TECHNISCHE UNIVERSITÄT MÜNCHEN

Lehrstuhl für Experimentelle Genetik

Significance of Apoptosis in Hepatitis B Virus Infection

Silke Arzberger

Vollständiger Abdruck der von der Fakultät Wissenschaftszentrum Weihenstephan für Ernährung, Landnutzung und Umwelt der Technischen Universität München zur Erlangung des akademischen Grades eines

Doktors der Naturwissenschaften

genehmigten Dissertation.

Vorsitzender: Univ.-Prof. Dr. B. Küster

Prüfer der Dissertation:

1. Univ.-Prof. Dr. M. Hrabé de Angelis
2. Univ.-Prof. Dr. U. Protzer-Knolle
3. apl. Prof. Dr. V. Bruss
   (Georg-August-Universität Göttingen)

Die Dissertation wurde am 25.06.2009 bei der Technischen Universität München eingereicht und durch die Fakultät Wissenschaftszentrum Weihenstephan für Ernährung, Landnutzung und Umwelt am 07.12.2009 angenommen.

Contents

Abbreviations

A

Ab	antibodies
Ad	adenoviral vector
ADCC	antibody-dependent cell-mediated cytotoxicity
ALT	alanine aminotransferase
APC	antigen presenting cells
approx	approximately

B

BCR	B cell receptor

C

cccDNA	covalently closed circular DNA
CD	cluster of differntiation
CsCl	cesium chloride
CTL	cytotoxic T lymphocytes

D

ddH_2O	double distilled water
DHBV	duck hepatis B virus
DC	dendritic cells
DMSO	dimethylsulfoxid
DNA	desoxyribonucleic acid
DR	directed repeat
dsDNA	double-stranded DNA

E

EDTA	ethylenedinitrilotetraacedic acid
e.g.	exempli gratia
EtBr	ethidiumbromide
ELISA	enzyme linked immunosorbent assay
Enh	enhancer
ER	hepatocellular transcription factors

F

FADD	Fas-associated death domain
FCS	fetal calf serum

G

GFP	green fluorescent protein

H

h	hour
HBcAg	hepatitis B core antigen
HBeAg	hepatitis B e antigen
HBsAg	hepatitis B surface antigen
HBV	hepatitis B virus
H&E	hematoxylin-eosin stain
HIV	human immunodeficiency virus
HNF	hepatocellular transcription factors

I

IFN	interferon
IFA	incomplete Freunds adjuvant
Ig	immunglobulin
IL-	interleukine
i.p.	intraperitoneal
i.v.	intravenously

K

kb	kilo base
kDa	kilo dalton

L

L	ligand
LAL	liver-associated lymphocytes
LC	Light Cycler
LSEC	liver sinusoidal endothelial cells

M

µg	microgram
MHC	major histocompatibility complex
ml	milliliter
mM	millimolar
MOI	multiplicity of infectious units

MOMP	mitochondria outer membrane permeabilisation
mRNA	messenger ribonucleic acid

N

NK	natural killer

O

ORF	open reading frame

P

PAA	polyacrylamid
PAGE	polyacrylamid gel electrophorese
PBS	phosphate buffered saline
PCR	polymerase chain reaction
PreC	precore protein
PEG	polyethyleneglycol
pgRNA	pregenomic RNA
PHH	primary human hepatocytes

Q

qPCR	quantiative PCR

R

rcDNA	relaxed circular DNA
RNA	ribonucleic acid
RT-PCR	reverse transcription PCR
RLU	relative light units

S

SDM	second derivative maximum
subgRNA	subgenomic RNA
SVP	subviral particle

T

TAE	tris-acetat-EDTA buffer
TCR	T cell receptor
TEMED	N,N,N',N'-Tetramethylethylendiamin
Th	T helper
TLR	Toll-like receptor
TNF-α	tumor necrosis factor alpha
TNFR	tumor necrosis factor receptor
TRAIL	TNF related apoptosis inducing ligand

U

UV-C	ultraviolet light C

W

WHV	woodchuck hepatitis virus

V

VP	virus particle

Abstract

The hepatitis B virus (HBV) is a highly infectious, small hepatotrophic para-retrovirus (hepadnavirus) that replicates by reverse transcription within hepatocytes and strongly promotes acute and chronic liver diseases worldwide. The pathogenesis of HBV is still a poorly understood process, which is caused by the cellular immune response attacking infected liver cells. This work focused on apoptosis as an important cellular defense mechanism.

(A) The first part of this thesis considered the consequence of apoptosis for HBV life cycle. The goal of this study was to determine if apoptosis of HBV-infected hepatocytes supports viral propagation. Moreover, we addressed the questions of whether or not the expression of viral HBx protein sensitizes HBV-replicating cells towards apoptosis.

In order to substantiate the relevance of apoptosis for HBV propagation, we designed a cell culture model that consists of both HBV-producing cell lines and primary human hepatocytes (PHH). We revealed that apoptotic hepatocytes released huge amounts of immature non-enveloped HBV capsids. Second round of infections on PHH demonstrated that those particles were non-infectious. Comparative analyses of *wild type* (wt) HBV- and *HBx-deficient* (Δx) HBV-producing hepatoma cell lines showed that wtHBV-producing hepatoma cells were partially resistant towards UV-C induced apoptosis. cDNA microarray analyses of HepG2, wtHBV- and ΔxHBV-producing hepatoma cell lines indicated that HBV-replication hardly influenced the cellular transcriptome. Especially, we found no hints that viral protein expression alters the transcription of cellular proteins involved in pro- and anti-apoptotic signaling pathways. However, we detected slight differences between ΔxHBV- and wtHBV-producing cell lines.

Taken together, this work has shown for the first time that apoptosis of HBV infected hepatocytes blocks viral propagation to neighbouring cells. Consistent with this finding we have demonstrated that HBV-replication does not sensitize host cells towards apoptosis. Our data imply that the viral HBx protein actively prevents apoptosis.

(B) The second part of this thesis focused on the immune response of an acute HBV infection. In detail, we addressed the question of what happens to the clearance of an acute HBV infection if cytotoxic T lymphocytes cannot kill HBV infected liver cells either by perforin/granzyme or CD95-receptor mediated apoptosis. To this end, we used a mouse model of an acute, self-limiting HBV-infection by adenoviral vector gene transfer (AdHBV). We compared the establishment and the clearance of an acute HBV infection in different mouse lineages bearing a generalized lymphocyte deficiency (gld) or a conditional, hepatocyte-specific deficiency of CD95-receptor signaling (FADDfl/fl x Alb-Cre= FADD-/-$_{hep}$). Furthermore, we analyzed the clearance in mice deficient for perforin/granzyme-mediated killing using perforin knockout mice (perf k/o).

We found that mice deficient for CD95- or perforin/granzyme mediated killing were able to clear an acute HBV infection. However, mice deficient for CD95-induced apoptosis (gld and FADD-/-$_{hep}$) exhibited a significant reduced cellular and especially humoral HBV-specific immune response. The data suggest that priming of the adaptive immune system against HBV is insufficient. Reports on the requirement for help showed that B cells efficiently capture HBV capsids and present them to naïve T cells. Thus, we hypothesized that CD95-induced apoptosis of infected hepatocytes is connected with HBV particle release, which in turn might be necessary to induce priming of adaptive immunity. To substantiate this notion, we induced artificial apoptosis in HBV-infected gld mice using *anti*-CD95 antibody treatment. Additionally, we immunized HBV-infected FADD-/-$_{hep}$ and gld mice with HBV capsids. To this end, we revealed that the humoral HBV-specific immune response is significantly increased by both *anti*-CD95 antibody treatment and capsid immunization. Based on this data, we have developed the revolutionary theory that B cells play a key role as antigen presenting cells during HBV infection in priming the adaptive immunity by efficiently taking up HBV capsids released after CD95-induced apoptosis.

1 Introduction

1.1. Overview of Hepatitis B

1.1.1 Epidemiology

With about 2 billion people infected worldwide, the human hepatitis B virus (HBV) is a major global health problem and represents one of the most important occupational hazards for health workers (Hepatitis B Foundation, 2009).

HBV possesses a high organ and species specificity. In addition to humans, only chimpanzees and other higher order primates are naturally susceptible to HBV. The virus specifically infects hepatocytes. Thereby, it causes an acute liver inflammation (hepatitis) with variable extent ranging from asymptomatic to fulminant hepatic failure. In most cases, however, a mild to moderate liver pathology has been observed. The clinical manifestation of hepatitis is caused by cellular anti-viral defense responses attacking HBV-infected cells. Viral replication, assembly and egress do not cause any cellular disruptions (Schulze-Bergkamen *et al.* 2003); therefore, the virus is considered as non-cytopathic. The most prominent clinical symptoms of acute HBV-infection are jaundice, fatigue and nausea.

The majority of HBV-infected adults (90%) resolved spontaneously from acute infection within six months. However, the patients who become persistently infected have a high risk to develop liver cirrhosis and later hepatocellular carcinoma (HCC). Presently, about 400 million chronic carriers live with HBV worldwide and estimated one million individuals die each year due to the consequence of HBV-related diseases (Hepatitis B Foundation, 2009). However, the prevalence of HBV varies significantly between different regions of the world. High epidemic areas are Asia, Africa, and China with about 10% of chronic HBV carriers in the population. Most of them become infected during childhood and 80% developed HCC. Low epidemic areas include Western Europe and North America. These countries have HBV infection-rates below 1% and HBV is mostly transmitted between adults. The actual incidence of *de-novo* HBV infections per year is estimated to be about 60,000 in the USA (CDC; 2004) and about 30,000 in Germany (www.impf-info.de; 2007). It is important to note that the estimated number of unknown cases is extremely problematic because it builds up the major reservoir of new infections.

A prophylactic vaccination against HBV is available since 1982 (Francis *et al.* 1982); however, no therapeutic treatment is on the market that completely eradicates persistent HBV-infections, and thereby preventing the formation of HCC.

HBV is highly infectious: 50 to 100 times more potent than the human immunodeficiency virus (HIV) (WHO, 2008). A tremendous study in chimpanzees has shown that a single HBV virion intravenously applied is sufficient to induce viral infection (S.Wieland and F.Chisari, personal communication, 2007). HBV is transmitted horizontally by percutaneous and permucosal exposure of infected blood and body fluids during sexual contact, unsafe injection, blood transfusion, and infected household objects. Additionally, HBV is transmitted vertically from an infected mother to infant. About 90% of HBV-infected infants developed HBV persistence.

In conclusion, the clinical outcome, extent and severity of HBV infection depend on various viral and host factors. However, no satisfactory answer has yet to be forthcoming to why some individuals recover from HBV-infection whereas others have not. Several lines of evidence indicate that the antiviral immune response of the host is the most critical variable.

1.1.2 Classification

The term “viral hepatitis” describes infections of the liver caused by at least five distinct hepatotropic viruses including Hepatis A (picornaviridae), Hepatitis B (hepadnaviridae), Hepatitis C (flaviviridae), Hepatitis D (viriod-like) and, Hepatitis E (caliciviridae).

Blumberg originally identified the human HBV in 1968 (Blumberg *et al.* 1968). It represents the prototype of hepatotrophic viruses belonging to the family of hepadnaviridae (*hepa*totropic-*DNA*-*Viruses*). Relatives to this virus family are the woodchuck hepatitis virus (WHV), the ground squirrel hepatitis virus (GSHV), and the duck hepatis B virus (DHBV) (Ganem & Schneider 2001). All these viruses share common properties: (i) replication via an RNA-intermediate within nucleocapsids; (ii) comparable genomic organizations (described in 2.2.1); (iii) secretion of different types of virus-related particles; (iv) viral persistence; (v) high species and organ specificity.

Since mammalian and avian hepadnaviruses exhibit some prominent distinctions, two separate genera have been generated denoting the *Ortho*hepadnaviridae and *Avi*hepadnaviridae. The latter genus shows: (i) less sequence homology with HBV, and (ii) a less pronounced hepatotropism, (iii) they encode only two surface proteins (L and S) but lack the M protein, and (iv) they carry no regulatory HBx protein (Ganem & Schneider 2001). Despite these differences, DHBV infection of ducks has been an important animal model for the understanding of the biology of hepadnaviral infections.

1.1.3 Experimental Models for HBV

Due to the narrow host-range and the organ-specificity of HBV, experimental models are still limited. However, over the last forty years a multiplicity of models has been developed that allow the study of different steps in the HBV life cycle, or even virus-host immune reactions.

1.1.3.1. Cell Culture Models

Different hepatoma cell lines have been established like HuH7 or HepG2 that support the HBV life-cycle upon transfection with plasmids carrying an HBV-genome (Sureau *et al.* 1986, Sells *et al.* 1987). In addition, stably HBV-transformed cell lines like HepG2.2.15, HepG2-H1.3 or HepG2-H1.3x- (K6) have been generated by molecular cloning that produce high amounts of HBV particles (Acs *et al.* 1987, Protzer *et al.* 2007); results part I). Nevertheless, the cell lines are not permissive for natural infection. Only primary human hepatocytes (PHH) and surprisingly hepatocytes from the Tupaia belangeri, a squirrel-like animal, are susceptible to HBV particles (Rumin *et al.* 1996, Schulze-Bergkamen *et al.* 2003, Kock *et al.* 2001). Since 2002, a cell line (HepRG) has been established that also becomes susceptible to HBV after differentiation under special cell culture conditions (Gripon *et al.* 2002). All these HBV-permissive cell culture models have in common that they are difficult to handle. Furthermore, the availability of PHH from surgical liver resections and the isolation procedure by collagenase digestion and perfusion are extremely sumptuous (Schulze-Bergkamen *et al.* 2003). This is combined with an unpredictable and permanently altered quality of cells because the donors are mostly HCC patients. Moreover, the infection of PHH and HepRG cells is polyethyleneglycol (PEG)-dependent and the cultivation of these cells needs high concentrations of dimethylsulfoxide (DMSO).

1.1.3.2. Animal Models

To analyze the early steps of HBV infection and especially virus-host interactions in combination with immune responses, an animal model is necessary.

As already mentioned, besides humans only chimpanzees are naturally susceptible to HBV but the access to chimpanzees is extremely limited due to ethical aspects, availability, and high costs. The woodchuck and Peking duck are alternative natural animal models that are based on HBV-related hepadnaviruses. Both models brought fundamental knowledge into the biology of hepatitis B (Mason *et al.* 1983, Summers *et al.* 1978). However, these animals are not convenient to keep and furthermore they lack genetically characterization.

Therefore, HBV transgenic mouse lineages expressing partial or complete HBV genomes have been generated as an inbreed animal model with well defined immune system (Guidotti *et al.* 1995, Chen *et al.* 2000, Chisari *et al.* 1985). These transgenic mouse models provided important insights into viral pathobiology and hepatocellular injury, especially upon lymphocyte transfer (Ando *et al.* 1993, Guidotti *et al.* 1996b, Guidotti *et al.* 1994a, Nakamoto *et al.* 1997, Milich *et al.* 1998). However, it is important to note that hepatocytes of mice are not permissive to HBV infection, although they support HBV-life cycle and secrete huge amounts of virions upon transduction of viral genomes (Guidotti *et al.* 1995). The reason why viral entry is hampered remains still an unknown. Moreover, mouse hepatocytes do not establish cccDNA, the natural template for HBV transcription. Thus, viral RNA is synthesized from a linearized transgene.

In the last few years, two different mouse models of acute-self limiting HBV infection by either adenoviral HBV genome transfer or by hydrodymamic injection of plasmids carrying an HBV genome have been independently developed (Yang *et al.* 2002, Sprinzl *et al.* 2001, Huang *et al.* 2006, John von Freyend M. *et al.* 2009). These models allow detailed studies of virus-host interactions in an immune competent environment. Thus, they are suitable to analyze the onset, the establishment and the dynamic of an acute HBV-infection in a well defined immune system. A further advantage of the transient genome transfer is the fact that HBV genomes, used for viral transcription, stayed in an extra-chromosomal organization like cccDNA.

A chimeric mouse with humanized hepatocytes represents an additional small-animal system. The advantage of this system is that the humanized liver can be infected by

HBV and cccDNA will be formed. However, this mouse model is very complex: it is based on a liver-toxic phenotype in urokinase-type plasminogen activator (uPA) immunodeficient transgenic mice. In this model, the mouse-hepatocytes expressing the uPA transgene become depleted and transferred PHH repopulate in a functional manner (Dandri *et al.* 2001, Mercer *et al.* 2001, Katoh *et al.* 2008). The major disadvantage of this system is the use of immune deficient mice (RAG-I, SCID). Therefore, this model system cannot be used to address immunological questions.

1.1.3.3. Applied Model Systems

In the first part of this PhD thesis, we worked with stable HBV-transformed hepatoma cell lines in conjunction with PHH to analyze the significance of apoptosis for HBV spreading. In the second part of this PhD thesis we took advantage of adenoviral HBV genome transfer to analyze the clearance of an acute HBV-infection under conditions when cytotoxic lymphocytes are restricted in their effector functions. The corresponding models are explained in detail in the respective result sections.

1.2. The Hepatitis B Virus

1.2.1 Particle Structures

The hepadnaviruses produce and secrete different types of virus-related particles as presented in Figure 1 (Bayer *et al.* 1968).

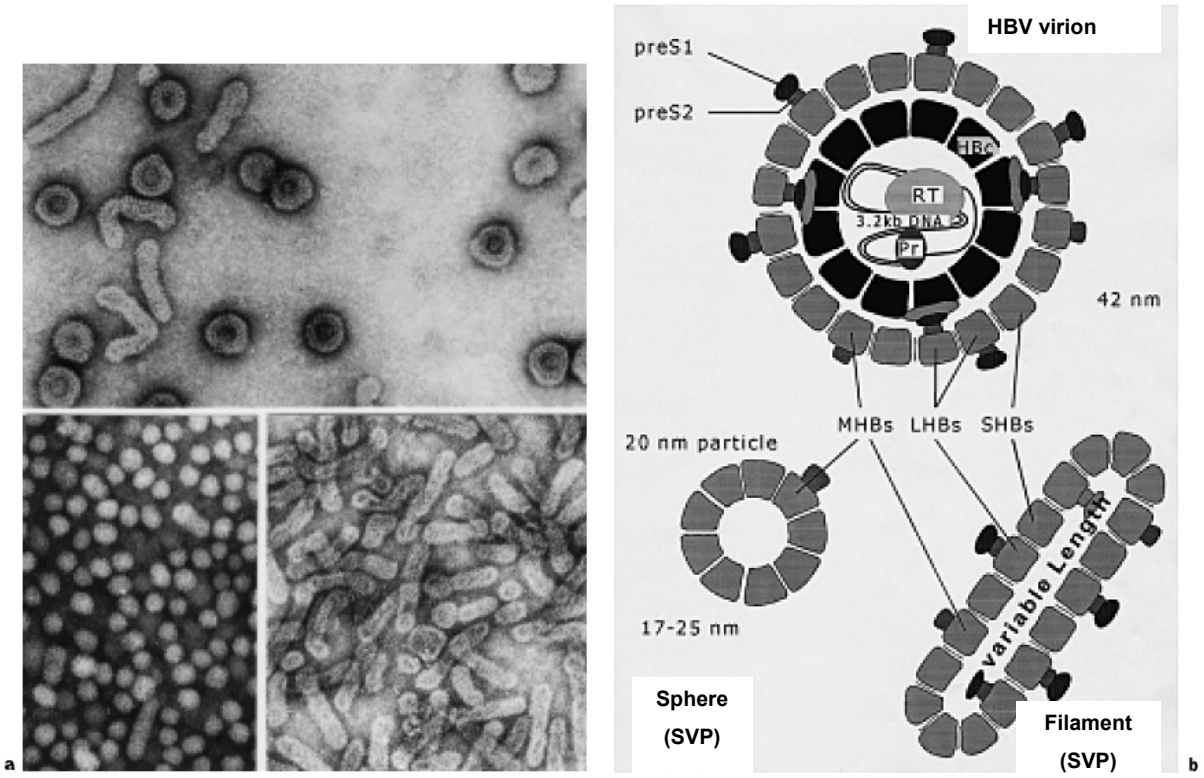

Figure 1 HBV Particles a) Electron micrograph of HBV particles (top), SVP bottom: spheres (bottom left), filaments (bottom right) b) Scheme of virions and SVP. L, M, and S hepatitis B surface (HBs) proteins with S, pres1 and preS2 domain; core protein (HBc); reverse transcriptase (RT); RNA cap primer (Pr) Infus Ther Transfus Med 2000; 27:226-234(Copyright)

1.2.1.1. Virion

The infectious virion is termed a Dane particle after its discoverer (Dane *et al.* 1970). The virion has a spherical structure about 42 nm and consists of the nucleocapsid enveloped in a host-derived lipoprotein membrane. Three different Hepatits B surface (HBs) glycoproteins are integrated into the lipid-envelope termed *small* (S), *middle* (M) and *large* (L) proteins with the domains S, preS2 and preS1 (Fig.1). The ratio of these HBs proteins is about 4:1:1 in virions (Heermann *et al.* 1984). Of note, despite its low abundance, the preS1 domain of the L protein plays a key role in viral assembly and infectivity (Bruss *et al.* 1996, Ishikawa & Ganem 1995, Lenhoff & Summers 1994). The 27-nm icosahedral nucleocapsid consist of 180 or 240 viral

core proteins, respectively (Bottcher *et al.* 1997), and contains the HBV genome as well as the viral polymerase (P-protein) (Robinson *et al.* 1974).

1.2.1.2. Subviral Particles (SVP)

In addition to the Dane particle, two different forms of non-infectious SVP, denoted as spheres and filaments, are secreted from HBV replicating hepatocytes. They are composed of host-derived lipids and viral S glycoproteins. Note that SVP carry no viral capsid and no nucleic acid content. Spheres are 20 nm in diameter and are secreted in **10,000- to 100,000-fold** excess over virions (Ganem & Schneider 2001). Filaments are found in smaller quantities; they are 20 nm in diameter and variable in length.

Of note, the viral S protein is abundant in the envelope-structures of all virus-related particles and serologically detectable as *hepatitis B surface antigen* (HBsAg). In keeping with this, HBsAg are present in enormous quantities in the serum of infected patients and most of them are composed of spheres. The SVP might have an immune regulatory function, possibly by absorbing *anti*-HBsAg neutralizing antibodies.

1.2.2 Genomic Structure and Organization

The HBV exhibit an extraordinary and extremely compact genomic structure, of which two different constitutions are distinguished: (i) the capsid-restricted rcDNA within virions and (ii) the nucleus-restricted cccDNA episome.

1.2.2.1. Virion

The capsid-restricted infectious HBV-genome is relaxed circular (rc), partially double-stranded and with a size of 3.2 kb, it is one of the smallest DNA genomes known so far. The circular structure is composed of two coiled DNA strands that are not perfectly symmetric. A gap of fixed polarity is formed between the 5´- and 3´-end of the negative (-) DNA strand. Additionally, the 5´-ends of both DNA strands carry unusual modifications derived from the primers of the hepadnaviral replication strategy. The (-) DNA strand is of unit length and its 5´-end is covalently linked to the viral P-protein. The positive (+) DNA strand is of variable length and its 5´-end bears a capped oligoribonucleotide.

1.2.2.2. cccDNA

Within the nucleus of the host cell, the rcDNA genome converts into a *covalently closed circular* DNA (cccDNA) and serves as a template for viral transcription. Note, rcDNA and cccDNA can be discriminated due to the gap structure of rcDNA by PCR.

1.2.2.3. HBV Transcripts

Two classes of HBV transcripts are distinguished: **subgenomic (subg)** and **pregenomic (pg) RNA**s. The subgRNAs encode for the viral surface proteins and a regulatory protein termed HBx. The subgRNAs function exclusively as “normal” mRNAs for translation. The pgRNAs exceed by about 3.5 kb the genomic size of HBV-DNA because their transcription is initiated approximately 6 bp upstream of the direct repeat (DR) 1 region (Fig.2). Additionally, their transcription proceeds along the entire DNA molecule, pasts the initiation site, and terminates at the commonly used polyadenylation (Poly(A)) site located within the open reading frame C (Fig.2) (Summers & Mason 1982, Will *et al.* 1987). HBV generates two 3.5 kb RNAs; both encode the complete sequence of the viral genome, but they differ slightly in length at the 5´-end. This difference in length has a dramatic influence on their functions: the 3.5 kb **pgRNA** is **bifunctional,** meaning it works as a “normal” mRNA template for translation of the viral P and Core protein and additionally as template for viral replication. By contrast, the slightly extended 3.5 kb RNA functions exclusively as mRNA for translation of PreC protein. The extension is a signal sequence targeting the template to the secretory pathway. This pgRNA is not used as template for viral replication.

1.2.2.4. Viral Proteins

In general, HBV encodes for seven viral proteins:

- **P-protein**, a multifunctional enzymatic protein carrying **viral reverse transcriptase** (RT) -, DNA polymerase-, RNase H- activity and additionally serving as a primer for (-) DNA strand synthesis.

- **Core protein**, an important structure component for building up the viral **capsid**. Serologically, known as *c antigen* (**HBcAg**).

- **PreC**, a non-structural protein showing substantial sequence overlaps with Core. Immunologically, the PreC protein is identified as a nonparticulate form of HBcAg and termed *e antigen* (**HBeAg**). The function of HBeAg remains mysterious as it is neither required for infection nor for viral replication. HBeAg is secreted and evidence from the last decade indicates that it has **immunoregulatory functions**.

- **L** - **M** - **S** HBs **glycoproteins**. Immunologically identified as HBsAg.

- **HBx**, a regulatory protein with enigmatic functions. Its participation in apoptosis induction is discussed in 1.4.2

1.2.2.5. Genomic Organization

The seven viral proteins are encoded in four open reading frames (ORF P - ORF C - ORF S – ORF X) and their transcription is controlled by four promoters (C/P - preS1 - preS2 - X) and two enhancer (Enh) elements (Fig.2). Enh I strongly upregulates the transcription of all five promoters, whereas Enh II exclusively stimulates the transcription of the C/P promoter.

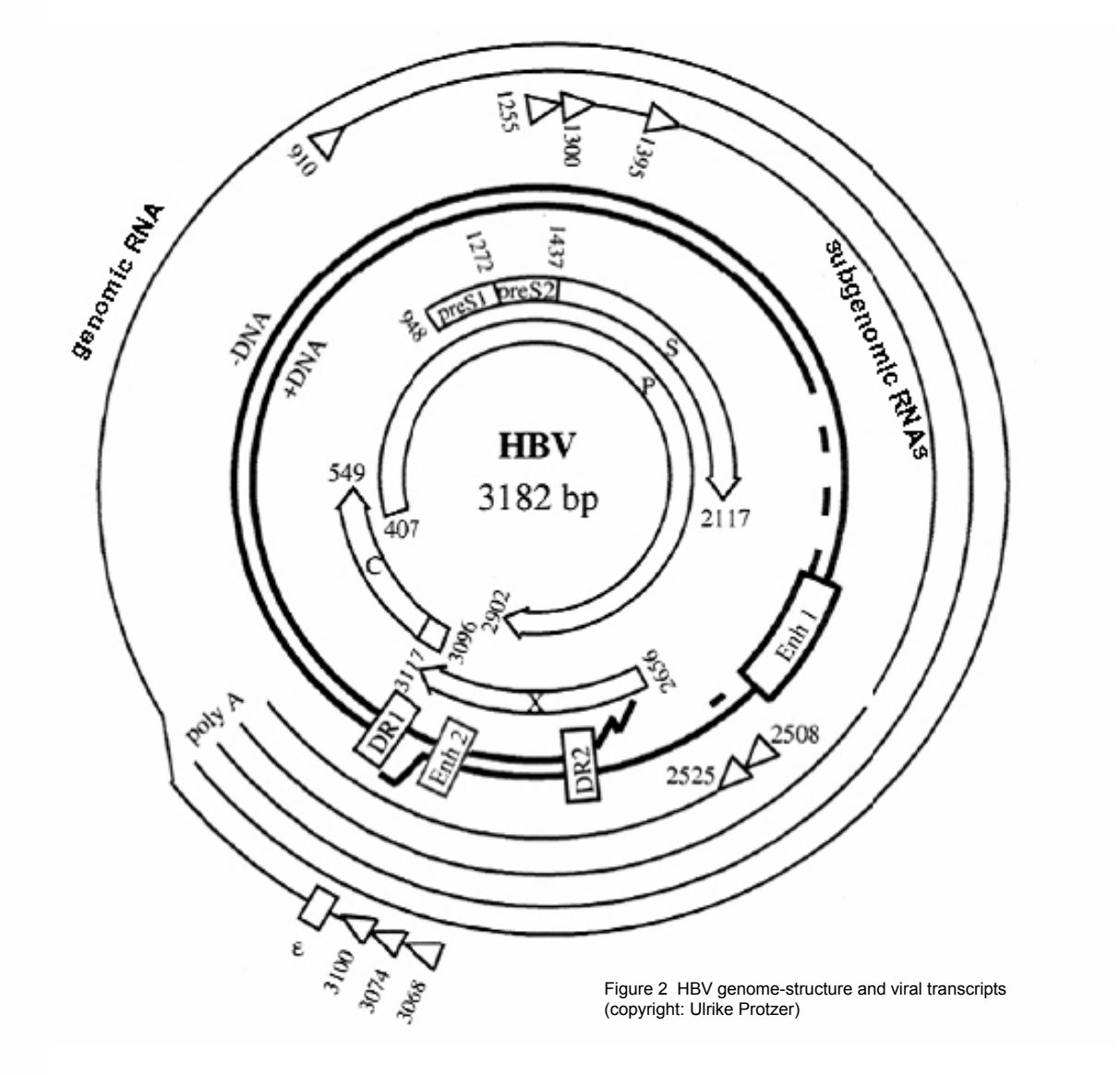

Figure 2 HBV genome-structure and viral transcripts
(copyright: Ulrike Protzer)

As mentioned above, the genome organization of HBV is extremely compact: every nucleotide is part of at least one coding region, and most of the sequences are translated in more than one frame (Galibert *et al.* 1979). In addition to the overlapping open reading frames, the virus employs multiple initiation codons (AUG side) within the in-frame readings to generate structurally related but functionally distinct viral proteins.

In particular, the coding organization of the surface glycoproteins on the one hand - and of P, Core, and PreC protein on the other hand are highly complex as described in the following:

- The glycoproteins (L-M-S) are coded in-frame within the ORF S. Thus, all proteins share a common C-terminal domain corresponding to the S protein, but vary in length at the N-terminus. This coding organization requires a complex regulation: transcription of the L-protein is regulated separately by the Pre-S1 promoter. By contrast, the transcription of M and S are controlled by a common promoter (Pre-S2). A leaking scanning mechanism and different initiation sites generate two distinct transcripts: the transcription of the M-protein starts at the first AUG site upstream of the Pre-S2 promoter lacking a TATA-Box, therefore the transcription of the S protein, initiated from an internal AUG site, is favored by RNA Polymerase II (Cattaneo *et al.* 1983, Standring *et al.* 1984).

- The preC, Core and P-protein are also coded in a complex fashion: the coding sequence of preC and Core are almost identical. However, the templates of both proteins are different. One promoter (C/P), but two different initiator regions (preC and C/P) regulate distinct transcription within the ORF C by a still unknown mechanism. - Curiously, the P and Core gene are transcribed in one run controlled by the C/P promoter, although their ORFs (C and P) overlap, generating a bicistronic RNA. Therefore, expression of both proteins must be controlled at the translational level by a poorly understood process, leaky scanning or ribosome re-initiation mechanisms are assumed (Fouillot *et al.* 1993, Hwang & Su 1998, Chen *et al.* 2005). Of note, the activity of the C/P promotor and Enh II, which both control the transcription of the P and Core protein, are restricted to hepatocytes. Both regulatory elements require hepatocellular transcription factors like HNF3, HNF4 and HBF1 (Yee 1989, Yuh & Ting 1993). Therefore, replication of HBV is exclusively confined to hepatocytes.

1.2.3 Viral Life Cycle

Although the replication cycle of HBV via an RNA intermediate has been largely clarified since 1982 (Summer and Mason), details concerning all important steps within the HBV life-cycle such as entry, intracellular transport, maturation and egress are hitherto enigmatic as mentioned in the following. The replication cycle of HBV is represented in Figure 3.

1.2.3.1. Delivery to Hepatocytes

HBV is highly infectious: the half-life of the virions in the blood stream averaged about four hours (Murray *et al.* 2006, Dandri *et al.* 2008) and one particle is still sufficient to induce an infection (Jilbert *et al.* 1996);S. Wieland and F. Chisari, personal communication, 2007). This implies that HBV particles are efficiently removed from the circulation within the liver. However, it remains unclear how this process is achieved and how HBV particles get in contact with hepatocytes. Preliminary data suggest that HBV virions are bound loosely to apolipoproteins in the blood stream. Thereby, they are efficiently taken up by scavenger receptors of Kupffer cells. Within Kupffer cells, the virion envelope structure is altered and the particles translocate to the space of *Dissé* (K. Esser and U. Protzer, personal communication 2009).

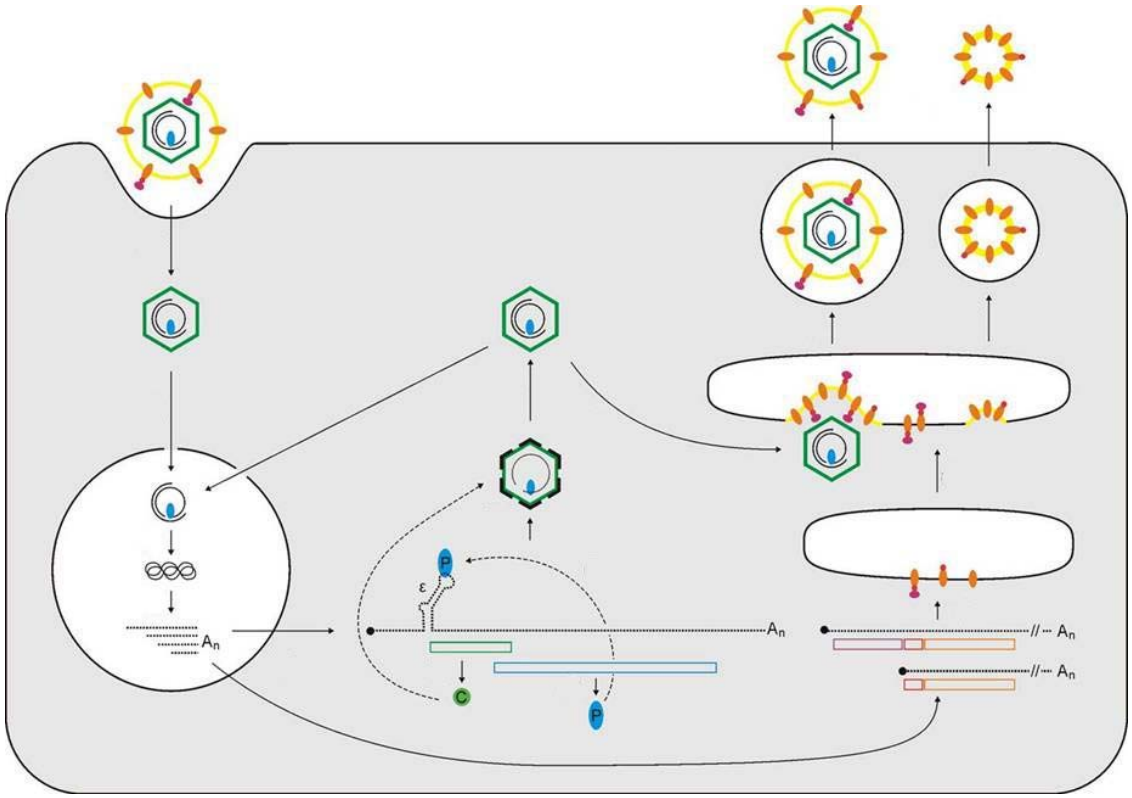

Figure 3 Overview of HBV life cycle. Kindly provided by Volker Bruss; description see text.

1.2.3.2. Entry

How the virus enters the hepatocytes is another mystery. Evidence from a number of groups indicates that a multistep process involving viral, cellular and extracellular components form the basis for infiltration. Especially, the viral large surface glycoprotein (Schulze *et al.* 2007) and the cholesterol content of the viral envelope (Bremer *et al.* 2009, Funk *et al.* 2008) are important structures for viral entry. Depletion of one of these components strongly reduces viral infectivity. It has been suggested that the myristoylated L-protein interacts with glycosaminoglycans associated with hepatocytes before internalization is initiated. Possibly, a still unknown high-affinity receptor is linked to this process (Schulze *et al.* 2007). The high cholesterol content in the envelope of the virions seems to be necessary for viral fusion with endosomal membranes to deliver HBV capsids into the cytoplasm (Funk *et al.* 2008), which has been shown to be pH independent (Rigg & Schaller 1992, Kock *et al.* 1996).

1.2.3.3. Intracellular Transport to the Nucleus

Upon uncoating, the viral capsid has to be delivered to the nucleus by a still incompletely identified process. It has been assumed that capsids are transported via microtubules to the perinuclear-located microtubule organization center. Afterwards, the capsid is directed to the nuclear pore complex by its nuclear localization signal, where the rcDNA genome is released from the capsids and translocates to the nucleus (Bock *et al.* 1996, Kann *et al.* 2007). Interestingly, no capsids are found in the nucleus but rare amounts of core protein are detectable, indicating that rcDNA might be released at the nuclear pores (Bock *et al.* 1996, Ning & Shih 2004).

Inside the nucleus the rcDNA genome is converted into the stable cccDNA form by cellular enzymes. This involves completion of the (+) DNA strand, removal of the primers at the 5´-ends of both DNA strands, and ligation of compatible DNA ends (Miller *et al.* 1984). Additionally, cccDNA becomes wrapped by cellular histones and other proteins (Bock *et al.* 1994, Bock *et al.* 2001). These epigenetic modifications have substantial influences on viral transcription (Pollicino *et al.* 2006); and own observations). By note, the episomal HBV genome has the potential to persist in the host cell over years. However, the reader should be reminded that cccDNA is not replicated during mitosis by the cellular DNA-polymerase, it requires the viral life

cycle (reverse transcription of pgRNA in viral capsids and re-import into the nucleus as described below).

1.2.3.4. Transcription

The viral pg- and subgenomic transcripts are generated from cccDNA by cellular RNA polymerase II. All viral transcripts are intronless, but they carry a 5´-end capped RNA structure and a 3´-end Poly(A) tail that is generated at a common Poly (A) site (for a detailed description, see section 2.2.2). The export of viral RNAs is regulated by post-transcriptional regulatory elements (PRE) (Huang, 1993).

1.2.3.5. Translation

The viral surface glycoproteins and the preC protein are translated by ribosomes bound to the endoplasmatic reticulum (ER) entering the secretory pathway. By contrast, HBx, P- and Core proteins are transcribed by free ribosomes at low efficiency (Hwang & Su 1998, Su *et al.* 1998).

1.2.3.6. Replication

HBV replication via the pgRNA template takes place within the capsid located in the cytoplasm (Summers & Mason 1982). The replication process can be divided into three parts: encapsidation of the pgRNA plus the P-protein, (-) DNA strand-, and (+) DNA strand synthesis. Regarding the circular HBV genome structure, permanent exchanges of the template are a characteristic of hepadnaviral replication. Requisites for this process are regions with sequence homologies called "*directed repeats"* (DR) (Fig.3). In addition, the spatial arrangement of the template within the capsid might also be important for viral replication. Recent data indicate that cellular chaperons are also involved in the packaging process (Beck & Nassal 2007).

Before capsid self-assembly is initiated, a threshold concentration of core proteins must be reached (Seifer & Standring 1993). It should be noted that capsid formation is independent of packaging (Birnbaum & Nassal 1990, Cohen & Richmond 1982). The selective encapsidation of P-protein and pgRNA is triggered by a small hairpin-loop at the 5´-end of the pgRNA termed *epsilon* (ε) (Junker-Niepmann *et al.* 1990, Bartenschlager *et al.* 1990) (Fig.4). It is assumed that the nascent P-protein co-translationally binds to the ε-structure of its own pgRNA template (Bartenschlager *et al.* 1990).

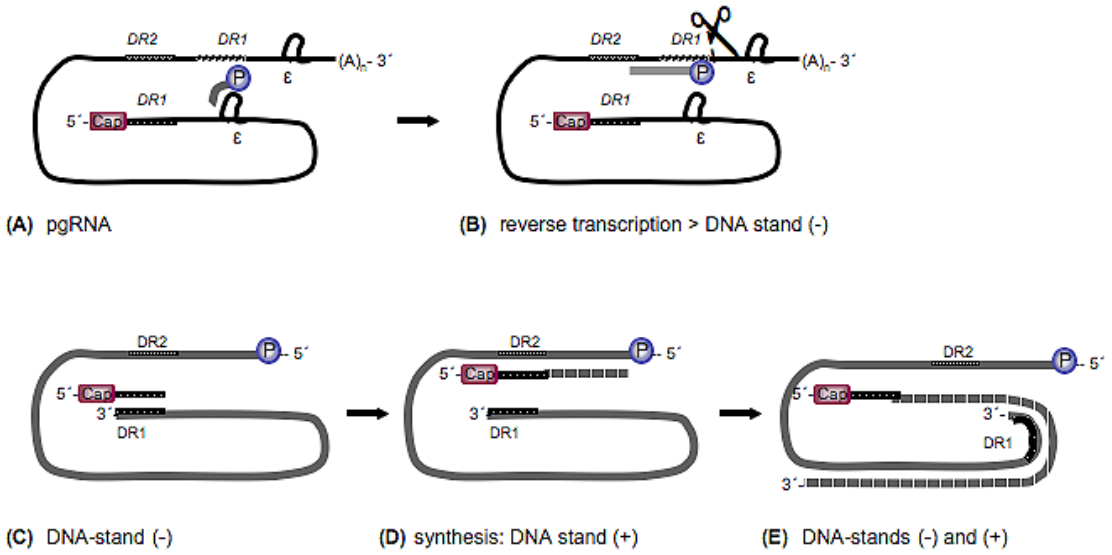

Figure 4 HBV Genomic Replication (description see Text)

Upon encapsidation, **reverse transcription** starts immediately, primed by the N-terminal tyrosine residue of the P-protein and by a specific DNA sequence located at the bulge of the ε-structure (Fig.4A). Due to this process, the P-protein becomes covalently attached to the 5´-end of the growing **(-) DNA strand**. After a short oligonucleotide has been synthesized at the ε-structure, the synthesis of the (-) DNA strand stops and the **first template exchange** takes place (Fig.4B) (Rieger & Nassal 1996, Wang & Seeger 1993). The (-) DNA strand polymerization continues at the DR1 region at the 3´-end of the pgRNA and finishes upon the complete copying of the pgRNA template. Concomitantly to the reverse transcription, the transcribed **RNA-template is degraded** by the RNase H activity of the P protein.

A short RNA molecule, corresponding to the 5´-end RNA cap of the pgRNA and including the DR1 region, is not digested by RNase H and serves as a primer for the **(+) DNA strand** synthesis (Fig.4C) (Lien *et al.* 1986). The (+) strand synthesis is initiated by a **second translocation step**: the RNA-primer changes to the DR2 position near the 5´-end of the (-) DNA strand (Fig.4D) (Seeger *et al.* 1986). In order to obtain a circular DNA genome, a second **intramolecular template exchange** must take place during (+) strand synthesis at a later time point (Fig.4E).

1.2.3.7. Morphogenesis and Release

Nucleocapsids follow **two different routes** in the cytoplasm: one is the **re-import** of rcDNA to the nucleus amplifying the pool of viral cccDNA (about 10-50 genomes per cell) (Tuttleman *et al.* 1986, Mason *et al.* 1998), whereas the other is directed to **virion-formation** by budding into intracellular membranes as described in the following.

To acquire a glycoprotein envelope, progeny cores bud into the pre-Golgi compartments. One requisite for envelopment is the completion of genomic DNA synthesis because only capsids with **reverse transcribed** genomes are competent for intracellular **budding** (Gerelsaikhan *et al.* 1996, Schormann *et al.* 2006). Therefore, it is intriguing to speculate that the structure of the capsids changes during genome replication. Recently, it has been shown that a special arrangement of four amino acids on the surface of the capsid is essential for envelopment. These residues are located at the base and between the spikes protruding from the capsid (Bruss 1997); Bruss, personal communication 2008). A second requisite is a high concentration of L- and S-proteins at the pre-Golgi membrane, and especially, a cytosolic deposition of the Pre-S1 domain of the L-protein (Bruss & Ganem 1991, Bruss & Thomssen 1994, Bruss & Vieluf 1995). Furthermore, it became evident that two cellular host factors, 2γ-adaptin and Nedd4 ubiquitin ligase, coordinate the budding process (Rost *et al.* 2006).

Since hepatocytes are polarized cells, enclosing the bile canaliculi with their apical site and facing the sinusoidal endothelium with the basolateral surface (Wisher & Evans 1975), it is still a mystery how virions enter the blood stream. A recent study speculated that the virus exploits the sorting machinery of multivesicular bodies (MVB) with the aid of 2γ-adaptin (Lambert *et al.* 2007). The MVB system is possibly used to trigger viral release at the basolateral cell surface. However, to enter the circulation, the liver sinusoidal endothelial cells (LESC) barrier must be passed a second time. Recently, it became evident that virions, SVP, and nucleocapsids are released through distinct pathways (Lambert *et al.* 2007, Watanabe *et al.* 2007).

1.3. Hepatitis B Infection

1.3.1 Pathogenesis of an acute HBV-infection

Horizontally acquired HBV infections in humans mostly become apparent just with the onset of clinical symptoms approximately three to six month after infection. At this time point, HBV-replication has already declined to borderline levels in most cases.

Figure 5 represents the typical dynamic of an acute self-limiting HBV-infection in humans followed by serological parameters. The infection shows two distinctive features. First, there are successive causes of viremia and liver inflammation characterized by HBV DNA and alanine aminotransferase (ALT), respectively. Second, HBV-DNA is hardly detectable during the first two to four weeks. This indicates that viral replication and/or progeny secretion are not efficient in the earlier stages. Interestingly, higher doses of transmitted HBV virions (inoculum) do not accelerate the onset of the exponential replicating phase (Thimme *et al.* 2003). High titers of HBV-DNA are detectable six weeks after infection.

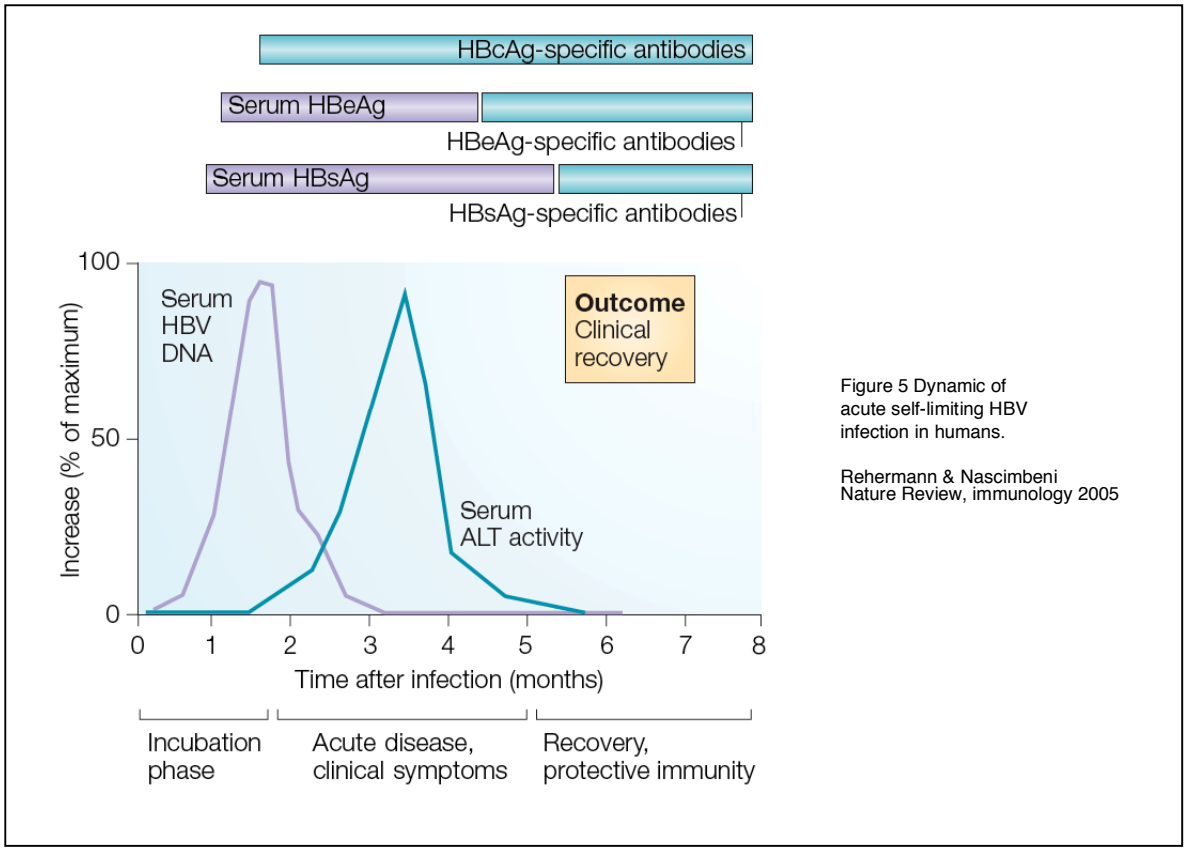

Figure 5 Dynamic of acute self-limiting HBV infection in humans.

Rehermann & Nascimbeni Nature Review, immunology 2005

At the same time, HBeAg, HBsAg and HBcAg-specific IgM appear. Approximately eight weeks after infection, ALT levels start to rise and peak six weeks later. At this point, all virions are cleared. It is important to note that more than 90% of horizontally infected patients get rid of all clinical symptoms and develop life-long protection against HBV by producing *anti*-HBs- and *anti*-HBe-specific antibodies. However, residual cccDNA molecules persist in the nucleus of some hepatocytes that are controlled by cellular and humoral immune responses (Rehermann & Nascimbeni 2005).

1.3.2 Innate Immunity

The innate immunity is the first line of host defense against microbes including viruses. Moreover, it has indispensable controller functions programmed to react to “danger signals” by alerting and modulating the adaptive immunity. The innate immune system reacts immediately because the weapons are already in place. Components of innate immunity are (i) the epithelial barriers, (ii) the complement system and other circulating effector proteins (iii) professional phagocytes including macrophages and neutrophils, (iv) natural killer cells (NK), (v) cytokines, and (vi) the cell-autonomous defense system.

1.3.2.1. Liver Environment

Applying the components of innate immunity to the hepatic environment as an immune-privileged organ, we found the following micro-anatomic structures: (i) liver sinusoidal endothelial cells (**LSEC)** line the hepatic sinus and separate hepatocytes from leukocytes in the sinusoidal lumen marking the space of Dissé; (ii) **Hepatocytes**, the most prominent hepatic cell population, are producers of proteolytic plasma proteins belonging to the complement system and the acute-phase response; (iii) **Kupffer cells** are the resident macrophages of the liver patrolling through the sinus. Kupffer cells and LSEC efficiently clear antigen from the blood by receptor-mediated endocytosis. LSEC can also function as antigen-presenting cells as described below. **Neutrophils** are professional phagocytes on call. They are recruited from the blood stream by adhesion molecules and cytokines upon infection. (iv) **Liver-associated lymphocytes (LAL)** are a heterogeneous population in the liver consisting of NK, NK-T, T-cells, dendritic cells (DC); Stellate cells (also called Ito cells) are a population of liver cells situated within the space of Dissé. Although Stellate cells are involved in liver fibrosis (Friedman 2004), their

immune-modulating functions are not yet fully defined. A recent report indicates that Stellate cells might activate $CD8^+$ or NK-T responses (Winau *et al.* 2007).

Compared to other hepatic viruses like HCV, HBV induce only a marginal detectable innate immune response during the first weeks of infection (Wieland *et al.* 2004); however, the importance of the innate immunity in controlling HBV infection at early time points should not be dismissed, as explained in the following.

1.3.2.2. Important Cytokines Controlling HBV-Infection

The different cell populations of the liver communicate with each other through cytokines that are produced in response to microbes. **Interferons** (IFN) are the most important cytokines in controlling viral infection: they block viral replication by inducing the synthesis of a number of enzymes, such as 2´5´oligoadenylate-activated RNaseL, Mx protein or inducible nitric oxide (NO) synthase. Furthermore, IFN intensify the cell-mediated immunity by increasing the expression of MHC class I molecules, enhancing the cytolytic activity of NK cells and promoting the T helper 1 (Th1) responses. Due to its origin, two types of IFN are distinguished with comparable anti-viral functions. IFN-α and IFN-β are belong to type I; they are directly trigged by viral-replication through cellular mechanisms. IFN-α is produced by phagocytes and IFN-β is secreted by infected host cells like hepatocytes. IFN-γ are type II interferons; they are produced by activated immune cells and as such by NK, $CD8^+$ and Th1 cells.

TNF-α and **IL-6** are also important cytokines involved in controlling acute HBV infection. TNF-α and IL-6 are both produced by activated phagocytes, like Kupffer cells and activated $CD4^+$ cells. They act on hepatocytes by increasing the synthesis of acute-phase plasma proteins (>systemic function) and stimulate the recruitment of leukocytes into the liver parenchyma. In addition, TNF-α has the ability to induce apoptosis via the TNF receptor (see 1.4.1.3.2). It is important to note that overwhelming cytokine-mediated leukocyte recruitment and activation are responsible for liver injury.

Diverse studies marked the importance of IFNs and TNF-α in controlling acute HBV infection non-cytopathically at early time points (Guidotti *et al.* 1994b, Guidotti *et al.* 1996a). These studies supported the concept that infected cells are not passive victims during HBV infection. Intriguing studies in chimpanzees and humans showed that virions are cleared from serum before a detectable adaptive immune response

could be triggered by cytokines (Guidotti *et al.* 1999a, Webster *et al.* 2000). The intracellular antiviral mechanisms through which IFNs and TNF-α control viral replication are still not understood, but it is known that they influence the degradation of nucleocapsids as well as the posttranscriptional destabilization of HBV-RNA (Guidotti *et al.* 1996b, Guidotti *et al.* 2002). It is possible that these antiviral mechanisms are not mediated by the "classical" IFN-induced proteins like Mx1 or RNase-L (Guidotti *et al.* 2002). The degradation of capsids might be proteosome-dependent (Robek *et al.* 2002). However, despite intensive research we could not detect any ubiquitin-modification on the viral Core protein (Silke Arzberger, unpublished results, 2007; Robek, personal communication, 2008).

1.3.2.3. Recognition of Invaders by Innate Immunity

With just about everything else in the immune system, cellular components of the innate immunity must be activated before they can function. However, the innate immunity requires **no priming** in comparison to the adaptive immunity. The activation of the innate immunity can generally happen by two ways. The first pathway is based on the direct recognition of microbes by germline-encoded receptors. This pathway is especially important for the detection of extracellular invaders. The second pathway discriminates between the presence and absence of common cell surface markers. This control system is useful to identify intracellular invaders like viruses that actively suppress antigen presention via MHC molecules class I.

1.3.2.3.1 Pathogen-Associated Molecular Patterns (PAMP)

Microbial invaders possess many unique features that are not present in eukaryotic cells. Recognition of these PAMP forms the basis of most defense reactions because the cells receive a "**danger signal**" prompting cellular defense mechanisms. At first, the affected cell immediately alerts the local environment by cytokine secretion and/or by expression of co-stimulatory cell surface markers like CD40L. PAMP are recognized by cellular pattern recognition receptors (PRR) that are abundant in a variety of immune and non-immune cells. PRR are present on the cell surface, as well as in the cytoplasm or in intracellular compartments like the endosome.

Three important PRR families that might detect HBV-derived structures are: (i) the Toll-like receptors (**TLR**) and the two intracellular helicase-receptors including (ii) melanoma differentiation associated gene 5 (**MDA5**) and (iii) retinoic acid-inducible genes (**RIG-I**). Recently, we showed for the first time that HBV triggers PRR

activation on Kupffer cells that leads to the release of IL-6. We supposed that the IL-6 controls viral replication non-cytopathically early after infection (Hösel M *et al.* 2009). In addition, a number of groups provided evidence that diverse PRR-signaling pathways suppress HBV replication non-cytopathically, as in TLR-signaling (Isogawa *et al.* 2005) Broxtermann and Protzer, personal communication, 2009), MDA5- and RIG-I-activation (Guo *et al.* 2009) Ebert and Protzer, personal communication, 2009). However, in those studies, HBV-derived products did not necessarily induce PRR-activation. Interestingly, recent studies indicate that HBV actively counteract TLR-signaling (Xu *et al.* 2008, Chen *et al.* 2008, Wu *et al.* 2009).

1.3.2.3.2 Detection of Infected Cells by NK and NK-T Cells

NK cells represent the lymphocyte population of innate immunity that recognizes intracellular invaders. They play an important role during the first few days after viral infection because they can kill infected cells **without MHC-I restriction** and therefore they can operate before antigen-specific CTL become fully active. That is why NK cells are termed *"natural killers".* NK cells express no T cell receptor (TCR); the balance of different signals generated from "activating" and "blocking" stimuli regulates their activation. Inhibitory signals for NK cells are MHC-I molecules that are constitutively expressed in all healthy cells in the body. Low expression levels of MHC-I molecules, possibly due to viral infections, are a powerful killing-signal for NK cells. The respective receptor on NK cells is NKG2D. A second population of lymphocytes that act without MHC-restriction is **NK-T** cells. These cells express T cell- and NK-markers, but they recognize antigens bound to CD1d (MHC-like molecule). Independent of the described activation, NK and NK-T cells kill their targets in the same fashion, than CTL by CD95-mediated or perforin/granzyme-induced apoptosis. In addition to the cytotoxic function, activated NK and NK-T cells produce huge amounts of IFN-γ. NK cells are also involved in antibody-dependent cell-mediated cytotoxicity (ADCC) by recognizing antibody-coated targets through FcγRIIIa (CD16), a low-affinity receptor for the Fc region of IgG1 and IgG3 antibodies.

The knowledge about NK and NK-T cells during acute and chronic HBV infections is rudimentary at best. A previous study in humans of acute HBV infection revealed that the kinetics of NK and NK-T in liver tissue is faster than of HBV-specific $CD8^+$ and $CD4^+$ (Webster *et al.* 2000, Fisicaro *et al.* 2009). These data indicate that the innate

immunity is not silent at early time points of acute HBV infection. Two further interesting studies of tg-mice suggest that the acute liver inflammation is mediated by NKG2D receptor-activity of NK-T cells during HBV-infection (Vilarinho *et al.* 2007, Chen *et al.* 2007). Intrahepatic NK and NK-T cells are possibly activated by the cell surface of stress signals on infected hepatocytes (Trobonjaca *et al.* 2001) or by direct recognition of viral components (Baron *et al.* 2002).

1.3.3 Priming Adaptive Immunity

Before a T cell can function as a $CD8^+$ CTL or as $CD4^+$ helper cell, it must be activated for a special antigen. For this to happen, a naïve T cell must recognize at least two signals, its cognate antigen presented by a major histocompatibility complex (MHC) and a co-stimulus (B7). Cells that capture and display antigens in an appropriate fashion to lymphocytes are called antigen-presenting cells (APC). Presently, four different populations of APC are known, and each of them plays a different role in T cell responses: (i) dendritic cells; (ii) activated macrophages; (iii) B cells and (iv) LSEC, recently discovered as APC. As a dogma, initial priming of adaptive immunity occurs exclusively in **secondary lymphatic organs**, i.e. draining lymph nodes. However, it is still a focus of intensive research whether the liver can also prime lymphocytes under inflammatory conditions.

1.3.3.1. Dendritic Cells (DC)

DC are regarded as the most potent APC for initiating T cell responses. They are distributed all over the body and function as “sentinels”. During macropinocytosis of extracellular fluid, they capture microbial proteins and transport the antigen to the draining lymph nodes. In a resting state, DC are poor APC because they express low levels of MHC and B7 molecules. However, after receiving a “danger signal” the expression profile of DC changes. During their migration to the lymph nodes, DC mature and become extremely efficient at presenting antigens and stimulating naïve T cells. By the time they reach the lymph node, high levels of B7, MHC-I, and MHC-II molecules are displayed at their cell surface. Note, activated DC live for only a few days; this insures that the represented antigens are up-to-date. The magnitude of induced T cell responses is proportional to DC activation.

At present, there is controversial debate over whether hepatic DC might induce tolerance during HBV-infection rather than stimulating immune defenses. For instance it has been shown that hepatic DC have a reduced capacity to induce a vigorous T cell response. This supports the theory that the incomplete DC activity might forward viral-infections (Lau & Thomson 2003, De Creus *et al.* 2005).

1.3.3.2. Macrophages

Macrophages are tissue-resting cells; they do not travel to the lymph node. However, they are also “sentinels”, and they become activated upon recognition of “danger signals”. The functions of macrophages in antigen presentation are mainly restricted to re-stimulation of activated T cells at the place of defense. However, the function of Kupffer cells in viral antigen presentation seems to be negligible, since they do not produce MHC-I molecules (Limmer *et al.* 2000).

1.3.3.3. B Cells

B cells are highly efficient at presenting exogenous proteins that have specifically bound to their membrane surface immunoglobulin (BCR, see next chapter). The captured antigens are internalized through BCR-mediation; diverse peptide-fragments of the processed antigen are efficiently displayed on MHC-II complexes. By note, the surface immunoglobulin of B cells has an incredible **magnet function** because BRC-mediated presentation of specific antigen is 100 to 10,000 fold more efficient than the presentation by other APC. This is most prominent when relatively low concentrations of antigen are present (Lanzavecchia 1987, 1990, Pape *et al.* 2007). In addition, the presentation of antigens by B cells is extremely fast; less than half an hour elapses between BCR-capturing and MHC-presentation (Milich *et al.* 1997a, Cheng *et al.* 1999). However, the contribution of B cells for **priming CD4** T cells still remains controversial because the required co-stimulatory molecules to activate naïve T cells are mostly not present on B cells. But in the recent years, numerous studies provided convincing evidence that B cells can activate naïve T cells *in vivo* (Milich *et al.* 1997a, Ron & Sprent 1987, Kurt-Jones *et al.* 1988, Constant 1999, Rodrigues *et al.* 2005, Crawford *et al.* 2006).

The second experimental part of this PhD thesis provides strong indications that antigen-presentation by B cells has an important function during HBV infection to trigger effective humoral and cytotoxic immune responses. Of special interest in this

regard is one intriguing study by Milich (1987) showing that HBV nucleocapsids are captured, processed and presented by B cells. These B cells become activated and express co-stimulatory B7 molecules on their surfaces and are able to prime naïve T cells.

1.3.3.4. Liver Sinusoidal Endothelial Cells (LSEC)

LSEC display a prominent antigen-presenting capacity in priming CD4+ and CD8+ T cells (Knolle & Gerken 2000). However, antigen-presentation by LSEC induces a state of anergy rather than T cell activation (Knolle *et al.* 1999, Limmer *et al.* 2000). The induction of tolerance of hepatic T cells might be important for oral antigens and points out the immune privileged role of the liver. At present, it is still a focus of extensive research whether LSEC diminish or possibly promote T cell responses against HBV.

1.3.3.5. Cross-Presentation

Professional APC are specialized to present exogenous peptides on MHC-II and endogenous peptides on MHC-I molecules to stimulate antigen-specific CD4+ and CD8+ T cell responses. However, exogenous antigens can also be shuttled to the class I MHC presentation pathway; this process is termed “cross-presentation”. Over a long period of time it has been assumed that this process is restricted to **DC**. However, in the last few years an increasing number of evidence demonstrated that **B cells** also participate in cross-presentation (Ke & Kapp 1996, Lazdina *et al.* 2003, Heit *et al.* 2004, Tobian *et al.* 2005). These findings opened a new area of CD8+ T cell priming and it might be especially important in situations when low antigen is present or low numbers of DC bear the respective antigen (Hon *et al.* 2005). In keeping with this, combined with the finding that T cell priming by hepatic DC is partially insufficient, cross-presentation by B cells might play in important role in inducing HBV-specific T cell responses (see discussion part II of this PhD thesis). A recent report indicated that B cells could elicit CD8+ cells priming by cross-presentation (Lazdina *et al.* 2003).

1.3.4 Cell-Mediated Immunity

Different cell populations are involved in the cell-mediated immunity. The effector phase of the adaptive immunity is controlled by T lymphocytes.

1.3.4.1. Antigen Recognition by T Lymphocytes

T lymphocytes recognize their cognate antigen processed on MHC molecules. Of note, T cells recognize **only a small peptide fragment** of a processed antigen; they are not able to identify tightly folded proteins like B cells do. However, T cells are able to recognize targets of exogenous antigens that are hidden in the tridimensional structure from the view of the BCR. One interesting example for this phenomenon might be HBV capsids captured and processed by B cells (as described in 1.3.3.5 and 1.3.5.4). Such “capsid-capturing” by B cells generates multiple B cell clones presenting different peptides from the capsid on MHC molecules. These epitopes elicit a T-cell dependent immunity against the viral surface proteins and especially the L-protein (Milich *et al.* 1997a). Note that the L protein is mostly present on the virions and only in small amounts on SVP that are found in excess in serum.

1.3.4.2. T Cell Receptor (TCR) and Co-Receptor

The receptor complex by which T cells recognize antigenic determinants on MHC is composed of different structural elements: the extracellular, extreme variable “**antigen-recognition-part**” is generated by **somatic recombination** of gene segments. It consists of two protein chains (αβ or γδ). Four different protein chains comprise the intracellular constant signaling portion, defined as the CD3 complex. In addition to the TCR, a co-receptor, which is either CD4 or CD8, is required to trigger MHC-restricted T cell activation. The co-receptor interacts with the constant region of the MHC molecule: CD4 binds specifically to MHC class II whereas CD8 binds specifically to MHC class I. Since each T cell expresses either CD4 or CD8, this surface molecule is used to classify T lymphocytes due to their functions. MHC class I molecules are expressed on almost all somatic cells; they represent processed antigens of mostly endogenous origin. By contrast, MHC class II molecules are only expressed on APC representing processed antigens of exogenous origin.

1.3.4.3. $CD4^+$ T cells

The **main function** of activated $CD4^+$ T helper cells (Th) is to modulate the activity of other immune cells in the **local** surroundings by the **release of diverse cytokines**.

One part of Th cells stays in the lymphatic circulation, which provides help for B and T cells; the other part migrates to the focus of invasion and provides help for macrophages and NK cells. Depending on the mixture of the released cytokines, two different Th responses are defined because no phenotypic marker exists that reflects the activation status of Th cells.

Th1-response is mediated mainly by IFN-γ and TNF-α. This cytokine milieu induces a strong cellular immune response that is mostly associated with tissue inflammation. IFN-γ and TNF-α increase the phagocytic activities and degradative reactions of macrophages, strengthen NK reactions and favor IgG3 class switching of B cell to trigger antibody-dependent cell-mediated cytotoxicity (ADCC) reactions. It also helps in the generation of CTL.

Th2-response consists mainly of IL-4, IL-5, IL-6 and IL-10. This immune response is less destructive for tissues because it inhibits degradative reactions of macrophages and down-regulates CTL responses. In the lymph node, the Th2 cytokine profile triggers the isotype switching of B cells towards IgA, IgE, IgG1.

Numerous studies of HBV-infected individuals revealed that a Th1 cytokine profile is the basis for recovery from HBV (Ferrari *et al.* 1990, Penna *et al.* 1997, Rehermann *et al.* 1995, Webster *et al.* 2004). Furthermore, it has been shown that HBcAg and HBeAg elicit different Th subsets. HBeAg down-regulates antiviral clearance mechanisms and favors an anti-inflammatory Th2-response (Milich *et al.* 1997b).

1.3.4.4. $CD8^+$ T cells

Following activation of naïve $CD8^+$ T cells by specific antigen in secondary lymph organs, the CD8 T cells differentiate into cytotoxic T lymphocytes (CTL), which are ready to kill the infected target cells that represent the cognate antigen on MHC-I. In general, CTL are able to lyse target cells by two mechanistically distinct but functionally similar mechanisms: one is the secretory membranolytic pathway via perforin and granzyme, and the other is the receptor-mediated pathway via CD95 (Lowin *et al.* 1994).

The CD8 T cells are regarded as the main effector cells responsible for clearing acute HBV infections mediated by cytolytic and noncytolytic effector functions (Thimme *et al.* 2003). The second section of this PhD thesis addresses the question of which cytolytic pathway is most relevant in clearing acute HBV.

1.3.5 Humoral Immunity

Humoral immunity is mediated by secreted antibodies (Ab). They are produced by mature B lymphocytes and plasma cells in the lymphoid node. However, Ab perform their physiologic function at distant sites in the body. The effector functions of Ab are neutralization of extracellular microbes and microbial products and elimination of infected cells by ADCC.

1.3.5.1. B Cell Receptor (BCR) and Antigen Recognition

The BCR is a membrane bound immunoglobulin (Ig) that consists of two parts: (i) the cell surface region defines the “antigen-specific recognition zone”; two heavy and two light protein chains make up the antibody molecule. (ii) The constant region consists of intracellular signaling molecules called Igα and Igβ that convert the received information upon receptor engagement. The extremely high variability of the recognition part is generated by **gene rearrangement**, that is, the random assembly of genes into unique segments. It is important to note that each B cell produces only one kind of BCR, which recognizes one specific antigen. The BCR recognizes **conformational determinants** of proteins **(tertiary folded),** but also of lipids, polysaccharides and nucleic acids. Therefore, the BCR identifies antigens in their “natural” state in contradiction to TCR as described above.

1.3.5.2. Activation of B cells and Antibody Production

The Ab production is a multi-step process initiated by recognition of antigens through the BCR. To activate naïve B cells, at least two stimuli are required: first, the receptor engagement by a specific antigen (cross-linking) and second, a co-stimulus. This is usually provided by a helper T cell through direct cell-cell contact (CD40-CD40L). By contrast, the T-cell-independent B cell stimulation needs no co-stimulus, however a high IFN-γ concentration might be conductive (Snapper *et al.* 1992, Mond *et al.* 1995, Su & David 1999, Maloy *et al.* 1998). A secondary activation of already primed B cells requires only the cognate antigen.

Following antigenic stimulation of naïve B cells, gene expression changes. Activated B cells display antigens in association with MHC-II (see 1.3.3.3) and additionally they express different cell surface molecules. Furthermore, activated B cells start to proliferate by clonal expansion, building up a large cell population with the same receptor specificities. Upon initial activation, B cells differentiate along two distinct

pathways. One part of the cells become extrafollicular plasma cells and produces rapidly neutralizing IgM antibodies. The other part enters the germinal center of the lymph node to differentiate into plasma and memory cells by the help of T helper cells. In order to produce **high-affinity antibodies**, B cells run through different maturation processes involving (i) **class switching**, (ii) **somatic hypermutation** and (iii) affinity maturation.

1.3.5.3. Isotype-Switching

Class switching is restricted to the **constant (Fc)** region of the BCR and determines the antibody class (isotype). This region defines how the AB will function. Somatic hypermutation and affinity maturation is restricted to the Fab-region and strengthens its affinity to a specific antigen by changing single amino acids. Note, the maturation steps are influenced by cytokines and require continuous re-stimulation of the cognate antigen. A cytokine milieu dominated by **IFN-γ** influences the isotype switching to IgG2a and IgG3 and thereby enforces the cell-mediated immunity denoted as the **Th1-response**. Since IgG3 forms a bridge between infected target cells (Fab-region) and NK cells (Fc-region), the killing of NK cells becomes more effective, a process called ADCC. An **IL-4 and IL-10** dominated cytokine milieu (**Th2-response**) favors the production of IgG1 molecules that opsonize invaders for ingestion by macrophages.

1.3.5.4. T Cell-Independent Activation of B Cells by HBcAg

The highly immunogenic nucleocapsid of HBV (HBcAg) can elicit T cell-dependent and T cell-independent antigen production in humans and mice (Milich *et al.* 1998, Cao *et al.* 2001). The molecular foundation for the T cell-independent B cell activation is based on structural properties of the capsid as well as of the BCR: protruding protein spikes at the cell surface of the capsid, build up the basis for this unusual B cell activation (Conway *et al.* 1998). These spikes bind with high frequency to a linear motif at the BCR that is located at the junction of heavy and light chain present in a large proportion of naïve B cells (Lazdina *et al.* 2001).

1.4. Apoptosis

In a biological system two types of cell death are distinguishable due to their physiological, biochemical and morphological features. **Apoptosis** is the physiologically induced cell death, tightly controlled from initiation to disposal. It is indispensable for development, homeostasis and defense reactions. Apoptosis is genetically encoded, initiated and counteracted by multiple mechanisms as described below. By contrast, **necrosis** represents the accidental collapse of cells by physical injury.

The immune system responds to both kinds of cell death in fundamentally different manners. Necrosis is characterized by the loss of cell membrane integrity. Thus, intracellular contents diffuse into the extracellular space and trigger an inflammatory immune response because these components are "**danger-signals**" for macrophages and monocytes (Matzinger 2002). By contrast, apoptosis is an intracellular enzymatic self-destructing process with intact membrane structures. Morphologically, apoptosis is defined by cytoplasmatic shrinkage (pyknosis), detachment, plasma membrane blebbing, DNA fragmentation and condensation. In most cases, the apoptotic cells collapse into numerous apoptotic bodies. Since apoptotic cells expose phosphatidylserine on the outer plasma membrane, they are rapidly engulfed by macrophages without danger signaling (Taylor *et al.* 2008, Voll *et al.* 1997).

1.4.1.1. Initiation of Apoptosis

The intracellular apoptotic signaling pathways can be divided into two parts. The first part is restricted to initiation of apoptotic signaling cascades by activating the **initiator caspases** 8, 2, or 10. During this phase, apoptosis can be blocked, modified or abrogated by diverse anti-apoptotic signaling pathways, such as stabilization of NFκB or rapid induction of heat shock proteins (Beere 2005). The second phase of apoptosis comprises the execution process. Once the **execution caspases** 3, 6, 7 become active, the point of no return is reached, which leads to irreversible self-destruction of the cell by cellular enzymes (Thornberry 1998).

Caspases are aspartate-specific cysteine proteases that are present in the cytoplasm of all cells in inactive forms (zymogene).

Three main routes lead to the activation of caspases (Fig.6): (i) **perforin and granzyme** release onto the cell surface; (ii) **death-receptor stimulation** including CD95R, TNFR and TRAIL; (iii) **mitochondria** outer membrane permeabilisation (**MOMP**).

Perforin/granzyme release and death-receptor stimulation are both defined as the extrinsic apoptosis pathways induced by cells of the immune system. MOMP is also called an intrinsic apoptosis pathway triggered by intracellular stress and loss of survival signals like growth factors, co-stimulatory molecules, or receptors. The extrinsic and intrinsic apoptosis pathways converge both on caspase-3.

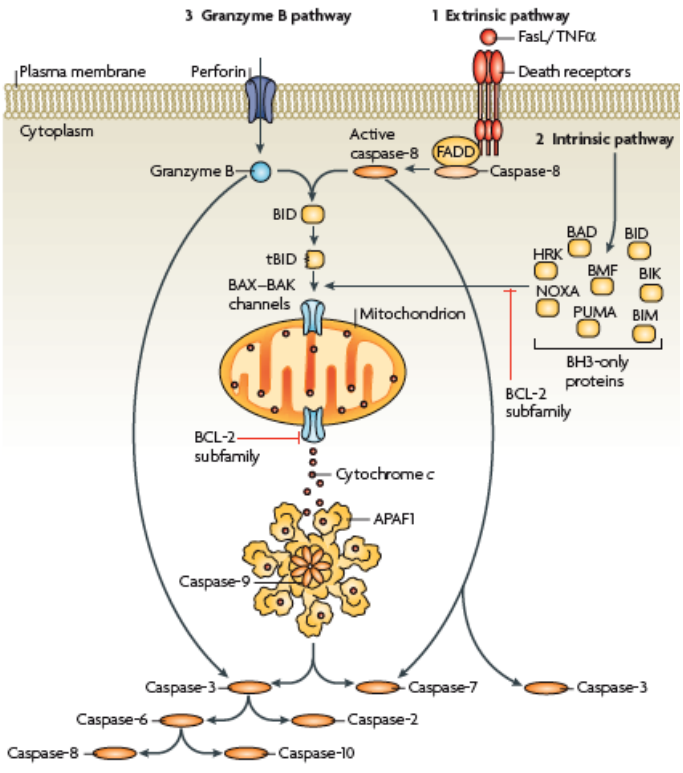

Figure 6 Three main routes of apoptosis-induction: 1. Death Receptor 2. MOMP via Bcl-2 proteins 3. Perforin/Granzyme

Taylor *et al.*
Nature Reviews,
Molecular Cell Biology 2008

1.4.1.2. Characteristic Features of Hepatocytes

Hepatocytes show an exquisite sensitivity to CD95-mediated apoptosis (Ogasawara *et al.* 1993). However, the extrinsic apoptotic stimulus must be amplified in hepatocytes by the intrinsic MOMP pathway *via* cleavage of Bid (Scaffidi *et al.* 1998, Peter & Krammer 2003). This kind of CD95-signaling is unique to hepatocytes; therefore, **hepatocytes** are defined as **type II** cells to emphasize their "special" death-receptor signaling pathway. All other cells in the body, except tumor cells, are

typ I cells by which Caspase-8 activation by death-receptor stimulation directly leads to caspase-3 activation. The importance of MOMP-amplified apoptosis in hepatocytes is evident in overexpression of the anti-apoptotic proteins Bcl-2 and Bcl-xL that prevent MOMP (Scaffidi *et al.* 1998, Terradillos *et al.* 2002).

1.4.1.3. Extrinsic Pathway

Extrinsic stimuli of apoptosis are mostly mediated by release of perforin/granzyme or CD95-receptor stimulation. Both pathways are involved in **killing infected cells** as well as in **regulating the size of lymphocytes** at many stages of maturation and after activation (Matloubian *et al.* 1999, Rathmell *et al.* 1995). However, it remains a mystery under which conditions lymphocytes kill their target cells, either by CD95 or by perforin/granzyme (Nakamoto *et al.* 1997). It is also assumed that both pathways cooperate with each other because the ligand of CD95 is also stored in lytic granules of murine CTL and NK cells (Kojima *et al.* 2002).

Nonetheless, a requisite of both apoptotic pathways is a stable binding between effector and appropriate target cell by engagement of TCR and co-receptors, which results in the formation of an immunologic synapse.

1.4.1.3.1 Perforin and Granzyme

Perforin and granzyme are stored in cytoplasmic granules of CTL. Both components become activated upon release into a Ca^{2+}-rich surrounding, like the extracellular space. **Perforin** is a 65 kDa monomeric protein that rapidly self-assembles into a polymeric pore forming structure inserted into the target cell membrane. Thereby, the cell membrane loses its integrity and becomes permeable to water, ions and proteins. Granzymes are serine proteases that share substrate specificity with caspases for cleavage after aspartate residues (Poe *et al.* 1991). **Granzyme B** directly activates Caspase-3 (Yang *et al.* 1998). However, Granzyme B also signals through the mitochondrial amplification-loop by activating Bax and Bak (MacDonald *et al.* 1999, Metkar *et al.* 2003).

1.4.1.3.2 Death Receptor Signaling

CD95 (synonym: FasR or Apo1) is the prototype of the death receptors belonging to the tumor necrosis factor receptor **(TNFR) superfamily**. More than 20 members of this superfamily have been identified. However, only a few members of the TNFR superfamily are death receptors like CD95 and to a minor extent TNFR and TRAIL

(*TNF related apoptosis inducing ligand*) (Fig.7). TNFR are all homotrimers, defined by similar cysteine-rich extracellular domains. The “death-receptors” of this family also contain a homologous **cytoplasmatic “death domain” (DD)**. The ligands that activate these receptors are structurally related molecules belonging to the TNF family (Ashkenazi & Dixit 1998). Most of these ligands are membrane-associated molecules like the Fas ligand (FasL syn. CD95L).

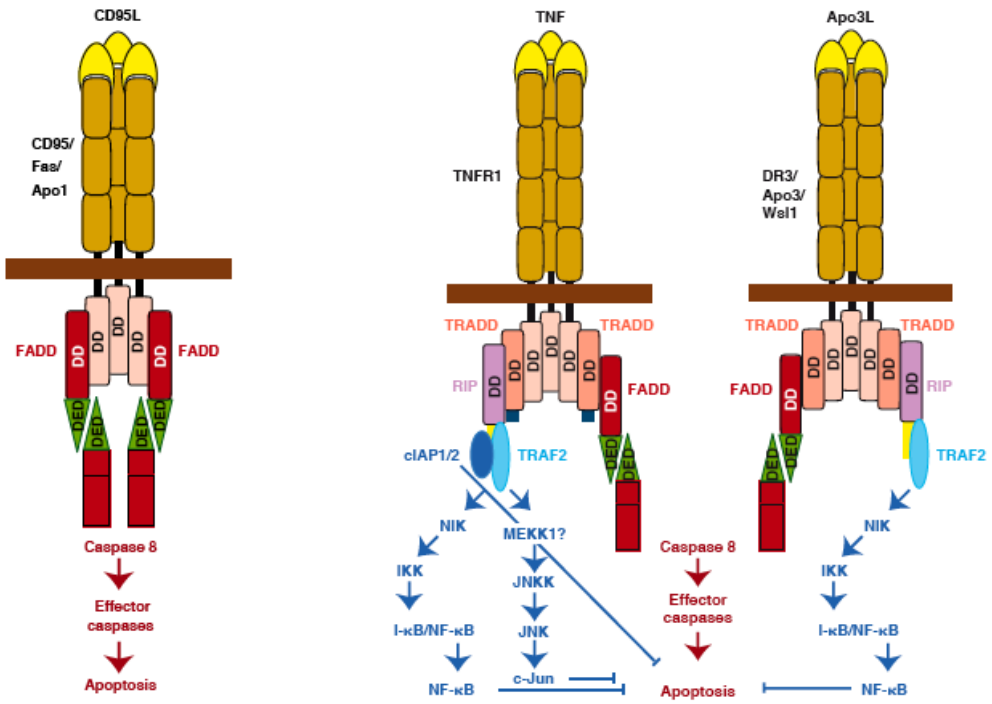

Figure 7 Death Receptors of TNF superfamily
Ashkenzi & Dixit. Science, 1998

Ligation of CD95R with CD95L or with agonistic antibodies (*anti*-Apo1 or Jo2) triggers trimerization, clustering of cytoplasmic DD and recruitment of dual adaptor molecules called **FADD** (Fas-associated death domain). The FADD molecules consist of N-terminal DD that binds to the CD95R and of a N-terminal “death effector domain” (DED) that allows the recruitment and activation of **procaspase-8** (also known as FLICE). The complex consisting of FasL-FasR-FADD is called the “death-inducing signaling complex” (DISC), and is able to recruit huge amounts of procaspase-8 (Muzio *et al.* 1998).

Similarly, trimerized TNFR1 or TRAIL (Apo3) recruits corresponding adaptor molecules called TRADD (TNFR-associated death domain), which in turn recruit

FADD and procaspase-8 to trigger the apoptotic signaling pathway. However, TNFR1 and TRAIL additionally activate **anti-apoptotic** signaling cascades by recruiting the receptor-interacting protein (RIP). RIP in turn stimulates the NFκB and JNK/AP-1 survival pathways (Micheau & Tschopp 2003). Although TNFR1 and TRAIL are constitutively expressed in hepatocytes, they usually do not trigger apoptosis. However, under pathological circumstances, hepatocytes might become sensible to TNFα or TRAIL induced apoptosis (Varfolomeev *et al.* 2007,Dunn *et al.* 2007, Liang *et al.* 2007).

1.4.1.4. Intrinsic Pathway

The intrinsic pathway is also called the mitochondrial-induced pathway. The “point of no return” for apoptosis-induction is the outer mitochondria membrane permeabilization controlled by pro- and anti-apoptotic proteins of the Bcl-2 family.

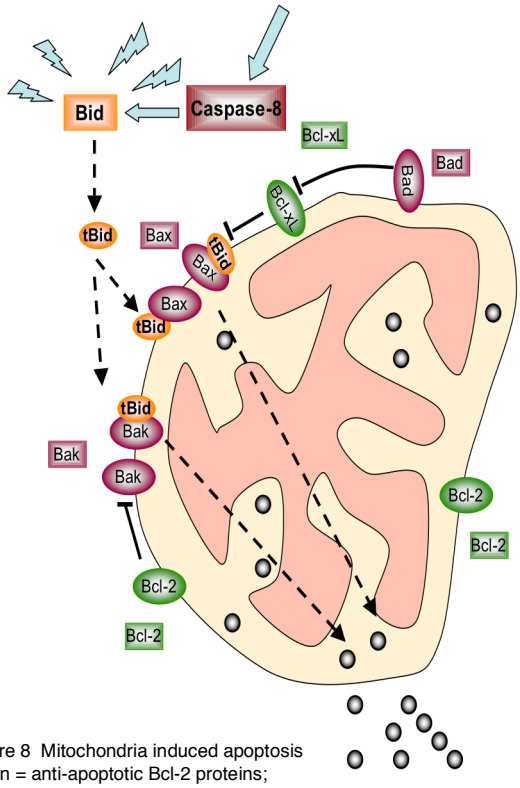

Figure 8 Mitochondria induced apoptosis
green = anti-apoptotic Bcl-2 proteins;
red = pro-apoptotic Bcl-2 proteins;
grey = proteins in mitochondrial intermembrane space;
rectangular shape = cytoplasmatic localization;
round shape = mitochondrial outer membrane localization

The initiator of this pathway is the cleavage of Bid that leads to the catalytically active form called truncated **tBid**. The activation of tBid can be triggered by external stimuli like the CD95R-activated Caspase-8 as well as numerable internal stress stimuli like UV-C irradiation. Upon activation, tBid interacts with cytosolic **Bax** and **Bak** and induces the mitochondrial membrane insertion of both proteins. Thereby, the membrane loses its integrity and becomes permeable for proteins that reside in the intermembrane space, e.g. cytochrome c, apoptosis inducing factor (AIF), Smac and Diablo (Joza *et al.* 2001).

In the cytoplasm, cytochrome c interacts with the apoptotic peptidase activating factor 1 (Apaf-1) and dATP generating the **apoptosome**, a immense structural complex, that in turn activates caspase-3 (Li *et al.* 1997, Zou *et al.* 1997). An additional consequence of MOMP is the loss of the inner transmembrane potential

between the intermembrane space and the mitochondrial lumen that is necessary to generate ATP (Crompton 2000). Pro-apoptotic proteins like **Bcl-2** or **Bcl-xL** prevent the catalytic activity of tBid and thereby block MOMP (Lovell *et al.* 2008). However, pro-apoptotic proteins like **Bad** also counteract these proteins.

1.4.2 Interference of HBx with Apoptotic Cell Signaling Pathways

Many enigmatic functions have been ascribed to the viral HBx protein (reviewed in (Tang *et al.* 2006, Bouchard & Schneider 2004). One prominent functions is its regulator activity influencing pro- and anti-apoptotic signaling pathways during HBV infection. Since the first experimental part of this thesis is based on the still disputed question of whether or not HBV induces apoptosis of its host cell, the following paragraph summarizes the literature that considers HBx to be either a **promoter** or an **inhibitor** of apoptotic cell death during HBV infection.

Conclusions about the potential apoptotic functions of HBV have mostly been obtained from cell culture experiments in which the HBx protein was **highly overexpressed**. It has been shown in transient transfections that HBx sensitizes liver cells to apoptosis in a dose-dependent manner (Pollicino *et al.* 1998, Terradillos *et al.* 1998, Miao *et al.* 2006, Kim & Seong 2003, Shirakata & Koike 2003). Moreover, stably transformed cell lines with inducible HBx expression exhibited an increased sensitivity to apoptotic treatments when the expression was turned on (Kim *et al.* 1998, Shintani *et al.* 1999).

Therefore, it has been discussed intensely that **HBx might have opposing functions on cell viability**: on the one hand, HBx might boost viral replication early after hepatocyte infection, and on the other hand, HBx might **sensitize host cells to apoptosis** in later stages which might lead to **efficient HBV particle release** (Kim *et al.* 1998, Pollicino *et al.* 1998, Terradillos *et al.* 1998, Shintani *et al.* 1999, Kim *et al.* 2005, Miao *et al.* 2006).

However, **these assumptions have not yet been proven due to the lack of a suitable experimental** setting. Furthermore, the mechanisms through which HBx might modulate the apoptotic turnover are still disputed and results previously presented are contradictory. It has been reported that HBx induces apoptosis both in a p53-dependent (Chirillo *et al.* 1997, Wang *et al.* 2008) and p53-independent

manner (Terradillos *et al.* 1998, Shintani *et al.* 1999), or by harming the integrity of mitochondrial membranes (Miao *et al.* 2006, Terradillos *et al.* 2002). However, a possible **pro-apoptotic effect of HBx** during **natural infection** has **not** to be **documented**.

Only one publication has mentioned a potentially apoptotic function of HBx during viral replication by sensitizing Chang liver cells transformed with woodchuck hepatitis B virus to TNF-α-induced apoptosis (Su & Schneider 1997). A successive publication from the same research group described impressively that a special set of conditions might be required for triggering apoptosis by HBx (Su *et al.* 2001) comparable to the multistep process of tumorigenesis from cellular oncogenes. Su *et al.* (2000) indicated that either ablation of NFκB signaling or a strong elevation of *myc* gene expression plus exposure of hepatocytes to TNF-α are necessary to induce apoptosis. Thus, it has been suggested that apoptosis of infected hepatocytes increases the release of hepatocyte growth factors, enhances the generation in liver tissue and raises the level of uninfected hepatocytes for new infection.

In contradiction to the proposed pro-apoptotic functions of HBx, diverse publications described anti-apoptotic functions of HBx. It has been shown that HBx abrogates p53-induced apoptosis (Elmore *et al.* 1997, Wang *et al.* 1995, Huo *et al.* 2001). Further studies demonstrated that HBx inhibits the activity of Caspase-3 (Gottlob *et al.* 1998, Lee *et al.* 2001, Marusawa *et al.* 2003) and prevents CD95- and TGF-β-mediated apoptosis (Diao *et al.* 2001, Pan *et al.* 2001, Shih *et al.* 2000). Although the precise mechanism by which HBx interferes with pro-apoptotic signaling is still unknown, most researchers provided concurrent evidence that HBx modulates the phosphatidylinositol-3-kinase survival-signaling cascade. The presented opposing pro-survival and pro-apoptotic effects of HBx might explain the tumorgenic potential of HBV. Thus, HBx might exert a selective pressure on hepatocyte growth, promoting the emergence of mutations, which might lead to the development of HCC 40-50 years after viral infection.

Beside HBV, pro-apoptotic functions have also been described for numerous other viruses that cause persistent infections including HIV, HTLV-1 or HPV (Desaintes *et al.* 1997, Westendorp *et al.* 1995, Yamada *et al.* 1994). However, the physiological relevance of apoptosis-induction has not yet been analyzed for any persistent virus.

Therefore, the first results section of this PhD thesis elucidates the biological significance of apoptosis for HBV spreading. Furthermore, we analyze whether or not HBx sensitizes host cells toward apoptosis when HBx is expressed under “natural” conditions during HBV replication.

2 Experimental Part I

Does HBV replication sensitize host cells towards apoptosis to enhance the spread of progeny through liver tissue?

In previous studies we have shown that neither infection nor replication of HBV induces spontaneous apoptosis of primary human hepatocytes (PHH) (Schulze-Bergkamen *et al.* 2003). Therefore, we assumed that survival of the host cell is crucial for HBV propagation. However, contradictory data reported that HBV infection sensitizes host cells towards apoptosis (see introduction “Interference of HBx with apoptotic cell signaling pathways). Most of these data are attributed to the over-expression of the viral HBx protein. Since the potential role of HBx in inducing apoptosis of the host cell is a seeming contest for its established function in viral replication, a number of groups argued that apoptosis might facilitate HBV particle release and enhances the spread of progeny in the host (Kim *et al.* 2005, Shintani *et al.* 1999, Terradillos *et al.* 1998, Pollicino *et al.* 1998, Kim *et al.* 1998, Miao *et al.* 2006). Although this assumption remains attractive, especially at the onset of an acute HBV infection, no direct experimental evidence has yet to be shown due to the lack of a suitable experimental setting.

1. To address this important issue, we designed a cell culture model, which allows us to substantiate the physiological relevance of apoptosis for HBV proliferation. Thus, we determined quality, quantity, and infectivity of HBV particles released from apoptotic liver cells using HBV-producing hepatoma cell lines, as well as HBV infected PHH.

2. Moreover, we took the advantage of HBV-producing cell lines to analyze the influence of the viral HBx protein in sensitizing host cells towards apoptosis during viral replication.

3. Additionally, we compared the gene expression profiles of different HBV-replicating hepatoma cells (expressing and non-expressing HBx) with the corresponding parental cell line to analyze whether HBV-replication modulates the cellular transcriptome. In detail, we focused on genes encoding for proteins involved in pro- and anti-apoptotic cellular signaling pathways.

2.1.1.1. HBV-transformed Hepatoma Cell Lines

Since we used different kinds of stably HBV-transformed hepatoma cell lines as tools to analyze the virus-host interactions, the following section shortly introduce the cell lines and emphasizes their cell culture conditions necessary for HBV virion secretion.

HepG2.2.15 cell line has been generated by stable transfection of HepG2 cells with HBV genome dimers (Acs *et al.* 1987). Due to the long-term culture for more than two decades, the cellular transcriptome of HepG2.2.15 and HepG2 cells might be substantially different. In order to have an alternative, we previously generated two further HBV-producing cell lines, which we compared with each other. On the one hand, we generated a second wild type (wt) HBV-producing cell line by transforming the 1.3 over-length genome of HBV into HepG2 cells. This cell line was named HepG2-H1.3 and was produced by Felix Bohne in 2003 (Protzer *et al.* 2007). On the other hand, we have generated a series of corresponding ΔxHBV producing cell lines from which we selected clone HepG2-H1.3x- (K6). These cells replicate and produce HBV virions in absence of viral HBx protein. The translation of HBx has been blocked by a premature stop codon at the 5´ end in both copies of x open reading frame (diploma thesis Silke Arzberger, 2005).

Although the HBV genome is stably integrated, the level of viral replication and virion secretion strongly depends on cellular differentiation (Quasdorff *et al.* 2008). Serial passaging of HBV-transformed cells impedes HBV-replication. Therefore, HBV particles could not be detected in cell culture medium of growing cells using sedimentation through cesium chloride (CsCl) gradients and subsequent HBV-DNA dot blot analysis (Fig.1a I). In contrast, when HepG2.2.15 and HepG2-H1.3 cells were grown to confluence and henceforward were cultured under conditions supporting cell differentiation, HBV virions were detected in culture medium (Fig.1a II). If HepG2-H1.3 cells were maintained several weeks in culture without passaging, the release of HBV virions increased (Fig.1b).

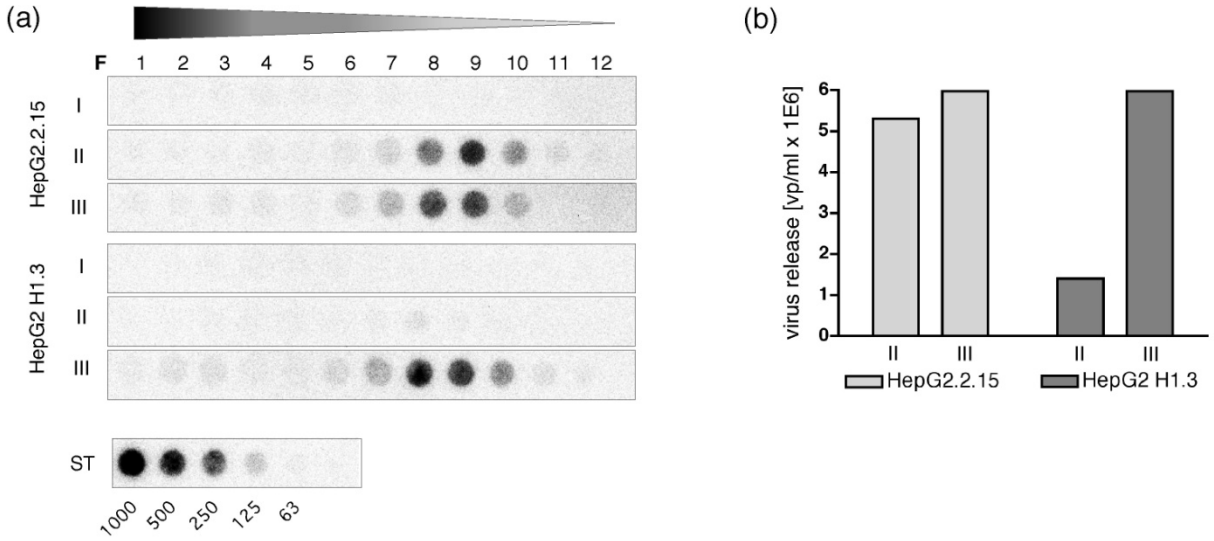

Figure 1 Cell culture conditions boosting HBV replication in HBV transformed HepG2 cell lines.
(a) HBV-DNA dot blot analysis of cell culture medium of HBV replicating cell lines separated by CsCl gradient centrifugation. ^{32}P-labeled DNA probe was prepared by random priming of HBV-DNA fragment. Mature, enveloped HBV virions are detected in fractions F7-F11. Cone illustrates density gradient. Upon 2d culturing, media were collected from cells maintained under following conditions: (I) three weeks in conventional medium supporting cell division; (II) one week in differential medium reducing cell division and boosting HBV replication; (III) cells sustained three weeks in differential medium **(b)** Densitometric quantification of HBV-DNA dot blot analysis of fractions F7-12. Plasmid DNA encoding HBV genome was used as standard (ST).

The culture conditions of HBV-transformed hepatoma cell lines strongly influences HBV replication. In order to use stably HBV-transformed hepatoma cell lines as a model system to mimic HBV-infection in vitro and to analyze virus-host interactions, the level of HBV-replication must be regarded. In the following experiments, we used differentiated HBV-replicating cell lines producing at least 5x10^6 virions per ml culture medium.

2.2. Results

2.2.1 Sensitivity of HBV-replicating hepatoma cells towards apoptosis

To investigate whether HBV replication sensitizes cells towards apoptosis, we compared the sensitivity of HBV-replicating HepG2.2.15 cells with parental HepG2 cells upon apoptosis induction using UV-C irradiation. Cell viabilities were quantified before and 24 h after UV-C exposure, respectively, by determining changes in cell metabolism via XTT measurement and visualizing dead cells using fluorescence microscopy.

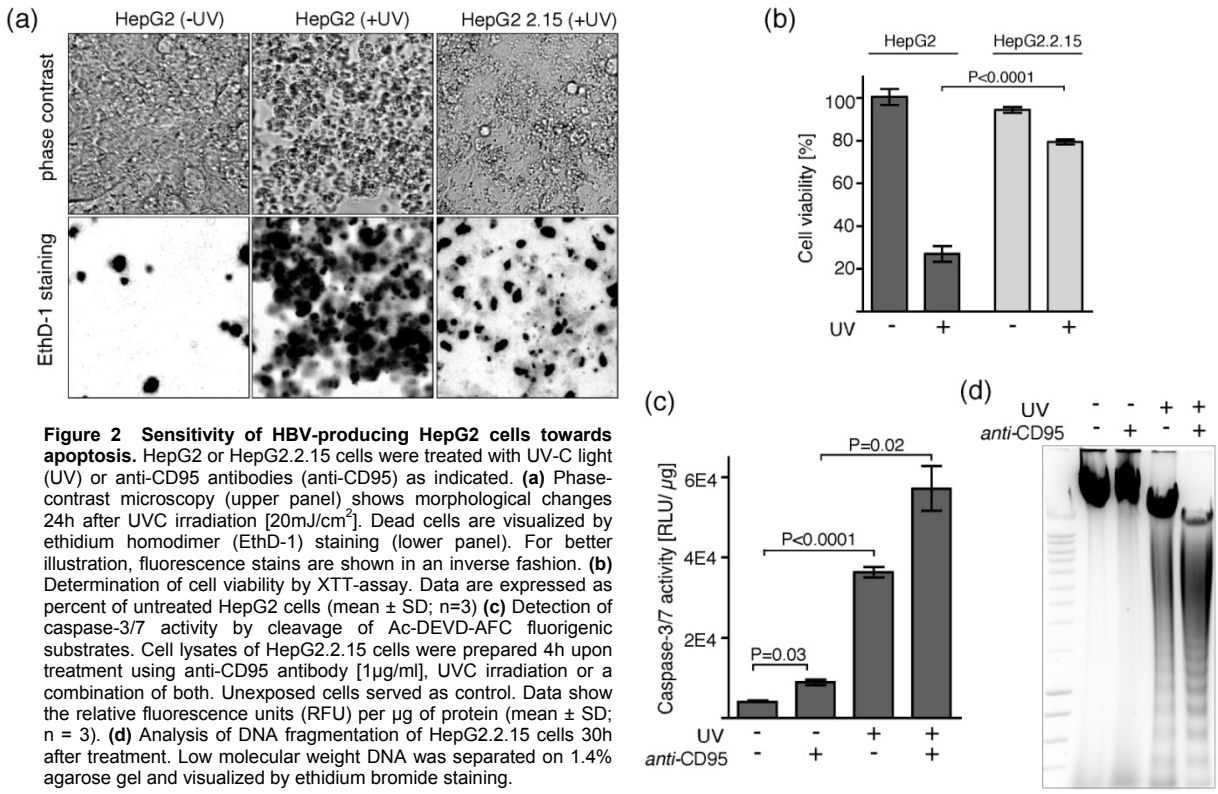

Figure 2 Sensitivity of HBV-producing HepG2 cells towards apoptosis. HepG2 or HepG2.2.15 cells were treated with UV-C light (UV) or anti-CD95 antibodies (anti-CD95) as indicated. **(a)** Phase-contrast microscopy (upper panel) shows morphological changes 24h after UVC irradiation [20mJ/cm^2]. Dead cells are visualized by ethidium homodimer (EthD-1) staining (lower panel). For better illustration, fluorescence stains are shown in an inverse fashion. **(b)** Determination of cell viability by XTT-assay. Data are expressed as percent of untreated HepG2 cells (mean ± SD; n=3) **(c)** Detection of caspase-3/7 activity by cleavage of Ac-DEVD-AFC fluorigenic substrates. Cell lysates of HepG2.2.15 cells were prepared 4h upon treatment using anti-CD95 antibody [1µg/ml], UVC irradiation or a combination of both. Unexposed cells served as control. Data show the relative fluorescence units (RFU) per µg of protein (mean ± SD; n = 3). **(d)** Analysis of DNA fragmentation of HepG2.2.15 cells 30h after treatment. Low molecular weight DNA was separated on 1.4% agarose gel and visualized by ethidium bromide staining.

We found that HBV-replicating HepG2.2.15 cells were significantly (P<0.0001) more resistant towards UV-C irradiation than HepG2 cells (Fig.2a+b). Almost 80% of HepG2.2.15 cells but only 25% HepG2 cells were viable 24 h after UV-C irradiation (Fig.2b). However, in both cell types, we observed a change in cell morphology: HepG2 cells rounded up, typical for apoptotic cell death, whereas HepG2.2.15 cells were retained in a confluent cell layer, but exhibited an increased granule content in the cytoplasm (Fig.2a). In contrast, undifferentiated HepG2.2.15 establishing HBV replication at low levels were as sensible to UV-C irradiation as HepG2 cells (data not shown).

To confirm apoptosis induction, we measured activation of the execution caspases-3 and -7 and analyzed the fragmentation of genomic DNA in HepG2.2.15 cells. Besides UV-C irradiation, we tested anti-CD95 antibody treatment and a combination of both as apoptotic stimuli. We found that HepG2.2.15 cells were partially resistant to anti-CD95 antibody application (Fig.2c and 1d). However, a combination of UV-C irradiation plus anti-CD95 antibody application synergistically increased caspases-3 and -7 activity about 57% (Fig.2c and 1d).

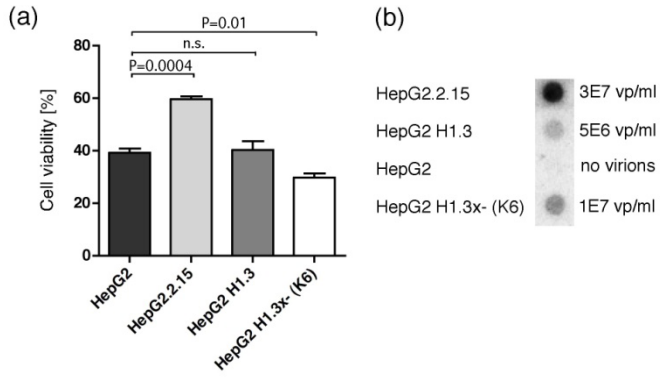

Figure 3 Comparative sensitivity of wtHBV- and ΔxHBV-replicating cells towards apoptosis. **(a)** Cell viability was determined by an XTT-assay 24h after UVC irradiation [20mJ/cm^2]. Data are expressed as percent of untreated cells (mean ± SD; n=3). For statistical analysis the student t-test was used. **(b)** Dot blot analysis of HBV particles released into the cell culture medium of untreated cells within 24 h. HBV-DNA was hybridized using a ^{32}P-labeled HBV-DNA probe. Total amount of particles was densitometrically quantified and compared with plasmid HBV standard .

In an extended experiment, we compared the sensitivity of wtHBV- and ΔxHBV-replicating cell lines towards apoptosis to analyze the influence of the viral HBx protein. In detail, we compared the viabilities of HepG2.2.15, HepG2-H1.3 and HepG2-H1.3x- (K6) cell lines with that of HepG2 cells, respectively, 24h after UV-C irradiation (Fig.3). We found that HepG2-H1.3 cells, which produced about 8-fold lower amounts of HBV than HepG2.2.15, were as sensitive as HepG2 cells (Fig3a). By contrast, HepG2-H1.3x- (K6) cells, which produced about 2.5-fold higher amounts of HBV than HepG2-H1.3 cells, exhibited a significantly (P = 0.01) increased sensitivity to UV-C irradiation although they express no HBx protein.

These results demonstrate that neither HBV replication nor the expression of the viral HBx protein sensitizes host cells towards apoptosis. By contrast, wtHBV-replicating cell lines like HepG2.2.15 and HepG2-H1.3 cells are partially resistant towards UV-C-induced apoptosis compared with parental cells. The observation that HepG2-H1.3x-(K6) cells are even more sensitive towards apoptosis than parental cells straighten the notion that HBx interferes with cell signaling pathways to prevent apoptosis.

2.2.2 Microarray Analysis of HBV-replicating hepatoma cell lines

In the present study, we attempted to identify hepatocellular genes whose transcriptional regulation is tightly linked to HBV replication in the presence and absence of the viral HBx protein. In particular, we restricted our focus to genes associated with apoptosis and cell survival and searched for transcripts that were either induced or suppressed in HBV-replicating hepatoma cell lines compared to parental cells. In detail, we compared the gene expression profiles of HepG2 with HepG2-H1.3x- (K6), HepG2-H1.3 (clone 2), HepG2-H1.3 (clone 5) and HepG2.2.15, respectively. Since we were aware that different sides of integration of the HBV genome and long-term culture periods may alter the cellular expression patterns independently of HBV replication, comparative analyses of three different wtHBV-transformed cell lines were performed. Thus, we differentiate between cell line- and clone-specific and HBV-induced changes in cellular transcriptomes. Unfortunately, we were unable to perform comparative analyses of different cell clones of ΔxHBV-producing cell lines. Because we selected only one cell clone HepG2-H1.3x- (K6) which carried the point mutation and therefore did not express HBx. All other selected ΔxHBV-producing cell clones mutated back to wild type like HepG2-H1.3x- (K4) (see appendix: sequencing data of HBx ORF).

Before total cellular RNAs were isolated and complementary DNAs (cDNA) were synthesized, all hepatoma cell lines were cultured for six weeks under identical conditions supporting hepatocyte differentiation. Additionally, HBV virion secretion was monitored continuously (data not shown). The cDNAs were hybridized to Illumina human WG-6 microarray gene chips comprising 48,000 probe sets designed to detect 25,400 unique human transcripts. The results were quantified using Illumina BeadStudio software, which calculates a fold change as well as the actual intensity value for each gene. The data set obtained from HepG2 cells was used as baseline. Those values were compared in pairs with the data sets of the HBV-transformed cell lines (mentioned above). We considered mRNA to be significantly regulated during HBV-replication if its fold change was 2-fold or greater. On this basis, we found that approximately 1,090 transcripts were differentially regulated during HBV-replication in all HBV-transformed cell lines corresponding to about 1.3% of the cellular transcriptome (data not shown). These data indicated that HBV replication influences the cellular gene expressions only to a marginal extent.

In order to identify cellular transcripts encoding for proteins associated with apoptosis and cell survival, we used gene ontology annotations. Thus, we filtered the obtained data sets of differentially regulated mRNA in HBV-transformed cell lines with respect to their potential functions in apoptosis or cell survival. On average, 51 transcripts of all analyzed HBV-transformed cell lines (□0.06% of the cellular transcriptome) matched to this category. The complete lists of clustered transcripts are presented in Table 1. Those transcripts encode for diverse cellular structures and regulatory proteins which are located at (I) the extracellular membrane (ALB, ANGPTL4, TNFRSF21, TNFSF14, VEGFA); (II) the mitochondrial outer membrane (Bax, Bik, FIS1, BNIP3); (III) the endoplasmatic reticulum (SELS, SGK, HSPA1B); (IV) the cytoplasm and involved in cellular stress response (SQSTM1, SGK, PRODH, PRDX2, TRIB3) or (V) caspase activation (CASP4, MOAP1).

We found a complex regulation of genes associated with apoptosis and cell survival in all analyzed cell lines. Furthermore, we detected differences but also remarkable similarities in mRNA expression patterns between the different cell lines (Table 1). The highest total number of regulated transcripts was found in HepG2-H1.3x- (K6) cells, whereas the lowest number was detected in HepG2.2.15 cells (Table 1). Importantly, the calculated values of fold-changes of respective mRNAs were remarkably similar between all HBV-transformed cell lines suggesting a specific response to HBV replication. As an exception, we found that the expression of the cellular mRNAs encoding for Mx1 and BIRC7 were contrarily regulated in HepG2-H1.3x- (K6) cells compared to wtHBV-producing cells: the mRNA expression level of Mx1, an interferon-responsive gene which encodes for a protein with antiviral activity against RNA viruses, was more than two-fold down-regulated in HepG2-H1.3x- (K6) cells, whereas in HepG2.2.15 cells a two-fold increase was detected. In contrast, Mx1 mRNA was not differentially regulated in HepG2-H1.3 cell lines. More importantly, the mRNA encoding for the anti-apoptotic protein BIRC7 was about three-fold down-regulated in HepG2-H1.3x- (K6) cells, whereas a more than two-fold increase was detected in HepG2.2.15 as well as in HepG2-H1.3 cell lines.

Table 1 HBV-induced alteration of cellular gene expression patterns of gene products with pro-apoptotic (orange) and anti-apoptotic potential (green). Table describes three different wtHBV and one ΔxHBV stably transformed cell lines. The HepG2 H1.3x-(K4) cell line mutated back to wtHBV-producing cells. Data show relative fold changes of gene expression levels (+ increase / - decrease) relative to HepG2 cells. Actual intensity value are depicted for HepG2 cells. Orange fields show changes in gene expression with are associated with pro-apoptotic cell signaling; Green fields show changes in gene expression with are associated with anti-apoptotic cell signaling (cell survival). Note: blank fields demonstrate that the mRNA was not differentially regulated in the respective cell line when compared to HepG2 cells.

genes	wtHBV			ΔxHBV	wt/ΔxHBV	reference	GenBank accession number
	HepG2.2.15	HepG2 H1.3		HepG2 H1.3x-		HepG2	
		(clone 2)	(clone 5)	(clone K6)	(clone K4)	(baseline)	
	fold change			fold change		actual intensity value	
ALB	-2,12	-2,29	-2,85	-5,82		7398	NM_000477.3
ANGPTL4	-2,59	-3,94	-3,27	-10,31	-2,6	802	NM_139314.1
APAF1				-2		207	NM_181869.1
APOH		-2,79	-3,09	-8,29		2675	NM_000042.1
ASNS	2,16	2,27	3,01	3,02	2,38	1450	NM_133436.1
BAX				**2,99**		282	NM_138765.2
BCL6	4,96			-2,11		1170	NM_001706.2
BIK				3,32		73	NM_001197.3
BIRC3				-2,11	-2,54	748	NM_182962.1
BIRC7	3,16		2,47	**-2,97**	2	175	NM_139317.1
BNIP3				-3,1		3370	NM_004052.2
BNIP3L				-2,39	2,08	420	NM_004331.2
BNIPL	-4,44	-3,65	-3,75	-3,28	-3,29	194	NM_138278.1
C10orf97				2,03		168	NM_025161.3
C8orf4	-2	-2,09	-2,09	-4,44	-2,1	372	NM_020130.2
CASP4		-4,06	-3,94	-2,31	-4,08	750	NM_033306.2
CBX4				2,38	2,14	317	NM_003655.2
CD24		-3,5	-3,39	-2,74	-6,92	562	NM_013230.2
CD74		-2,59	-2,23	-4,25	-2,18	641	NM_001025158.1
CDKN1A	-2,48	-2,68	-2,37	-2,39	-3,05	2873	NM_078467.1
CIDEB				-3,42		162	NM_014430.1
CIDEC		-2,33		-2,64		286	NM_022094.2
CRYAA	-3,35	-4,33	-4,55		-2,83	544	NM_000394.2
CTNNAL1				2,15		279	NM_003798.1
CTSB				-4,2		3859	NM_001908.3
CYCS		2,32	2,21		2,54	98	NM_018947.4
CYFIP2	2,78	2,45	2,23		5,44	45	NM_001037333.1
DDIT4	2,33	2,02	2,61	2,1	2,98	658	NM_019058.2
DNM2	-3,07	-2,57	-2,82	-2,27	-2,29	427	NM_004945.2
EEF1E1				2,16		548	NM_004280.2
EGLN3		-2,35	-2,32	-5,86		300	NM_022073.2
EIF5A				2,15		493	NM_001970.3
FIS1	2,27	2,24	2,16	2,02		191	NM_016068.1
FOXO3A				-2,57		1540	NM_001455.2
GADD45B	-2,61			-2,98		308	NM_015675.1
HSPA1B		3,54	3,03			1707	NM_005346.3
HSPA9B				2,27		1181	NM_004134.4
HSPB1	-2,61	-2,48	-2,81	-2,33	-3,76	2638	NM_001540.2
IGFBP1	2,29	2,38	2,6	2,2	2,76	2331	NM_000596.2
ITGB2				-4,25		589	NM_000211.2
LGALS1				-2,11		1502	NM_002305.2
LITAF		2,91	2,39		2,21	530	NM_004862.2
MAGED1		-2,32	-2,59	-3,6	-2,12	838	NM_001005333.1
MOAP1	-3,37	-2,68	-2,97	-3,15	-2,21	961	NM_022151.4
MX1	**2,75**			**-4,57**	-2,21	227	NM_002462.2
NEK6	-2,76	-2,67	-2,54	-2,69	-2,44	513	NM_014397.3
NFKBIA		-2,41	-2,39	-2,79	-2,15	2039	NM_020529.1
NGFRAP1				-10,51		303	NM_206917.1
NME1				3,3		1552	NM_198175.1
P2RX1	5,09	6,32	7,61	4,36	4,6	37	NM_002558.2
PDCD2		2,34	2,62		2,82	211	NM_144781.1
PDCD5				2,1		288	NM_004708.2
PEG3				-6,2		1601	NM_006210.1
PERP		-2,12	-2,61	-2,66		445	NM_022121.2
PPP1R13L		-2,25		-2,23		270	NM_006663.2
PPP2CA	2,12			2,12		239	NM_002715.2
PRDX2		2,21	2,29		2,82	184	NM_181738.1
PRKCZ				2,27		266	NM_002744.4
PRODH	5,43	3,79	4,76		4,91	109	NM_021232.1
PTPRH		2,13	2,34		2,08	172	NM_002842.2
SCARB1				-3,06		1598	NM_005505.3
SELS	2,37	2,33	2,88	3,04	2,06	874	NM_018445.4
SEMA6A	2,46			2,74		68	NM_020796.2
SGK	-3,64	-3,92	-3,99	-6,1	-4,98	441	NM_005627.2
SH3GLB1				2,06		546	NM_016009.2
SIAHBP1				2,33		825	NM_014281.3
SQSTM1	2,43	2,16	2,38	3,42	2,24	650	NM_003900.3
TBX3	-2,02			-2,15		658	NM_016569.3
TNFAIP3	-2,53			-3,87		443	NM_006290.2
TNFRSF12A	3,41	3,13	3,3	3,53	3,09	272	NM_016639.1
TNFRSF19	-3,91	-3,14	-3,61	-2,02	-2,77	964	NM_148957.2
TNFRSF21	-2,28	-2,15	-2,07		-2,44	1858	NM_014452.3
TNFSF14		-2,17	-2,13	-2,1	-2,67	599	NM_172014.1
TOP2A	-2,2	-3,21	-3,26		-4,1	200	NM_001067.2
TRIB3	2,2	2,01	2,53	2,7	2,11	1725	NM_021158.3
TSPO	-12,16	-2,93	-2,84		-2,16	872	NM_000714.4
VEGFA		-2,06	-2,31	-2,94		602	NM_003376.4
YARS	2,1			2,22		1035	NM_003680.2
ZDHHC16				2,09		508	NM_198044.1

To assess the influence of HBV-replication in sensitizing cells towards apoptosis on the mRNA level, we quantified the selected mRNAs according to two criteria: (i) with respect to either pro-apoptotic or anti-apoptotic functions of their encoded proteins and (ii) with regard to the regulation level of the respective genes, if they were induced or suppressed. Data are summarized in Figure 4.

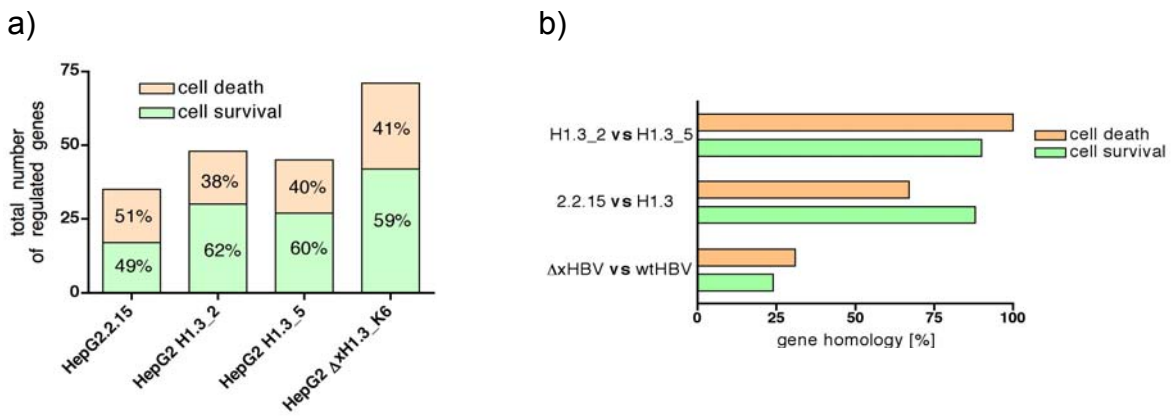

Figure 4 Evaluation of HBV-induced changes in cellular transcriptome. **(a)** Total amount of mRNAs encoding proteins associated with pro- and anti-apoptotic potential. The percentages present the relative amount of mRNA supporting cell survival and cell death. **(b)** Comparative analysis of regulated pro- and anti-apoptotic genes. Different clones (2 and 5) of HepG2-H1.3 cells were matched with each other and in relation to the long term cultured HepG2.2.15 cells. ΔxHBV transformed cells were aligned to all three wtHBV-expressing cells.

We observed that the gene expression patterns of transcripts encoding for proteins associated with pro- and anti-apoptotic signaling pathways were balanced in HepG2.2.15 cells (Fig.4a). Furthermore, about 60% of the regulated transcripts in HepG2-H1.3 as well of HepG2-H1.3x- (K6) favored cell survival (Fig.4a) indicating that HBV replication per se does not sensitize host towards apoptosis on mRNA level. Comparing the gene expression profiles between the cell lines listed in Table1, we revealed about 93% homology between the HepG2-H1.3 cell clones 2 and 5 (Fig.4b). (Note, both clones carry the same HBV-construct but were independently selected.) This finding indicates that the random integration site of the HBV genome has no influence on the cellular transcriptome. In addition, about 78% similarity was observed between HepG2-H1.3 cell lines and HepG2.2.15 cells. In contrast, the lowest similarity in gene expression patterns with about 28% was found between HepG2-H1.3x- (K6) cells aligned to all wtHBV-transformed cell lines (Fig.4b). This most probably is a consequence of the higher amount of the total number of regulated genes in HepG2-H1.3x- (K6) cells (see Table1).

In the overall analysis, it is important to consider the fold change of the gene transcripts as well as the actual intensity values that correspond to the total amount

of the respective transcripts in the sample used for hybridization. The actual intensity values are only shown for the reference HepG2 cells (Table 1). The intensities of all listed mRNAs in Table 1 spanned a range of more than two orders of magnitude, from approximately 37 (P2RX1) to 6,060 (IGFBP1). We considered actual intensity values below 100 as low, from 100 to 500 as mild, 500 to 1,000 as medium, and above 1000 as high expression intensities. The majority of the listed mRNA of HBV-transformed cell lines, approximately 85%, was detected with intensities around 100 to 350. Thus, they represented low but reliable expression values. Table 2 juxtaposes identical expression patterns in HBV-transformed cell lines and highlights genes exclusively regulated in HepG2-H1.3x- (K6) cells. We grouped those transcripts into four different categories:

The first group comprised mRNAs encoding proteins involved in pro-apoptotic signaling pathways, which were down-regulated in both wtHBV- and ΔxHBV-producing cell lines. This includes mRNAs encoding proteins that may directly activate caspases (CASP4, MOAP1) or are involved in NFκB signaling cascade (NFKBIA, NEK6) or in the TNF-α receptor signaling pathway (TNFAIP19, TNFRSF21, TNFSF14). Notably, the actual intensity values of mRNAs encoding NFKBIA and TNFRSF21 in HepG2 cells were more than 1,850 and therefore considered as a high expression values.

The second group comprised mRNAs encoding proteins involved in pro-apoptotic signaling pathways, which were up-regulated in wtHBV- and/or ΔxHBV-producing cell lines. We found an increased expression of mRNAs encoding proteins involved in stress-response signaling pathways like SQSTM1 and TRIB3. Conspicuously, we detected the highest fold-change value between 4.3- and 7.6-fold by one transcript encoding for the integral membrane protein (P2RX1). This protein is a ligand of a protein channel gate influencing the Ca2+ activity. However, the actual intensity value of the P2RX1 mRNA was very low in HepG2 cells about 37. In contrast, in all HBV-transformed cell lines, we detected P2RX1 mRNA at still low but reliable expression values. However, the role of P2RX1 in HBV-replicating cells remains to be determined.

Furthermore, we revealed that two mRNAs encoding pro-apoptotic Bcl-2 family proteins Bax and Bik were 3-fold up-regulated in HepG2-H1.3x- (K6) cells. These proteins are involved in mitochondrial-induced apoptosis. Comparing the actual

intensity values of these mRNAs in parental and HepG2-H1.3x- (K6) cells, we found that the values increased from a low expression value (e.g. Bik: 73) in HepG2 to a mild (Bik: 244) or medium value (Bak: 850) in HepG2-H1.3x- (K6) cells.

Table 2 Comparison of transcriptional alternations indicating pro- (green) and anti-apoptotic (orange) signaling in HBV transformed cell cells. Values show fold changes of mRNA levels relative to parental HepG2 cells. Transcripts are grouped due to the proposed functions of their gene products in apoptosis pathways and due to their regulation by HBV-replication. Functional classifications are assigned to gene ontology annotations.

A) pro-apoptotic function; decreased (↓) in HBV producing cell lines

	wtHBV			ΔxHBV	
	HepG2.2.15	HepG2 H1.3	HepG2 H1.3	HepG2 ΔxH1.3	
gene		(clone 2)	(clone 5)		**functions of the gene product / localization**
BNIPL	-4,44	-3,65	-3,75	-3,28	apoptosis,nucleus, cytosol, negative regulation of cell proliferation
CASP4		-4,06	-3,94	-2,31	induction of apoptosis, **caspase activity**, proteolysis, cysteine-type peptidase activity
CD24		-3,5	-3,39	-2,74	induction of apoptosis, **immune response, T cell costimulation**, positive regulation of MAPKKK cascade
CD74		-2,59	-2,23	-4,25	apoptosis, immune response, **antigen processing and presentation**
CDKN1A	-2,48	-2,68	-2,37	-2,39	induction of apoptosis, cellular response to extracellular stimulus
DNM2	-3,07	-2,57	-2,82	-2,27	positive regulation of apoptosis
MOAP1	-3,37	-2,68	-2,97	-3,15	apoptosis, **caspase activation**, cell structure disassembly during apoptosis
NEK6	-2,76	-2,67	-2,54	-2,69	apoptosis, **positive regulation of I-kappaB kinase/NF-kappaB cascade**
NFKBIA		-2,41	-2,39	-2,79	apoptosis, **cytoplasmic sequestering of NF-kappaB**
SGK	-3,64	-3,92	-3,99	-6,1	apoptosis, response to stress, nucleus, cytoplasm, endoplasmic reticulum, protein serine/threonine kinase activity,
TNFAIP3	-2,53			-3,87	apoptosis, **negative regulation of I-kappaB kinase/NF-kappaB cascade,** ubiquitin cycle
TNFRSF19	-3,91	-3,14	-3,61	-2,02	induction of apoptosis, tumor necrosis factor receptor activity, JNK cascade, integral to membrane
TNFRSF21	-2,28	-2,15	-2,07		apoptosis, receptor activity, , signal transduction, integral to membrane
TNFSF14		-2,17	-2,13	-2,1	induction of apoptosis, immune response, signal transduction, **release of cytoplasmic sequestered NF-kappaB, caspase inhibitor activity**
TSPO	-12,16	-2,93	-2,84		apoptosis, **mitochondrial outer membrane**, protein targeting to mitochondrion

B) pro-apoptotic function; increased (↑) in HBV producing cell lines

	wtHBV			ΔxHBV	
	HepG2.2.15	HepG2 H1.3	HepG2 H1.3	HepG2 ΔxH1.3	
gene		(clone 2)	(clone 5)		**functions of the gene product / localization**
BAX				**2,99**	induction of apoptosis, **mitochondrial outer membrane**, **caspase activation**
BIK				**3,32**	induction of apoptosis, **mitochondrial outer membran**
DDIT4	2,33	2,02	2,61	2,1	apoptosis, cytoplasm, negative regulation of signal transduction
FIS1	2,27	2,24	2,16	2,02	apoptosis, **mitochondrial outer membrane**, peroxisomal membrane
P2RX1	5,09	6,32	7,61	4,36	apoptosis, signal transduction, purinergic nucleotide receptor activity, integral to plasma membrane, ion transport
SQSTM1	2,43	2,16	2,38	3,42	apoptosis, **response to stress, immune response**, nucleus, cytoplasm, late endosome, **regulation of I-kappaB kinase/NF-kappaB cascade**, ubiquitin binding receptor tyrosine kinase/ SH2 domain binding,
TNFRSF12A	3,41	3,13	3,3	3,53	apoptosis, receptor activity, integral to membrane
TRIB3	2,2	2,01	2,53	2,7	apoptosis, **response to stress**, nucleus, transcription, regulation of MAP kinase activity

C) anti-apoptotic function; increased (↑) in HBV producing cell lines

	wtHBV			ΔxHBV	
	HepG2.2.15	HepG2 H1.3	HepG2 H1.3	HepG2 ΔxH1.3	
gene		(clone 2)	(clone 5)		**functions of the gene product / localization**
ASNS	2,16	2,27	3,01	3,02	anti-apoptosis, asparagine biosynthetic process, positive regulation of cell cycle
BIRC7	3,16		2,47	**-2,97**	anti-apoptosis, nucleus, cytoplasm, activation of JNK activity, IAP
HSPA1B		3,54	3,03		anti-apoptosis, nucleus, cytoplasm, mitochondrion, endoplasmic reticulum, protein folding
IGFBP1	2,29	2,38	2,6	2,2	regulation of cell growth, signal transduction
SELS	2,37	2,33	2,88	3,04	anti-apoptosis, antioxidant activity, receptor activity, unfolded protein response, retrograde protein transport

D) anti-apoptotic function; decreased (↓) in HBV producing cell lines

	wtHBV			ΔxHBV	
	HepG2.2.15	HepG2 H1.3	HepG2 H1.3	HepG2 ΔxH1.3	
gene		(clone 2)	(clone 5)		**functions of the gene product / localization**
ALB	-2,12	-2,29	-2,85	-5,82	anti-apoptosis, **mitochondrion** localization
ANGPTL4	-2,59	-3,94	-3,27	-10,31	anti-apoptosis, receptor binding, extracellular region
BIRC3				**-2,11**	anti-apoptosis, ubiquitin-protein ligase, IAP2 (inhibitor of apoptosis)
BIRC7	3,16		2,47	**-2,97**	anti-apoptosis, nucleus, cytoplasm, activation of JNK activity, IAP
CRYAA	-3,35	-4,33	-4,55		anti-apoptosis, protein folding, Bcl2 interacting protein
HSPB1	-2,61	-2,48	-2,81	-2,33	anti-apoptosis, nucleus, cytoplasm, regulation of translational initiation, protein folding

The third group comprised mRNAs encoding proteins involved in anti-apoptotic signaling pathways, which were up-regulated in HBV-producing cell lines. We revealed that the abundant basal expression of the mRNA encoding the hepatocytes-derived IGF binding protein (IGFBP1) was more than 2-fold increased in all HBV-transformed cell lines. Note the actual intensity value of IGFBP1 mRNA was high in HepG2 cells of about 2,331. IGFBP1 has been described as an important hepatocyte-specific growth factor required for liver generation and for reducing pro-apoptotic signals. In addition, we found an up-regulation of mRNAs encoding proteins involved in protein folding and were located at the endoplasmatic reticulum like SELS and HSPAIB.

The fourth group comprised mRNAs encoding proteins involved in anti-apoptotic signaling pathways, which were down-regulated in HBV-producing cell lines. Hereby, we found mRNAs encoding proteins involved in protein folding like CRYAA or HSPB1. Notably, we detected that the expression levels of mRNAs encoding BIRC3 and BIRC7 were exclusively down-regulated in HepG2-H1.3x- (K6) cells. Those proteins belong to the caspase-inhibitor family (IAP). In contrast, the mRNA of BIRC7 was up-regulated in all wtHBV-producing cells. The actual intensity value of BIRC7 mRNA in HepG2 cells was about 175 and was considered as a mild but reliable expression value.

Taken together, the gene expression profiling of different HBV-replicating hepatoma cell lines revealed that HBV replication influences the cellular gene expression profile only marginally indicating the sophisticated adaptation of the virus to the host cell. We have found no evidence that viral replication either disrupts the cellular balance between pro- and anti-apoptotic genes expressions or sensitizes cells towards apoptosis. Moreover, we found that some apoptosis inhibitors, for instance IGFBP1, a hepatocyte-derived anti-apoptotic protein, were substantially up-regulated at the mRNA level in all HBV-transformed cell lines. Furthermore, genes encoding for pro-apoptotic proteins like members of the TNF-receptor family or caspase activators were significantly down-regulated in all HBV-transformed cell lines. Importantly, we observed minor, but distinct differences between ∆xHBV- and wtHBV-producing cell lines. Especially, mRNAs encoding proteins controlling mitochondrial apoptosis check points (Bax, Bik) were up-regulated and mRNAs encoding apoptosis inhibitors (BIRC/IAP) were down-regulated in ∆xHBV replicating cells. These findings suggest that HBx might be important for prevention of apoptosis induction.

2.2.3 Structure and Infectivity of HBV particles released from apoptotic cells

2.2.3.1. HBV-transformed hepatoma cell lines

In order to address the question if apoptosis of HBV infected hepatocytes facilitates the release of infectious HBV particles and enhances viral propagation, we used a cell culture model consisting of HBV-replicating hepatoma cell lines and primary human hepatocytes (PHH) (Fig.5). Thereby, we took advantage of the HBV-producing HepG2.2.15 cell line to analyze viral progeny release after apoptosis induction and PHH as a tool to determine the infectivity of particles released.

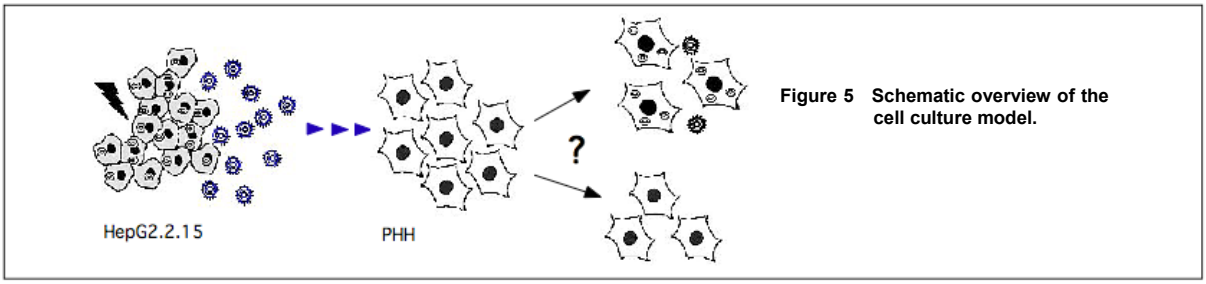

Figure 5 Schematic overview of the cell culture model.

At first, we characterized HBV particles released from HepG2.2.15 cells during the first 24 h after apoptosis-induction.

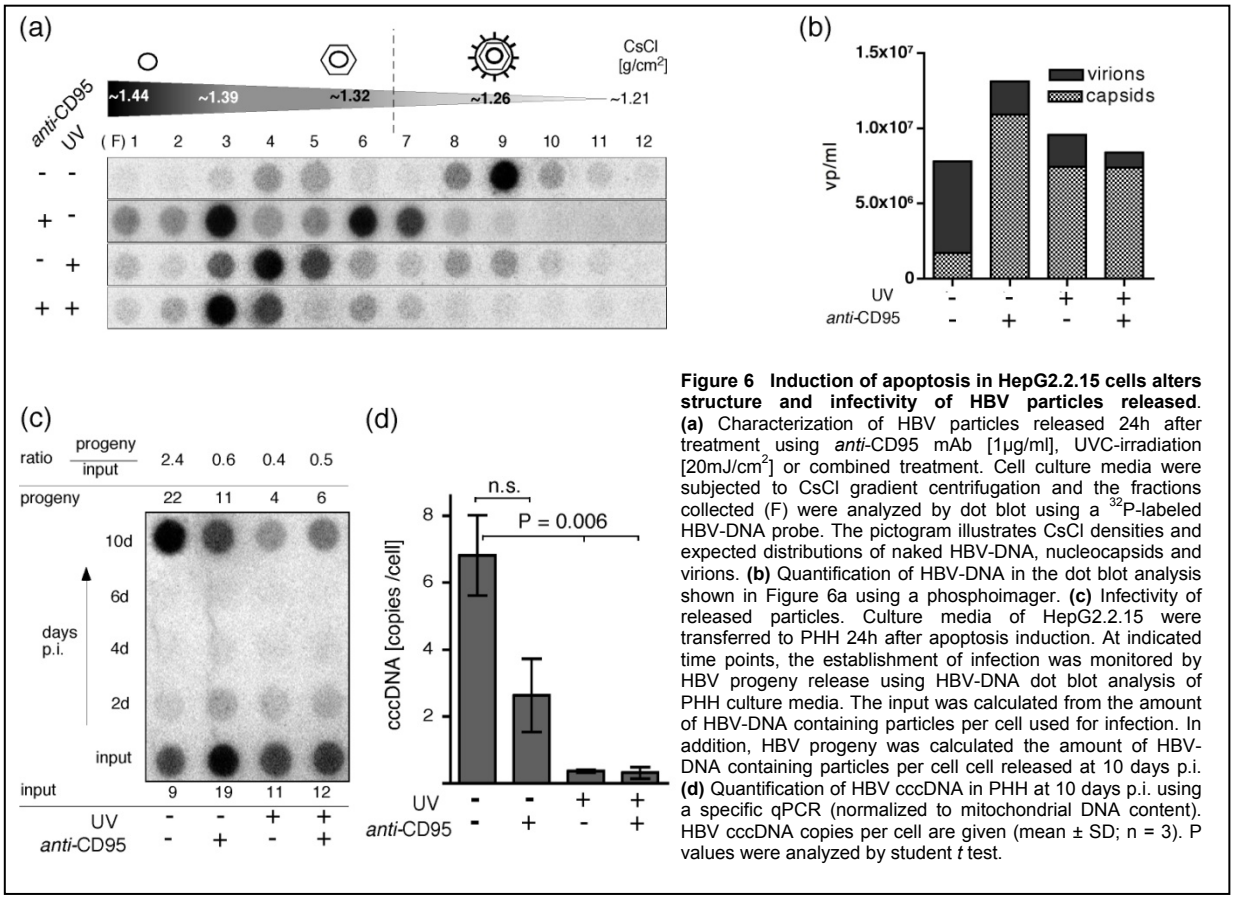

Figure 6 Induction of apoptosis in HepG2.2.15 cells alters structure and infectivity of HBV particles released. **(a)** Characterization of HBV particles released 24h after treatment using *anti*-CD95 mAb [1µg/ml], UVC-irradiation [20mJ/cm^2] or combined treatment. Cell culture media were subjected to CsCl gradient centrifugation and the fractions collected (F) were analyzed by dot blot using a ^{32}P-labeled HBV-DNA probe. The pictogram illustrates CsCl densities and expected distributions of naked HBV-DNA, nucleocapsids and virions. **(b)** Quantification of HBV-DNA in the dot blot analysis shown in Figure 6a using a phosphoimager. **(c)** Infectivity of released particles. Culture media of HepG2.2.15 were transferred to PHH 24h after apoptosis induction. At indicated time points, the establishment of infection was monitored by HBV progeny release using HBV-DNA dot blot analysis of PHH culture media. The input was calculated from the amount of HBV-DNA containing particles per cell used for infection. In addition, HBV progeny was calculated the amount of HBV-DNA containing particles per cell cell released at 10 days p.i. **(d)** Quantification of HBV cccDNA in PHH at 10 days p.i. using a specific qPCR (normalized to mitochondrial DNA content). HBV cccDNA copies per cell are given (mean ± SD; n = 3). P values were analyzed by student *t* test.

Therefore, we used CsCl gradient centrifugation to separate mature enveloped HBV virions from HBV capsids and HBV-DNA due to their densities.

Subsequently, HBV-DNA dot blot analysis was performed. Depending on the strength of the apoptotic stimulus, we found a shift of released HBV particles from enveloped virions to naked capsids (Fig.6a). Without any treatment, about 80% of released viral genomes was in enveloped particles (buoyant density, 1.24 to 1.28 g/cm^3). In contrast, upon anti-CD95 antibody treatment, which we showed to be a weak apoptotic stimulus for HepG2.2.15 cells (Fig.2c), only 20% of released genomes were detected in enveloped virions, whereas 80% were in naked capsids (buoyant density, 1.32 to 1.39 g/cm^3). Interestingly, we observed two distinct populations of capsids sedimenting at a density of 1.32 and 1.39 g/cm^3, respectively. We hypothesized that these populations attribute to different maturation levels of capsids within the HBV-replication cycle and therefore we analyzed RNA/DNA content of the particles (see chaper 3.1.6). After a strong apoptotic stimulus, such as the combination of UV-C-irradiation and anti-CD95 antibody treatment, more than 90% of the released genomes was in naked capsids sedimenting at a density of 1.39 g/cm^3 (Fig.6a). It is important to note that the total amount of released HBV particles did not changed significantly during the first 24 h after apoptosis induction.

Furthermore, we examined the infectivity of the HBV particles released. Thus, we collected the cell culture medium of HepG2.2.15 cells 24 h after apoptosis induction or mock treatment, respectively, and used the HBV particles contained to infect PHH. We followed the establishment of an HBV infection up to 10 days post infection (p.i.). Although the total amount of HBV genomes used for infection was equal in all settings or even higher in the samples subjected to apoptotic treatment, we observed a four- to six- fold reduction of HBV progeny released (Fig.6c) and cccDNA levels (Fig.6d), respectively.

The data indicate that after apoptosis-induction of HepG2.2.15 cells, predominantly noninfectious HBV particles (naked capsids) were released. We found an inverse correlation between the strength of the apoptotic stimulus, the structure of the released viral genomes, and their infectivity: the more potent an apoptotic stimulus was, the higher the ratio of capsids to virions was and the lower was the infectivity.

2.2.3.2. HBV-infected PHH

Since apoptosis pathways in hepatoma cell lines are altered due to the nature of these cells, we confirmed our results in a more natural system using PHH. In detail, we analyzed viral propagation after CD95-receptor mediated apoptosis induction of HBV-infected PHH (Fig.7).

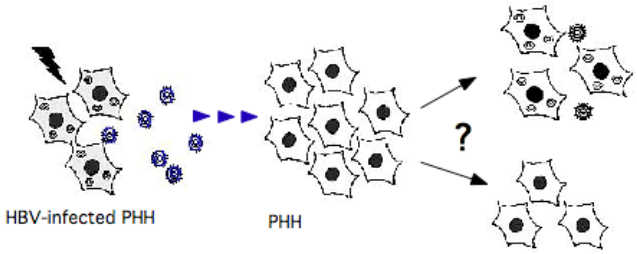

Figure 7 Schematic overview of cell culture model.

At first, we monitored the dynamic of HBV-infection in PHH cultures up to 10 days p.i. to determine the time point of HBV particles released sufficient in quantity to infect a second PHH culture. Additionally, we compared the infectivity of HBV particles bearing or non-bearing intact envelope structures, respectively. Therefore, we infected freshly isolated PHH *in vitro* with HBV obtained from HepG2.2.15 using a multiplicity of infection (moi) of 200 enveloped, DNA containing virus particles / cell. The amount of infectious HBV particles was calculated by quantitative HBV-DNA dot blot analysis of cell culture medium subjected to CsCl gradient centrifugation.

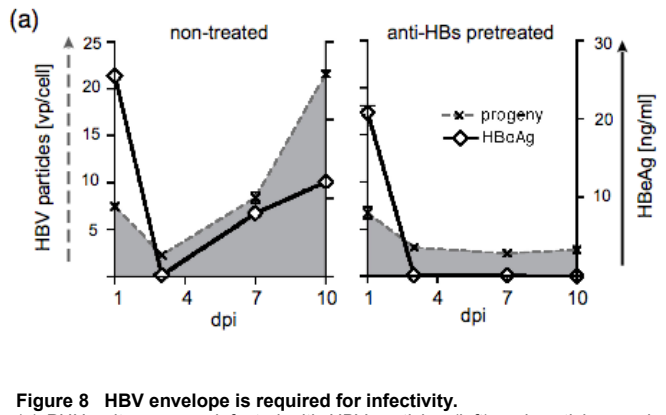

Figure 8 HBV envelope is required for infectivity.
(a) PHH cultures were infected with HBV particles (left) and particles pre-incubated with neutralizing *anti*-HBs antibodies (right), respectively. Up to 10 day post infection, the establishment of productive infection was monitored by progeny HBV-DNA dot blot analysis (filled area) and HBeAg secretion (continuous line). HBV-DNA containing particles per cell were quantified using a phosphoimager (mean ± SD; n = 3). (b) Quantification of HBV cccDNA at day 10 p.i. using qPCR relative to mitochondrial DNA content. The cut-off for detection was 50 copies cccDNA per 10^4 cells. Data are expressed as copies of cccDNA per ten cells (mean ± SD; n = 3)

Upon polyethylenglycan mediated HBV infection, the establishment of a productive HBV infection in PHH was measured every second day by determining the secretion of newly synthesized HBeAg and release of HBV progeny. As shown in Figure 9, the

productive infection started at 3 days p.i. and increased more than 10-fold until 10 days p.i. (Fig. 8a). However, we detected neither the establishment of a productive HBV infection (Fig. 8a) nor the formation of cccDNA (Fig. 8b) after blocking the surface proteins of HBV virions with neutralizing anti-HBs antibodies. This indicates that an intact envelope of HBV is required for PHH infection. Therefore, we considered only enveloped particles as infectious.

To analyze HBV propagation after apoptosis-induction in PHH, we firstly infected PHH with 200 moi and allowed the establishment of viral infection for 8 days before we induced apoptosis by anti-CD95 antibodies. (Note that PHH are resistant to high dosis of UV-C irradiation (up to 80 mJ/cm^2) for still undefined reasons (diploma thesis Silke Arzberger), whereas they are sensitive to anti-CD95 antibody treatment (Schulze-Bergkamen *et al.* 2003).

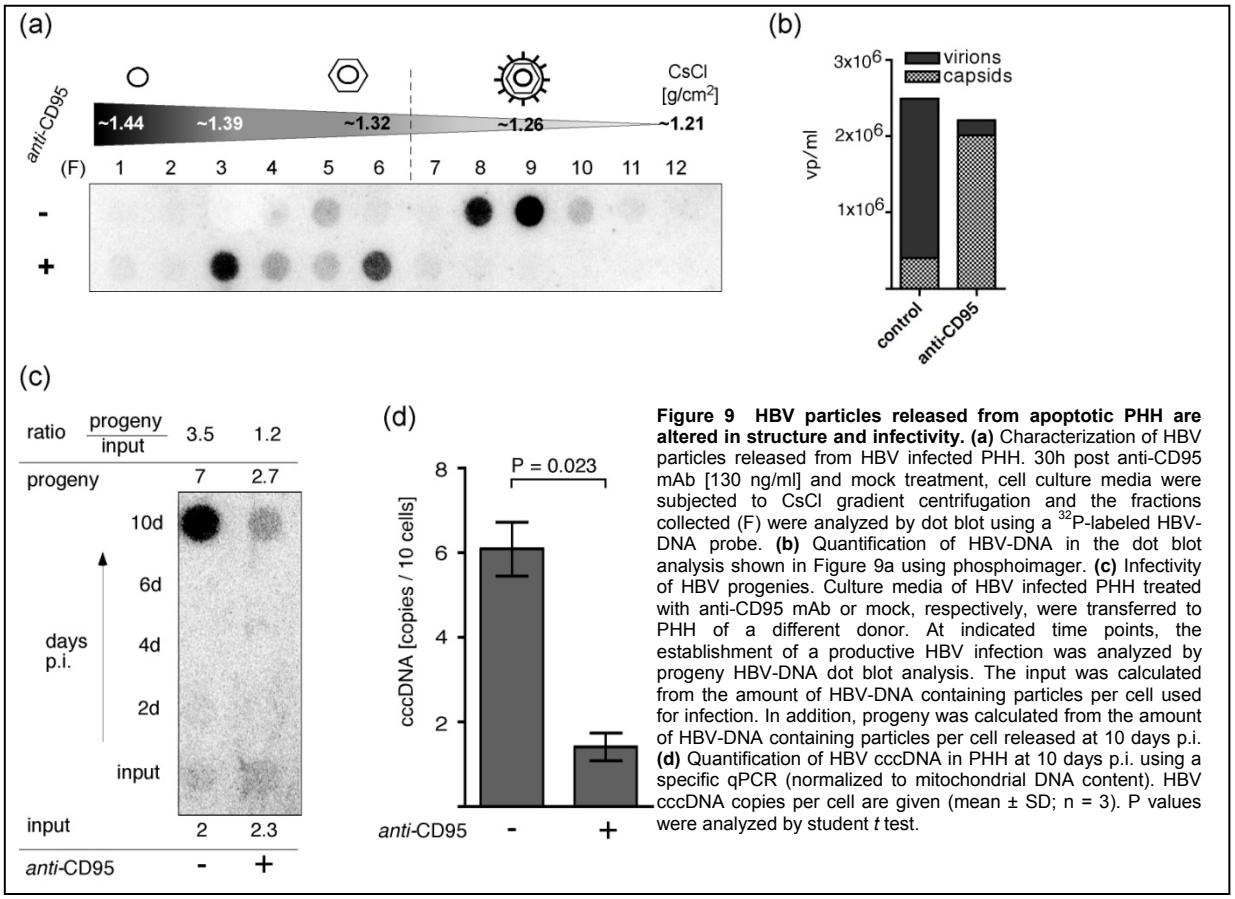

Figure 9 HBV particles released from apoptotic PHH are altered in structure and infectivity. (a) Characterization of HBV particles released from HBV infected PHH. 30h post anti-CD95 mAb [130 ng/ml] and mock treatment, cell culture media were subjected to CsCl gradient centrifugation and the fractions collected (F) were analyzed by dot blot using a ^{32}P-labeled HBV-DNA probe. **(b)** Quantification of HBV-DNA in the dot blot analysis shown in Figure 9a using phosphoimager. **(c)** Infectivity of HBV progenies. Culture media of HBV infected PHH treated with anti-CD95 mAb or mock, respectively, were transferred to PHH of a different donor. At indicated time points, the establishment of a productive HBV infection was analyzed by progeny HBV-DNA dot blot analysis. The input was calculated from the amount of HBV-DNA containing particles per cell used for infection. In addition, progeny was calculated from the amount of HBV-DNA containing particles per cell released at 10 days p.i. **(d)** Quantification of HBV cccDNA in PHH at 10 days p.i. using a specific qPCR (normalized to mitochondrial DNA content). HBV cccDNA copies per cell are given (mean ± SD; n = 3). P values were analyzed by student *t* test.

Comparing the sedimentation characteristics of the released HBV genomes after apoptosis induction, we found similar patterns as observed in HepG2.2.15. The released HBV-DNA containing particles from untreated HBV-infected PHH consisted of about 85% of enveloped virions (buoyant density, 1.24 to 1.28 g/cm^3), whereas about 90% of the released particles after anti-CD95 antibody treatment were naked

capsids sedimenting in two populations at 1.32 to 1.39 g/cm^3, respectively (Fig.9a). We assume that they attribute to different maturation levels.

In order to analyze whether the particles released still allowed spread of HBV infection to other hepatocytes, we transferred the culture media from both anti-CD95 treated and mock treated HBV-infected PHH to freshly isolated PHH from a different donor. Prior to infection, the recipient PHH was incubated with caspase inhibitors zVAD and DEVD for two hours to block residual activity of the anti-CD95 antibodies. The establishment of the secondary infection was followed by measuring HBV progeny release up to 10 days p.i. (Fig.9b). Moreover, the formation of HBV cccDNA was determined at 10 days p.i. (Fig.9c). Although the amount of HBV-DNA containing particles used for infection were comparable in these parallel experiments, we revealed that the infection with culture medium of apoptotic PHH was significantly ($P = 0.023$) less effective compared with the culture medium of apoptotic PHH.

We found that CD95-induced apoptosis-induction of HBV-infected PHH leads to the release of naked capsids. Secondary infection experiments revealed that those particles were substantially noninfectious. Therefore, our data clearly demonstrated that CD95-induced apoptosis of HBV-infected PHH does not support HBV propagation.

2.2.3.3. Structure analysis of HBV particles released from PHH

Distinct types of HBV particles were detected in the cell culture medium of mock treated and apoptotic hepatocytes. In order to characterize those particles in more detail, we analyzed on the one hand the formation of a viral envelope by measuring the small surface antigen (HBsAg) in collected fractions using ELISA (Fig.10a). On the other hand, we explored the maturation levels of the viral capsids by quantifying the nucleic acid content using one-step RT-PCR. We discriminated between HBV-DNA and HBV-RNA containing capsids by distinct nucleic acid digestions (Fig. 10b-d). The onset of both analyses was the separation of HBV particles released from HBV-infected PHH 30h after apoptosis induction or mock treatment, respectively, using CsCl gradient centrifugation.

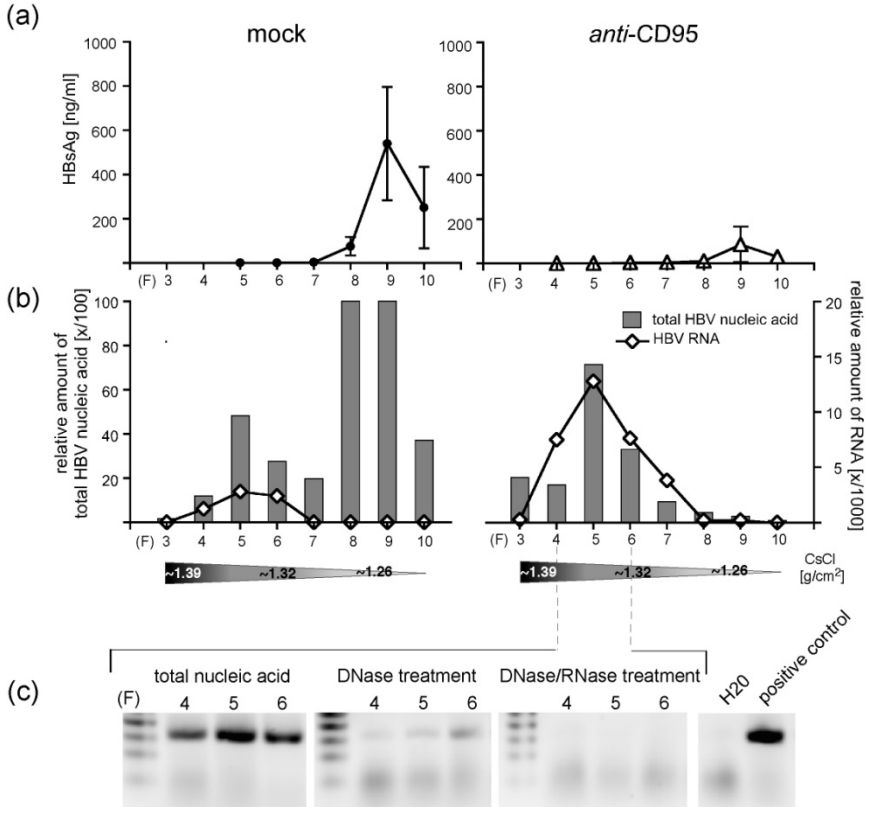

Figure 10 Characterization of HBV particles released from apoptotic PHH. Supernatant of HBV infected PHH cultures were subjected to CsCl gradient centrifugation 24h post anti-CD95 mAb [130 ng/ml] and mock treatment, respectively. Twelve fractions (F) with decreasing densities (F1 to F12) were collected; for further characterization only F3-F10 were used. **(a)** HBsAg ELISA visualising enveloped HBV particles. Averages of three experiments ± standard deviation of the means are given. **(b)** Qualitative and quantitative analysis of encapsidated viral nucleic acids using one-step RT-PCR. To discriminate between DNA and RNA, DNase digestion was performed. The total amount of HBV nucleic acids (DNA+RNA, grey bars) detected in F8 of mock treated cells was set to 100%. HBV RNA levels (continued line) of all samples are reported as parts per thousand. **(c)** Amplifications products of qPCR runs of F4-F6 with indicated treatments were separated on 2% agarose gel and visualized by ethidium bromide staining.

As shown in Figure 10a, HBsAg was exclusively detected in fractions eight to ten (buoyant density, 1.24 to 1.28 g/cm^3) of the mock treated HBV-infected PHH. These data confirmed the separation of HBV capsids and enveloped virions by CsCl gradient centrifugation. Accordingly, in these fractions we detected the highest amount of total HBV nucleic acids (Fig.10b). A second peak of total-HBV nucleic acids was found in fraction five (density, 1.34 g/cm^2) corresponding to naked HBV

capsids. In fractions four to six (buoyant density, 1.36 to 1.32) of mock-treated cells, we also detected small amounts of HBV-RNA suggesting that reversed transcription of pre-genomic HBV genomes was incomplete. Particularly, no RNA was detected in fractions eight to ten corresponding to mature enveloped virions. After apoptosis-induction the released particles exhibited about 6-fold increased values of HBV-RNA in fractions four to six (Fig.10c). This finding corroborates our assumption that those particles are mainly non-mature HBV capsids. In agreement with HBV-DNA dot blot analysis (Fig.9a), the qPCR reaction confirmed that no HBV-DNA was detectable in fractions eight to ten (Fig.10c). Indicating that no enveloped HBV particles were released after apoptosis induction.

In conclusion, we confirmed that after apoptosis-induction by anti-CD95 exclusively naked, immature HBV capsids were released from HBV-infected PHH using HBsAg ELISA and qPCR methods. The increased amount of HBV-RNA containing capsids suggests that apoptosis interrupts HBV-replication and prevents the reverse transcription step.

2.3. Discussion

This study was designed to investigate the biological significance of apoptosis induction of HBV-infected cells. This question is on current interest because it is still disputed whether or not HBV induce apoptosis of its host cell to enhance its progeny release and to minimize the onset of antiviral inflammatory responses (Miao *et al.* 2006, Shintani *et al.* 1999, Terradillos *et al.* 1998, Pollicino *et al.* 1998). The focus of this debate is based on divers *in vitro* studies showing that the viral HBx protein sensitizes host cells towards apoptosis. Therefore, it has been argued that HBV induce apoptosis, probably at the onset of an acute infection, to increase the spread of progeny to neighbouring cells as described for cytopathic viruses like adenovirus or simian virus (Hay & Kannourakis 2002, Heise *et al.* 2000, Fromm *et al.* 1994).

In this study we shows for the first time in a biological context that (i) HBV-replication does not sensitizes hepatoma cells towards apoptosis and (ii) more importantly, apoptosis of HBV-infected hepatocytes do not support viral propagation. Thus, we demonstrated under experimental conditions that closely match the natural HBV infection that apoptosis-induction severely interrupts HBV-replication and significantly reduces the spread of progeny in the host. Furthermore, we provided strong indications that HBV has evolved strategies to prevent apoptosis to allow the production of high yields of progeny virus.

2.3.1 Apoptosis-Induction of Hepatocytes

Since we revealed that HBV-producing hepatoma cell lines and HBV-infected PHH exhibit different sensitivities towards CD95-receptor mediated and UV-C induced apoptosis (diploma thesis, Silke Arzberger), we took advantage of both apoptotic stimuli: CD95-receptor clustering effectively induces apoptosis in PHH but barely harms the viability of hepatoma cell-lines. By contrast, hepatoma cell lines were susceptible to UV-C irradiation, whereas PHH did not show any changes in viability upon increasing doses of UV-C exposure.

The cell type specific protein expression profile might account for distinct sensitivities towards apoptosis. This is probably related to (i) the basal expression of proteins modulating apoptotic-signaling pathways, (ii) the density of CD95-receptor on cell surface and (iii) the cytoplasmic storage of secondary signaling molecules of the death-receptor pathway like FADD.

Gene expression analysis showed that the hepatoma cell line HepG2 expressed 98% of the genes detectable in cultured PHH (Harris *et al.* 2004). However, 31% of the HepG2 transcriptome was unique to the cell line, which might explain the different sensitivity towards apoptosis compared to PHH. Furthermore, UV-C irradiation elicits a complex cellular response, which substantially varies in different cell types and involves different signaling pathways. Apoptosis induction by UV-C irradiation strongly depends on cellular differentiation level and age of the cells (Latonen & Laiho 2005): UV-C exposure transmits energy to photo-sensitive molecules like DNA and reactive oxygen-generating proteins; they harm their structures for instance by cross-linking adjacent DNA bases or DNA and proteins. This cell damage elicits a complex cell-specific defense mechanism including (I) activation of transcription factors (like p53, NFκB, AP-1), (II) inducing signaling cascades (p38, JNK, Ras/Rac), (III) clustering and internalization of cell surface receptors in a ligand-independent manner and (IV) activation of the nucleotide excision repair machinery.

Based on our results, we supposed that PHH might cushion the energy transfer by UV-C. This could possibly be linked to its quiescent differentiation state and a pronounced expression of proteins associated with anti-apoptotic functions. We found for instance that the gene expression of p53 is 7-fold reduced in PHH compared to hepatoma cell lines, which may explain the resistance towards UV-C irradiation (Marianna Hösel, unpublished results, 2006). Previously, it has been described that UV-C light induces clustering of CD95 receptors in the same fashion as CD95 ligands (Rathmell *et al.* 1995, Aragane *et al.* 1998). In keeping with this, it is hard to explain why anti-CD95 antibody treatment induces apoptosis in PHH while UV-C irradiation does not. One reason might be the strength of CD95-receptor activation. Concerning hepatoma cell lines, we assume that a weak CD95-receptor density might be responsible for its resistance to *anti*-CD95 antibody application. Gene expression analysis of CD95 corroborates this notion. We found that CD95 gene expression was up to 10-fold increased in PHH compared with hepatoma cell lines (Marianna Hösel, unpublished results, 2006).

2.3.2 HBV nucleocapsids are released from apoptotic hepatocytes

Irrespective of whether CD95 was triggered or cells were subjected to UV-C light, we demonstrated that the release of enveloped HBV virions from hepatoma cell lines and PHH was abolished in a dose-dependent manner upon apoptosis. More

importantly, we revealed in this study that dying hepatocytes released huge amounts of unenveloped nucleocapsids for hitherto unknown reasons.

The release of HBV nucleocapsid upon apoptosis was unexpected, however it has also been observed in AdHBV-L^- infected hepatocytes in which intracellular budding and virion secretion was blocked due to the absence of the viral L glycoprotein (Sprinzl *et al.* 2001). Nucleocapsids are hardly found in the blood of infected patients and chimpanzees (Possehl *et al.* 1992), indicating that this kind of particle release does either not occur during natural HBV infection in the absence of hepatocyte killing or that non-enveloped particles are rapidly phagocytosed.

Moreover, the mechanism of HBV nucleocapsids release remains elusive; indeed, it is hardly to explain why the capsids are not directly degraded by activated caspases. The majority of the potential aspartyl cutting sides are probably hidden in the tri-dimensional structure of the HBV capsid. We assume that the release of capsids is linked to cell autonomous defense mechanisms purging out foreign protein aggregations. An alternative interpretation is the lost of cell membrane integrity upon apoptosis-induction. However, this possibility appears to be unlikely since CD95-receptor mediated apoptosis as well as UV-irradiation are both considered as intracellular killing mechanisms with intact membrane structures (Lowin *et al.* 1994).

Noteworthy, analyzing the particle released of HBV-infected cells after CD95-apoptosis induction, we revealed two characteristic populations of nucleocapsids sedimenting at different densities. This observation is astonishing since hepatoma cell lines and PHH exhibit different sensitivities towards CD95-induced apoptosis as aforementioned. We assume that the distinct populations of nucleocapsids released are different in terms of their nucleic acid content and/or constitution of the protein shell, which might reflect different maturation levels.

Differential analysis distinguishing between HBV-RNA and HBV-DNA within nucleocapsids revealed that no correlation consisted between the nucleic acid content and the densities of nucleocapsids. However, we observed that the contingent of HBV-RNA containing nucleocapsids was overall increased after apoptosis-induction indicating that apoptosis somehow blocks the reverse transcription.

According to our hypothesis that the protein structure of the nucleocapsids changed during maturation, recent publications revealed that only capsids with reverse

transcribed genomes are competent for intracellular budding and virion secretion (Schormann *et al.* 2006, Gerelsaikhan *et al.* 1996). These findings strongly support the theory that HBV nucleocapsids have different constitutions, which might be linked to characteristic densities.

2.3.3 Apoptosis abolished HBV-propagation

Second round infection-experiments of PHH with cell culture medium of either apoptotic or normal hepatocytes documented that the released nucleocapsids were not infectious since they established no HBV cccDNA in the inoculated PHH. (Note that cccDNA represents a prerequisite to initiate the HBV replication in a newly infected cell.) The remaining low-level infection observed was most likely attributed to enveloped virions that were present in the culture medium of apoptotic cells, which we used for inoculation. This assumption is supported by the observation that an intact HBV envelope is necessary for viral entry.

Collectively, this study provides for the first time compelling evidences that apoptosis of HBV-infected hepatocytes seriously blocks the dissemination of HBV progenies in the host. However, we could not rule out the possibility that nucleocapsids released from apoptotic cells are engulfed by surrounding hepatocytes in an *in vivo* situation, which might lead to a productive HBV infection. But even though this kind of viral propagation might take place *in vivo*, it may direct the capsids to the wrong cellular compartment. Since it is hardly conceivable that the virus actively initiates this kind of propagation, our study clearly refutes the generally discussed assumption that apoptosis of infected hepatocytes may facilitate efficient HBV particle spread.

2.3.4 HBV-replicating cell lines are partially resistant to apoptosis

The HBx protein is generally considered as the main regulator of apoptosis. However, most of these observations were obtained from cell culture experiments in which only the HBx protein was over-expressed (Pollicino *et al.* 1998, Terradillos *et al.* 1998, Miao *et al.* 2006, Kim & Seong 2003, Shirakata & Koike 2003). Since the HBx protein is hardly detectable in hepatocytes of infected patients (Su *et al.* 1998) as well as in hepatitis B infected woodchucks (Su & Schneider 1997, Dandri *et al.* 1998), we assumed that over-expression of HBx does not reflect its physiological function.

In this study we analyzed for the first time the apoptotic potential of HBx during HBV replication using HBV transformed hepatoma cell lines. We found that wtHBV-producing hepatoma cells were significantly more resistant towards UV-C-induced apoptosis, whereas ΔxHBV-producing hepatoma cells were as sensible as the parental HepG2 cell line. This result clearly demonstrates that neither HBV replication nor the expression of HBx during viral replication sensitizes host cells towards apoptosis. Furthermore, the result substantiates that HBx increased pro-apoptotic signaling.

Consistent with our data, it has recently been shown that HepG2.2.15 and HBx-expressing HepG2 cells were partially resistant to apoptosis (Pan *et al.* 2001). Pan and coworkers pointed out that the ability of HBx to promote or inhibit apoptosis depends on the hepatocellular differentiation state and whether hepatocytes are quiescent or generating. We support this assumption and revealed that wtHBV-transformed hepatoma cell lines, which released only marginal amounts of HBV particles, were as sensitive to apoptosis as their parental HepG2 cells (data not shown). This observation supports the notion that the cellular differentiation state influences HBV-replication which in turn increases the resistance of the HBV-replicating cell to apoptosis.

2.3.5 HBV-replication does not sensitize cells towards apoptosis on mRNA level

cDNA microarray analyses were performed to identify hepatocellular genes whose transcriptional regulation is tightly linked with HBV-replication in the presence and in the absence of the viral HBx protein. Therefore, we compared the gene expression profiles of parental HepG2 with wtHBV- and ΔxHBV-producing hepatoma cell lines, respectively. The evaluation of the cDNA microarray data sets was restricted to mRNAs encoding for proteins associated with apoptosis and cell survival.

We found that HBV replication influences the cellular basal expression only to a minimal extent, which emphasizes the sophisticated adaptation of the virus to the host. Our observations are in accordance with the cDNA microarray data of acutely HBV-infected chimpanzees (Wieland *et al.* 2004), which shows that HBV does not induce any genes during entry and expansion early in the infection. Therefore, HBV was considered as a stealth virus and the authors proposed this might be linked to the replication strategy of HBV within nucleocapsids.

However, we observed some differences in gene expression profile between HepG2 and HBV-transformed cell lines. We revealed a complex regulation of genes associated with apoptosis and cell survival. In all HBV-transformed cell lines, we found that the balance of mRNAs encoding proteins associated with pro- and anti-apoptotic functions is directed to cell survival. Our observations are in agreement with the cDNA microarray data of wtHBV-infected PHH (Marianna Hösel et al., manuscript in preparation, 2009). Particularly, we found that mRNAs encoding proteins associated with pro-apoptotic functions, like members of the TNF-receptor super family, inhibitors of NFκB signaling, and activators of caspases are down regulated in all HBV-transformed cell lines. This indicates that HBV-replication (i) modulates the transcription machinery of the host independent of the expression of the viral HBx gene and (ii) their modulations do not sensitize cells towards apoptosis. The viral preS/S and pre-S1 proteins (Kekule *et al.* 1990, Ono *et al.* 1998) have previously been described as transcriptional activators which might possibly modify cellular gene expressions.

In contrast to wtHBV-replicating cell lines, we observed that ΔxHBV producing cells exhibited a significantly increased level of mRNAs encoding Bcl-2 family proteins like Bax and Bik. Those proteins have been described to initiate and amplify apoptosis at mitochondrial checkpoints (Adams & Cory 1998, Danial 2007). In keeping with this observation, we hypothesized that the cell autonomous defense mechanism might recognize HBV infection and respond with the up-regulation of pro-apoptotic genes. HBV, however, circumvent the cellular defense mechanisms directly and indirectly. The passive mechanism might be independent of the viral HBx protein and consist of hijacking the cellular transcription machinery and favoring viral gene expressions. The active mechanism, the transcriptional suppression of proteins associated with pro-apoptotic functions like the Bcl-2 family, is probably HBx dependent. Although this theory is encouraging, further excessive examinations are necessary to confirm this preliminary data.

Since apoptosis induction in hepatocytes depends on mitochondrial membrane permeabilization (Scaffidi *et al.* 1998), the suppression of Bax and Bik would provide a highly effective viral escape mechanism. Blocking apoptosis at mitochondrial checkpoints has been described for numerous other DNA viruses like CMV, HSV, HPV, Adenovirus, Myoma virus or Vaccina virus (Ogg *et al.* 2004, Jurak *et al.* 2008,

Stewart *et al.* 2005, Magal *et al.* 2005). However, most of those viruses express viral proteins which directly interfere with Bax (Jurak *et al.* 2008, Sundararajan *et al.* 2001). Down-regulation of the Bax mRNA has been shown for HPV (Magal *et al.* 2005).

In accordance with our data, the gene expression profile of HBV-transformed Huh-6 hepatoma cell lines revealed that Bax is significantly down regulated (Nakanishi *et al.* 2005). Additionally, in agreement with our results, it has been shown that the expression of the hepatocyte-derived secretory IGF binding protein 1 (IGFBP1) is strongly increased during HBV replication. IGFBP1 is a crucial hepatic survival factor: on the one hand, it reduces the extracellular level of pro-apapototic signals (Leu *et al.* 2003) and on the other hand, it binds to Bak and antagonizes mitochondrial pro-apoptotic checkpoints (Leu & George 2007). We assume that HBV specifically up-regulates IGFBP1 to abrogate apoptotic signaling.

In sharp contrast to our results is the gene expression profile analysis of (Han *et al.* 2000) comparing transient HBx-transfected HepG2 with parental cells. This study shows that HBx actively induces the expression of mRNAs encoding proteins associated with pro-apoptotic functions like MCH4, Fast kinase, Bak and GST. The over-expression of HBx and the artificial context might account for this discrepancy. Furthermore, Pan *et al.* (2001) described that in HepG2.2.15 and in HBx-expressing HepG2 cells, Fas-mediated apoptosis is abrogated whereas NFκB signaling is enhanced by down-regulation of IκB mRNA. Our data confirm that HBV replication transcriptionally reduces IκB but this effect is independent of the expression of HBx.

In conclusion, we demonstrated for the first time that induction of apoptosis in HBV-infected hepatocytes interrupts HBV propagation. We support the concept that apoptosis is a powerful antiviral defense mechanism erasing HBV infection. In keeping with this, it is not conceivable that the virus actively sensitizes its host cell towards apoptosis, but rather explains why viral replication abrogates the sensitivity of hepatoma cells towards apoptosis.

3 Experimental Part II:

CD95-induced apoptosis of HBV-infected hepatocytes influenced the priming of B and T cells

The clearance of an acute HBV infection is coupled to the induction of a vigorous polyclonal MHC-I restricted, cytotoxic T lymphocyte (CTL) response to viral antigens expressed by HBV-infected hepatocytes. This adaptive CTL response is essential to eliminate HBV-infected cells by direct lysis, as well as to control viral replication by non-cytopathic mechanisms. The resulting cytodestructive liver inflammation causes the clinical manifestation of an acute HBV infection.

Although it is presently accepted that the control of an acute HBV infection is not simply determined by the cytotoxic potential of CTL (Ando *et al.* 1993, Guidotti *et al.* 1999b, Guidotti *et al.* 1996b, Guidotti *et al.* 1994a), the direct lysis of HBV-infected hepatocytes remains important (Ando *et al.* 1994, Ando *et al.* 1993, Moriyama *et al.* 1990). Particularly, a tremendous study in chimpanzees demonstrated that CTL are the main effector cells responsible for viral clearance by using cytopathic and non-cytopathic defense mechanisms (Thimme *et al.* 2003). Furthermore, previous studies including gene expression analyses of human liver biopsies of chronic HBV carriers (Lee *et al.* 2004, Ibuki *et al.* 2002) and immunological analyses within HBsAg-transgenic mice (Kondo *et al.* 1997), indicated that CD95-induced apoptosis has an essential role in the development of hepatitis. However, the function of CD95-induced apoptosis in clearing an acute HBV infection remains unknown.

The following study was designed to analyze the clearance of an acute HBV infection under conditions where CTL were unable to kill their target cells either by perforin/granzyme or CD95-receptor mediated apoptosis. Therefore, we compared the establishment and the clearance of an acute HBV infection in different mouse lineages. We used lineages that exhibited a generalized, or a conditional hepatocyte-specific deficiency of CD95-receptor signaling, in addition to a lineage that carried a generalized deficiency in perforin/granzyme production. HBV infection was documented by virological, immunological, histopathological, and molecular biological analyses of liver tissue and serum.

3.1.1.1. Mouse model of acute self-limiting HBV infection

HBV virions cannot simply infect mice due to the viral species specificity. However, if HBV genomes are transduced into mouse-hepatocytes, the HBV life cycle is initiated and virions, subviral particles and HBeAg are secreted. In order to transfer HBV genomes, we used systemically applied adenoviral vectors carrying a linearized replication-competent HBV genome (AdHBV) (John von Freyend M. *et al.* 2009, Sprinzl *et al.* 2001).

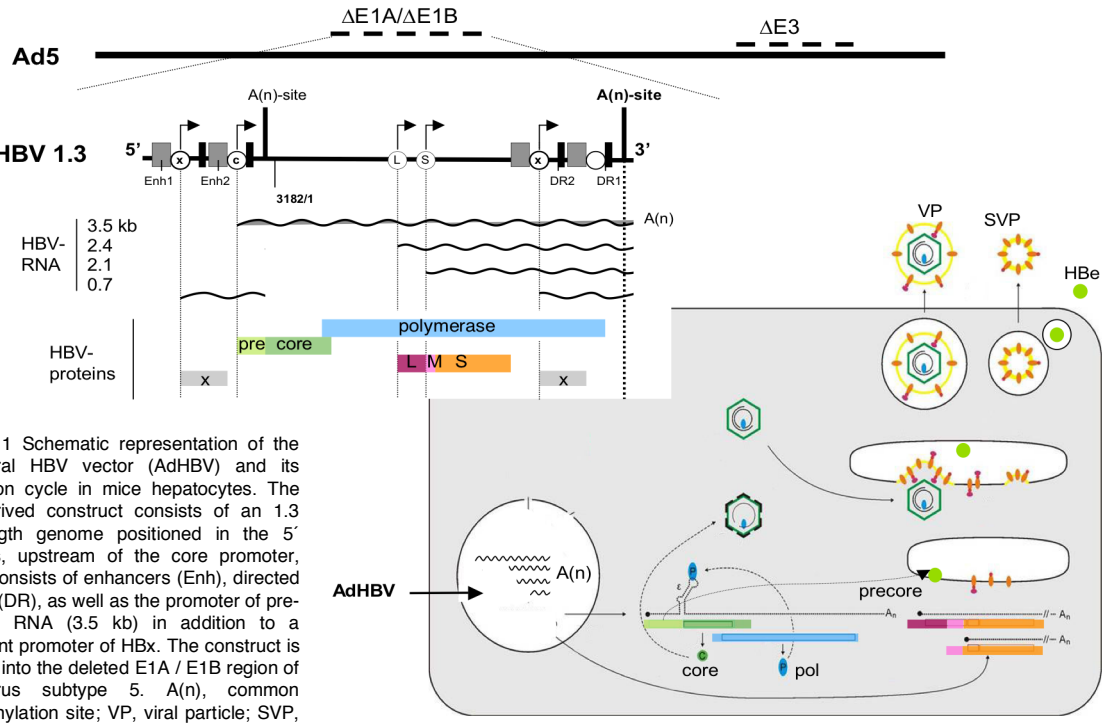

Figure 1 Schematic representation of the adenoviral HBV vector (AdHBV) and its replication cycle in mice hepatocytes. The HBV-derived construct consists of an 1.3 over-length genome positioned in the 5´ terminus, upstream of the core promoter, which consists of enhancers (Enh), directed repeats (DR), as well as the promoter of pre-genomic RNA (3.5 kb) in addition to a redundant promoter of HBx. The construct is inserted into the deleted E1A / E1B region of adenovirus subtype 5. A(n), common polyadenylation site; VP, viral particle; SVP, subviral particle

The AdHBV construct is depicted in Figure 1: it consists of a 1.3 over-length HBV genome inserted into the deleted E1 site of the adenoviral genome. Thus, the vector is replication-deficient if E1 proteins are not complemented *in trans*. By contrast, HBV replication can take place in the cytoplasm of hepatocytes via reverse transcription of the 3.5 kb pre-genomic HBV-RNA. Thus, the HBV replication-cycle is independent of the adenoviral genome's replication cycle. Although the AdHBV vectors have no liver-tropism, HBV transcription is exclusively initiated within hepatocytes because HBV promoters control the transduced HBV genomes, which themselves require hepatocellular transcription factors (Quasdorff *et al.* 2008, Guidotti *et al.* 1995).

3.2. Progression of acute HBV infection in mice deficient for different stimuli of apoptosis

In the first mouse experiment, we compared the clearance of an acute HBV infection in congenic C57BL/6 lineages harboring a generalized deficiency for CD95-signaling, or perforin/granzyme mediated apoptosis, respectively.

- The *gld* lineage expresses non-functional Fas ligands (FasL) on cell surfaces due to a natural spontaneous point mutation within the coding region of the FasL gene (Takahashi et al., 1994): phenylalanine has been replaced by leucine, which abolishes the ability of FasL to bind to the Fas receptor. Therefore, lymphocytes of *gld* mice are unable to kill target cells by CD95-mediated apoptosis.

- The *perforin* knockout (*k/o*) lineage carried a targeted mutation in the pore-forming protein. Those mice exhibit normal numbers of CD8+ and NK cells, but they are deficient for perforin-mediated apoptosis. Therefore, *perforin k/o* mice cannot clear certain viral infections, e.g., lymphocytic choriomeningitis (Kagi *et al.* 1994a).

- The C57BL/6 are the control (wild-type) lineage containing a functional immune system.

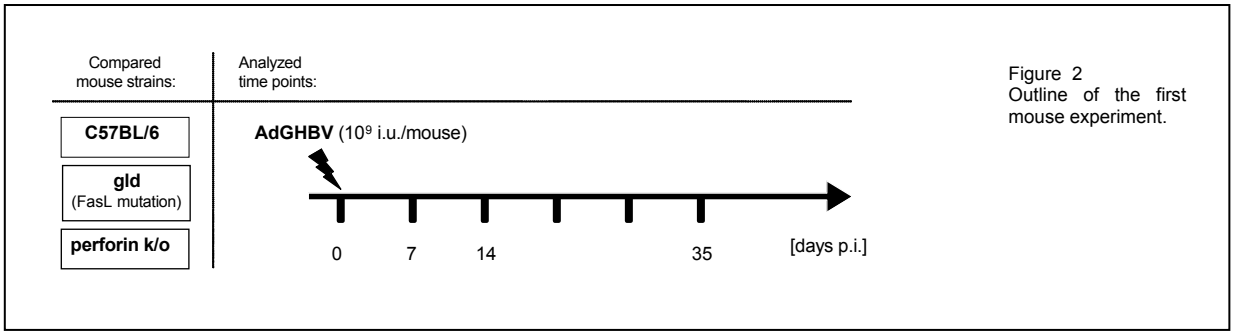

Figure 2
Outline of the first mouse experiment.

Figure 2 represents an overview of the first mouse experiment. Mice were intravenously injected into the tail vein using an amount of infectious units (i.u.) of 10^9 AdGHBV. The applied adenoviral vector carried additional to the 1.3 overlength HBV genome, the DNA sequence for the green fluorescent protein (GFP). Therefore, we were able to track transduced tissues by monitoring GFP-expression. All mice were challenged with the same batch of AdGHBV. Two mice of each lineage were left untreated and served as controls (day 0). Seven, fourteen and thirty-five days post infection (p.i.), three mice per lineage were sacrificed and analyzed as listed below. The mice we used were twelve- to sixteen-weeks old.

3.3. Results I

3.3.1 Serology

At first, we monitored the establishment of an acute HBV infection by diagnostic markers including: HBeAg, HBsAg and ALT (Takahashi *et al.* 1976). HBeAg is a non-structural viral protein that is secreted into the circulation. The amount of HBeAg in serum well correlates to the level of HBV-replication (Magnius & Espmark 1972). The HBsAg is a structure component of all HBV envelope proteins present in the lipomembrane of all released viral-particles including virions and SVP. Pathological alanine aminotransferase (ALT) levels in serum (>60 U/l) characterizes the manifestation of liver-inflammation caused by the immune attack of CTL (Chisari *et al.* 1989).

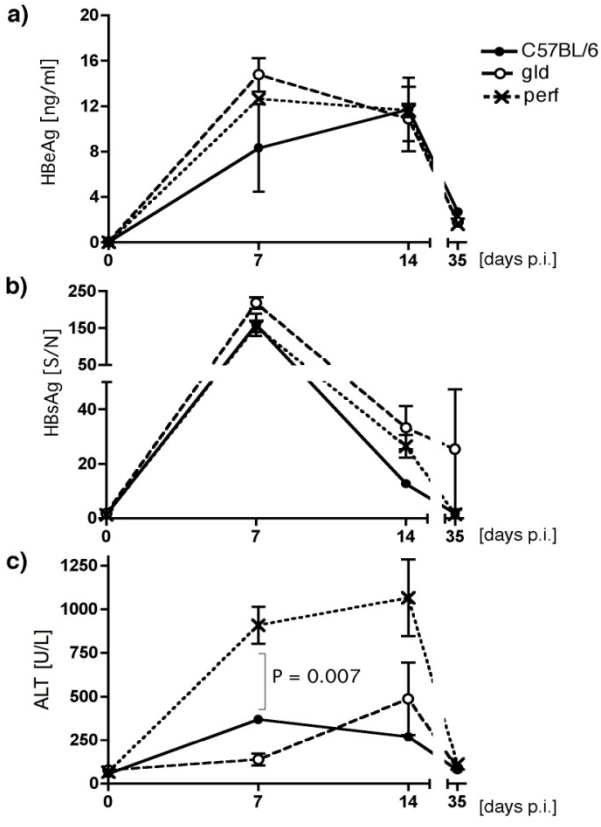

Figure 3 Establishment of an acute HBV-infection monitored by serological parameters.
HBeAg (a) and HBsAg (b) titers were determined in mouse serum diluted in PBS (1:20) before the Axsym was performed. The obtained S/Co ratio of HBeAg was converted to ng/ml by applying a standard curve. (c) Detection of liver injury by release of alanine aminotransferase (ALT) in undiluted mouse serum. Data represent means ± standard deviation of the results of 3 mice per group.

As shown in Figure 3, high levels of HBeAg and HBsAg were detected in the serum of all lineages at 7 days p.i.. The dynamics were quite similar between the lineages during the studied period of time (Fig.3 a+b): the highest HBeAg and HBsAg levels were measured at 7 days p.i.; HBeAg levels remained constant up to 14 days p.i., whereas HBsAg declined about 90% between 7 and 14 days p.i.. At 35 days p.i., HBeAg and HBsAg levels returned to the baseline in *perforin k/o* and C57BL/6 mice.

By contrast, HBsAg levels in the *gld* mice remained elevated (but note the high standard deviation) (Fig. 3b), despite detecting a decline of HBeAg (Fig. 3a).

The ALT levels differed significantly (P=0.007) between the lineages after AdGHBV injection (Fig. 3c): the highest elevation of ALT at about 15-fold was detected in sera of *perforin k/o* mice at 7 and 14 days p.i.. By contrast, C57BL/6 and *gld* mice exhibited approximately an 8-fold increase in ALT levels at 7 or 14 days p.i., respectively. It is important to note that the ALT levels of *gld* mice rose at later time points (14 days p.i.) compared with C57BL/6 and *perforin k/o* mice (7 days p.i.) (Fig. 3c). At 35 days p.i., normal ALT levels, without any pathological findings, were documented in all lineages indicating the termination of liver inflammation.

Taken together:

1) All mice lineages (C57BL/6, gld, and perforin k/o) developed a productive HBV infection at 7 days p.i..

2) We observed extremely high ALT levels in perforin k/o mice at 7 and 14 days p.i. for still undefined reasons.

3) The gld lineage showed two distinctive features: (i) ALT elevations were not detected before 14 days p.i. and (ii) HBsAg levels remained increased up to 35 days p.i.. The data suggested that a deficiency in CD95-receptor signaling might lead to a delayed induction of an effective immune response against HBV.

3.3.2 Viral transcription and replication in liver tissue

To analyze HBV transcription and HBV virion production independently of surrogate parameters like HBeAg and HBsAg, we performed Northern blot analyses (Fig.4a) and quantitative PCR (qPCR) reactions (Fig.4b).

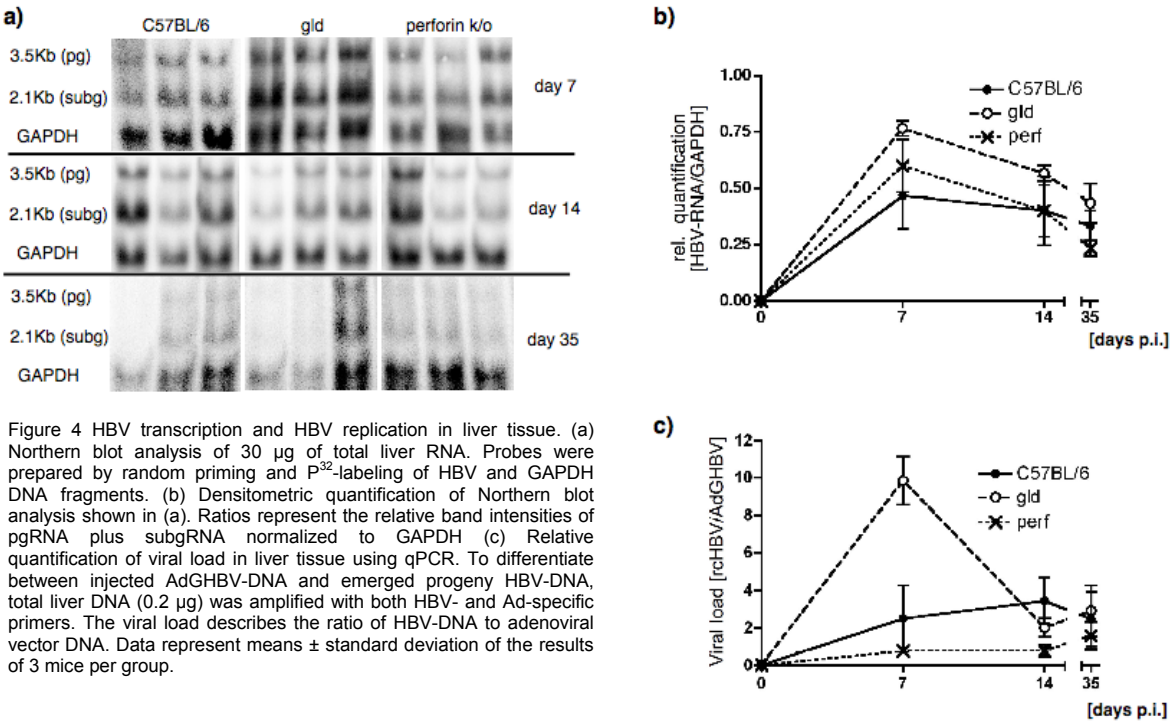

Figure 4 HBV transcription and HBV replication in liver tissue. (a) Northern blot analysis of 30 µg of total liver RNA. Probes were prepared by random priming and P^{32}-labeling of HBV and GAPDH DNA fragments. (b) Densitometric quantification of Northern blot analysis shown in (a). Ratios represent the relative band intensities of pgRNA plus subgRNA normalized to GAPDH (c) Relative quantification of viral load in liver tissue using qPCR. To differentiate between injected AdGHBV-DNA and emerged progeny HBV-DNA, total liver DNA (0.2 µg) was amplified with both HBV- and Ad-specific primers. The viral load describes the ratio of HBV-DNA to adenoviral vector DNA. Data represent means ± standard deviation of the results of 3 mice per group.

Seven days after AdGHBV injection, we detected HBV-RNA in liver tissue of all lineages (Fig.4a). The ratio of subg- to pgRNA was approximately 2:1 up to 3:1 indicating that the transcription of the subgRNAs was much more efficient than of pgRNAs. We detected about 1.9-fold and 1.5-fold higher HBV-RNA levels in *gld* and *perforin k/o* mice, respectively, than in C57BL/6 mice (Fig.4b). HBV-RNA levels declined in all lineages during the studied time period; however, HBV-RNA were still detectable 35 days p.i. (Fig.4a).

Significant differences were detected in the levels of hepatic HBV-DNA (viral load) between the lineages (Fig.4c): *gld* mice exhibited a 5-fold higher viral load at 7 days p.i. than C57BL/6 mice. Thus complements the previous observation that the onset of an antiviral immune response is delayed in *gld* mice (Fig.3). In parallel with the ALT elevation at 14 days p.i. (Fig.3c), the hepatic HBV-DNA decreased dramatically in *gld* mice at 14 days p.i. (Fig.4c). By contrast, hepatic HBV-DNA levels of *perforin k/o* mice remained nearly undetectable during the entire study period (Fig.4c). This

observation is disputable because we detected the same amount of HBsAg at 7 days p.i. in *perforin k/o* than in C57BL/6 or *gld* mice, respectively (Fig.3b).

In summary:

1) Viral transcription was detected in all lineages over the observed period of time. The highest amount of HBV-RNA was observed at 7 days p.i., afterwards the viral RNA levels declined constantly.

2) High levels of HBV replication (intrahepatic HBV-DNA) were determined in gld mice 7 days post infection. By contrast, the viral load in perforin k/o mice remained at background levels for hitherto unknown reasons.

3.3.3 Intrahepatic T cell response

In order to monitor the intrahepatic antiviral immune response in addition to ALT measurement (Fig.3c), we characterized the lymphocyte infiltration into liver tissue by biomolecular methods (Fig.5). Thus, we quantified the relative amount and composition of liver associated lymphocytes (LAL) at indicated time points by gene expression analysis of lymphocyte-specific cell surface markers (CD4 and CD8) and lymphocyte-derived cytokines (IFN-γ). Note that the principal cellular sources of IFN-γ secretion are T_H1 CD4, activated NK and CD8 T cells. Therefore, detection of IFN-γ during an acute HBV-infection should correlate with T cells responses that recognize HBV-infected hepatocytes through representing viral antigens on MHC molecules class I.

C57BL/6 and *perforin k/o* mice show the same dynamic of intrahepatic T cell infiltrations after HBV infection, however the magnitudes of T cell expression levels were different. At 7 days p.i., we detected a surge of hepatic CD8 and IFN-γ mRNA levels, which was about 70-fold and 7-fold, respectively, in C57BL/6 and about 24-fold and 3-fold, respectively, in *perforin k/o* mice. The levels of CD8 mRNA remained increased at 14 days p.i., whereas IFN-γ returned almost completely to the pre-injection level. At 35 days p.i., CD8 and IFN-γ mRNA levels correspond to pre-injection levels. In contrast to C57BL/6 and *perforin k/o* mice, the *gld* lineage showed a temporal delayed T cell response to HBV. Increased hepatic CD8 and IFN-γ mRNA levels were not detected until 14 days p.i., but they remained elevated up to 35 days p.i..

Throughout the lineages we detected more than 10-fold lower CD4 mRNA levels than those of CD8.

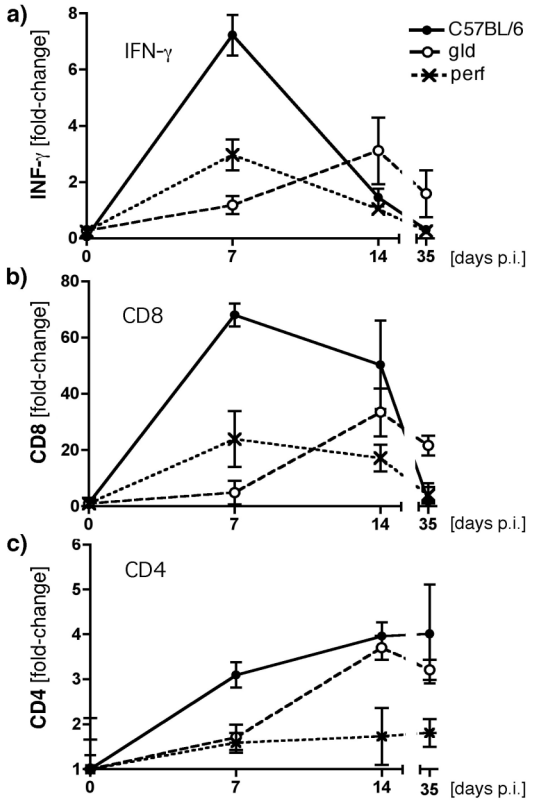

Figure 5 Dynamics of intra-hepatic T cells during the cause of acute HBV infection. Gene expression of IFN-γ (a), CD8 (b) and CD4 (c) were analyzed at indicated time points using qPCR. 0.7 μg of total liver RNA was reversed transcribed and applied for qPCR analysis using specific primers for target and reference genes, respectively. Values of indicated target genes were normalized to GAPDH. Data represent the relative levels of gene expression of HBV challenged mice compared to control (d 0). Data include means ± standard deviation of the results of 3 mice

Taken together:

1) All lineages showed a surge of intrahepatic CD8 and IFN-γ mRNA levels 7 days p.i. indicating that the elicit immune response mainly depends on activated CTL.

2) The intrahepatic T cells infiltration was more than 3.5-fold lower in gld and perforin k/o mice compared with C57BL/6 mice suggesting that apoptosis induction via CD95 and perforin/granzyme release act synergistically to induce a vigorous T cell response to HBV.

3) Two distinctive features were observed in gld mice: delayed intrahepatic T cell infiltration and elevated CD8 T levels up to 35 days p.i.. Thus, we speculate that the CD95-receptor signaling pathway is important for a rapid induction of a HBV-specific immune response.

3.3.4 Seroconversion

We documented the establishment of a humoral immune response to HBV by determining antibodies (Ab) to hepatitis B surface antigens (*anti*-HBs) in mouse sera of all lineages at 35 days p.i..

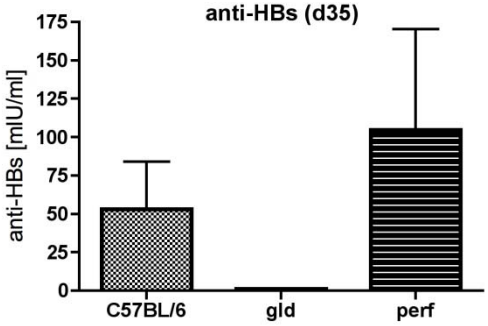

Figure 6 Anti-HBs Ab production at 35 days p.i.. Titers were determined in mouse serum diluted in PBs (1:20) before Axsym assay was performed. Data represent means ± standard deviation of the results of 3 mice per group.

As shown in Figure 6, the lineage C57BL/6 and *perforin k/o* developed *anti*-HBs *Ab* whereas no *anti*-HBs *Ab* were detectable in the *gld* lineage.

Since we wondered about the absence of *anti*-HBs Ab in the serum of the *gld* mice, we determined neutralizing *anti*-Adeno *Ab* to exclude that those lineage exhibit a generalized deficiency in the humoral immune response. For this purpose we performed AdGHBV infection assays on Hek293 cells in the presence of serum from AdGHBV challenged and non challenged *gld* mice. The idea is that if neutralizing *anti*-Adeno *Ab* were present in the serum of challenged *gld* mice, no productive infection should be possible.

A positive AdGHBV infection in Hek293 cells is generally documented by two parameters: first, through GFP expression and second, through the cytopathic cell destruction as a result of adenoviral vector progeny release at later time points.

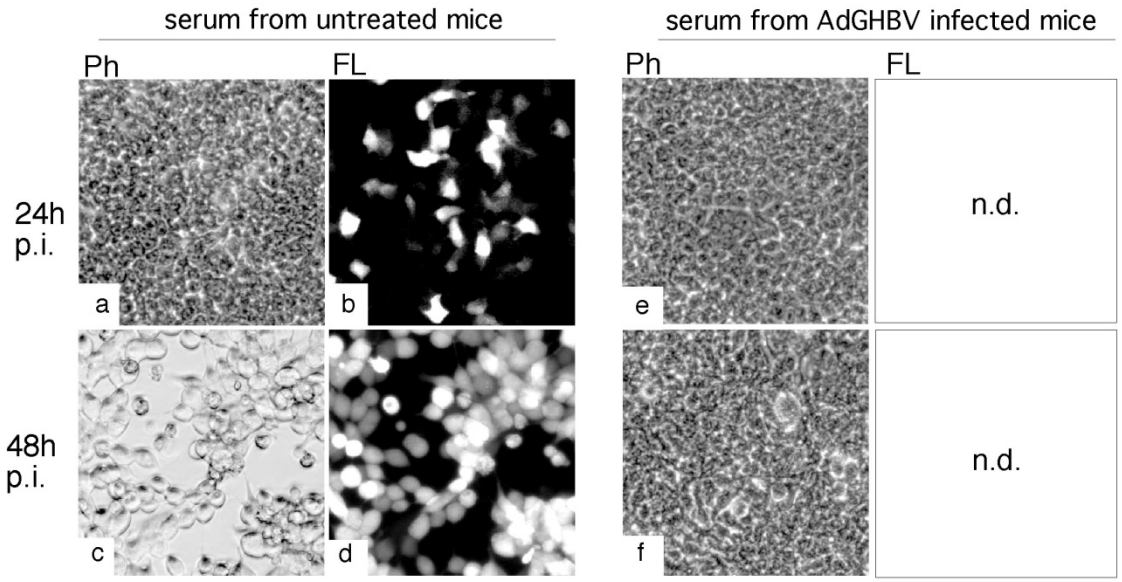

Figure 7 Neutralizing anti-Adeno Ab in sera of gld mice. Pictures show Hek293 cells 24 h and 48 h after infection with AdGHBV ($5x10^8$ particles) in the presence of 20 µl mice sera obtained from control group (a-d) and AdGHBV challenged mice at 35 days p.i. (e+f). Phase-contrast (Ph) microscopy points out cythopatic effect upon productive adenovirus infection (c). Fluorescence (FL) microscopy visualized GFP expression in AdGHBV infected cells (b+d). No fluorescence was observed in Hek293 cells infected with AdGHBV plus serum of challenged mice. (Original magnification, x100)

As shown in Figure 7, Hek293 cells infected with AdGHBV pre-incubated with sera of unchallenged *gld* mice showed a productive adenoviral infection (Fig.7 b,c,d). By contrast, no infection was observed by pre-incubating AdGHBV particles with sera of AdGHBV challenged *gld* mice (Fig.7 e+f). This result clearly shows that neutralizing *anti*-Adeno Ab are present in the serum of AdHBV challenged mice.

In summary, C57BL/6 and perforin k/o mice developed a humoral immune response to HBV at 35 days p.i.. In sharp contrast, no anti-HBs Ab were found in the gld lineage. However, we detected neutralizing anti-Adeno Ab in all lineages. Therefore, we assumed that CD95-receptor signaling is necessary for the induction of an efficient humoral immune response to HBV by a still unknown mechanism.

3.3.5 Histology

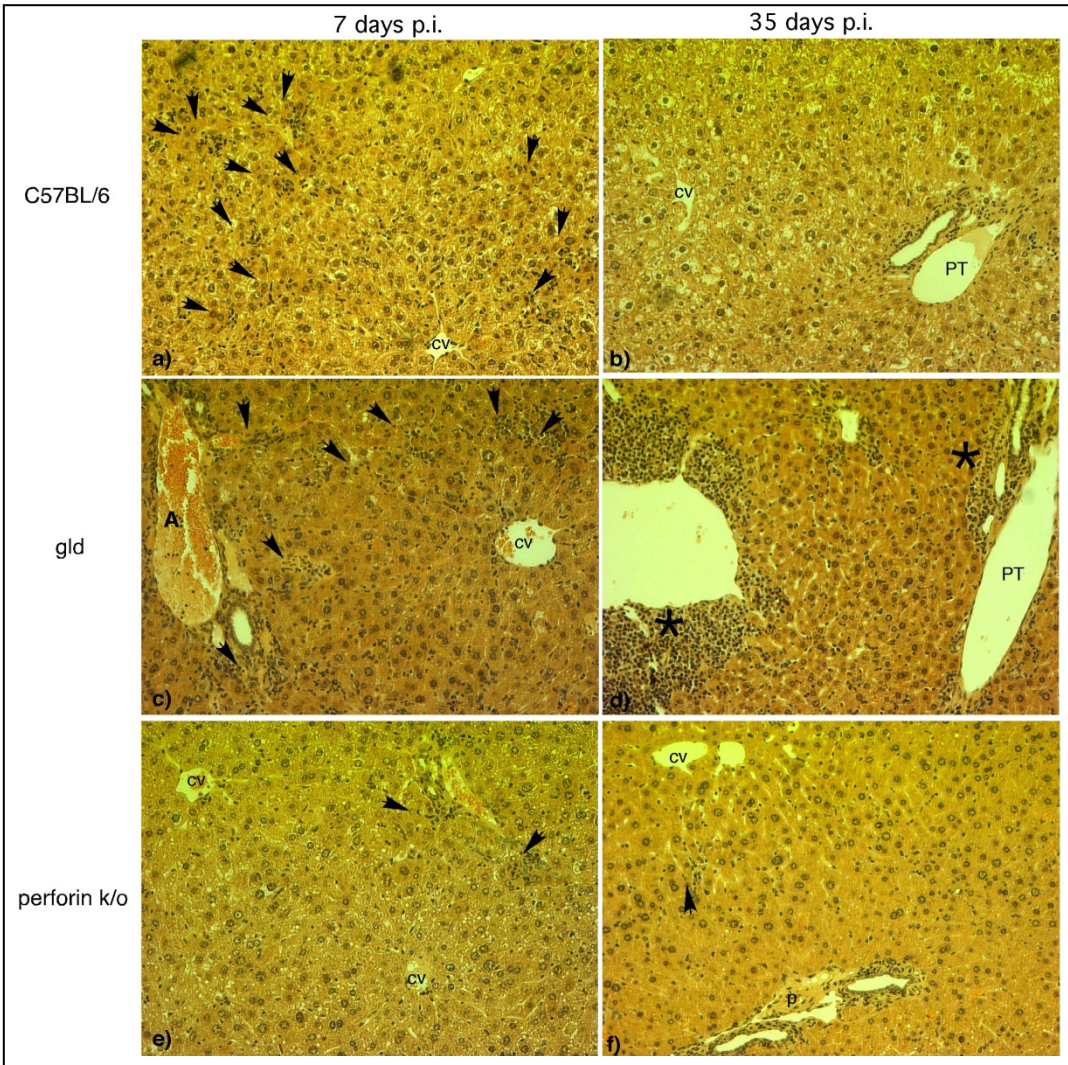

Figure 8 Histopathological manifestations of acute hepatitis in mice at 7 (a,c,e) and 35 (b,d,f) days p.i.. Liver tissues were stained with H&E (orginal magnification, x200). Arrows indicate necroinflammatory foci; Asterisks mark portal inflammatory infiltration; P, portal tract; CV, central vein

The histopathological examination confirmed that all three lineages developed an acute hepatitis seven days after AdGHBV injection, characterized by mononuclear infiltrates into the liver parenchyma and numerous sinusoidal inflammatory foci (Fig. 8 a,c,e). The highest extent of inflammatory activity was found in C57BL/6 mice at 7 days p.i. (Fig. 8a) whereas the lowest one was documented in *perforin k/o* mice (Fig. 8b). This result is unexpected because the ALT levels of *perforin k/o* mice were extremely high at 7 days p.i. (Fig. 3c). Importantly, at 35 days p.i. we found distinctive histological features between the lineages: C57BL/6 and *perforin k/o* mice showed increased regenerating activities in liver tissue characterized by a disarray of liver cells and nuclei with different sizes (Fig.8 b+d). By contrast, the *gld* lineage exhibited a massive accumulation of mononuclear cells around the portal tract (Fig.8f) also observed as a sign of chronic hepatitis.

3.4. The Clearance of acute HBV infection in mice harboring a hepatocyte-specific deficiency of CD95-receptor signaling

Based on the results presented above, we assumed that an intact CD95-receptor signaling pathway is important for the rapid induction of HBV-specific immunity as well as for the development of a long-lasting protection against HBV infection. However, we could not exclude that the *gld* lineage bears an immature immune system that was concurrently causative for the incomplete viral clearance.

In order to assess the functional significance of CD95-induced apoptosis of HBV-infected hepatocytes in more detail, we took advantage of liver specific conditional $FADD_{hep}$ k/o mice. This transgenic (*tg*) mouse lineage exhibits a complete executable immune system but the CD95-receptor signaling is impaired in hepatocytes due to the cell-specific deletion of FADD, an essential adaptor protein of the CD95-signaling cascade. Therefore, CTL cannot kill HBV-infected hepatocytes by CD95-mediated apoptosis.

In the following experiments we therefore analyzed the clearance of an acute HBV infection in $FADD_{hep}$ k/o mice. A second objective in this study was to determine whether the *gld* lineage developed a humoral immune response to HBV at later time points. Moreover, in contrast to the first mouse experiment (4.1.2), we monitored the dynamics of acute HBV infection in all lineages more frequently.

3.4.1 Hepatocyte-specific FADDhep k/o Mice

The hepatocyte-specific conditional FADD k/o mouse lineage has been engineered in the lab of Prof. Dr. M. Pasparakis, it based on the Cre-lox technology, a site-specific recombination methode: the FADD gene has been flanked with loxP sites in the germline of C57BL/6 mice. Therefore, the genetic modified C57BL/6 lineage carries floxed FADD (fl) genes. If FADD floxed mice are crossed back with a second tg C57BL/6 lineage that carry the cre recombinase (Cre+) gene under the control of a hepatocyte specific albumin promotor, a hepatocyte-specific $FADD_{hep}$ k/o lineage emerged. Since the floxed FADD gene are deleted in hepatocytes of littermates conditional on hepatic Cre expression.

In the following experiment we worked with two different subtypes of transgenic FADD mice: both subtypes of were homozygous for the floxed FADD gene (FADD fl/fl) but only one subtype additionally carried the heterozygote Cre recombinase (cre -/+) under the control of an albumin promotor. In order to obtain mice that were FADD positive (+) or FADD negative (-) in hepatocytes, we matched FADD(+)$_{hep}$ *[FADD fl/fl; Cre -/-]* with FADD(-)$_{hep}$ *[FADD fl/fl; Cre +/-]* mice for breeding corresponding to a likelihood of 50% to obtain FADD(+)$_{hep}$ and FADD(-)$_{hep}$ mice, respectively.

3.4.1.1. Genotyping

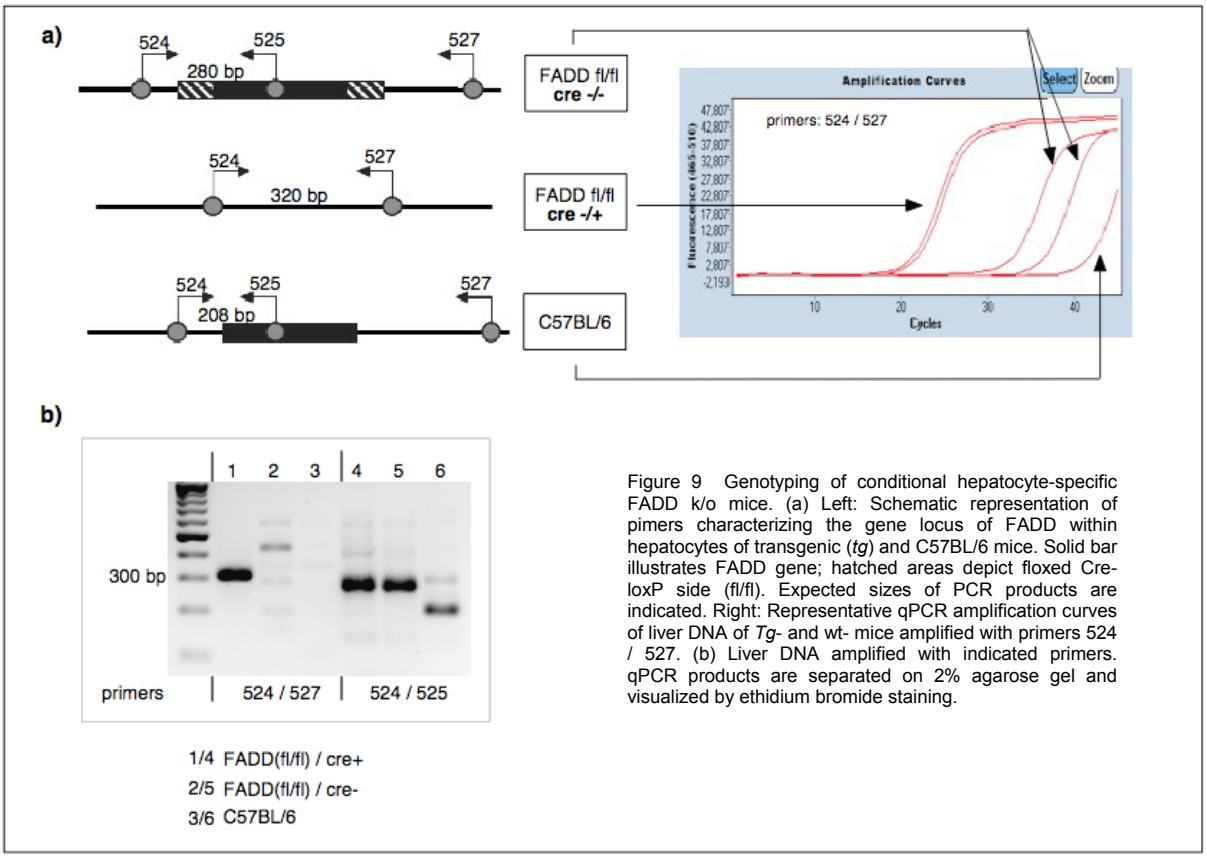

Figure 9 Genotyping of conditional hepatocyte-specific FADD k/o mice. (a) Left: Schematic representation of pimers characterizing the gene locus of FADD within hepatocytes of transgenic (*tg*) and C57BL/6 mice. Solid bar illustrates FADD gene; hatched areas depict floxed Cre-loxP side (fl/fl). Expected sizes of PCR products are indicated. Right: Representative qPCR amplification curves of liver DNA of *Tg*- and wt- mice amplified with primers 524 / 527. (b) Liver DNA amplified with indicated primers. qPCR products are separated on 2% agarose gel and visualized by ethidium bromide staining.

It is important to note that we characterize the phenotype of the FADD mice twice:

1. At birth, we screened somatic cells obtained from the tails of the littermates to the presence and absence of the cre gene. This information was used to refer back to their genetic phenotype in hepatocytes: FADD(-)$_{hep}$ or FADD(+)$_{hep}$.

2. On the day of sacrifice, we confirmed the hepatocyte-specific deletion of FADD gene by real time qPCR analysis (Fig.9a). Thus, we characterized genomic DNA from liver tissue by two different sets of primers: the first primer set named 524/527 amplified a specific DNA sequence conditional on the floxed FADD gene has being

removed (Fig.9a). The second primer set denoted 524/525 amplified a specific DNA sequence that requires the presence of the FADD gene. Thus, we used the second primer-set in order to document that the FADD gene had been removed in hepatocytes but not in all other hepatic cell types such as LSEC, LAL or Kupffer cells (Fig.9b).

3.4.2 Experimental Design

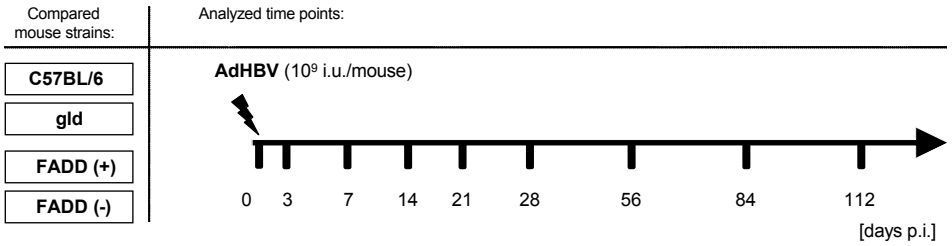

Figure 10 Outline of the second mouse experiment:

Figure 10 represents an overview of the second mouse experiment. The four different lineages (C57BL/6, *gld*, FADD(+)$_{hep}$, and FADD(-)$_{hep}$) were intravenously challenged with the same batch of AdHBV (10^9 i.u.). At indicated time points, four mice per strain were sacrificed. Subsequently, we increased the number of animals for the later time points up to twelve mice. Thus, it was unavoidable to change the virus batch due to its restricted availability. Seven days after injection, we bled all mice and checked the establishment of an acute HBV infection by ALT measurement (data not shown).

3.5. Results II

3.5.1 Serology

We monitored the dynamics of an acute HBV-infection by serological parameters (as described in 3.3.1). As shown in Figure 11, the dynamics of HBV-infection were quite similar between the lineages. The establishment and the clearance of an acute HBV infection mainly occurred within the first 28 days p.i.. Within this period of time, we could define three distinct stages, which were partially specific for the respective mouse lineages.

The first stage can be defined up until 7 days p.i., reflecting the establishment of acute HBV infection. High levels of HBeAg, HBsAg and viremia were already detectable at 3 days p.i. in all lineages. By contrast, ALT levels were not elevated until 7 days p.i.. The virological parameters in C57BL/6 and *gld* mice remained constant during this period. However, we had already detected a decline of HBeAg and virimia in FADD mice of about 1.4-fold (Fig.11b) and 2-4 logs (Fig.11f), respectively, during 3 and 7 days p.i..

The second stage is defined between 7 and 21 days p.i.. It is characterized by a substantial decline of all virological parameters throughout the lineages. In C57BL/6 and *gld* mice, the HBeAg levels decreased similarly about 2.3-fold (Fig.11a). Interestingly, the dynamic of HBsAg and viremia were significantly different (P=0.006; P=0.003) in those lineages (Fig.11 c+e): in C57BL/6 mice the levels of HBsAg and viremia decreased continuously about 5-fold and 4 logs whereas in *gld* mice the level of HBsAg and viremia declined to a minor extent about 1.6-fold and 1 log. In accordance with this observation, we measured 2-fold reduced ALT levels in *gld* mice compared with C57BL/6 at 7 days p.i. (Fig.11g). All these data indicate that *gld* mice combat the HBV infection less efficiently.

The dynamics of lineage FADD showed distinctive features to C57BL/6 and *gld* during the regarded period of study. However, we found no significant differences between FADD$(+)_{hep}$ and FADD$(-)_{hep}$ mice: between 7 and 14 days p.i., the levels of HBeAg remained constant, whereas HBsAg declined about 4-fold (Fig.11b+d). Moreover, the HBsAg levels were generally 2-fold lower in FADD mice compared to C57BL/6 and *gld* (Fig.11d). For this observation was no obvious explanation because the levels of HBeAg were quite comparable throughout the lineages. Furthermore,

FADD exhibited higher, and particularly prolonged elevated ALT levels that increased until 14 days p.i. (Fig.11h). Notably, the rising of ALT was reciprocal to HBsAg and viremia, suggesting that the antiviral immune response blocked HBV replication.

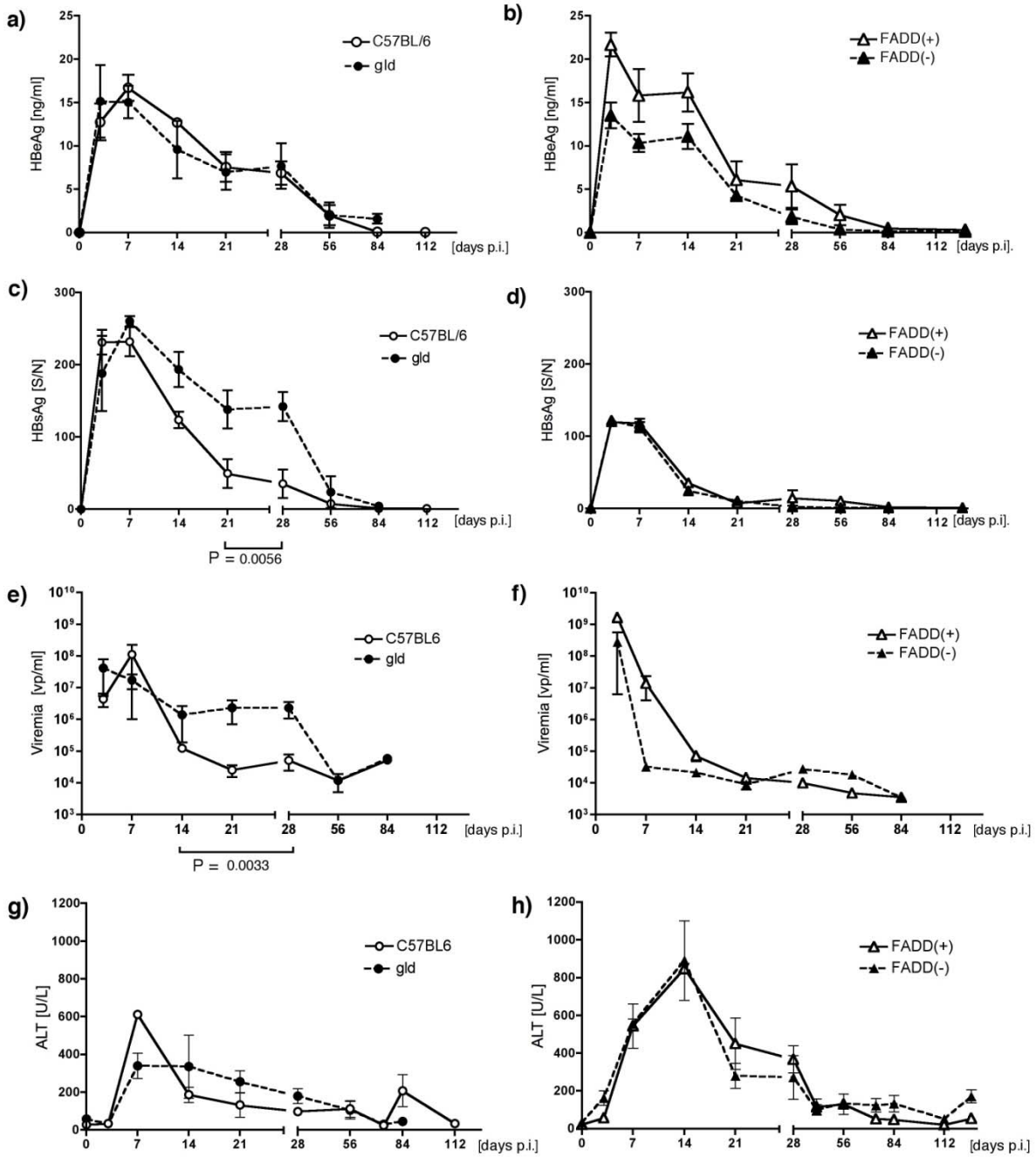

Figure 11 Comparative dynamics of acute HBV infection characterized by serological parameters including HBeAg, HBsAg, viremia, and viral load in liver tissue. HBeAg (a,b) and HBsAg (c,d) titers were determined in mouse serum diluted in PBS (1:20) before Axsym assay was performed. The obtained S/Co ratios of HBeAg were converted to ng/ml by applying a standard curve. (e,f) Viremia. Viral DNA was extracted from 50 µl serum. HBV-DNA levels were determined by qPCR using rcHBV-DNA specific primers and calculated in copy/ml relative to plasmid-HBV standard. (g,h) Detection of liver injury by ALT measurement in undiluted mouse serum. Data represent means ± standard deviation of the results of 4 mice per group. Statistical significance (between indicated mice lineages) was performed by a student´s t-test

The third stage of an acute HBV infection is defined between 21 and 28 days p.i.. All virological parameters remained constant. Remarkably, the levels of HBsAg and

virimia in *gld* mice were still elevated, indicating that the onset of an antiviral immune response was markedly delayed.

Between 28 and 56 days p.i., almost all virological parameters declined to background levels in all lineages. Interestingly, we observed a flare-up of ALT levels in C57BL/6 mice around 84 days p.i.. This observation is concurrent with studies of Miriam John von Freyend (John von Freyend et al., submitted 2009).

Taken together:

1) Upon AdHBV infection, all mice lineages developed a productive infection at day 3 p.i. which has been cleared approximately after 2 months. High levels of HBeAg were determined in all lineages until 28 days p.i., whereas HBsAg declined at 7 days p.i.. The data suggest that virion and SVP secretion, on the one hand, and HBV transcription, on the other hand, might be controlled by different cellular defense mechanisms.

2) The levels of HBsAg were significantly lower in FADD than in C57BL/6 and gld mice, respectively. However, the ratios of HBeAg and virimia were comparable between the lineages at 3 days p.i.. Therefore we assumed that FADD mice produced lower amounts of subviral particles for still undefined reasons.

3) It is important to note that the dynamic of ALT is different between FADD and C57BL/6 or gld mice, respectively. We observed that the levels of ALT, viremia and HBsAg peaked at the same time in C57BL/6 and gld mice, whereas in FADD mice the ALT levels raised reciprocal. This might be linked to different antiviral defense mediators present in the respective lineage.

4) Comparing the dynamic of ALT in gld mice with previous results (see first mouse experiment 3.3.1 Fig.3c), we could not confirm the delay in the onset of ALT elevation. Nevertheless the levels of HBsAg, viremia, and ALT levels remained increased in gld mice up to 28 days p.i.. This corroborates the notion that gld exhibits an attenuated immune response against HBV. However, it remains a matter of debate if the attenuated immune response of gld mice is related to a deficiency of CD95-mediated apoptosis of HBV-infected hepatocytes because hepatocyte-specific FADD(-)$_{hep}$ mice showed no increased levels of *HBsAg, viremia, and ALT up to 28 days p.i..*

3.5.1.1. Viral transcription and replication in liver tissue

We determined HBV-replication and HBV-transcription in liver tissue by real time PCR and Northern blot analysis. The dynamics of HBV replication (Fig.12 a+b) can be divided into two different stages characterized by the two distinct peaks of hepatic HBV-DNA.

The first HBV-DNA peak was detected at 3 days p.i. in C57BL/6, FADD(+)$_{hep}$, and FADD(-)$_{hep}$ mice. This was followed by a 1.2-fold reduction until 7 days p.i.. By contrast, the viral load in *gld* constantly increased up to 7 days p.i. and declined 2-fold until 14 days p.i. (Fig.12a).

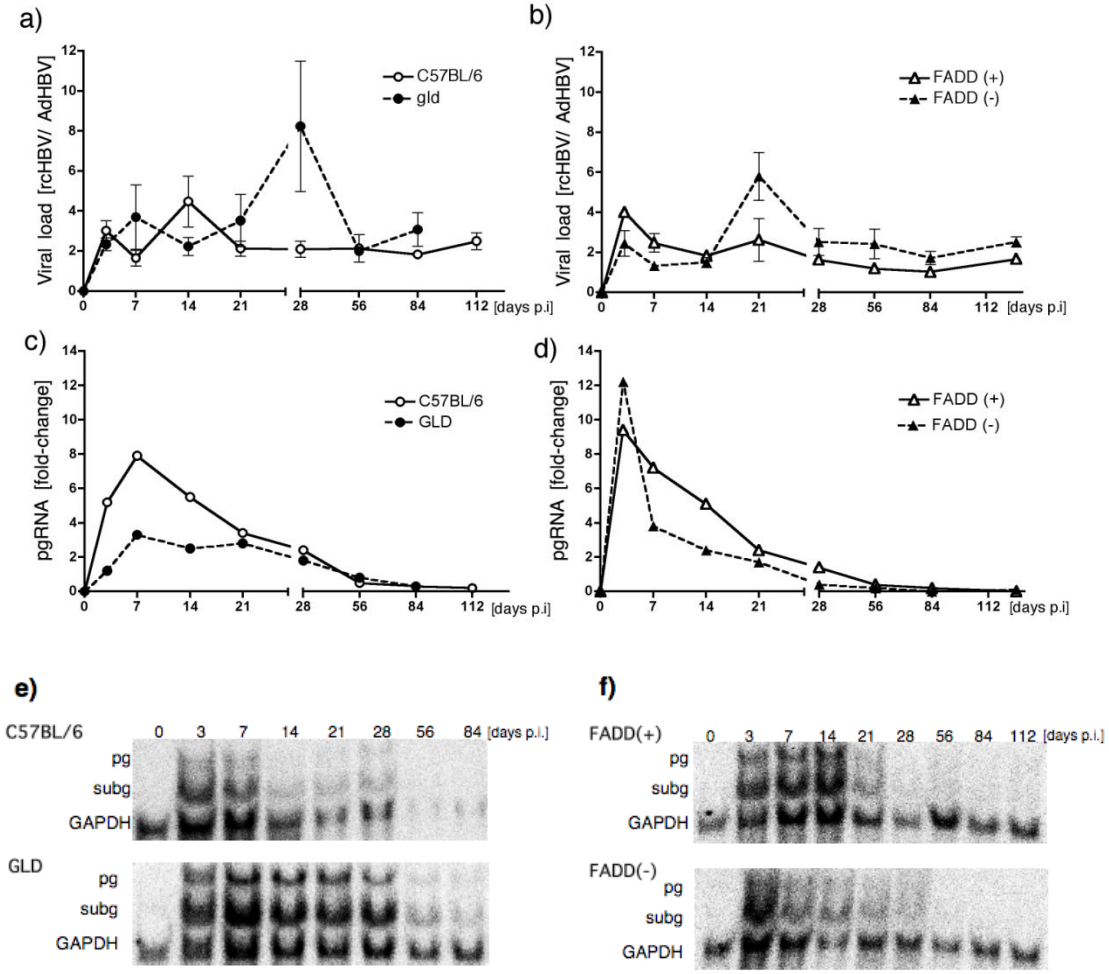

Figure 12 HBV transcription and replication within liver tissue. (a,b) Viral load quantified by qPCR. To differentiate between injected AdHBV-DNA and progeny HBV-DNA, total liver DNA (0.2 µg) was amplified with both HBV- and Ad-specific primers. The viral load describes the ratio of HBV- to adenoviral vector DNA. Data represent means ± standard deviation of the results of 4 mice per group. (c,d) Relative quantification of pgRNA was performed using qPCR. 0.7 µg of total liver RNA was reversed transcribed and applied for qPCR analysis using specific primers for pgRNA, GAPDH, and HPRT, respectively. Values show normalized ratios of pgRNA to the mean of GAPDH+HPRT (reference genes). (e,f) Northern blot analysis of 30 µg of total liver RNA (pool of 4 mice per group). ^{32}P-labeled HBV- and GAPDH DNA specific probes were prepared by random priming. pg, pregenomic HBV-RNA; subg, subgenomic HBV-RNA)

The second stage of HBV replication differs in magnitude and time between all lineages. It is important to note that the second intrahepatic HBV-DNA elevation was much more pronounced in *gld* and FADD(-)$_{hep}$ mice.

In C57BL/6 mice, the viral load increased 2-fold between 7 and 14 days p.i., whereas in *gld* mice the second hepatic HBV-DNA peak was 7 days delayed, 6-fold increased and prolonged. In FADD(+)$_{hep}$ and FADD(-)$_{hep}$ mice, the hepatic HBV-DNA level increased simultaneously between 14 and 21 days p.i.. However, the HBV-DNA levels were 3-fold lower in FADD(+)$_{hep}$ than in FADD(-)$_{hep}$ mice (Fig.12b). After 56 days p.i., the amount of hepatic HBV-DNA remained at borderline levels in all lineages.

In contrast to the biphasic dynamic of hepatic HBV-DNA, the kinetics of HBV-RNA declined constantly after peaking, except those of *gld* mice. The content of hepatic HBV-RNA was determined by two independent methods: (i) we performed real time qPCR of pgRNA (Fig.12 c+d) and (ii) Northern blot analyses of subg- and pgRNAs (Fig.12 e+f). With both methods, we detected pgRNA in C57BL/6 and *gld* mice up to 28 days p.i. and in FADD mice up to 21 days p.i.. However, the absolute expression levels of pgRNA varied between the applied techniques and among the lineages. The first remark probably depend on separate runs of RNA extractions and on separate poolings of the RNA samples from groups of four mice at each time point.

The dynamics of HBV-RNA provides following results: (i) in all lineages the total amount of subgRNA was approximately 3-fold higher than the amount of pgRNA (Fig.12 c+d); (ii) the levels of HBV-RNA expression in the *gld* mice remained consistently high between 7 and 28 days p.i., whereas they declined about 4-fold in all other lineages (Fig.12 c+e); (iii) in FADD(-)$_{hep}$ mice, the content of pgRNA declined rapidly between 3 and 7 days p.i. for still unknown reasons (Fig.12 d+f). However, this observation was seemingly in accordance with the decrease of viremia during the same time period (Fig.11f). *In summary*:

1) We detected a biphasic course of HBV-replication peaking at 3-7 days p.i. and 21-28 days p.i., respectively, in all mice lineages.
2) By contrast, HBV-transcription peaked at 3-7 days p.i. and declined continuously afterwards; 2 months p.i. HBV RNA remained at borderline levels in all lineages.
The different kinetics of HBV-replication and HBV-transcription indicate that both processes might be controlled by different cellular defense mechanisms.

3.5.1.2. Intrahepatic T cells response

The intrahepatic antiviral immune response was documented by lymphocyte infiltration. In detail we analyzed the gene expression of T cell markers and lymphocyte-derived cytokines in liver tissue as described in 3.3.3.

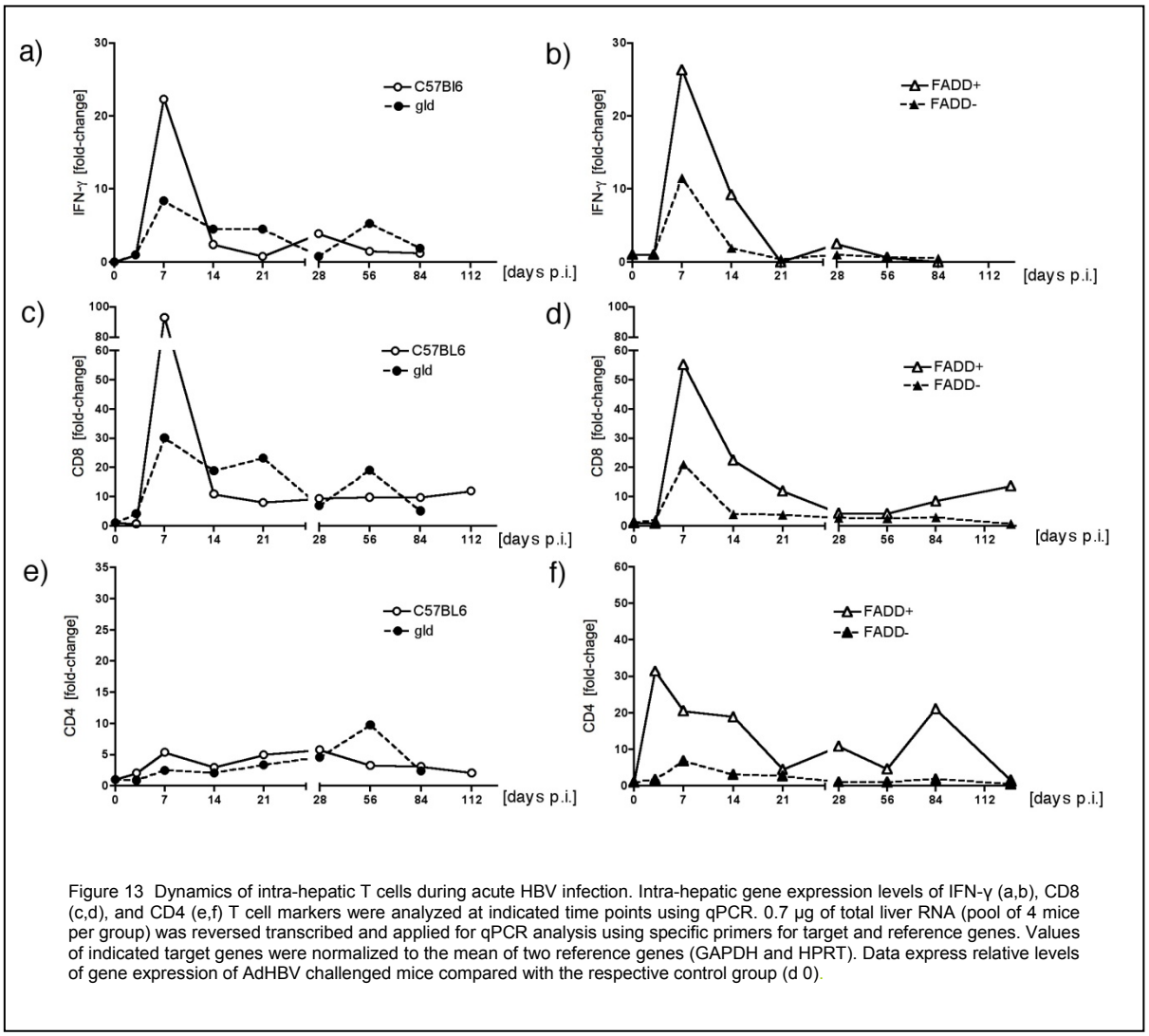

Figure 13 Dynamics of intra-hepatic T cells during acute HBV infection. Intra-hepatic gene expression levels of IFN-γ (a,b), CD8 (c,d), and CD4 (e,f) T cell markers were analyzed at indicated time points using qPCR. 0.7 µg of total liver RNA (pool of 4 mice per group) was reversed transcribed and applied for qPCR analysis using specific primers for target and reference genes. Values of indicated target genes were normalized to the mean of two reference genes (GAPDH and HPRT). Data express relative levels of gene expression of AdHBV challenged mice compared with the respective control group (d 0).

The dynamics of the hepatocellular T cell responses were very similar between C57BL/6 and FADD(+)$_{hep}$ mice on the one hand, and *gld* and FADD(-)$_{hep}$ mice on the other hand. At 7 days p.i., we found a surge of intrahepatic CD8 and IFN-γ mRNAs levels in all lineages about 20- to 90-fold and about 3- to 28-fold, respectively (Fig.13 a-d). However, the gene expression levels were about 3-fold lower in lineages deficient for CD95-mediated apoptosis. At 14 days p.i., CD8 and IFN-γ mRNA levels returned to pre-injection levels in C57BL/6, FADD(+)$_{hep}$, and FADD(-)$_{hep}$ mice. Importantly, CD8 and IFN-γ expression levels remained continuously elevated in *gld* mice, indicating that the induced CTL response did not subside (Fig.13 a+c).

In contrast to CD8 mRNA expression levels, we detected no characteristic surge of intrahepatic CD4 mRNA after AdHBV injection; however, the levels of CD4 mRNAs remained slightly elevated over the regarded time period (Fig.13 e-f). Particularly, the CD4 mRNA levels of FADD(+)$_{hep}$ mice were flaring up and down. With respect to CD4 mRNA being expressed in intrahepatic macrophages (Hume et al., 1987) and natural killer T cells (Bendelac et al., 1997) that are abundant in normal liver tissue, we did not really expect a significant increase in number of those cell types, rather than an activation that still needs to be measured.

Taken together:

1) CD8 positive T cells infiltrate into liver tissue approximately 7 days after AdHBV injection.

2) The intrahepatic expression levels of CD8 and IFN-γ mRNAs were 3-fold reduced in gld and FADD(-)$_{hep}$ mice compared with corresponding control (wild type) mice. Therefore, we assumed that CD95-mediated apoptosis of HBV-infected hepatocytes is important to induce a vigorous CTL response against HBV.

3) In accordance with the our previous results (see first mouse experiment (3.3.3 Fig.5), the intrahepatic expression levels of CD8 and IFN-γ remained elevated in gld mice up to 2 months. However, we cannot detect a delayed antiviral immune response in this lineage as documented before.

3.5.2 Seroconversion

3.5.2.1. anti-HBs / anti-HBc

In order to analyze the establishment of a humoral immune response to HBV-infection, we determined the amount of *anti*-HBs and *anti*-HBc *Ab* in mouse sera at 84 days p.i..

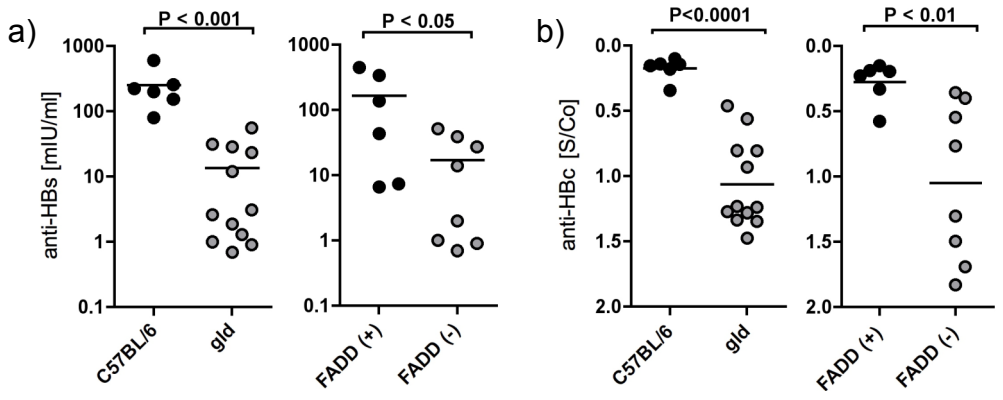

Figure 14 Seroconversion. Anti-HBs and anti-HBc Ab titers were determined at 84 days p.i. Mouse serum was diluted in PBS (1:20) before Axsym assay was performed. (a) anti-HBsAg ELISA. Values are directly proportional to Ab concentration. (b) anti-HBcAg titers were determined by competitive ELISA. Values are reciprocal to Ab concentration. Internal controls (negative/positive) are shown. Each data point represents the result of one mouse and the horizontal bar represents the mean. Statistical significance was performed by the student's t-test.

We detected in all lineages *anti*-HBs and *anti*-HBc *Ab*. However, the titers were significantly lower in lineages harboring deficiencies in CD95-signaling. We found in *gld* and FADD(-)$_{hep}$ mice about 10-fold lower *anti*-HBs and about 50% lower *anti*-HBc Ab titers, respectively.

3.5.2.2. IgG Isotype Profiling

In order to reveal why the humoral immune response is reduced in *gld* and FADD(-)$_{hep}$ mice, we compared the IgG isotype profiles by ELISA. Thus, we determined whether different T cell populations (Th1 or Th2) might account for the reduced *anti*-HBs and *anti*-HBc titers.

IFN-γ secretion elicits a Th1-response reflected by Ab switching to IgG2a and IgG3, whereas IL-4 secretion elicits a Th2-response defined by IgG1. TNF-β favors IgG2b Ab switching.

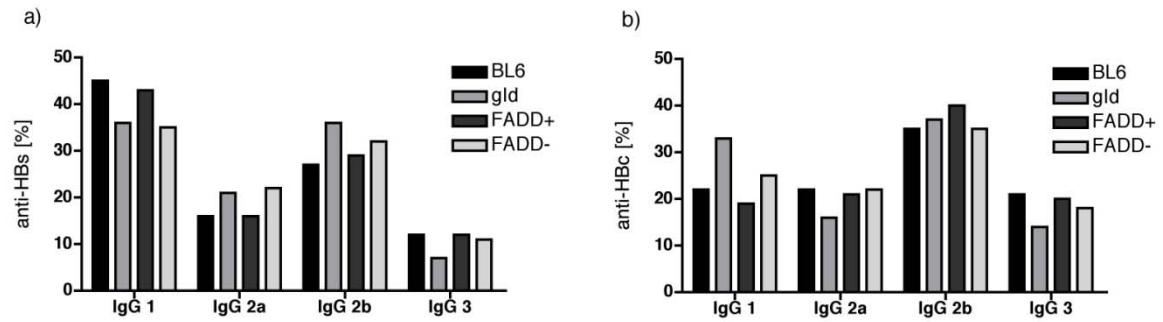

Figure 15 IgG isotype-specific anti-HBs (a) and anti-HBc (b) Ab measured by ELISA. Mouse sera obtained at 84 days p.i. were pooled from four mice per group and diluted as indicated: C57BL/6 1:250 - gld 1:5 - FADD(+) 1:250 - FADD(-)$_{hep}$ 1:50. The sera-dilutions were adjusted between the lineages in order to obtain comparable OD 492 onset values of total IgG of anti-HBs or anti-HBc, respectively. Values are expressed as percentage of total IgG [∑(1+2a+2b+3)] of anti-HBs or anti-HBc specific Ab in diluted serum.

Mixed IgG isotype profiles of *anti*-HBs and *anti*-HBc were detected in all lineages, however their distributions were slightly different (Fig.15).

In C57BL/6 and FADD(+)$_{hep}$ mice, the IgG isotype patterns of *anti*-HBs comprised with about 45% of IgG1, wheareas IgG2a and IgG3 were represented below 20% (Fig. 15a). Interestingly, the corresponding *anti*-HBc isotype profiles consisted about 35-40% of IgG2b whereas IgG1, IgG2a, and IgG3b were distributed in comparable amounts of about 20% (Fig. 15b). The data indicated that a mixed Th1/Th2-like T cell profile was present in the periphery of C57BL/6 and FADD(+)$_{hep}$ mice, which is slighly balanced towards the anti-inflammatory Th2-phenotype.

The isotype patterns of *anti*-HBs and *anti*-HBc in the *gld* and FADD(-)$_{hep}$ lineage were quite similar: comparable amounts of IgG1 and IgG2b about 30-35%, IgG2a about 20-24% and IgG3 below 20% were detected (Fig. 15a +b).

Taken together:

1) Gld and FADD(-)$_{hep}$ mice produce significantly less anti-HBs and anti-HBc Ab than C57BL/6 and FADD(+)$_{hep}$ mice for hitherto unknown reasons.

2) All lineages show a broaden IgG isotype profile of anti-HBs and anti-HBc including IgG2a, IgG2b, IgG3 and IgG1.

3) The anti-HBs IgG profile in C57BL/6 and FADD(+)$_{hep}$ is slightly pronounced to the anti-inflammatory Th2 response (IgG1). Interestingly, gld and FADD(-)$_{hep}$ mice shows comparable amounts of IgG1 and IgG2b. Since IgG2b is not assigned to either a Th2- or Th1-response, convincing conclusions about the corresponding Th-response are missing.

3.5.3 Histology

3.5.3.1. H&E stain

The extent of the induced hepatitis infection was analyzed in hematoxylin-eosin (H&E) stained liver tissues of all lineages at different time points. Therefore, we used a grading system that scored various parameters describing the inflammatory activity within liver tissue (Tabel 1). Thus includes: (i) presence and location of mononuclear infiltrates like portal or acinar/parenchyma; (ii) the amount of observed cell deaths; (iii) the level of liver regenerative activity like mitotic cells. Prof. Dr. Peter Schirmacher performed the assessment of histologically relevant findings and the author processed data.

Table 1 Assessment of histological relevant findings based on H&E staining. Grading describes value of histological features. Infiltration of portal tract (PT inf.); apoptotic hepatocytes / necroinflammatory foci (apo./nec); hepatocyte regeneration / proliferation (reg./prol.)

C57BL/6

dpi	nr	PT infl.	Parenchym apo./nec.	Parenchym reg./prol.
0	M3	0		
3	F1	1	1	2
	M2	0	1	2
7	F2	1	3	2
	M4	1	3	2
14	M3	2	2	2
	M4	0	2	1
21	F2	1	1	1
	M4	1	1	2
28	F2	2	2	2
	M4	1	1	2
56	F1	1	1	1
	F2	1	1	2
	M3	2	2	3
84	F1	1	1	1
	F2	1	1	2
	M3	1	2	1

GLD

dpi	nr	PT infl.	Parenchym apo./nec.	Parenchym reg./prol.
0	M3	0		
3	F2	3	2	2
	M4	1	0	0
7	F1	2	2	2
	M4	2	3	2
14	F1	2	2	2
	M3	3	3	2
21	F1	2	3	2
	F2	3	3	2
	F4	3	3	1
28	F1	3	2	1
	M4	2	3	2
56	F1	3	3	3
	F2	3	3	3
	M3	2	3	3
	M4	3	3	3
84	F1	2	3	2
	F2	3	2	2
	M3	3	3	2
	M4	3	2	2

FADD+

dpi	nr	PT infl.	Parenchym apo./nec.	Parenchym reg./prol.
0	F1	0		
3	M1	0	1	3
	M4	0	1	3
7	F1	2	3	2
14	F1	1	2	2
	M4	1	3	3
21	F2	1	3	2
	M3	2	3	2
28	F1	0	1	1
	F2	1	1	1
	M3	1	2	2
56	F1	1	1	1
	M4	1	2	2
84	M3	1	1	1
	M4	1	1	1

FADD-

dpi	nr	PT infl.	Parenchym apo./nec.	Parenchym reg./prol.
0	F1	0		
3	F1	1	3	2
	M4	0	2	2
7	F2	2	3	2
	M4	2	3	2
14	F1	1	3	2
	M4	1	3	2
21	F1	1	3	2
	M4	2	3	2
28	F1	1	2	2
	M3	1	2	3
	M3	1	2	2
56	F1	1	2	1
	M3	1	2	2
84	M3	1	1	2
	M4	1	1	1

0 no distinctive features

1 minimal level

2 mild-moderate level

3 moderate-severe level

All lineages developed a mild acute hepatits at 7 days p.i., characterized by numerous parenchymal inflammatory foci, numerous single cell or grouping necrosis and apoptotic and regenerating hepatocytes (Fig.16 a+b). At 28 days p.i., the lineages C57BL/6, FADD(+)$_{hep}$ and FADD(-)$_{hep}$ recovered from acute hepatits and the amount of inflammatory foci in the parenchyma declined substantially (Table 1). However, in the *gld* lineage we observed a predominant and persistent necroinflammation at the portal tract with chronic signs (Fig.16c). Additionally, the extent of hepatocellular cell deaths and generations was increased up to 84 days p.i. (Table 1). The detailed record of pictures showing liver sections of all lineages at different time points is presented in appendix.

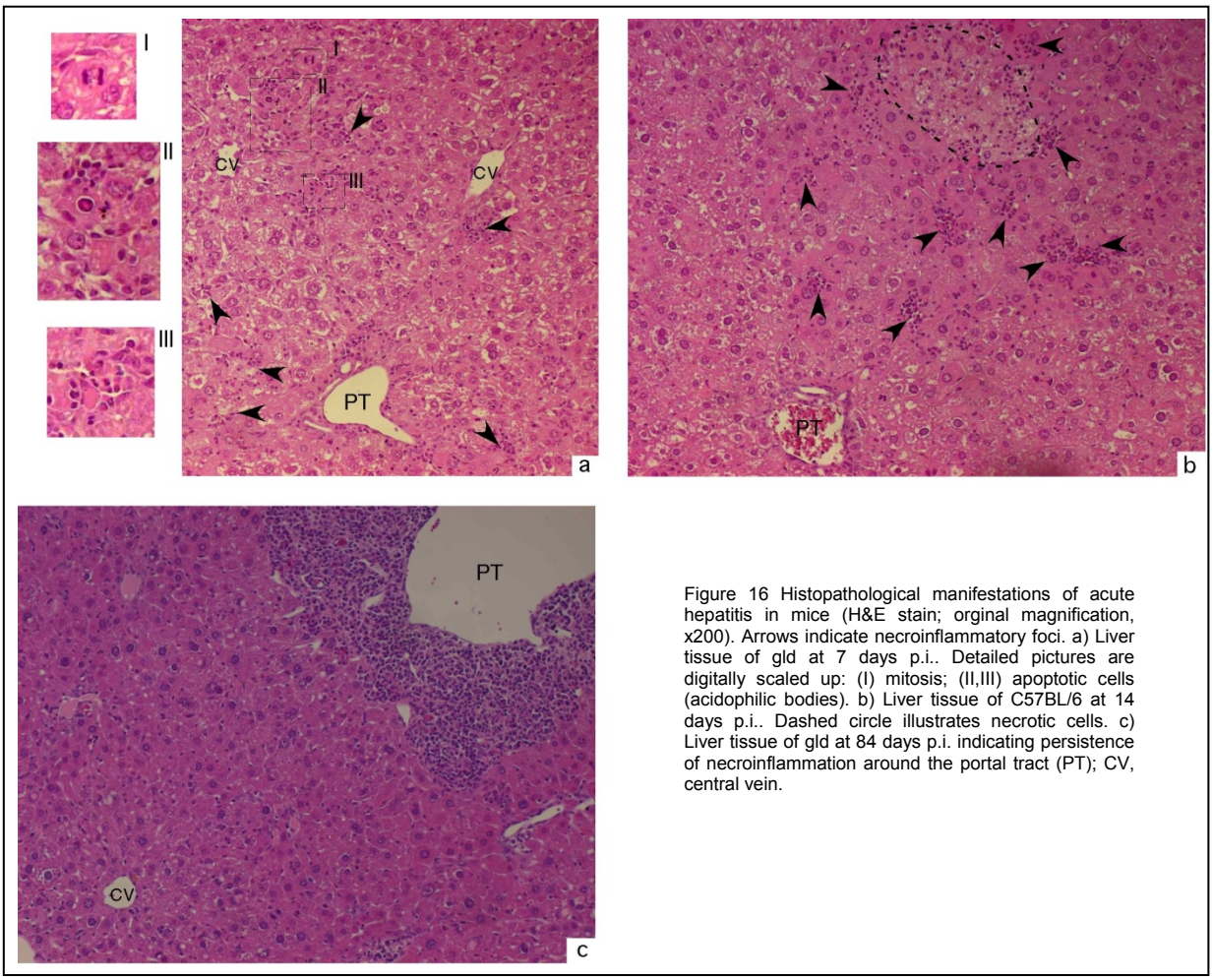

Figure 16 Histopathological manifestations of acute hepatitis in mice (H&E stain; orginal magnification, x200). Arrows indicate necroinflammatory foci. a) Liver tissue of gld at 7 days p.i.. Detailed pictures are digitally scaled up: (I) mitosis; (II,III) apoptotic cells (acidophilic bodies). b) Liver tissue of C57BL/6 at 14 days p.i.. Dashed circle illustrates necrotic cells. c) Liver tissue of gld at 84 days p.i. indicating persistence of necroinflammation around the portal tract (PT); CV, central vein.

3.5.3.2. HBc stain

We performed immunohistochemical HBcAg stains to document, histologically, the amount the viral replication during the period under observation (Fig.17). Especially, we were interested in confirming the biphasic dynamic of HBV replication in liver tissue measured by real time qPCR (Fig.12a). For staining we simply compared the lineage *gld* and FADD(+)$_{hep}$. The detailed record of immunohistochemical analyses of liver sections is presented in the appendix.

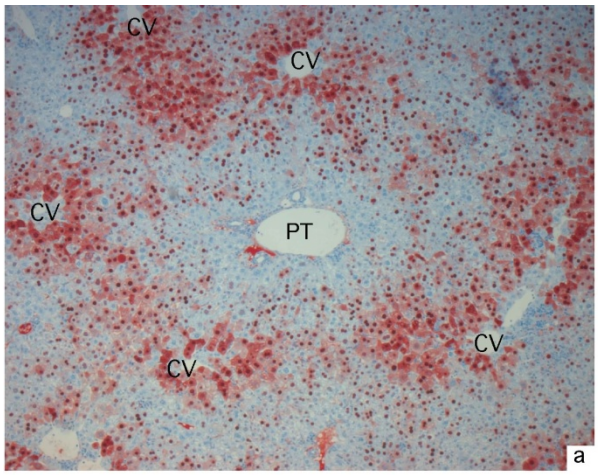

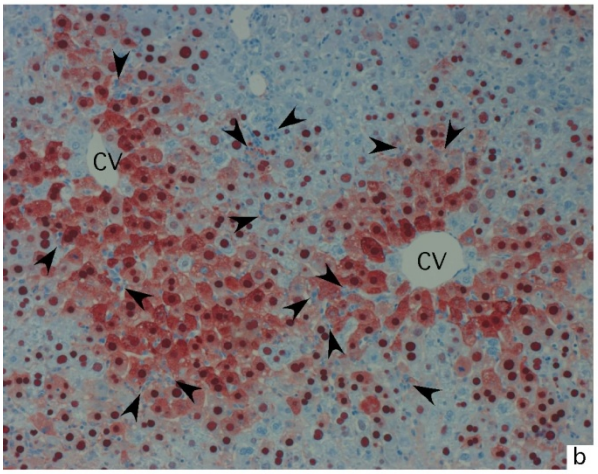

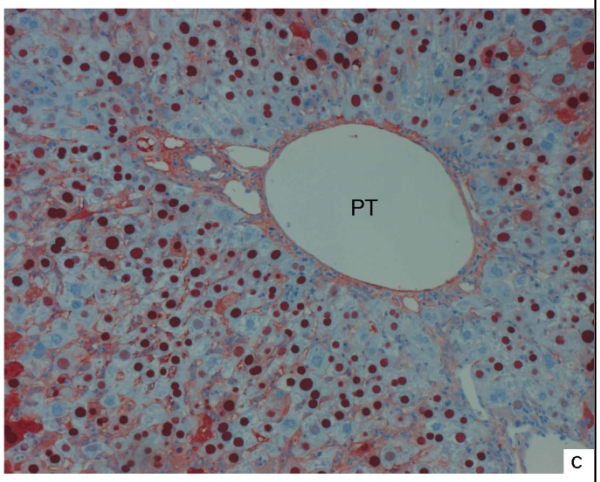

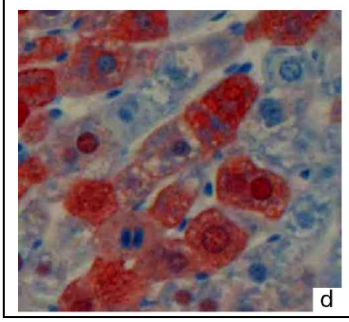

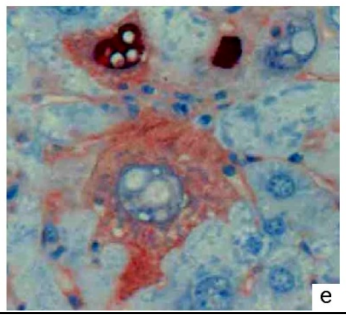

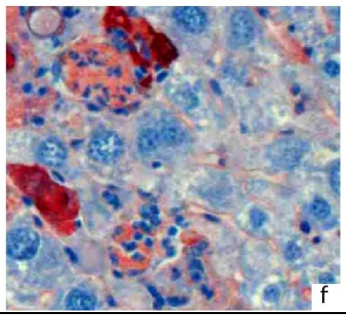

Figure 17 Immunohistochemical HBcAg staining of mice liver at 7 days p.i..
a) Overview of stained liver section. Orginal magnification, x100. b) Centrolobular hepatocytes showing primarily cytoplasmic staining. c) Hepatocytes around the portal region exhibited HBcAg positive nuclei; orginal magnification, x200.
(d-f) Detailed pictures digitally scaled up d) mitosis of HBV infected hepatocyte; e) hypertrophic hepatocyte with enlarged nucleus beleaguered by mononuclear lymphocytes; f) necroinflammatory foci. PT, portal tract; CV, central vein.

Generally, no homogenous distribution of HBcAg expression was documented in liver tissues of mice upon AdHBV injection. Predominantly, we revealed a cytoplasmic

expression of HBcAg in centrilobular hepatocytes surrounding the central vein indicating that cellular factors might influence HBV life cycle (Fig.17 a+b). By contrast, hepatocytes around the portal region showed only a nuclear HBcAg staining (Fig.17c).

Comparing the amount of cytoplasmic positive HBcAg hepatocytes in liver sections of mice sacrificed at different time points, different expression patterns were observed, which apparently correlate with a biphasic dynamic of HBV replication. However, the number of assessed sections must be increased to attain statistical significance. Cytoplasmic positive HBcAg hepatocytes were still detectable at 3 days p.i. and numbers increased until 7 days p.i.. At 14 days p.i., we detected a decline before the number increased a second time at 21 days p.i.. Low levels of HBcAg remained detectable at later time points (56 days p.i.), however HBcAg was predominantly located in the nuclei.

Furthermore, It is important to note that mononuclear infiltrates, which overwhelmed the liver tissue during 7 and 14 days p.i., exclusively adhered to hepatocytes that were cytoplasmic positive for HBcAg (Fig.17 e+f). This observation confirmed that CTL specifically targeted HBV-replicating cells.

3.5.4 Maturation level of LAL in *gld* mice

We observed that *gld* mice challenged with AdHBV predominately accumulation lymphocyte in liver tissue (see Fig.16c). Since it is known that *gld* developed lymphadenopathy by accumulating abnormal lymphocytes carrying B cell (B220+) and T cell (Thy1+) markers but do not express CD8+ or CD4+ antigens (Sidman *et al.* 1992, Nagata & Suda 1995), we analyzed whether these phenotype might account for the sustained lymphocyte accumulation around the portal tract. Therefore, we isolated LALs of *gld* and C57BL/6 mice and performed cell surface staining (Fig.18).

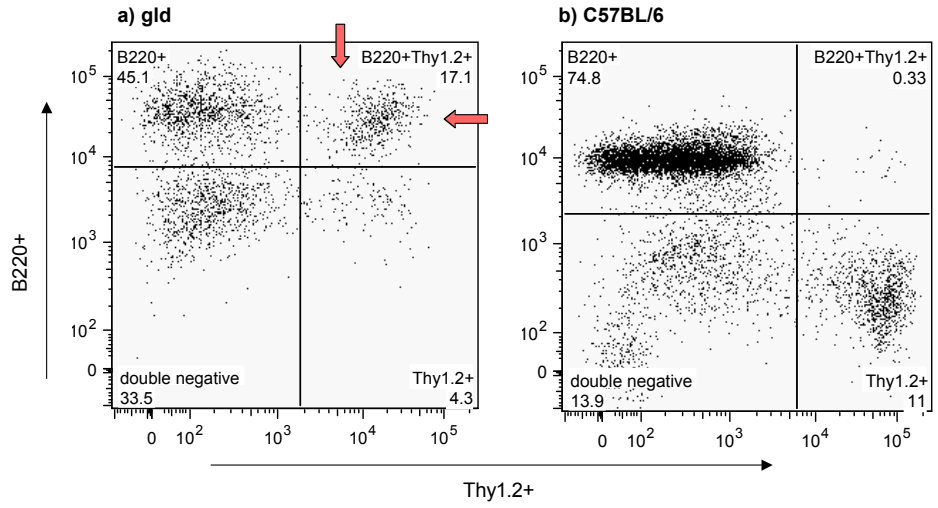

Figure 18 Cytofluorometric analysis of LAL. Dot plots represents non T-lymphocytes expressing B220 and/or Thy1.2 on cell surface. (Cells were gated on live and negative for CD4- and CD8- T cell markers.) LAL were obtained from (a) gld and (b) C57BL/6 mice at 130 days p.i.. The percentage of B220/Thy1.2 cells is given in each panel. Data are representative of four and two independently analyzed sets of gld and C57BL/6 mice, respectively. Arrows mark abnormal lymphocyte population characteristic for the gld lineage.

The isolated LALs were stained with four different cell surface markers: CD4, CD8, B220 and Thy1.2. In the following analysis, we focused on cells that were CD4 and CD8 negative. About 75% of LAL isolated from C57BL/6 that match to this category were pure B lymphocytes (Fig18b). In marked contrast, the *gld* lineage exhibited a mixed population of lymphocyte expressing B220: 45% of those cells correspond to pure B lymphocytes (B220+/Thy1.2-) and 17% correspond to the described abnormal lymphocyte (B220+/Thy1.2+) (Fig18a). Additionally, the percentage of LAL that carried neither T cell nor B cell markers were about 2.4-fold higher in the *gld* lineage compared to C57BL/6 (Fig18a). This data indicate that the accumulation of lymphocyte in liver tissue of *gld* mice might based on abnormal immune cells in a considerable extent.

3.5.5 The Influence of HBV capsids on seroconversion

Our results presented above indicate that the CD95-signaling pathway plays an important role in inducing a humoral immune response to HBV. With respect to our results that HBV capsids are released from apoptotic cells (see results of part I of this thesis), we hypothesize that CD95-induced apoptosis of HBV-infected hepatocytes is important for HBV capsid release *in vivo*. This might be necessary to stimulate B cells to induce the production of antibodies against HBV structure proteins. In order to prove this intriguing hypothesis, we infected *gld* and FADD lineages with AdHBV and additionally immunized them with recombinant capsids to simulate HBV capside release. HBV capsids were applied on two routes: at 3 days p.i., they were delivered intraperitonally in incomplete Freunds adjuvant (IFA) to allow prolonged particle release. At day 5 p.i., a small amount of capsids were applied intravenously to boost the reaction and to mimic the natural route of HBV particle release.

Moreover, we induced artificially CD95-mediated apoptosis in AdHBV-infected *gld* mice by the use *anti*-CD95 antibodies. In both settings, we analyzed *anti*-HBs and *anti*-HBc Ab production at 54 days p.i..

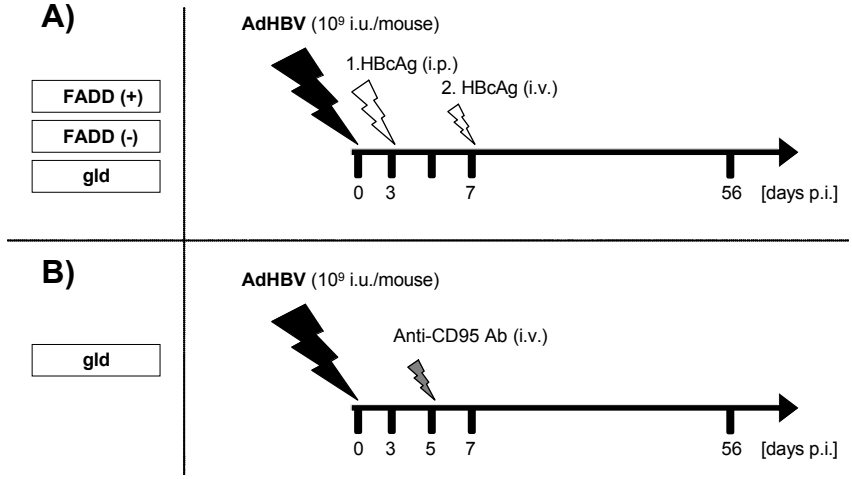

Figure 19 Outline of third mouse experiment: analyzing the influence of capsids on seroconversion.
(a) Immunization with HBcAg upon challaging with AdHBV at indicated time points. HBcAg was applied intraperitoneally (4 µg i.p.) with IFA and additionally intravenously (0.5 µg i.v.) in 5% NaCl at indicated time points. (b) Induction of CD95-induced apoptosis in gld mice at 5 days p.i.. Anti-CD95 Ab (5 µg) was applied intravenously (i.v.)

An outline about this experiment series is given in Figure 19.

At first, we compared the *anti*-HBs *Ab* titers at 54 days p.i. in mice challenged with AdHBV and additionally treated with recombinant capsids.

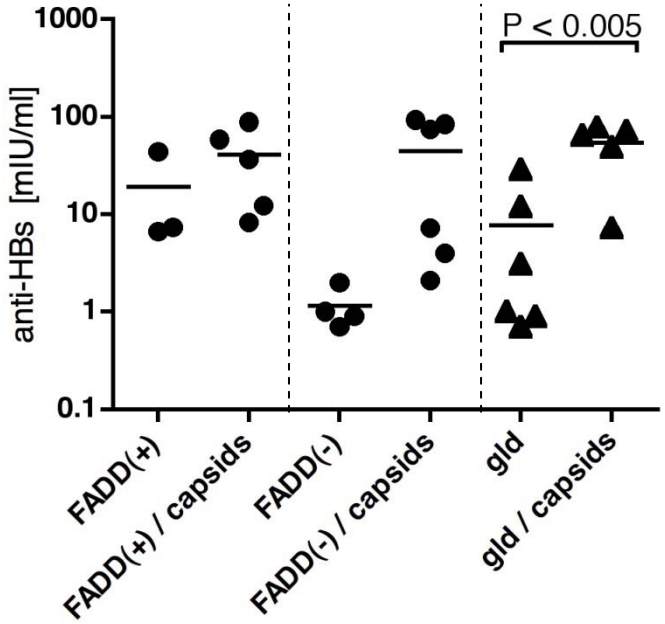

Figure 21 Seroconversion in AdHBV-infected FADD mice immunized with HBcAg. Mouse serum (54 days p.i.) was diluted in PBS (1:20) before titers were determined by Axsym assay. Immunization with HBcAg (4µg in IFA; i.p.) was performed at 3 days p.i. and an additional boost reaction was applied at 7 days p.i. (0.2 µg HBcAg; i.v.).
Anti-HBsAg ELISA. Values are directly proportional to Ab concentration in serum. Each data point represents the result of one mouse and the horizontal bar represents the mean. Statistical significance was performed by a student's t-test.

Preliminary data indicate that upon capsid immunization FADD(-)$_{hep}$ and gld mice obtained comparable *anti*-HBs titers than FADD(+)$_{hep}$ mice (Fig.21a). This result corroborates our theory that capsids are important for lymphocyte priming.

HBcAg application alone was immunogenic in eliciting anti-HBc Ab response as expected (data not shown). IFA treatment (without capsids) of AdHBV challenged mice did not boost the humoral immune response against HBV.

Secondly, we compared the *anti*-HBs and *anti*-HBc *Ab* production at 54 days p.i. in *gld* mice challenged with AdHBV and additionally treated with *anti*-CD95 *Ab*.

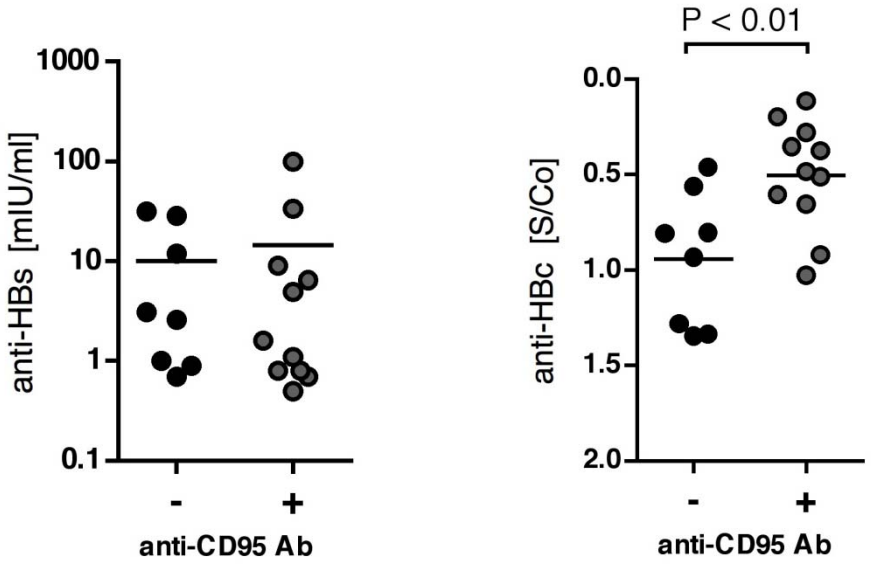

Figure 20 Seroconversion in AdHBV-infected gld mice treated with anti-CD95 Ab or immunized with HBcAg. Titers were determined at 54 days p.i. Mouse serum was diluted in PBS (1:20) before Axsym assay was performed. Anti-CD95 Ab (Jo2; 6.5 ng/mouse: i.v.) was applied at 5 days p.i.. HBcAg immunization (4 µg in IFA; i.p.) was performed at 3 days p.i. and additional boost reaction was applied at 7 days p.i. (0.2 µg HBcAg; i.v.). (a) Anti-HBsAg ELISA; Values are directly proportional to Ab concentration. (b) Anti-HBcAg determined by competitive ELISA. Values are reciprocal to Ab concentration. Internal controls (negative/positive) are shown. Each data point represents the result of one mouse and the horizontal bar represents the mean. Statistical significance was performed by the student's t-test.

We detected a significantly increased amount of *anti*-HBs titers (P< 0.01) upon recombinant capsids immunization (Fig.20) indicating that *anti*-CD95 induced apoptosis leads to the release of HBV capsids which stimulate *anti*-HBc *Ab* production. However, no significant difference in *anti*-HBs *Ab* production was measured.

3.6. Discussion

This study provides several new and important aspects of HBV-host cell interactions and describes the contribution of different apoptosis pathways in the clearance of HBV-infection. We demonstrated for the first time that the mode of killing of HBV-infected hepatocytes has dramatic influence in priming the adaptive immune response.

In detail, the study was undertaken to examine the relative contribution of perforin/granzyme and CD95-mediated apoptosis in controlling an acute HBV infection. Both apoptotic pathways are considered to be the major mechanisms of T cell-mediated cytotoxicity (Lowin *et al.* 1994, Kagi *et al.* 1994b). However, intracellular invaders are combat with different efficiencies even though both CD95- and perforin/granzyme converge on caspase-3 (Balkow *et al.* 2001).

In this study, we analyzed the clearance of an acute self-limiting HBV infection in different congenic C57BL/6 mouse lineages after AdHBV injection under conditions where lymphocytes were unable to kill their target cells either by CD95-receptor mediated apoptosis or by perforin/granzyme release.

We revealed that the intrahepatic T cell infiltration and lymphocyte-derived IFN-γ production, caused by HBV infection, was reduced and partially delayed when lymphocytes were restricted in their cytotoxic effector functions. More importantly, we found that the HBV-specific humoral immune response was dramatically reduced in mice deficient for CD95-mediated apoptosis of virus-infected hepatocytes. Predominately, the strongly reduced titers of *anti*-HBs and *anti*-HBc in the *gld* lineage were unexpected since those mice are prone to develop huge amounts of autoantibodies due to its genetic constitution (Nagata & Suda 1995, Sidman *et al.* 1992). Interestingly, *gld* mice developed normal titers of neutralizing Ab against the adenoviral vector.

The putative nature of these observations is surprising at first glance because all mouse lineages are able to control HBV infection after two months. The apparent discrepancy between “reduced lymphocyte activation” and nonetheless “clearance of viral infection” might become much clearer after regarding both aspects separately.

We assume that the reduced T and B cell response against HBV have an insufficient priming process in common which is probably not important in controlling an acute

HBV-infection in mice but might have dramatic influence in humans as discussed in the following section. Since HBV re-infection of mouse-hepatocytes is precluded by viral up-take, HBV-replication in mice declines as soon as either AdHBV-infected hepatocytes are eliminated by CTL or viral replication becomes controlled by non-cytopathic effector functions. In humans, however, HBV progeny released continually infect hepatocytes if not controlled by the immune system. Therefore, we supposed that reduced HBV-specific lymphocyte activation strongly influences the clinical outcome.

3.6.1 CD95-induced apoptosis of HBV-infected hepatocytes is important in priming the adaptive immune response

Since we observed a reduced HBV-specific adaptive immune response in *gld* and FADD(-)$_{hep}$ mice, we reason that CD95-mediated apoptosis of infected cells is essential in priming lymphocytes against HBV. Note that *gld* mice express non-functional CD95 ligands; therefore, lymphocytes of *gld* are unable to kill by CD95-mediated apoptosis. FADD(-)$_{hep}$ mice in contrast have a genetic defect in hepatocytes in converting death-receptor stimuli such as CD95R-, TNFR- and TRAIL.

To explain why HBV-specific T and B cell priming is reduced in *gld* and FADD(-)$_{hep}$ mice, we developed a theory which predominately is based on two observations: first, we revealed that apoptotic HBV-infected hepatocytes released huge amounts of HBV nucleocapsids ((Arzberger *et al.* 2009, submitted); see first experimental part of this PhD thesis). Second, Milich *et al.* showed that nucleocapsids were efficiently captured by B cells which in turn become activated and were able to function as APC in priming naïve T cells (Milich *et al.* 1987).

Therefore, we hypothesized that the release of nucleocapsids during apoptosis might be essential for priming lymphocytes towards HBV infection by an “unusual” mechanism involving B cells. This priming mechanism is termed “unusual” because only a few publications still described T cell priming by B cells (see introduction APC and cross-presentation). The reader should be remind that priming of naïve T cells is usually restricted to DC according to traditional textbook knowledge.

T cell priming by B cells might be important during HBV infection for several reasons:

(i) Evidences from a number of groups indicate that DC, the classical antigen presenting cells, are incompletely active in liver tissue. The data suggest that hepatic DC favor tolerance induction rather than triggering anti-viral immune responses (De Creus *et al.* 2005, Lau & Thomson 2003). If this assumption is correct, T and B cell priming by DC is probably insufficient to elicit an adaptive immunity against HBV.

(ii) Although capsids are usually undetectable in serum (Possehl *et al.* 1992), they are highly immunogenic and able to trigger T cell-dependent and -independent antigen productions (Cao *et al.* 2001, Milich *et al.* 1998).

(iii) BCRs have an incredible magnet function especially in capturing antigens that are present in serum at low concentrations (Pape *et al.* 2007, Lanzavecchia 1990). Therefore, it is possible that B cells capture nucleocapsids much more efficiently than DC do during phagocytosis. The location of antigen capturing by B cells is probably the cortex of lymphnodes; however, capsid capturing by B cells could also directly occur in the liver.

(iv) Capsid capturing by B cells is not specific in terms that the BCR recognize capsids within their variable antigen-binding region. However, it has been shown that capsids bind with high affinity to a **linear motif** within the **constant** region of BCR. This motif is present in a large proportion of naïve B cells (Lazdina *et al.* 2001).

(v) Moreover, one intriguing study showed that “capsid-capturing” by B cells generates multiple B cell clones. Some of these clones elicit T cell-dependent Ab production against the viral L-protein (Milich *et al.* 1987). Therefore, capsid capturing by B cells might be an important process in generating neutralizing Ab against virions. Note that the L-protein is necessary for infection but it is present only in low quantities on infectious virions as well as on SVP (Niederau *et al.* 1996, Budkowska *et al.* 1988).

(vi) Finally, a recent study showed that B cells can crosspresent capsid-derived peptides and trigger CLT activation (Lazdina *et al.* 2003).

Integrating all these findings into one context, we developed the following hypothesis: CD95-induced apoptosis of HBV-infected hepatocytes might be required to trigger nucleocapsid release. The nucleocapsids in serum can be captured and processed by APC cells. With respect to the aforementioned publications, we hypothesized that B cells play a key function in capsid capturing. This kind of antigen presenting might be important during HBV-infection in priming the adaptive immunity, probably because activation of DC is incomplete. If this hypothesis is correct, it would explain why the activity of lymphocytes is strongly reduced in mice harboring deficiencies in CD95-mediated apoptosis of hepatocytes such as the *gld* and FADD(-)$_{hep}$ lineage.

To corroborate this intriguing assumption, we artificially induced CD95-mediated apoptosis in AdHBV-infected *gld* mice or challenged *gld* and FADD(-)$_{hep}$ mice with recombinant capsids. Both lineages showed significantly increased *anti*-HBc Ab titers after treatment. However, the *anti*-HBs titer was only increased after capsid-immunization, but not after *anti*-CD95 application. These findings partially support our theory that CD95-induced apoptosis of infected hepatocytes might be important in eliciting an effective adaptive immune response. However, it only tentatively confirmed the observation of Milich et al. (1987) that capsid-capturing by B cells elicits Ab production against viral envelope proteins. Further studies are warranted in confirming these preliminarly conclusions.

Advanced studies corroborating our intriguing theory can go in the following direction: (i) Characterization of HBV particles released *in vivo* upon death-receptor mediated apoptosis. (ii) Neutralization of capsids in serum to examine whether HBV-specific lymphocyte priming is possible in the absence of nucleocapsids. Therefore, capsid-neutralizing Ab should be applied before mice are challenged with AdHBV. (iii) Depletion of either DC or specific B cells (if possible) to clarify which kind of APC is essential for lymphocyte priming during HBV infection. The depletion of B cells should be restricted to the pool of cells carrying the aforementioned motif within the constant region of the BCR able to capture nucleocapsids.

3.6.2 Comparing cytolytic pathways during viral infection

A possible explanation for why the mode of killing of HBV-infected hepatocytes has different influences in triggering adaptive immunity might be linked to different killing strategies of CD95-mediated apoptosis and perforin/granzyme release. Both apoptosis pathways might differ in causing a loss of membrane integrity, in inducing

enzymatic effector functions and probably in the time-lapse between initiation and execution of apoptosis.

Apoptosis-induction via perforin/granzyme is extremely rapid and linked to pronounced membrane-damage; the membrane integrity is lost about seven to ten minutes after target cell contact that subsequently leads to the release of cytotoxic granules (Lowin *et al.* 1996). By contrast, CD95-induced apoptosis shows an prevailing intracellular killing mechanism and signs of cytotoxicity are detectable after a lag period of several hours (Lowin *et al.* 1994). In keeping with this, viral clearance and tissue injury should not be regarded as one interrelated consequence of cellular immune responses. It might well be that the rapid loss of membrane integrity induced by perforin averts the “local” immunity like macrophages and enforces an inflammatory immune response in liver tissue.

Mouse studies with cytopathic orthopoxvirus ectromelia (Ect) showed that the presence of perforin and granzyme is necessary to combat viral infection. By contrast, membrane insertion of perforin is sufficient to block viral replication of the noncytopathic lymphocytic choriomeningitis virus (LCMV) (Balkow *et al.* 2001). Interestingly, their data provided evidence that liver damage but not viral clearance of LCMV is based on CD95- mediated apoptosis. These discrepancies might be linked to different viral replication and transmission strategies. For HBV infection the contribution of perforin/granzyme and CD95 are still undefined. One interesting study of Chisari and coworkers showed that IFN-γ secretion of CTL dominates CD95-mediated and perforin/granzyme-dependent pathways in inducing liver disease in HBs-transgenic mice upon lymphocyte transfer from wild type mice (Nakamoto *et al.* 1997). Moreover, they postulated that the physiological state of the hepatocytes determines the death pathway.

Numerous studies in humans and transgenic mice emphasized the contribution of CD95 ligand as an important effector molecule during hepatocellular injury (Tang *et al.* 2003, Ibuki *et al.* 2002, Kondo *et al.* 1997, Luo *et al.* 1997, Galle *et al.* 1995). However, these studies neither excluded the activity of perforin/granzyme nor did they examine whether CD95-mediated killing is necessary to control HBV infection. Most of these studies were performed in descriptive fashions on human liver biopsies (Lee *et al.* 2004, Tang *et al.* 2003, Ibuki *et al.* 2002, Tagashira *et al.* 2000) and on primary human hepatocytes (Galle *et al.* 1995) showing that intrahepatic expression levels of CD95 ligand were highly elevated during HBV infection but not in normal

tissues. Two of those studies also mentioned increased intrahepatic mRNA levels of perforin during chronic HBV infection, suggesting that both cytotoxic apoptosis pathways are involved in hepatocellular injury in humans (Lee *et al.* 2004, Tagashira *et al.* 2000). The expression of CD95 ligand was found primarily in areas with lymphocyte infiltration visualized by the use of *in situ* hybridization of liver tissues (Luo, 1997). Moreover, administration of soluble anti-CD95L antibodies in transgenic mice prevents T cell mediated hepatitis (Kondo *et al.* 1997). Note that hepatocytes need the intracellular mitochondrial amplification of death-receptor-mediated apoptosis to activate execution caspases (see introduction). Collectively, all these findings strengthen our notion that CD95-induced apoptosis is important in controlling HBV infection.

Despite reduced B and T cells activation, mice with deficiencies in CD95-induced apoptosis recover from acute HBV-infection. This might be linked to a combination of non-cytopathic activities and on perforin/granzyme-mediated killing. However, the situation could be different in humans since the virus spread through the liver if it is not sufficiently controlled by the immune system. In keeping with this, the absence or reduced amounts of HBV neutralizing Ab might facilitate HBV spread in humans. Therefore, reduced B and T cells activation might seriously influence the clinical outcome of an acute HBV-infection.

3.6.3 Contribution of perforin/granzyme in controlling HBV infection

Although we revealed that the absence of perforin is not as serious as a deficiency in CD95 in eliciting immunity against HBV, the contribution of perforin/granzyme should not be disregarded in the elimination of a HBV infection. Since we did not prove in our studies what happens to the clearance of an acute HBV infection in mice if perforin/granzyme as well as CD95-mediated killing failed. Moreover, the data obtained in these mouse models indicate that perforin/granzyme and CD95-mediated apoptosis act synergistically because the recruitment of inflammatory cells to the liver is reduced if lymphocytes are restricted in one of both cytotoxic effector functions.

An interesting study of woodchuck hepatitis B virus (WHV) infection (a natural animal model for hepadnaviral infections) indicated that perforin-mediated apoptosis is pronounced during the acute phase (Hodgson, 1999). The authors concluded that NK cells, the cellular effectors of the non-specific innate immunity, are presumably

responsible for the cytopathic cell death. We basically support this assumption; however, we revealed no difference in the course of HBV-infection (characterized by HBeAg, HBsAg or HBV replication) between wild-type C57BL/6 and perforin k/o mice during the first 14 days. By contrast, we observed a higher viral load in *gld* than wild-type mice. (Note that *gld* mice are able to kill via perforin/granzyme.) The data imply that CD95-mediated apoptosis might be much more pronounced than perforin-mediated apoptosis in controlling the early phase. However, this finding could not be confirmed in FADD(-)$_{hep}$ and FADD(+)$_{hep}$ mice. In this lineage, we detected no difference in the extent and in the dynamic of the HBV infection at early time-points (up to 14 dpi) suggesting that perforin as well as non-cytophathic mechanisms are probably the main effectors in the primary control of HBV. These inconsistent observations might be linked to the genetic constitutions of the *gld* lineages. Consequently, the results in the FADD lineages are in accordance with the woodchuck model.

An interesting publication of Kojima *et al.* (2002) (Kojima *et al.* 2002) showed that CD95 ligands are also stored in lytic granules of murine CD8 CTLs and NK cells which might translocate to the cell surface after receptor engagement and thereby participate in CD95-mediated cell lysis of the target cell. If this assumption is correct, it explains how NK cells can kill via CD95 and especially how NK cells of perforin k/o mice can participate in controlling viral infections.

3.6.4 Liverpathology and ALT

We revealed unexpectedly that perforin k/o mice have substantially increased ALT levels compared to all other mice lineages at 7 and 14 days post AdHBV infection. This phenomenon is challenging to explain; it is probably related to an unspecific release of granzyme B into the extracellular hepatic surroundings upon target-cell-recognition, including formation of an immunological synapse and release of cytoplasmic granules. In contrast to the elevated ALT levels in perforin k/o mice, we did not observe pronounced liver inflammation histologically. This might be related to the fact that increased ALT levels in serum are not mandatorily interrelated with histopathological findings like lymphocyte infiltration and necroinflammatory foci. Therefore, hepatocellular injuries caused by uncontrolled granzyme B release might be detectable by ALT elevations but not lead to the infiltration of lymphocytes into the liver tissue.

A similar discrepancy between ALT levels and histopathological findings was observed in the *gld* lineage: the massive accumulation of mononuclear cells around the portal-tact is classified histologically as sign of chronic liver inflammation. However, ALT elevations in the *gld* lineage were not as pronounced as expected especially compared with the FADD lineage. FACS analysis revealed that the overwhelming hepatocelular lymphocyte infiltration in *gld* mice was based in parts (17%) on an accumulation of abnormal nonfunctional lymphocytes carrying B cell (B220+) and T cell (Thy1+) surface markers. The fact that not all of these lymphocytes have cytodestructive activities, might explain why the histopathological assessment in *gld* mice did not directly correlate with the ALT level. Since homeostasis of lymphocytes is predominately regulated by CD95 ligand and receptor interactions, we propose that recruited lymphocytes additionally accumulate in liver tissue of *gld* mice because they cannot be eliminated by CD95 receptor/ligand interactions.

The analysis of the HBV-specific IgG isotype profiles revealed that all lineages have a mixed Th1/Th2-like cytokine profile with bias towards the anti-inflammatory Th2 response. These data suggest that neither the *gld* lineage with a massive accumulation of mononuclear cells around the portal tract nor the FADD lineage with pronounced ALT elevations have an overwhelming activity of activated macrophages or recruited monocytes. (Note that a pronounced Th1-like cytokine profile enhances the activity of macrophages and monocytes in producing degradative molecules like nitric oxide; this might lead to unspecific destructions in liver tissue.)

3.6.5 Non-cytopathic effector functions in controlling HBV infection

The clearance of HBV-infection solely through elimination of infected-hepatocytes is unlikely for several reasons: (i) the magnitude of reduction in viral protein expression and viral replication within two weeks is not compatible with the minimal rate of cell deaths observed histologically (ii) the killing of infected hepatocytes by direct cell lysis is a one-on-one process and therefore relatively inefficient in eliminating all infected cells in a short period of time (Rehermann *et al.* 1995, Guidotti *et al.* 1996b).

Diverse studies in transgenic mice and chimpanzees revealed that non-cytopathic cytokine-dependent antiviral defense mechanisms are important in controlling HBV-infection (Guidotti *et al.* 1999b, Guidotti *et al.* 1996a, Guidotti *et al.* 1996b, Guidotti *et al.* 1994b, Guidotti *et al.* 1994a). All these studies provide evidence that HBV-specific

CTL just kill a small pool of infected hepatocytes and additionally secrete huge amounts of IFN-γ and TNF-α. The cytokines, in turn, rapidly diffuse into the liver parenchyma and control HBV-replication in a non-cytopathic manner. Chisari and co-workers proposed that cytokines trigger at least two different anti-viral defense mechanisms: first, increased degradation of nucleocapsid and second, posttranscriptional down-regulation of viral RNA templates (Guidotti *et al.* 1996b). Our data support this theory for two reasons: first, we observed a flaring up and down of the viral load in liver tissue that might be the result of non-cytopathic control of viral replication. Second, simultaneously with the peak of IFN-γ at 7 dpi, we detected a dramatic decline of viral replication markers in serum such as viremia, HBeAg or HBsAg. However, the number of HBc positive cells in liver tissue does not decline substantially during the first 21 days p.i. suggesting that virion secretion must be controlled non-cytolytically (see supplementary data: HBc immunostain).

An intriguing study of HBV-infection in chimpanzees showed that viral DNA is more sensitive to cytokine-dependent anti-viral mechanisms than HBcAg, suggesting that the turnover of HBcAg is slower than that of viral DNA (Guidotti *et al.* 1999b). In addition, this study supports the theory that the clearance of more than 90% of viral DNA did not require the destruction of 90% of infected cells. An alternative theory to the turn-over of HBV-infected hepatocytes is provided by Guo et al. (2000), suggesting that nearly every hepatocyte is killed by CTL in a Fas-dependent manner. However, killing of hepatocytes can occur over a prolonged period of time, well balanced between apoptosis and replacement of hepatocytes (Mason *et al.* 2007). It has been estimated that the entire liver of woodchucks could be replaced between six and ten weeks (Guo *et al.* 2009).

Collectively, cytokines are important in triggering anti-viral intracellular defense mechanisms. However, they are probably not sufficient in controlling HBV-infection. Otherwise, chronic HBV patients would completely recover from infection after treatment with interferons. This happens unfortunately only in about 10-15% of cases (Niederau *et al.* 1996). Therefore, it has been postulated that a combination of both cytopathic and non-cytophathic effector mechanisms is required in controlling HBV infection (Thimme *et al.* 2003). In accordance with this hypothesis, we observed immunohistochemically that mononuclear cellular infiltrates adhere exclusively to cytoplasmic HBc positive hepatocytes. This reinforced the theory that direct cell-lysis of infected cells is indispensable to clear HBV infection. However, to substantiate the

importance of direct cell-lysis for the clearance of an acute HBV infection further analyses in mice are warranted. For instance, it would be interesting to know what happens to the clearance of an acute HBV infection if mice are deficient for IFN-γ secretion or if mice cannot kill target cells neither by perforin nor by CD95-receptor mediated apoptosis.

3.6.6 Are mice a suitable model system to analyze acute-HBV infection?

Mice are genetically and immunologically well characterized, simply modifiable by genetic engineering, easy to breed and they support hepadnaviral replication. Therefore, we used mice to analyze the clearance of an acute HBV infection under conditions where lymphocytes were unable to kill their target cells either by perforin/granzyme or CD95-mediated apoptosis release. However, mice are not unrestrictedly suitable to analyze all aspects of an acute HBV infection. The following section describes the limitations of the mouse model system.

The largest weakness of the system is that mice are not susceptible to natural hepadnaviral infections since the viral up-take into hepatocytes is hampered for still undefined reasons. Therefore, HBV-genomes must be transduced into hepatocytes. This can be achieved by two different ways either by hydrodynamic injection or by adenoviral gene transfer. Both applications have in common that (i) they do not mimic the natural cause of infection and in addition, (ii) huge amount of hepatocytes are infected at once.

The HBV-unspecific route of infection might alert the innate immunity independent of HBV. For example, intravenously applied adenoviral vectors preferentially target hepatocytes (Yang *et al.* 1994), but also encounter APC and non-parenchymal cells. Since the protein shell of the vector is immunogenic, an adenovirus-dependent immune response might be induced in addition to HBV-specific immune response. Although the vector by itself only triggers a mild liver inflammation in mice at 7 dpi, determined by ALT elevation and intrahepatic lymphocyte infiltrations (John von Freyend M. *et al.* 2009), the vector may increase the HBV-dependent immune response to some extent. In keeping with this, is has been shown that adenovirus as well as other unrelated viral liver-infections inhibit HBV replication and viral protein expression in HBV-transgenic mice (Guidotti *et al.* 1996a, Cavanaugh *et al.* 1998). This inhibition is based on noncytopathic cytokine-dependent pathways such as the release of interferon and TNF-α. Although the infections with replication-competent

viruses are not directly comparable to adenoviral vector transduction, they indicate that an unrelated activation of the innate immunity in the liver has profound influences on HBV-infection. The unrelated activation could also be caused by physical injury such as cell damage or stress induced by hydrodynamic injection.

Moreover, the onset and the dynamic of an acute HBV infection in mice transduced by AdHBV fundamentally differ from those in natural hosts. In mice, dynamics of viral parameters (viremia, HBeAg, HBsAg) and dynamics of immunological markers (intrahepatic T cell infiltration and ALT) peaked simultaneously at early time points. These data indicate that immediately after transduction, HBV-infection is recognized by the immune system. By contrast, naturally acquired HBV infection remains undetectable during the first four weeks after infection (Wieland *et al.* 2004, Guidotti *et al.* 1999b, Rehermann & Nascimbeni 2005). In this case, viral parameters do not overlap with immunological markers: viremia declines mostly before the ALT elevations and intrahepatic T cell infiltration appear.

It is possible that at the beginning of the natural infection, only a small subset of hepatocytes becomes infected and probably remains protected from direct contact of lymphocytes by the LSEC barrier (Knolle & Gerken 2000). However, spreading of the virus through the liver parenchyma leads to its recognition by the innate immune system. This results in cytokine-mediated inhibition of HBV replication followed by intrahepatic T cell infiltration and further control of HBV infection by the adaptive immune response.

Collectively, the natural cause of HBV infection seems to be very specific and circumvents the early immune response whereas vector transduction of HBV directly elicits a vigorous immune response in the host. This means that the mouse model only partially mimics the early phase of an acute HBV infection in a natural host. Since analyses on chimpanzees are mostly performed in a descriptive manner and depletion experiments with neutralizing antibodies are allowed at best, mice are a potent and indispensable tool to analyze important immunological questions concerning virus host interaction; especially, if those questions require specific genetic modifications like we did. Therefore, HBV-infection experiments in mice provide the basis for further phenotypic analysis in chimpanzees and humans.

4 Materials and Methods

4.1. Cell Culture

4.1.1 Culture Media and Buffers

DMEM medium	Dubbeccos MEM	500ml
(plus Supplements)	FCS	50ml
	Glutamine, 200mM	5.5ml
	Non essential amino acids	5.5ml
Williams medium	Williams E medium	500ml
(plus Supplements)	FCS	50ml
	Glutamine, 200mM	5.5ml
	Non essential amino acids	5.5ml
Perfusion solution I	HBSS, Ca^{2+}/Mg^{2+}free	500 ml
	EGTA, 100 mM	2.5 ml
	Heparin, 5000 U/ml	1ml
Perfusion solution II	Williams E medium	250 ml
	Calcium Chlorid, 1M	0.9 ml
	Gentamycin, 10 ng/ml	2.5 ml
	Collagenase type IV	200 mg
Wash medium	Williams E medium	500 ml
	Glutamine, 200 mM	5.6 ml
	Glucose, 5%	6 ml
	Hepes, 1 M, pH 7.4	11.5 ml
	P/S, 5000 U/ml	5.6 ml
	Solutions were mixed and stored as premix at -20°C	
PHH medium	Wash medium	500 ml
	Gentamycin, 10 mg/ml	5 ml
	Hydrocortison	0.5 ml
	Insulin	0.45 mg
	DMSO	8.7 ml
	Inosine, 82.5 mg/ml	2 ml
1:1 Medium	PHH medium	250ml
	Williams E medium plus Suppl.	250ml

4.1.1.1. Calculation of cell numbers and cell viability

A Neubauer hemacytometer was used to determine the cell number of a homogenous cell suspension. Four large squares of hemacytometer were counted and the number of cells was calculated as follows:

Cell number/ ml = (total cell number x dilution factor x $10^{4)}$ / 4

Remark: The factor 10^4corresponds to the volume of cell suspension considered for counting.

The cell viability in the cell suspension was determined by trypan blue by mixing equal volumes of cell suspension and dye prior counting. The trypan blue diffuses into all cells and exclusively stained dead cells because viable cells continuously remove the dye via pumps. Therefore, dead cells can be distinguished from living ones by light microscopy.

4.1.2 Primary Human Hepatocytes (PHH)

4.1.2.1. Isolation of PHH using two step perfusion

PHH were isolated from surgical liver resections obtained from patients undergoing partial hepatectomy. Informed consent was obtained from each patient and the procedure was approved by the local Ethics Committee.

The protocol is based on a collagen two-step perfusion as described in Schulze-Bergkamen (2003). Before the perfusion started the “perfusion solutions (I + II)” and the “PHH culture medium” were warmed up to 37°C. The “wash medium” was cooled down to 4°C and culture dishes were coated with collagen. Therefore, dishes were incubated with a collagen solution (Serva, Heidelberg) diluted 1:10 in steril ddH_2O water for at least 30 min at 37°C.

Healthy liver tissue (approx. 30 g resection material preferentially closed to the liver capsule) was used for perfusion: we canulated a large branch of the portal vein and started perfusion with about 500 ml perfusion-medium-I using a flow rate between 20 and 40 ml/min. From time to time, we changed the vessel used for canulation. The first perfusion step is necessary to wash out blood sticking in intrahepatic capillaries and vessels. Upon successful perfusion, the color of the resection tissue changed from red to brown after about 20 to 25 min. The second perfusion step was continued with 250 perfusion-medium-II containing the collagenase (Worthington, Lakewood)

approx. 15 to 20 min. As soon as the tissue softened and liver cells appeared in the medium the perfusion was stopped. The liver was cut into small peaces and the tissue was scratched off with a scalpel. The cell suspension was firstly filtered through double-layered gaze, and at second through a 70 µm cell strainer. After centrifugation of the cell suspension in 50 ml tubes for 5 min at 50 x g, 10°C, the supernatant was discarded and the cell pellet was re-suspended in 40 ml wash medium. The washing step was repeated three times (consisting of centrifugation and re-suspension of the cell pellet). After washing, cells were re-suspended in PHH medium and cell number and viability was determined. The cells were seeded on collagenized cell culture dishes at a density of 8 x 10^5 cells/ml of PHH medium supplemented with 10% FCS and maintained at 37°C, 5% CO_2. After 3h, the culture medium was changed to remove non adherent cells. After incubation over night, cells were kept in medium containing 5% FCS. From day 2 post seeding, cells were cultured continuously in FCS-free PHH medium. In order to remove cell debris, adherent PHH were washed vigorously at 3 days post seeding by pipetting culture medium several times towards the cell layer.

4.1.2.2. PEG-triggered HBV infection

About 5 days post-seeding, PHH were infected with indicated amounts of enveloped HBV particles obtained from HBV-replicating cells in the presence of 5% polyethylenglycol (PEG 8000). Mostly, frozen virus stocks with a moi of 200 was used. The virus stocks consists of HBV enriched culture medium of HepG2.2.15 cells. Depending on experimental requirements, culture medium of HBV-replicating cell lines supplemented with 5% PEG was also directly transferred to PHH for infection. – After overnight infection, PHH were washed three times to remove residues of the inoculum. In order to monitor a productive HBV-infection, culture medium was collected every second day and HBsAg plus HBeAg was determined by commercial assays (Axsym, HBeAg 2.0, HBsAg V2, Abbott Laboratories, Wiesbaden, Germany).

If apoptosis has been induced by *anti*-CD95 antibodies (Jo2, Pharmingen) the recipient PHH cultures were pre-treated with two caspase inhibitors for 1h to prevent remaining any anti-CD95 antibody activity: 2µM DEVD-CHO (Biomol, Plymouth, PA) and 100µM z-VAD (Alexis, Lausen, Switzerland). After overnight incubation of PHH

with HBV/PEG- containing medium, cells were washed twice with phosphate-buffered saline (PBS) and further cultured in PHH medium.

4.1.3 HBV-replicating cell lines

4.1.3.1. Cell culture conditions

All hepatoma cell lines were seeded on collagen coated culture dishes. Therefore, dishes were incubated with a collagen solution (Serva, Heidelberg) diluted 1:10 in sterile ddH_2O water for at least 30 min at 37°C. Cells are maintained in complete DMEM medium at 37°C and 5% CO_2 atmosphere. Cells were passaged/splitted at a ratio of 1:5 when they were 90-100% confluent.

4.1.3.2. Culture conditions boosting HBV-production

Hepatoma cell lines were cultured in a 1:1 mixture of „PHH-medium“ and „complete Williams E medium“ without passaging/splitting up to 6 weeks. The culture medium was collected every 3 day and replaced by a new one.

4.1.4 Production of HBV

For virus preparation, the virus-containing medium of HBV-producing cell lines was collected every third day. Cell debris were removed by centrifugation at 1000 rpm for 5 min and the supernatant was transferred to centrifugal filter devices (Centricon Plus-70, Biomax 100, Millipore Corp., Billerica). The first centrifugation was performed at 3500 x g for 1 h at 4°C, to capture the virus particles in a filter. Due to the exclusion limit of 100 kDa, serum proteins flow through, while proteins larger than 100 kDa stuck in the filter. The virus concentrate was eluted from the filter system by a second, invert centrifugation step at 2600 x g for 10 min. The virus concentrate was supplemented with 10% glycerol and stored at -80°C. The titer of eluted HBV particles was determined with Caesium chloride density gradient centrifugation, followed by dot blot analysis, as outlined below. By note, only enveloped HBV particles were considered as infectious and counted for the titer.

4.1.5 Induction of Apoptosis

In order to induce apoptosis in hepatoma cell lines, cell culture medium was removed and adherent cells were exposed to UV-C [20 mJ / cm^2] using UV chamber [GS GENE Linker; BIO Rad]. Cells were subsequently covered with medium and cultured for 24 h as described. Anti-CD95 Ab treatment was applied to induce apoptosis in

PHH. For this, we used the monoclonal anti-Apo1 antibody (kindly provided by H.-P. Krammer, DKFZ Heidelberg, Germay) at concentrations of 100 ng/ml in the presence of 50 ng/ml protein A [Fluka, Germany] as described (Schulze-Bergkamen *et al.* 2003).

4.2. Production of Adenoviral Vectors

The production of pure and highly infectious AdHBV stocks used for animal experiments can be separated in different parts: (i) propagation of adenoviral vectors in 293 cells; (ii) cell harvest and cell disruption; (iii) purification of viral particles by CsCl gradient centrifugation; (iv) dialysis, and (v) titration.

The following protocol is designed to produce about 15 ml of highly infectious AdHBV stocks with titers ≥ $5x10^9$ infectious VP/ml.

4.2.1.1. Vector Propagation

293 cells were seeded into 15 to 17 culture flasks (175 cm^2) to be 80-90% confluent at time of infection. Every flask of 293 cells was infected with approximately $1x10^8$ infectious AdHBV particles corresponding to a moi of 3 to 5.

At 40 h post infection, the monolayer of 293 cells showed a significant cytopathic effect characterized by rounded cell shapes and cell detachment. Cells were harvested in their culture medium. To unhitch all cells, the culture flask was bead to the palm several times. The cell suspension of all flasks was combined and cells were pellet into two 50 ml falcon tubes by several rounds of centrifugation at 4000 rpm for 5 min. Since 90% of the produced vectors stuck inside the cells, they were disrupted by 3 freeze/thaw cycles. Therefore, cell pellets were re-suspended in about 30 ml of the collected culture medium, followed by alternating frozen in liquid nitrogen and thawing in 37°C waterbath. After sedimentation of the cell debris, supernatant containing adenoviral vectors were subjected to CsCl gradient centrifugation (see below).

4.2.1.2. CsCl Gradient

The total volume of 60 ml vector containing supernatant (2 falcons à 30 ml) were purified one after another by CsCl gradient ultra centrifugation. (One falcon was stored at 4°C until usage.) Therefore, the content of the falcon was filled up to 48 ml DMEM medium (without supplements) and 24.4 g CsCl were added. This solution

was portioned into 6 centrifugation tubes (SW-40 polyallomer vials; Beranek Laborgeräte) in equal amounts and balanced. The tubes were covered with mineral oil about 2 mm below the edge and balanced a second time. Ultra-Centrifugation was performed in SW40Ti rotor at 32,000 rpm for 40 h at 10°C. Figure 1 represents a CsCl gradient with concentrated bands of adenoviral vectors after 24h or 40h centrifugation, respectively. Upon 40 h centrifugation, the lower white band of adenoviral vectors was collected. Therefore, the gradient was pipette off from top to the respective band. The upper bands containing empty or defect particles were discarded.

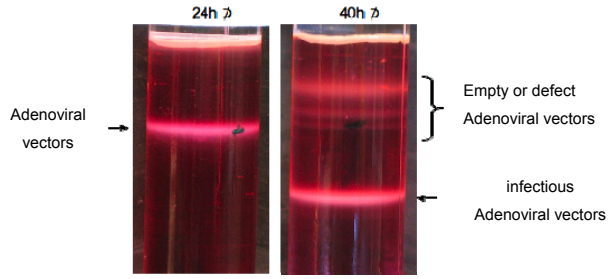

Figur 1 concentrated bands of adenoviral vectors upon CsCl centrfugation

4.2.1.3. Dialysis

The collected fractions of adenoviral particles were pooled and diluted to same amounts in dialysis buffer. The solution was filled in 15 ml dialyse chambers and stirred for about 16 h in 700 ml dialysis buffer to remove the toxic CsCl content. The buffer was replaced at least three times. (Upon dialysis, the virus was stored at 4°C until the second round of virus purification was performed (second falcon with 30 ml virus supernatant)). The dialyzed virus solutions were combined, aliquoted and frozen at -80°C.

Dialysis Buffer	NaCl	137 mM	16 g
	KCl	5 mM	0.74 g
	Tris	10 mM	2.42 g
	$MgCl_2$ $6H_2O$	1 mM	0.4 g
			add 2 l H_2O

4.2.1.4. Titration

The infectivity of the produced virus stock was estimated by cytopathic cell destruction in infected 293 cells. Therefore, 293 cells were seeded into 12 well plates to be 80-90% confluent at time of infection corresponding to $1x10^6$ cells per well. The wells were covered with 1 ml medium. A dilution serial of the frozen aliquots was performed as indicated in the following: viral stock solution of 100 µl, 30 µl, 10 µl and 3µl, respectively, were added to the wells in the top row and cautiously dispensed. 100 µl culture medium of each well were transferred to the well below (middle row). The medium was mixed again, and 100 µl were transferred a second time to the wells in the last row corresponding to a virus volume of 1 µl, 0.3 µl, 0.1 µl and 0.03 µl.

After 48h post infection, the cytophatic effect of the dilution serial was assessed. The well of cells infected with the lowest amount of virus inducing cell detachment was marked and used for titer calculation of the viral stock.

The calculation of virus titer is based on the following assumptions: (i) $1x10^6$ 293 cells per well were infected with corresponding volumes of virus; (ii) the minimal titer necessary to infect 100% of seeded cells (assessed by cell detachment) correspond to a moi of approx. 3-5 viral particles per cell.

100 µl	$5x10^7$ IU/ml	1 µl	$5x10^9$ IU/ml
30 µl	$2x10^8$ IU/ml	0.3 µl	$2x10^{10}$ IU/ml
10 µl	$5x10^9$ IU/ml	0.1 µl	$5x10^{10}$ IU/ml
3 µl	$2x10^9$ IU/ml	0.03 µl	$2x10^{11}$ IU/m

4.3. Quantitative Real Time PCR

4.3.1 Introduction into *Real Time* qPCR

The quantitative real time polymerase (qPCR) reaction is the most sensitive technique for cDNA and (microbial) DNA quantifications currently available; copy numbers of genes in starting material from 10 to $10x10^{10}$ could be discriminated. By contrast, a range of 2-3 logs of templates can be quantitated by traditional end-point PCR reactions after gel electrophoresis of PCR products and measurement by densitometry.

The real time PCR reaction is based on a "traditional" PCR reaction combined with a fluorescence detection format that is either SYBR Green-I, an intercalating fluorescent dye, or target-specific fluorescently labeled probes. The measurement requires a special thermocycler equipped with a sensitive camera that monitors the fluorescent intensity in each reaction after each amplification cycle. The measured fluorescent intensity directly correlates to the amount of PCR product formed during the exponential phase.

4.3.2 Quantification of qPCR

The **absolute quantification** determines the absolute number of copies per reaction and the **relative quantification** (fold-change calculation) defines the relative amount of a target gene normalized to a reference gene (loading control).

A reference for quantification should be a gene that is constantly expressed in tissues or cells being analyzed such as beta actin, MHC I, ribosomal RNA, GAPDH, HPTR and many others. Note that no "gold standard" exists, which can be used as reference for all tissues or species.

A very precise method to define the "loading" of a PCR reaction is the relative quantification by <u>two</u> or more reference genes. Thus, regulatory side effects of reference genes are minimized. [Fold-change (target gene) = relative amount (target) / relative amount (reference (A+B))]

4.3.2.1. Principles of Measurement

The software of the thermocycler plotted the detected fluorescent intensity (FL) against cycle number on a logarithmic scale and determined the threshold (see

below) for detection. The cycle at which the FL of the sample crosses the threshold is called cycle threshold (CT); this value is used for quantifications.

4.3.2.2. Threshold

Different methods exist to define the threshold. To quantify PCR templates, the threshold should be site to the exponential phase of the PCR reaction. In order to define the exponential phase of a PCR reaction the **second derivative maximum (SDM)** method was performed, provided by the LC quantification software. The SDM specifies the highest point of the exponential phase before the curve turns into a linear range. (Thus, the amplification of genes by PCR is exponential between the background and before SDM.) The LC software automatically set the threshold to SDM.

4.3.2.3. Efficiency of PCR reaction

Theoretically, the amount of DNA doubles with every cycle (efficiency of amplification correspond to 100%). Therefore, a CT difference of 3.3 between to samples means that the amount of template differs by a factor of 10 and a CT of 1 corresponds to a factor of 2. However, in most cases the efficiency of a PCR reaction is below 100%. Since small differences in efficiency of PCR reactions, make a lot differences in the amount of final product (e.g. an efficiency of 90% results in less than 25% total amount after 30 cycles), it is very important to determine the efficiency of genes being amplified; this is done by a dilution series of the respective gene quantified by the SDM method.

4.3.2.4. Melting curves

Since Syber Green unspecifically intercalates in dsDNA molecules, the product specificity is not award by real time PCR reactions. To confirm that the right PCR fragment corresponds to the fluorescence being measurement, a melting curve is performed at the end of a PCR reaction. All PCR products of a specific primer should have the same melting temperature. If two or more PCR products are present (e.g. primer dimer or unspecific PCR products), different melting temperatures are detectable. Note that random amplification products (like primer dimer) could be excluded from measurement by increasing the temperature chosen for fluorescence detection after each cycle.

4.3.3 Protocols of qPCR

4.3.3.1. Used thermcyclers

A) Light Cycler 2.0 (Roche Diagnostic, Mannheim, Germany)

B) Light Cycler 480 II (Roche Diagnostic, Mannheim, Germany)

4.3.3.2. PCR Mix

	LightCycler FastStart Masterplus SYBR Green I	LightCycler 480 SYBR Green I Master	
sample	2 µl	2 µl	2
PCR Mix	4 µl	10 µl	
Forward primer (20 nM)	1 µl	1 µl	
Reversed primer (20 nM)	1 µl	1 µl	
H_2O	12 µl	6 µl	

4.3.3.3. Running conditions

	cccDNA		Ad HBV/ Mito		rcDNA	
Start	95°C	5 min	95°C	5 min	95	
Cycles						
denaturation	95°C	15 sec	95°C	15 sec	95°C	15 sec
annealing	60°C	4 sec	55°C	10 sec	60°C	10 sec
elongation	72°C	25 sec	72°C	25 sec	72°C	25 sec
detection	88°C	2 sec	72°C	25 sec	83°C	1 sec
Melting	95°C	10 sec	95°C	10 sec	95°C	10 sec
	65°C	60 sec	65°C	60 sec	65°C	60 sec
	95°C	continuous	95°C	continuous	95°C	continuous
Final	40°C	hold	40°C	hold		

	All other genes (C3)		FADD PCR		OneStep-RT	
Start	95°C	5 min	94°C	3 min	61°C	20 min
					95°C	2 min
Cycles						
denaturation	95°C	15 sec	95°C	15 sec	95°C	15 sec
annealing	60°C	4 sec	55°C	15 sec	60°C	4 sec
elongation	72°C	25 sec	72°C	15 sec	72°C	25 sec
detection	72°C		72°C		78°C	2 sec
Melting	95°C	10 sec	95°C	10 sec	95°C	10 sec
	65°C	60 sec	65°C	60 sec	65°C	60 sec
	95°C	continuous	95°C	continuous	95°C	continuous
Final	40°C	hold	40°C	hold	40°C	hold

4.3.3.4. Primers

cccDNA recognizes pHT1.3	2760 (+) 156 (-)	5´ GACTCTCTCGTCCCCTTCTC 3´ 5´ ATGGTGAGGTGAACAATGCT 3´
cccDNA	2251 (+) 92 (-)	5´ AGCTGAGGCGGTATCTA 3´ 5´ GCCTATTGATTGGAAAGTATGT 3´
HBV	HBV 1844 (+) HBV 1745 (–)	5' GTTGCCCGTTTGTCCTCTAATTC 3' 5' GGAGGGATACATAGAGGTTCCTTGA 3'
Ad	Ad 156 (+) Ad 388 (–)	5' TAAGCGACGGATGTGG 3' 5' CCACGTAAACGGTCAAAG 3'
Mitochrial DNA	Mito 8686 (+) Mito 8796 (-)	5´CCCTCTCGGCCCTCCTAATAACCT 3´ 5`GCCTTCTCGTATAACATCGCGTCA 3
GAPDH		5' ACCAACTGCTTAGCCC 3' 5' CCACGACGGACACATT 3
HPRT		5´CACGTTTGTGTCATTAGTGAA 3 5´AAGATAAGCGACAATCTACC 3´
IFN		5' ATGGTGACATGAAAATCCTG 3' 5' GTGGACCACTCGGATGA 3'
CD8		5' GGATTGGACTTCGCCTG 3' 5' CAAGTATGCTTTGTGTCAAAGA 3'
CD4		5' AGCTCAACAATACTTTGACC 3' 5' CCCAGAAAGCCGAAGGA 3'
FADD PCR	524 (sense)	5´TCACCGTTGCTCTTTGTCTAC 3´
	525 (antisense)	5´GTAATCTCTGTAGGGAGCCCT 3´
	527 (antisense)	5´CTAGCGCATAGGATGATCAGA 3`
Afp-Cre	700 Alb-prom (sense)	5´TTCTGCACACAGATCACCTTTC 3`
	699 cre as (antisense)	5´GTGTACGGTCAGTAAATTGGAC 3`

4.4. Assays Detecting Apoptosis / Cell Viability

4.4.1 Viability Measurement by XTT

The cell viability of adherent cells plated in 96 well dishes was determined by XTT test (Cell Profiferation Kit II, XTT, Roche Diagnostics, Penzberg, Germany) upon manufactures instructions. The test is based on cleavage of the tetrazolium salt XTT by metabolic active cells. The formazan dye formed is soluble in culture medium and can directly be quantified by densitometry. We determined viability at 1h after addition of substrate using a scanning multiwell spectrometer (Tecan, Männedorf, Switzerland), absorbance 450nm, reference 650 nm

4.4.2 Immunofluorescence Microscopy

The LIVE/DEAD® Viability/Cytotoxicity kit (Molecular Probes, Europe BV) was used to detect live and dead cells simultaneously. Cell were stained for intracellular esterase activity using 2µM Calcein AM and plasma membrane integrity using 2µM Ethidium homodimer-1 (EthD-1). Viable cells appear green (Calcein), dead cells red (EtD-1).

4.4.3 Caspase 3/7 Assay

Caspase-3 assay. The activity of caspase-3/7 was determined as described elsewhere (Deveraux *et al.* 1998). Briefly, cytosolic protein extracts of cells cultured on 6-well plates were prepared in 200 µl buffer A (20 mM Hepes pH 7.5, 10 mM KCl, 1.5 mM $MgCl_2$, 1 mM EDTA, 1 mM dithiolthreitol, 0.1 mM PMSF). 5 µl cytosolic protein extracts were added to 100 µl caspase buffer (20 mM Pipes, 100mM NaCl, 10mM DTT, 1 mM EDTA, 0.1% CHAPS and 10% Sucrose) and incubated with 100 µM caspase-3 substrate Ac-DEVD-AFC (Alexis, Lausen, Switzerland). Release of fluorgenic AFC from cleaved caspase-3 substrate was compared after 30 min at 30°C using the Genios Pro fluorometric plate reader (Tecan, Männedorf, Switzerland)

4.4.4 DNA Fragmentation

Low molecular weight DNA was extracted from cells cultured on 6-well plates. Cells were harvested and resuspended in lysis buffer (100 mM Tris pH 8.5; 5 mM EDTA; 200 mM NaCl, 0.2% SDS) containing 3 µg/ml Proteinase K (Roche, Karlsruhe, Germany) for 16h at 37°C. Afterwards RNase A (Macherey-Nagel, Düren, Germany)

digestion was performed 30 min at 37°C and DNA was extracted with phenol and phenol/chloroform. The DNA was subjected to 1.5% agarose gel electrophoresis and laddering was visualized by ethidium bromide staining.

4.5. Molecular Biology

4.5.1 CsCl Density-Gradient Centrifugation

In order to separate HBV particle due to their densities, CsCl gradient centrifugation was performed. CsCl solutions of differend densities (see below) were layered one upon the other in SW-60 polyallomer vials (Beranek Laborgeräte). From botton to top 500 µl of 1.4 g/l, 1.3 g/l and 1.15 g/l were applied, followed by 500 µl of a 20% sucrose solution. The sample was layered on top and vials were filled up with PBS. Ultra-centrifugation was performed at 55000 rpm at 20°C for 10 h to over night using SW-60 swing bucket rotor (Beckman). Upon centrifugation, the gradient was fractionated from bottom to top with a Fraction recovery system (Beckman). Each fraction contained 6 drops, which correspond approx. to a volume of 175 µl. Afterwards the fractions were subjected to quantitative dot blot analysis.

4.5.2 Dot Blot Analysis

For quantitative and qualitative analysis of HBV particles, DNA dot blot analysis was performed. Collected fractions of the CsCl gradient, or simply culture media of HBV-replicating cells (approx. 500 µl), were dotted onto a nylon membrane (Roche Diagnostics, Mannheim) using a dot blot aperture (Schleicher & Schuell, Dassel). The doted samples were quantified relative to a dilution series of plasmid HBV DNA standard ranging from 8 pg to 1000 pg. The membrane was washed twice with PBS, before it was transferred to a Whatman paper soaked with 0.4 mM NaOH for 5 min (depurination of DNA molecules). Afterwards, the membrane was transferred to a Whatman paper soaked with SSC (2x) buffer. The dried membrane was cross-linked in an UV-oven. A ^{32}P-labelled HBV DNA probe was used for hybridization at 68°C over night. Upon washing with SSC (2x) buffer, the membrane was exposed to a phosphor-screen and quantified on Phosphoimager (Molecular Dynamics, Sunnyvale, CA).

4.5.3 Northern Blot Analysis

The Northern blot analysis is a technique to identify specific sequences of RNA. Thus, RNA molecules are separated by electrophoresis due to their size, transferred to nitrocellulose, and identified with a ^{32}P labeled hybridization probe complementary to parts of the target sequence.

4.5.3.1. Agarose Gel with formaldehyde

An amount of about 20-30 µg total RNA was separated on agarose gel (1%) containing formaldehyde (20%) as a denaturing agent. The gel was run in a vertical direction at 80 V for 5 h at 4°C. Running buffer was E-buffer (1x)

E-Buffer (10x):	300 mM NaH_2PO_4 50 mM EDTA	pH 7.0
stucking gel:	2% agarose in E-buffer (1x)	(1g add 50 ml)
resolving gel:	1% agarose in E-buffer (1x) supplemented with 20% formaldehyde (1.5 g agarose was heated in 120 ml ddH_2O; after cooling down to 50°C, 30 ml formaldehyde were added and the gel was carefully cast in respective camber.)	
preparation of samples	25 µg RNA 10 µl E-buffer (10x) 15 µl formaldehyde 40 µl formamid	RNA samples were heated at 65°C for 10 min and immediately put on ice. Each probe was supplemented with 5 µl loading buffer
Saline-sodium citrate (SSC) buffer (20x)	Natrium Cloride 350,6 g Tri-Sodium Citrate 176,5 g Add 2l	

4.5.3.2. Blotting

Capillary blotting (over night) was used to transfer RNA from the gel to a positive charged nylon membrane; transfere buffer: SSC (20x). The transferred RNA was immobilized through covalent linkage to the membrane by UV light before it was hybridized to specific probes.

4.5.4 Hybridization Probes (^{32}P)

For hybridization of nucleic acids fixed on Nylon membranes (see DNA dot blot or Nothern blot), a α^{32}P-dCTP labelled, sequence specific DNA probe was used. The

labeling was performed with 25 ng DNA using rediprime DNA Labeling System (Amersham, Buckinhamshire, England).

The hybridization solution consists of 25 ml hybridization buffer, 10 ng salmon sperm DNA and the specific probe. (By note, to separate DNA strands, salmon sperm DNA and the probe were heated at 95°C for 1 min and chilled on ice before they were added to the hybridization buffer!)

Hybridization was performed at 68°C degrees for at least 16h. After hybridization, membrane was washed 2-times with hybridization wash buffer I for at least 20 min at 68°C and 2-times with hybridization wash buffer II for at least 20 min at 68°C. Afterwards, membrane was laminated and exposed to a phosphor-screen for 48h and quantified on Phosphoimager (Molecular Dynamics, Sunnyvale, CA).

Hybridization buffer (Church)	0.25 M $NaPO_4$-buffer 1 mM EDTA 1% BSA 7% SDS
$NaPO_4$-buffer (0.5M; pH 7.2)	342 ml (A) + 158 ml (B) + 500 ml H_2O A) Na_2HPO_4 $2H_2O$ (1M): 177.9 g B) NaH_2PO_4 $2H_2O$ (1M): 156.0 g
Hybridisation Wash buffer I	SSC (2x) 0.1 % SDS
Hybridisation Wash buffer II	SSC (2x)

4.5.4.1. HBV Probe

Plasmid pCH-9/3091 (6338 kb) (HBV genome between Sal I and Nhe I)

1. Digestion (Sal I): 10 µg DNA, 5 µl buffer (orange), add 50 µl H_2O >> 2 h 37°C
2. PCR fragment purification: Mini Elute (Qiagen) > elution 40 µl
3. Digestion (Cui I (AlwNI 4872) + Nhe I): 10 µg DNA (elution 40 µl) 2 µl per Enzyme + 5 µl buffer (yellow), add 50 µl >> 2h 37°C
4. Preparative Gel (0.8% agarose) > 3,054 kb fragment correspond to the probe
5. Gel extraction kit (Qiagen) > elution 200 µl (probe: 2.5-25 ng)

4.5.4.2. GAPDH Probe

pBS-GAPDH (10 µg)> digestion BamHI/XbaI 2 h 37°C > preparative gel > GAPDH fragment: 814 bp.

4.5.5 RNA/DNA-Methods

4.5.5.1. Calculation of DNA/RNA Concentration

The concentrations of DNA and RNA were calculated from absorption of light at 260 nm and the Lambert- Beer´s law. (used photometer: NanoVue, GE, Haelthcare)

DNA concentration [µg|ml] = (A260) sample X 50 X dilution factor

RNA concentration [µg|ml] = (A260) sample X 40 X dilution factor

The purity of nucleic acids was determined by the ratio (A260/A280). By note, the ratio should be ≥ 1.7 for high quality and useful (RT) PCR results.

4.5.5.2. RNA Isolation

RNA Isolation with TRIzol (Invitrogen) after manufactures instruction.

RNA clean up with

4.5.5.3. cDNA Synthesis

SuperScript III First-Strand Synthesis SuperMix for qRT-PCR (Invitrogen) was used to transcribe 750 ng RNA after manufactures instructions.

4.5.5.4. DNA Isolation

DNA isolation was performed with different kit systems after manufactures instructions using QIAamp MiniElute Virus Spin Kit, QIAamp DNA blood, DNeasy Tissue

4.5.6 ELISA

Enzyme-Linked Immunosorbent assay (ELISA) is a biochemical technique to analyze the presence of an antigen or antibody in the sample. We performed different ELISA to determine (i) the structure of HBV particles (envelopment), (ii) to detect different viral antigens in serum of mice (HBe, HBs, anti-HBs, anti-HBc), (iii) to characterize the isotype profile of specific antibodies against viral antigens.

4.5.6.1. HBsAg (characterization of HBV particles)

To analyze HBV envelopment, HBV particles released were separated by CsCl gradient centrifugation. Collected fractions were dialyzed in Slide-A-Lyzer Mini Dialysis Units 10 K MWCO (Pierce). 2 µl of the dialyzed CsCl fractions were

analyzed by commercial available anti-HBsAg ELISA (Murex®; Abbott, Wiesbaden, Germany). Samples were quantified absolute to an external standard using a dilution series of recombinant HBsAg (Engerix®-B, GlaxoSmithKline, London, GB) (100 – 2 ng/ml).

4.5.6.2. HBs, HBe, anti-HBs and anti-HBc

The AXSYM assay system (Abbott laboratories, Abbott park, IL, USA) was used to determine viral antigens and antibodies in serum of mice. Samples were diluted 1:20 in PBS in a total volume of 600 µl.

4.5.6.3. Isotype Profiles

Commercial anti-HBsAg and anti-HBcAg ELISA assays (Dade Behring; Enzygnost; Anti-HBs II or anti-HBcAg monoclonal, Germany) were combined with HRP-conjugated IgG isotype-specific secondary anti-mouse antibodies IgG_3, IgG_1, IgG_{2b} and IgG_{2a} (SouthernBiotech, Birmingham, AL) (dilution: 1:2000) to measure the isotype profile of anti-HBs and anti-HBc antibodies in mouse sera.

4.6. cDNA Microarray

4.6.1 Principle of cDNA Microarray

The cDNA microarray is a multiplex technology, designed to compare the relative expression levels of thousands of genes simultaneously in different cells or tissues. Commercial gene chip consist of thousands of microscopic spots of oligonucleotides of known sequence “arrayed” on carrier. The gene chip is hybridized with the fluorescently labeled unknown mixture of cDNA being analyzed corresponding to the transcriptome of interest. After intensive washing, the chip is scanned by a laser measuring the intensity of fluorescence at each spot. To this end, the data are entered into a database and becomes analyzed by a number of statistical methods. The detected fluorescent intensity at each spot correlates to the amount of complementary cDNA molecules present in the sample. Importantly, changes in gene expression level are calculated by comparing of two or more samples hybridized to identical gene chips in parallel.

4.6.2 Performance of Microarray

Gene expression profiling was performed in the lab of Prof. Dr Joachim Schulze by Dr. Svenja Debey-Pascher. The obtained data (fold-change levels and assignment of gene functions), were further evaluated by the author.

Briefly, RNA was isolated from hepatoma cell lines (see results) by TRIzol (Invitrogen) and cleaned up by RNeasy (Qiagen). 100 ng RNA were reversed transcribed and 1.5 µg cDNA were hybridized to the Illumina Gene Chip WG-6. The arrays were scanned with Illumina BeadStation 500x. Raw data were extracted by BeadStudio software 3.1.1. – For further analysis Gene Ontology Annotation Database and Microsoft Excel was used.

4.7. FACS

4.7.1 Principle of FACS Measurement

Fluorescent-activated cell sorting (FACS) uses the principles of light scatting, excitation and emission of fluorochrome molecules to generate multi-parameter data from particles and cells, which are hydro-dynamically focused to a laser. FACS analysis is used to differentiate cells due to there seize and granularity combined with staining of specific cell surface structures as well as intracellular proteins (like cytokines) by antibodies conjugated to fluorescent dyes.

4.7.2 Cell Surface Staining

A total of $5x10^6$ to $1x10^7$ freshly isolated liver associated lymphocytes from mice were stained with CD4-Poly7 (1:100), CD8-FITC (1:100) , B220-PE (1:100) and Thy1.1-APC (1:500) conjugated antibodies for 1h. Afterwards, cells were washed with phosphate-buffered saline and analyzed on flow cytometer (FACSCalibur; BD Bioscience) using the CellQuest software.

4.8. Animal Experiments

Mice were kept in the mice facility department of the Institute of Pathology, University of cologne. C57BL/6, gld/B6Smn.C3-Tnfs6 and C57/BL/6-Perf1 were obtained from Charls River. FADDfl/fl mice were obtained from the lab of Prof. Dr. Manolis Pasparakis.

All mice were euthanized by carbon dioxide inhalation for harvesting of organs. If tissues were subjected to histological analyzes, the organs were fixed in 4% formalin.

4.8.1 Intravenous Injection (i.v.)

Mice were intravenously injected into the tail vain. Therefore, mice were warmed under a heating light to dilate the veins facilitating injection. The mouse was placed in a mouse holder, the tail was disinfected with 70% ethanol and hold firmly. A 25-gauge attached to a syringe was inserted into the lumen of the vein; if no resistance was felt by pushing the plunger, the material (virus (AdHBV $1x10^9$ vp) or anti-CD95 antibodies (Jo2, Pharmingen) or HBV capsids) was injected in a total volume of 200 µl (adjusted by physiological natrium chlorid solution). Upon retraction of the needle, the tail was disinfected a second time and pressure was applied to the site of injection for 5 seconds to ensure hemostasis.

4.8.2 Retro-Orbital Blood Collection

The peri-orbital sinus of the mouse was used as a source of venous blood. Up to 0.5 ml blood can be obtained by this method of mice older than 6 weeks. Therefore, mice were anaesthetized; per g body weight (mouse) 100 µl of anaesthethic solution (1 ml Ketanest (Ketavet; 100 mg/ml), 0.25 ml Rompun (2%) and 8.75 ml 0.9% NaCl) were applied intraperitonial. The mouse was restrained in one hand and a microhematocrit tube was insets into the lateral canthus of the eye at about 60° angle to the side of the head. The tube was quickly rotated to score the sinus. Once the sinus has been ruptured blood flow and was collected. As soon as the tube has been withdrawn the bleeding stops.

4.8.3 ALT-Measurement

For ALT measurement, 32 µl serum was used and quantified in Reflovet Plus System (Roche Diagnostics, Mannheim Deutschland).

5 References

Acs, G., Sells, M.A., Purcell, R.H., Price, P., Engle, R., Shapiro, M. & Popper, H. (1987) Hepatitis B virus produced by transfected Hep G2 cells causes hepatitis in chimpanzees. **Proc Natl Acad Sci U S A,** 84**,** 4641-4.

Adams, J.M. & Cory, S. (1998) The Bcl-2 protein family: arbiters of cell survival. **Science,** 281**,** 1322-6.

Ando, K., Guidotti, L.G., Wirth, S., Ishikawa, T., Missale, G., Moriyama, T., Schreiber, R.D., Schlicht, H.J., Huang, S.N. & Chisari, F.V. (1994) Class I-restricted cytotoxic T lymphocytes are directly cytopathic for their target cells in vivo. **J Immunol,** 152**,** 3245-53.

Ando, K., Moriyama, T., Guidotti, L.G., Wirth, S., Schreiber, R.D., Schlicht, H.J., Huang, S.N. & Chisari, F.V. (1993) Mechanisms of class I restricted immunopathology. A transgenic mouse model of fulminant hepatitis. **J Exp Med,** 178**,** 1541-54.

Aragane, Y., Kulms, D., Metze, D., Wilkes, G., Poppelmann, B., Luger, T.A. & Schwarz, T. (1998) Ultraviolet light induces apoptosis via direct activation of CD95 (Fas/APO-1) independently of its ligand CD95L. **J Cell Biol,** 140**,** 171-82.

Arzberger, S., Hoesel, M. & Protzer, U. (2009, submitted) Apoptosis of hepatitis B virus infected hepatocytes does not release infectious virus

Ashkenazi, A. & Dixit, V.M. (1998) Death receptors: signaling and modulation. **Science,** 281**,** 1305-8.

Balkow, S., Kersten, A., Tran, T.T., Stehle, T., Grosse, P., Museteanu, C., Utermohlen, O., Pircher, H., von Weizsacker, F., Wallich, R., Mullbacher, A. & Simon, M.M. (2001) Concerted action of the FasL/Fas and perforin/granzyme A and B pathways is mandatory for the development of early viral hepatitis but not for recovery from viral infection. **J Virol,** 75**,** 8781-91.

Baron, J.L., Gardiner, L., Nishimura, S., Shinkai, K., Locksley, R. & Ganem, D. (2002) Activation of a nonclassical NKT cell subset in a transgenic mouse model of hepatitis B virus infection. **Immunity,** 16**,** 583-94.

Bartenschlager, R., Junker-Niepmann, M. & Schaller, H. (1990) The P gene product of hepatitis B virus is required as a structural component for genomic RNA encapsidation. **J Virol,** 64**,** 5324-32.

Bayer, M.E., Blumberg, B.S. & Werner, B. (1968) Particles associated with Australia antigen in the sera of patients with leukaemia, Down's Syndrome and hepatitis. **Nature,** 218**,** 1057-9.

Beck, J. & Nassal, M. (2007) Hepatitis B virus replication. **World J Gastroenterol,** 13**,** 48-64.

Beere, H.M. (2005) Death versus survival: functional interaction between the apoptotic and stress-inducible heat shock protein pathways. **J Clin Invest,** 115**,** 2633-9.

Birnbaum, F. & Nassal, M. (1990) Hepatitis B virus nucleocapsid assembly: primary structure requirements in the core protein. **J Virol,** 64**,** 3319-30.

Blumberg, B.S., Sutnick, A.I. & London, W.T. (1968) Hepatitis and leukemia: their relation to Australia antigen. **Bull N Y Acad Med,** 44**,** 1566-86.

Bock, C.T., Schranz, P., Schroder, C.H. & Zentgraf, H. (1994) Hepatitis B virus genome is organized into nucleosomes in the nucleus of the infected cell. **Virus Genes,** 8**,** 215-29.

Bock, C.T., Schwinn, S., Locarnini, S., Fyfe, J., Manns, M.P., Trautwein, C. & Zentgraf, H. (2001) Structural organization of the hepatitis B virus minichromosome. **J Mol Biol,** 307**,** 183-96.

Bock, C.T., Schwinn, S., Schroder, C.H., Velhagen, I. & Zentgraf, H. (1996) Localization of hepatitis B virus core protein and viral DNA at the nuclear membrane. **Virus Genes,** 12**,** 53-63.

Bottcher, B., Wynne, S.A. & Crowther, R.A. (1997) Determination of the fold of the core protein of hepatitis B virus by electron cryomicroscopy. **Nature,** 386**,** 88-91.

Bouchard, M.J. & Schneider, R.J. (2004) The enigmatic X gene of hepatitis B virus. **J Virol,** 78**,** 12725-34.

Bremer, C.M., Bung, C., Kott, N., Hardt, M. & Glebe, D. (2009) Hepatitis B virus infection is dependent on cholesterol in the viral envelope. **Cell Microbiol,** 11**,** 249-60.

Bruss, V. (1997) A short linear sequence in the pre-S domain of the large hepatitis B virus envelope protein required for virion formation. **J Virol,** 71**,** 9350-7.

Bruss, V. & Ganem, D. (1991) The role of envelope proteins in hepatitis B virus assembly. **Proc Natl Acad Sci U S A,** 88**,** 1059-63.

Bruss, V., Hagelstein, J., Gerhardt, E. & Galle, P.R. (1996) Myristylation of the large surface protein is required for hepatitis B virus in vitro infectivity. **Virology,** 218**,** 396-9.

Bruss, V. & Thomssen, R. (1994) Mapping a region of the large envelope protein required for hepatitis B virion maturation. **J Virol,** 68**,** 1643-50.

Bruss, V. & Vieluf, K. (1995) Functions of the internal pre-S domain of the large surface protein in hepatitis B virus particle morphogenesis. **J Virol,** 69**,** 6652-7.

Budkowska, A., Dubreuil, P., Gerlich, W.H., Lazizi, Y. & Pillot, J. (1988) Occurrence of pre-S1 antigen in viremic and nonviremic carriers of hepatitis B surface antigen. **J Med Virol,** 26**,** 217-25.

Cao, T., Lazdina, U., Desombere, I., Vanlandschoot, P., Milich, D.R., Sallberg, M. & Leroux-Roels, G. (2001) Hepatitis B virus core antigen binds and activates naive human B cells in vivo: studies with a human PBL-NOD/SCID mouse model. **J Virol,** 75**,** 6359-66.

Cattaneo, R., Will, H., Hernandez, N. & Schaller, H. (1983) Signals regulating hepatitis B surface antigen transcription. **Nature,** 305**,** 336-8.

Cavanaugh, V.J., Guidotti, L.G. & Chisari, F.V. (1998) Inhibition of hepatitis B virus replication during adenovirus and cytomegalovirus infections in transgenic mice. **J Virol,** 72**,** 2630-7.

Chen, A., Kao, Y.F. & Brown, C.M. (2005) Translation of the first upstream ORF in the hepatitis B virus pregenomic RNA modulates translation at the core and polymerase initiation codons. **Nucleic Acids Res,** 33**,** 1169-81.

Chen, M., Sallberg, M., Thung, S.N., Hughes, J., Jones, J. & Milich, D.R. (2000) Nondeletional T-cell receptor transgenic mice: model for the CD4(+) T-cell repertoire in chronic hepatitis B virus infection. **J Virol,** 74**,** 7587-99.

Chen, Y., Wei, H., Sun, R., Dong, Z., Zhang, J. & Tian, Z. (2007) Increased susceptibility to liver injury in hepatitis B virus transgenic mice involves NKG2D-ligand interaction and natural killer cells. **Hepatology,** 46**,** 706-15.

Chen, Z., Cheng, Y., Xu, Y., Liao, J., Zhang, X., Hu, Y., Zhang, Q., Wang, J., Zhang, Z., Shen, F. & Yuan, Z. (2008) Expression profiles and function of Toll-like receptors 2 and 4 in peripheral blood mononuclear cells of chronic hepatitis B patients. **Clin Immunol,** 128**,** 400-8.

Cheng, P.C., Dykstra, M.L., Mitchell, R.N. & Pierce, S.K. (1999) A role for lipid rafts in B cell antigen receptor signaling and antigen targeting. **J Exp Med,** 190**,** 1549-60.

Chirillo, P., Pagano, S., Natoli, G., Puri, P.L., Burgio, V.L., Balsano, C. & Levrero, M. (1997) The hepatitis B virus X gene induces p53-mediated programmed cell death. **Proc Natl Acad Sci U S A,** 94**,** 8162-7.

Chisari, F.V., Klopchin, K., Moriyama, T., Pasquinelli, C., Dunsford, H.A., Sell, S., Pinkert, C.A., Brinster, R.L. & Palmiter, R.D. (1989) Molecular pathogenesis of hepatocellular carcinoma in hepatitis B virus transgenic mice. **Cell,** 59**,** 1145-56.

Chisari, F.V., Pinkert, C.A., Milich, D.R., Filippi, P., McLachlan, A., Palmiter, R.D. & Brinster, R.L. (1985) A transgenic mouse model of the chronic hepatitis B surface antigen carrier state. **Science,** 230**,** 1157-60.

Cohen, B.J. & Richmond, J.E. (1982) Electron microscopy of hepatitis B core antigen synthesized in E. coli. **Nature,** 296**,** 677-9.

Constant, S.L. (1999) B lymphocytes as antigen-presenting cells for CD4+ T cell priming in vivo. **J Immunol,** 162**,** 5695-703.

Conway, J.F., Cheng, N., Zlotnick, A., Stahl, S.J., Wingfield, P.T., Belnap, D.M., Kanngiesser, U., Noah, M. & Steven, A.C. (1998) Hepatitis B virus capsid: localization of the putative immunodominant loop (residues 78 to 83) on the capsid surface, and implications for the distinction between c and e-antigens. **J Mol Biol,** 279**,** 1111-21.

Crawford, A., Macleod, M., Schumacher, T., Corlett, L. & Gray, D. (2006) Primary T cell expansion and differentiation in vivo requires antigen presentation by B cells. **J Immunol,** 176**,** 3498-506.

Crompton, M. (2000) Bax, Bid and the permeabilization of the mitochondrial outer membrane in apoptosis. **Curr Opin Cell Biol,** 12**,** 414-9.

Dandri, M., Burda, M.R., Torok, E., Pollok, J.M., Iwanska, A., Sommer, G., Rogiers, X., Rogler, C.E., Gupta, S., Will, H., Greten, H. & Petersen, J. (2001) Repopulation of mouse liver with human hepatocytes and in vivo infection with hepatitis B virus. **Hepatology,** 33**,** 981-8.

Dandri, M., Murray, J.M., Lutgehetmann, M., Volz, T., Lohse, A.W. & Petersen, J. (2008) Virion half-life in chronic hepatitis B infection is strongly correlated with levels of viremia. **Hepatology,** 48**,** 1079-86.

Dandri, M., Petersen, J., Stockert, R.J., Harris, T.M. & Rogler, C.E. (1998) Metabolic labeling of woodchuck hepatitis B virus X protein in naturally infected hepatocytes reveals a bimodal half-life and association with the nuclear framework. **J Virol,** 72**,** 9359-64.

Dane, D.S., Cameron, C.H. & Briggs, M. (1970) Virus-like particles in serum of patients with Australia-antigen-associated hepatitis. **Lancet,** 1**,** 695-8.

Danial, N.N. (2007) BCL-2 family proteins: critical checkpoints of apoptotic cell death. **Clin Cancer Res,** 13**,** 7254-63.

De Creus, A., Abe, M., Lau, A.H., Hackstein, H., Raimondi, G. & Thomson, A.W. (2005) Low TLR4 expression by liver dendritic cells correlates with reduced capacity to activate allogeneic T cells in response to endotoxin. **J Immunol,** 174**,** 2037-45.

Desaintes, C., Demeret, C., Goyat, S., Yaniv, M. & Thierry, F. (1997) Expression of the papillomavirus E2 protein in HeLa cells leads to apoptosis. **EMBO J,** 16**,** 504-14.

Deveraux, Q.L., Roy, N., Stennicke, H.R., Van Arsdale, T., Zhou, Q., Srinivasula, S.M., Alnemri, E.S., Salvesen, G.S. & Reed, J.C. (1998) IAPs block apoptotic events induced by caspase-8 and cytochrome c by direct inhibition of distinct caspases. **EMBO J,** 17**,** 2215-23.

Diao, J., Khine, A.A., Sarangi, F., Hsu, E., Iorio, C., Tibbles, L.A., Woodgett, J.R., Penninger, J. & Richardson, C.D. (2001) X protein of hepatitis B virus inhibits Fas-mediated apoptosis and is associated with up-regulation of the SAPK/JNK pathway. **J Biol Chem,** 276**,** 8328-40.

Dunn, C., Brunetto, M., Reynolds, G., Christophides, T., Kennedy, P.T., Lampertico, P., Das, A., Lopes, A.R., Borrow, P., Williams, K., Humphreys, E., Afford, S., Adams, D.H., Bertoletti, A. & Maini, M.K. (2007) Cytokines induced during chronic hepatitis B virus infection promote a pathway for NK cell-mediated liver damage. **J Exp Med,** 204**,** 667-80.

Elmore, L.W., Hancock, A.R., Chang, S.F., Wang, X.W., Chang, S., Callahan, C.P., Geller, D.A., Will, H. & Harris, C.C. (1997) Hepatitis B virus X protein and p53 tumor suppressor interactions in the modulation of apoptosis. **Proc Natl Acad Sci U S A,** 94**,** 14707-12.

Ferrari, C., Penna, A., Bertoletti, A., Valli, A., Antoni, A.D., Giuberti, T., Cavalli, A., Petit, M.A. & Fiaccadori, F. (1990) Cellular immune response to hepatitis B virus-encoded antigens in acute and chronic hepatitis B virus infection. **J Immunol,** 145**,** 3442-9.

Fisicaro, P., Valdatta, C., Boni, C., Massari, M., Mori, C., Zerbini, A., Orlandini, A., Sacchelli, L., Missale, G. & Ferrari, C. (2009) Early kinetics of innate and adaptive immune responses during Hepatitis B Virus infection. **Gut**.

Fouillot, N., Tlouzeau, S., Rossignol, J.M. & Jean-Jean, O. (1993) Translation of the hepatitis B virus P gene by ribosomal scanning as an alternative to internal initiation. **J Virol,** 67**,** 4886-95.

Francis, D.P., Hadler, S.C., Thompson, S.E., Maynard, J.E., Ostrow, D.G., Altman, N., Braff, E.H., O'Malley, P., Hawkins, D., Judson, F.N., Penley, K., Nylund, T., Christie, G., Meyers, F., Moore, J.N., Jr., Gardner, A., Doto, I.L., Miller, J.H., Reynolds, G.H., Murphy, B.L., Schable, C.A., Clark, B.T., Curran, J.W. & Redeker, A.G. (1982) The prevention of hepatitis B with vaccine. Report of the centers for disease control multi-center efficacy trial among homosexual men. **Ann Intern Med,** 97**,** 362-6.

Friedman, S.L. (2004) Stellate cells: a moving target in hepatic fibrogenesis. **Hepatology,** 40**,** 1041-3.

Fromm, L., Shawlot, W., Gunning, K., Butel, J.S. & Overbeek, P.A. (1994) The retinoblastoma protein-binding region of simian virus 40 large T antigen alters cell cycle regulation in lenses of transgenic mice. **Mol Cell Biol,** 14**,** 6743-54.

Funk, A., Mhamdi, M., Hohenberg, H., Heeren, J., Reimer, R., Lambert, C., Prange, R. & Sirma, H. (2008) Duck hepatitis B virus requires cholesterol for endosomal escape during virus entry. **J Virol,** 82**,** 10532-42.

Galibert, F., Mandart, E., Fitoussi, F., Tiollais, P. & Charnay, P. (1979) Nucleotide sequence of the hepatitis B virus genome (subtype ayw) cloned in E. coli. **Nature,** 281**,** 646-50.

Galle, P.R., Hofmann, W.J., Walczak, H., Schaller, H., Otto, G., Stremmel, W., Krammer, P.H. & Runkel, L. (1995) Involvement of the CD95 (APO-1/Fas) receptor and ligand in liver damage. **J Exp Med,** 182**,** 1223-30.

Ganem, D. & Schneider, R.J. (2001) Hepadnaviridae: The Viruses and their Replication. **Fields - Virology,** Fourth Edition.

Gerelsaikhan, T., Tavis, J.E. & Bruss, V. (1996) Hepatitis B virus nucleocapsid envelopment does not occur without genomic DNA synthesis. **J Virol,** 70**,** 4269-74.

Gottlob, K., Fulco, M., Levrero, M. & Graessmann, A. (1998) The hepatitis B virus HBx protein inhibits caspase 3 activity. **J Biol Chem,** 273**,** 33347-53.

Gripon, P., Rumin, S., Urban, S., Le Seyec, J., Glaise, D., Cannie, I., Guyomard, C., Lucas, J., Trepo, C. & Guguen-Guillouzo, C. (2002) Infection of a human hepatoma cell line by hepatitis B virus. **Proc Natl Acad Sci U S A,** 99**,** 15655-60.

Guidotti, L.G., Ando, K., Hobbs, M.V., Ishikawa, T., Runkel, L., Schreiber, R.D. & Chisari, F.V. (1994a) Cytotoxic T lymphocytes inhibit hepatitis B virus gene expression by a noncytolytic mechanism in transgenic mice. **Proc Natl Acad Sci U S A,** 91**,** 3764-8.

Guidotti, L.G., Borrow, P., Brown, A., McClary, H., Koch, R. & Chisari, F.V. (1999a) Noncytopathic clearance of lymphocytic choriomeningitis virus from the hepatocyte. **J Exp Med,** 189**,** 1555-64.

Guidotti, L.G., Borrow, P., Hobbs, M.V., Matzke, B., Gresser, I., Oldstone, M.B. & Chisari, F.V. (1996a) Viral cross talk: intracellular inactivation of the hepatitis B virus during an unrelated viral infection of the liver. **Proc Natl Acad Sci U S A,** 93**,** 4589-94.

Guidotti, L.G., Guilhot, S. & Chisari, F.V. (1994b) Interleukin-2 and alpha/beta interferon down-regulate hepatitis B virus gene expression in vivo by tumor necrosis factor-dependent and -independent pathways. **J Virol,** 68**,** 1265-70.

Guidotti, L.G., Ishikawa, T., Hobbs, M.V., Matzke, B., Schreiber, R. & Chisari, F.V. (1996b) Intracellular inactivation of the hepatitis B virus by cytotoxic T lymphocytes. **Immunity,** 4**,** 25-36.

Guidotti, L.G., Matzke, B., Schaller, H. & Chisari, F.V. (1995) High-level hepatitis B virus replication in transgenic mice. **J Virol,** 69**,** 6158-69.

Guidotti, L.G., Morris, A., Mendez, H., Koch, R., Silverman, R.H., Williams, B.R. & Chisari, F.V. (2002) Interferon-regulated pathways that control hepatitis B virus replication in transgenic mice. **J Virol,** 76**,** 2617-21.

Guidotti, L.G., Rochford, R., Chung, J., Shapiro, M., Purcell, R. & Chisari, F.V. (1999b) Viral clearance without destruction of infected cells during acute HBV infection. **Science,** 284**,** 825-9.

Guo, H., Jiang, D., Ma, D., Chang, J., Dougherty, A.M., Cuconati, A., Block, T.M. & Guo, J.T. (2009) Activation of pattern recognition receptor-mediated innate immunity inhibits the replication of hepatitis B virus in human hepatocyte-derived cells. **J Virol,** 83**,** 847-58.

Han, J., Yoo, H.Y., Choi, B.H. & Rho, H.M. (2000) Selective transcriptional regulations in the human liver cell by hepatitis B viral X protein. **Biochem Biophys Res Commun,** 272**,** 525-30.

Harris, A.J., Dial, S.L. & Casciano, D.A. (2004) Comparison of basal gene expression profiles and effects of hepatocarcinogens on gene expression in cultured primary human hepatocytes and HepG2 cells. **Mutat Res,** 549**,** 79-99.

Hay, S. & Kannourakis, G. (2002) A time to kill: viral manipulation of the cell death program. **J Gen Virol,** 83**,** 1547-64.

Heermann, K.H., Goldmann, U., Schwartz, W., Seyffarth, T., Baumgarten, H. & Gerlich, W.H. (1984) Large surface proteins of hepatitis B virus containing the pre-s sequence. **J Virol,** 52**,** 396-402.

Heise, C., Hermiston, T., Johnson, L., Brooks, G., Sampson-Johannes, A., Williams, A., Hawkins, L. & Kirn, D. (2000) An adenovirus E1A mutant that demonstrates potent and selective systemic anti-tumoral efficacy. **Nat Med,** 6**,** 1134-9.

Heit, A., Huster, K.M., Schmitz, F., Schiemann, M., Busch, D.H. & Wagner, H. (2004) CpG-DNA aided cross-priming by cross-presenting B cells. **J Immunol,** 172**,** 1501-7.

Hon, H., Oran, A., Brocker, T. & Jacob, J. (2005) B lymphocytes participate in cross-presentation of antigen following gene gun vaccination. **J Immunol,** 174**,** 5233-42.

Hösel M, Quasdorff M, Webb D, Zedler U, Esser K, Arzberger S, Wiegmann K, Kirschning K, Langenkamp A & U., R.-J.S.a.P. (2009) Not interferon, but IL-6 controls early gene expression in Hepatitis B virus (HBV) infection. **submitted**.

Huang, L.R., Wu, H.L., Chen, P.J. & Chen, D.S. (2006) An immunocompetent mouse model for the tolerance of human chronic hepatitis B virus infection. **Proc Natl Acad Sci U S A,** 103**,** 17862-7.

Huo, T.I., Wang, X.W., Forgues, M., Wu, C.G., Spillare, E.A., Giannini, C., Brechot, C. & Harris, C.C. (2001) Hepatitis B virus X mutants derived from human hepatocellular carcinoma retain the ability to abrogate p53-induced apoptosis. **Oncogene,** 20**,** 3620-8.

Hwang, W.L. & Su, T.S. (1998) Translational regulation of hepatitis B virus polymerase gene by termination-reinitiation of an upstream minicistron in a length-dependent manner. **J Gen Virol,** 79 (Pt 9)**,** 2181-9.

Ibuki, N., Yamamoto, K., Yabushita, K., Okano, N., Okamoto, R., Shimada, N., Hakoda, T., Mizuno, M., Higashi, T. & Tsuji, T. (2002) In situ expression of Granzyme B and Fas-ligand in the liver of viral hepatitis. **Liver,** 22**,** 198-204.

Ishikawa, T. & Ganem, D. (1995) The pre-S domain of the large viral envelope protein determines host range in avian hepatitis B viruses. **Proc Natl Acad Sci U S A,** 92**,** 6259-63.

Isogawa, M., Kakimi, K., Kamamoto, H., Protzer, U. & Chisari, F.V. (2005) Differential dynamics of the peripheral and intrahepatic cytotoxic T lymphocyte response to hepatitis B surface antigen. **Virology,** 333**,** 293-300.

Jilbert, A.R., Miller, D.S., Scougall, C.A., Turnbull, H. & Burrell, C.J. (1996) Kinetics of duck hepatitis B virus infection following low dose virus inoculation: one virus DNA genome is infectious in neonatal ducks. **Virology,** 226**,** 338-45.

John von Freyend M., Untergasser A., Arzberger S., Oberwinkler H., Drebber U. & U., S.P.a.P. (2009) Sequential control of hepatitis B virus in a mouse model of acute, self-resolving hepatitis B. **submitted**.

Joza, N., Susin, S.A., Daugas, E., Stanford, W.L., Cho, S.K., Li, C.Y., Sasaki, T., Elia, A.J., Cheng, H.Y., Ravagnan, L., Ferri, K.F., Zamzami, N., Wakeham, A., Hakem, R., Yoshida, H., Kong, Y.Y., Mak, T.W., Zuniga-Pflucker, J.C., Kroemer, G. & Penninger, J.M. (2001) Essential role of the mitochondrial apoptosis-inducing factor in programmed cell death. **Nature,** 410**,** 549-54.

Junker-Niepmann, M., Bartenschlager, R. & Schaller, H. (1990) A short cis-acting sequence is required for hepatitis B virus pregenome encapsidation and sufficient for packaging of foreign RNA. **EMBO J,** 9**,** 3389-96.

Jurak, I., Schumacher, U., Simic, H., Voigt, S. & Brune, W. (2008) Murine cytomegalovirus m38.5 protein inhibits Bax-mediated cell death. **J Virol,** 82**,** 4812-22.

Kagi, D., Ledermann, B., Burki, K., Seiler, P., Odermatt, B., Olsen, K.J., Podack, E.R., Zinkernagel, R.M. & Hengartner, H. (1994a) Cytotoxicity mediated by T cells and natural killer cells is greatly impaired in perforin-deficient mice. **Nature,** 369**,** 31-7.

Kagi, D., Vignaux, F., Ledermann, B., Burki, K., Depraetere, V., Nagata, S., Hengartner, H. & Golstein, P. (1994b) Fas and perforin pathways as major mechanisms of T cell-mediated cytotoxicity. **Science,** 265**,** 528-30.

Kann, M., Schmitz, A. & Rabe, B. (2007) Intracellular transport of hepatitis B virus. **World J Gastroenterol,** 13**,** 39-47.

Katoh, M., Tateno, C., Yoshizato, K. & Yokoi, T. (2008) Chimeric mice with humanized liver. **Toxicology,** 246**,** 9-17.

Ke, Y. & Kapp, J.A. (1996) Exogenous antigens gain access to the major histocompatibility complex class I processing pathway in B cells by receptor-mediated uptake. **J Exp Med,** 184**,** 1179-84.

Kekule, A.S., Lauer, U., Meyer, M., Caselmann, W.H., Hofschneider, P.H. & Koshy, R. (1990) The preS2/S region of integrated hepatitis B virus DNA encodes a transcriptional transactivator. **Nature,** 343**,** 457-61.

Kim, H., Lee, H. & Yun, Y. (1998) X-gene product of hepatitis B virus induces apoptosis in liver cells. **J Biol Chem,** 273**,** 381-5.

Kim, K.H. & Seong, B.L. (2003) Pro-apoptotic function of HBV X protein is mediated by interaction with c-FLIP and enhancement of death-inducing signal. **EMBO J,** 22**,** 2104-16.

Kim, S.Y., Kim, J.K., Kim, H.J. & Ahn, J.K. (2005) Hepatitis B virus X protein sensitizes UV-induced apoptosis by transcriptional transactivation of Fas ligand gene expression. **IUBMB Life,** 57**,** 651-8.

Knolle, P.A. & Gerken, G. (2000) Local control of the immune response in the liver. **Immunol Rev,** 174**,** 21-34.

Knolle, P.A., Schmitt, E., Jin, S., Germann, T., Duchmann, R., Hegenbarth, S., Gerken, G. & Lohse, A.W. (1999) Induction of cytokine production in naive CD4(+) T cells by antigen-presenting murine liver sinusoidal endothelial cells but failure to induce differentiation toward Th1 cells. **Gastroenterology,** 116**,** 1428-40.

Kock, J., Borst, E.M. & Schlicht, H.J. (1996) Uptake of duck hepatitis B virus into hepatocytes occurs by endocytosis but does not require passage of the virus through an acidic intracellular compartment. **J Virol,** 70**,** 5827-31.

Kock, J., Nassal, M., MacNelly, S., Baumert, T.F., Blum, H.E. & von Weizsacker, F. (2001) Efficient infection of primary tupaia hepatocytes with purified human and woolly monkey hepatitis B virus. **J Virol,** 75**,** 5084-9.

Kojima, Y., Kawasaki-Koyanagi, A., Sueyoshi, N., Kanai, A., Yagita, H. & Okumura, K. (2002) Localization of Fas ligand in cytoplasmic granules of CD8+ cytotoxic T lymphocytes and natural killer cells: participation of Fas ligand in granule exocytosis model of cytotoxicity. **Biochem Biophys Res Commun,** 296**,** 328-36.

Kondo, T., Suda, T., Fukuyama, H., Adachi, M. & Nagata, S. (1997) Essential roles of the Fas ligand in the development of hepatitis. **Nat Med,** 3**,** 409-13.

Kurt-Jones, E.A., Liano, D., HayGlass, K.A., Benacerraf, B., Sy, M.S. & Abbas, A.K. (1988) The role of antigen-presenting B cells in T cell priming in vivo. Studies of B cell-deficient mice. **J Immunol,** 140**,** 3773-8.

Lambert, C., Doring, T. & Prange, R. (2007) Hepatitis B virus maturation is sensitive to functional inhibition of ESCRT-III, Vps4, and gamma 2-adaptin. **J Virol,** 81**,** 9050-60.

Lanzavecchia, A. (1987) Antigen uptake and accumulation in antigen-specific B cells. **Immunol Rev,** 99**,** 39-51.

--- (1990) Receptor-mediated antigen uptake and its effect on antigen presentation to class II-restricted T lymphocytes. **Annu Rev Immunol,** 8**,** 773-93.

Latonen, L. & Laiho, M. (2005) Cellular UV damage responses--functions of tumor suppressor p53. **Biochim Biophys Acta,** 1755**,** 71-89.

Lau, A.H. & Thomson, A.W. (2003) Dendritic cells and immune regulation in the liver. **Gut,** 52**,** 307-14.

Lazdina, U., Alheim, M., Nystrom, J., Hultgren, C., Borisova, G., Sominskaya, I., Pumpens, P., Peterson, D.L., Milich, D.R. & Sallberg, M. (2003) Priming of cytotoxic T cell responses to exogenous hepatitis B virus core antigen is B cell dependent. **J Gen Virol,** 84**,** 139-46.

Lazdina, U., Cao, T., Steinbergs, J., Alheim, M., Pumpens, P., Peterson, D.L., Milich, D.R., Leroux-Roels, G. & Sallberg, M. (2001) Molecular basis for the interaction of the hepatitis B virus core antigen with the surface immunoglobulin receptor on naive B cells. **J Virol,** 75**,** 6367-74.

Lee, J.Y., Chae, D.W., Kim, S.M., Nam, E.S., Jang, M.K., Lee, J.H., Kim, H.Y. & Yoo, J.Y. (2004) Expression of FasL and perforin/granzyme B mRNA in chronic hepatitis B virus infection. **J Viral Hepat,** 11**,** 130-5.

Lee, Y.I., Kang-Park, S. & Do, S.I. (2001) The hepatitis B virus-X protein activates a phosphatidylinositol 3-kinase-dependent survival signaling cascade. **J Biol Chem,** 276**,** 16969-77.

Lenhoff, R.J. & Summers, J. (1994) Coordinate regulation of replication and virus assembly by the large envelope protein of an avian hepadnavirus. **J Virol,** 68**,** 4565-71.

Leu, J.I., Crissey, M.A. & Taub, R. (2003) Massive hepatic apoptosis associated with TGF-beta1 activation after Fas ligand treatment of IGF binding protein-1-deficient mice. **J Clin Invest,** 111**,** 129-39.

Leu, J.I. & George, D.L. (2007) Hepatic IGFBP1 is a prosurvival factor that binds to BAK, protects the liver from apoptosis, and antagonizes the proapoptotic actions of p53 at mitochondria. **Genes Dev,** 21**,** 3095-109.

Li, P., Nijhawan, D., Budihardjo, I., Srinivasula, S.M., Ahmad, M., Alnemri, E.S. & Wang, X. (1997) Cytochrome c and dATP-dependent formation of Apaf-1/caspase-9 complex initiates an apoptotic protease cascade. **Cell,** 91**,** 479-89.

Liang, X., Liu, Y., Zhang, Q., Gao, L., Han, L., Ma, C., Zhang, L., Chen, Y.H. & Sun, W. (2007) Hepatitis B virus sensitizes hepatocytes to TRAIL-induced apoptosis through Bax. **J Immunol,** 178**,** 503-10.

Lien, J.M., Aldrich, C.E. & Mason, W.S. (1986) Evidence that a capped oligoribonucleotide is the primer for duck hepatitis B virus plus-strand DNA synthesis. **J Virol,** 57**,** 229-36.

Limmer, A., Ohl, J., Kurts, C., Ljunggren, H.G., Reiss, Y., Groettrup, M., Momburg, F., Arnold, B. & Knolle, P.A. (2000) Efficient presentation of exogenous antigen by liver endothelial cells to CD8+ T cells results in antigen-specific T-cell tolerance. **Nat Med,** 6**,** 1348-54.

Lovell, J.F., Billen, L.P., Bindner, S., Shamas-Din, A., Fradin, C., Leber, B. & Andrews, D.W. (2008) Membrane binding by tBid initiates an ordered series of events culminating in membrane permeabilization by Bax. **Cell,** 135**,** 1074-84.

Lowin, B., Hahne, M., Mattmann, C. & Tschopp, J. (1994) Cytolytic T-cell cytotoxicity is mediated through perforin and Fas lytic pathways. **Nature,** 370**,** 650-2.

Lowin, B., Mattman, C., Hahne, M. & Tschopp, J. (1996) Comparison of Fas(Apo-1/CD95)- and perforin-mediated cytotoxicity in primary T lymphocytes. **Int Immunol,** 8**,** 57-63.

Luo, K.X., Zhu, Y.F., Zhang, L.X., He, H.T., Wang, X.S. & Zhang, L. (1997) In situ investigation of Fas/FasL expression in chronic hepatitis B infection and related liver diseases. **J Viral Hepat,** 4**,** 303-7.

MacDonald, G., Shi, L., Vande Velde, C., Lieberman, J. & Greenberg, A.H. (1999) Mitochondria-dependent and -independent regulation of Granzyme B-induced apoptosis. **J Exp Med,** 189**,** 131-44.

Magal, S.S., Jackman, A., Ish-Shalom, S., Botzer, L.E., Gonen, P., Schlegel, R. & Sherman, L. (2005) Downregulation of Bax mRNA expression and protein stability by the E6 protein of human papillomavirus 16. **J Gen Virol,** 86**,** 611-21.

Magnius, L.O. & Espmark, A. (1972) A new antigen complex co-occurring with Australia antigen. **Acta Pathol Microbiol Scand [B] Microbiol Immunol,** 80**,** 335-7.

Maloy, K.J., Odermatt, B., Hengartner, H. & Zinkernagel, R.M. (1998) Interferon gamma-producing gammadelta T cell-dependent antibody isotype switching in the absence of germinal center formation during virus infection. **Proc Natl Acad Sci U S A,** 95**,** 1160-5.

Marusawa, H., Matsuzawa, S., Welsh, K., Zou, H., Armstrong, R., Tamm, I. & Reed, J.C. (2003) HBXIP functions as a cofactor of survivin in apoptosis suppression. **EMBO J,** 22**,** 2729-40.

Mason, A.L., Xu, L., Guo, L., Kuhns, M. & Perrillo, R.P. (1998) Molecular basis for persistent hepatitis B virus infection in the liver after clearance of serum hepatitis B surface antigen. **Hepatology,** 27**,** 1736-42.

Mason, W.S., Halpern, M.S., England, J.M., Seal, G., Egan, J., Coates, L., Aldrich, C. & Summers, J. (1983) Experimental transmission of duck hepatitis B virus. **Virology,** 131**,** 375-84.

Mason, W.S., Litwin, S., Xu, C. & Jilbert, A.R. (2007) Hepatocyte turnover in transient and chronic hepadnavirus infections. **J Viral Hepat,** 14 Suppl 1**,** 22-8.

Matloubian, M., Suresh, M., Glass, A., Galvan, M., Chow, K., Whitmire, J.K., Walsh, C.M., Clark, W.R. & Ahmed, R. (1999) A role for perforin in downregulating T-cell responses during chronic viral infection. **J Virol,** 73**,** 2527-36.

Matzinger, P. (2002) An innate sense of danger. **Ann N Y Acad Sci,** 961**,** 341-2.

Mercer, D.F., Schiller, D.E., Elliott, J.F., Douglas, D.N., Hao, C., Rinfret, A., Addison, W.R., Fischer, K.P., Churchill, T.A., Lakey, J.R., Tyrrell, D.L. & Kneteman, N.M. (2001) Hepatitis C virus replication in mice with chimeric human livers. **Nat Med,** 7**,** 927-33.

Metkar, S.S., Wang, B., Ebbs, M.L., Kim, J.H., Lee, Y.J., Raja, S.M. & Froelich, C.J. (2003) Granzyme B activates procaspase-3 which signals a mitochondrial amplification loop for maximal apoptosis. **J Cell Biol,** 160**,** 875-85.

Miao, J., Chen, G.G., Chun, S.Y. & Lai, P.P. (2006) Hepatitis B virus X protein induces apoptosis in hepatoma cells through inhibiting Bcl-xL expression. **Cancer Lett,** 236**,** 115-24.

Micheau, O. & Tschopp, J. (2003) Induction of TNF receptor I-mediated apoptosis via two sequential signaling complexes. **Cell,** 114**,** 181-90.

Milich, D.R., Chen, M., Schodel, F., Peterson, D.L., Jones, J.E. & Hughes, J.L. (1997a) Role of B cells in antigen presentation of the hepatitis B core. **Proc Natl Acad Sci U S A,** 94**,** 14648-53.

Milich, D.R., Chen, M.K., Hughes, J.L. & Jones, J.E. (1998) The secreted hepatitis B precore antigen can modulate the immune response to the nucleocapsid: a mechanism for persistence. **J Immunol,** 160**,** 2013-21.

Milich, D.R., McLachlan, A., Thornton, G.B. & Hughes, J.L. (1987) Antibody production to the nucleocapsid and envelope of the hepatitis B virus primed by a single synthetic T cell site. **Nature,** 329**,** 547-9.

Milich, D.R., Schodel, F., Hughes, J.L., Jones, J.E. & Peterson, D.L. (1997b) The hepatitis B virus core and e antigens elicit different Th cell subsets: antigen structure can affect Th cell phenotype. **J Virol,** 71**,** 2192-201.

Miller, R.H., Marion, P.L. & Robinson, W.S. (1984) Hepatitis B viral DNA-RNA hybrid molecules in particles from infected liver are converted to viral DNA molecules during an endogenous DNA polymerase reaction. **Virology,** 139**,** 64-72.

Mond, J.J., Lees, A. & Snapper, C.M. (1995) T cell-independent antigens type 2. **Annu Rev Immunol,** 13**,** 655-92.

Moriyama, T., Guilhot, S., Klopchin, K., Moss, B., Pinkert, C.A., Palmiter, R.D., Brinster, R.L., Kanagawa, O. & Chisari, F.V. (1990) Immunobiology and pathogenesis of hepatocellular injury in hepatitis B virus transgenic mice. **Science,** 248**,** 361-4.

Murray, J.M., Purcell, R.H. & Wieland, S.F. (2006) The half-life of hepatitis B virions. **Hepatology,** 44**,** 1117-21.

Muzio, M., Stockwell, B.R., Stennicke, H.R., Salvesen, G.S. & Dixit, V.M. (1998) An induced proximity model for caspase-8 activation. **J Biol Chem,** 273**,** 2926-30.

Nagata, S. & Suda, T. (1995) Fas and Fas ligand: lpr and gld mutations. **Immunol Today,** 16**,** 39-43.

Nakamoto, Y., Guidotti, L.G., Pasquetto, V., Schreiber, R.D. & Chisari, F.V. (1997) Differential target cell sensitivity to CTL-activated death pathways in hepatitis B virus transgenic mice. **J Immunol,** 158**,** 5692-7.

Nakanishi, F., Ohkawa, K., Ishida, H., Hosui, A., Sato, A., Hiramatsu, N., Ueda, K., Takehara, T., Kasahara, A., Sasaki, Y., Hori, M. & Hayashi, N. (2005) Alteration in gene expression profile by full-length hepatitis B virus genome. **Intervirology,** 48**,** 77-83.

Niederau, C., Heintges, T., Lange, S., Goldmann, G., Niederau, C.M., Mohr, L. & Haussinger, D. (1996) Long-term follow-up of HBeAg-positive patients treated with interferon alfa for chronic hepatitis B. **N Engl J Med,** 334**,** 1422-7.

Ning, B. & Shih, C. (2004) Nucleolar localization of human hepatitis B virus capsid protein. **J Virol,** 78**,** 13653-68.

Ogasawara, J., Watanabe-Fukunaga, R., Adachi, M., Matsuzawa, A., Kasugai, T., Kitamura, Y., Itoh, N., Suda, T. & Nagata, S. (1993) Lethal effect of the anti-Fas antibody in mice. **Nature,** 364**,** 806-9.

Ogg, P.D., McDonell, P.J., Ryckman, B.J., Knudson, C.M. & Roller, R.J. (2004) The HSV-1 Us3 protein kinase is sufficient to block apoptosis induced by overexpression of a variety of Bcl-2 family members. **Virology,** 319**,** 212-24.

Ono, M., Morisawa, K., Nie, J., Ota, K., Taniguchi, T., Saibara, T. & Onishi, S. (1998) Transactivation of transforming growth factor alpha gene by hepatitis B virus preS1. **Cancer Res,** 58**,** 1813-6.

Pan, J., Duan, L.X., Sun, B.S. & Feitelson, M.A. (2001) Hepatitis B virus X protein protects against anti-Fas-mediated apoptosis in human liver cells by inducing NF-kappa B. **J Gen Virol,** 82**,** 171-82.

Pape, K.A., Catron, D.M., Itano, A.A. & Jenkins, M.K. (2007) The humoral immune response is initiated in lymph nodes by B cells that acquire soluble antigen directly in the follicles. **Immunity,** 26**,** 491-502.

Penna, A., Del Prete, G., Cavalli, A., Bertoletti, A., D'Elios, M.M., Sorrentino, R., D'Amato, M., Boni, C., Pilli, M., Fiaccadori, F. & Ferrari, C. (1997) Predominant T-helper 1 cytokine profile of hepatitis B virus nucleocapsid-specific T cells in acute self-limited hepatitis B. **Hepatology,** 25**,** 1022-7.

Peter, M.E. & Krammer, P.H. (2003) The CD95(APO-1/Fas) DISC and beyond. **Cell Death Differ,** 10**,** 26-35.

Poe, M., Blake, J.T., Boulton, D.A., Gammon, M., Sigal, N.H., Wu, J.K. & Zweerink, H.J. (1991) Human cytotoxic lymphocyte granzyme B. Its purification from granules and the characterization of substrate and inhibitor specificity. **J Biol Chem,** 266**,** 98-103.

Pollicino, T., Belloni, L., Raffa, G., Pediconi, N., Squadrito, G., Raimondo, G. & Levrero, M. (2006) Hepatitis B virus replication is regulated by the acetylation status of hepatitis B virus cccDNA-bound H3 and H4 histones. **Gastroenterology,** 130**,** 823-37.

Pollicino, T., Terradillos, O., Lecoeur, H., Gougeon, M.L. & Buendia, M.A. (1998) Pro-apoptotic effect of the hepatitis B virus X gene. **Biomed Pharmacother,** 52**,** 363-8.

Possehl, C., Repp, R., Heermann, K.H., Korec, E., Uy, A. & Gerlich, W.H. (1992) Absence of free core antigen in anti-HBc negative viremic hepatitis B carriers. **Arch Virol Suppl,** 4**,** 39-41.

Protzer, U., Seyfried, S., Quasdorff, M., Sass, G., Svorcova, M., Webb, D., Bohne, F., Hosel, M., Schirmacher, P. & Tiegs, G. (2007) Antiviral activity and hepatoprotection by heme oxygenase-1 in hepatitis B virus infection. **Gastroenterology,** 133**,** 1156-65.

Quasdorff, M., Hosel, M., Odenthal, M., Zedler, U., Bohne, F., Gripon, P., Dienes, H.P., Drebber, U., Stippel, D., Goeser, T. & Protzer, U. (2008) A concerted action of HNF4alpha and HNF1alpha links hepatitis B virus replication to hepatocyte differentiation. **Cell Microbiol,** 10**,** 1478-90.

Rathmell, J.C., Cooke, M.P., Ho, W.Y., Grein, J., Townsend, S.E., Davis, M.M. & Goodnow, C.C. (1995) CD95 (Fas)-dependent elimination of self-reactive B cells upon interaction with CD4+ T cells. **Nature,** 376**,** 181-4.

Rehermann, B., Fowler, P., Sidney, J., Person, J., Redeker, A., Brown, M., Moss, B., Sette, A. & Chisari, F.V. (1995) The cytotoxic T lymphocyte response to multiple hepatitis B virus polymerase epitopes during and after acute viral hepatitis. **J Exp Med,** 181**,** 1047-58.

Rehermann, B. & Nascimbeni, M. (2005) Immunology of hepatitis B virus and hepatitis C virus infection. **Nat Rev Immunol,** 5**,** 215-29.

Rieger, A. & Nassal, M. (1996) Specific hepatitis B virus minus-strand DNA synthesis requires only the 5' encapsidation signal and the 3'-proximal direct repeat DR1. **J Virol,** 70**,** 585-9.

Rigg, R.J. & Schaller, H. (1992) Duck hepatitis B virus infection of hepatocytes is not dependent on low pH. **J Virol,** 66**,** 2829-36.

Robek, M.D., Wieland, S.F. & Chisari, F.V. (2002) Inhibition of hepatitis B virus replication by interferon requires proteasome activity. **J Virol,** 76**,** 3570-4.

Robinson, W.S., Clayton, D.A. & Greenman, R.L. (1974) DNA of a human hepatitis B virus candidate. **J Virol,** 14**,** 384-91.

Rodrigues, A.R., Heise, N., Previato, J.O., Mendonca-Previato, L. & Pecanha, L.M. (2005) B cell response during infection with the MAT a and MAT alpha mating types of Cryptococcus neoformans. **Microbes Infect,** 7**,** 118-25.

Ron, Y. & Sprent, J. (1987) T cell priming in vivo: a major role for B cells in presenting antigen to T cells in lymph nodes. **J Immunol,** 138**,** 2848-56.

Rost, M., Mann, S., Lambert, C., Doring, T., Thome, N. & Prange, R. (2006) Gamma-adaptin, a novel ubiquitin-interacting adaptor, and Nedd4 ubiquitin ligase control hepatitis B virus maturation. **J Biol Chem,** 281**,** 29297-308.

Rumin, S., Gripon, P., Le Seyec, J., Corral-Debrinski, M. & Guguen-Guillouzo, C. (1996) Long-term productive episomal hepatitis B virus replication in primary cultures of adult human hepatocytes infected in vitro. **J Viral Hepat,** 3**,** 227-38.

Scaffidi, C., Fulda, S., Srinivasan, A., Friesen, C., Li, F., Tomaselli, K.J., Debatin, K.M., Krammer, P.H. & Peter, M.E. (1998) Two CD95 (APO-1/Fas) signaling pathways. **EMBO J,** 17**,** 1675-87.

Schormann, W., Kraft, A., Ponsel, D. & Bruss, V. (2006) Hepatitis B virus particle formation in the absence of pregenomic RNA and reverse transcriptase. **J Virol,** 80**,** 4187-90.

Schulze, A., Gripon, P. & Urban, S. (2007) Hepatitis B virus infection initiates with a large surface protein-dependent binding to heparan sulfate proteoglycans. **Hepatology,** 46**,** 1759-68.

Schulze-Bergkamen, H., Untergasser, A., Dax, A., Vogel, H., Buchler, P., Klar, E., Lehnert, T., Friess, H., Buchler, M.W., Kirschfink, M., Stremmel, W., Krammer, P.H., Muller, M. & Protzer, U. (2003) Primary human hepatocytes--a valuable tool for investigation of apoptosis and hepatitis B virus infection. **J Hepatol,** 38**,** 736-44.

Seeger, C., Ganem, D. & Varmus, H.E. (1986) Biochemical and genetic evidence for the hepatitis B virus replication strategy. **Science,** 232**,** 477-84.

Seifer, M. & Standring, D.N. (1993) Recombinant human hepatitis B virus reverse transcriptase is active in the absence of the nucleocapsid or the viral replication origin, DR1. **J Virol,** 67**,** 4513-20.

Sells, M.A., Chen, M.L. & Acs, G. (1987) Production of hepatitis B virus particles in Hep G2 cells transfected with cloned hepatitis B virus DNA. **Proc Natl Acad Sci U S A,** 84**,** 1005-9.

Shih, W.L., Kuo, M.L., Chuang, S.E., Cheng, A.L. & Doong, S.L. (2000) Hepatitis B virus X protein inhibits transforming growth factor-beta -induced apoptosis through the activation of phosphatidylinositol 3-kinase pathway. **J Biol Chem,** 275**,** 25858-64.

Shintani, Y., Yotsuyanagi, H., Moriya, K., Fujie, H., Tsutsumi, T., Kanegae, Y., Kimura, S., Saito, I. & Koike, K. (1999) Induction of apoptosis after switch-on of the hepatitis B virus X gene mediated by the Cre/loxP recombination system. **J Gen Virol,** 80 (Pt 12)**,** 3257-65.

Shirakata, Y. & Koike, K. (2003) Hepatitis B virus X protein induces cell death by causing loss of mitochondrial membrane potential. **J Biol Chem,** 278**,** 22071-8.

Sidman, C.L., Marshall, J.D. & Von Boehmer, H. (1992) Transgenic T cell receptor interactions in the lymphoproliferative and autoimmune syndromes of lpr and gld mutant mice. **Eur J Immunol,** 22**,** 499-504.

Snapper, C.M., McIntyre, T.M., Mandler, R., Pecanha, L.M., Finkelman, F.D., Lees, A. & Mond, J.J. (1992) Induction of IgG3 secretion by interferon gamma: a model for T cell-independent class switching in response to T cell-independent type 2 antigens. **J Exp Med,** 175**,** 1367-71.

Sprinzl, M.F., Oberwinkler, H., Schaller, H. & Protzer, U. (2001) Transfer of hepatitis B virus genome by adenovirus vectors into cultured cells and mice: crossing the species barrier. **J Virol,** 75**,** 5108-18.

Standring, D.N., Rutter, W.J., Varmus, H.E. & Ganem, D. (1984) Transcription of the hepatitis B surface antigen gene in cultured murine cells initiates within the presurface region. **J Virol,** 50**,** 563-71.

Stewart, T.L., Wasilenko, S.T. & Barry, M. (2005) Vaccinia virus F1L protein is a tail-anchored protein that functions at the mitochondria to inhibit apoptosis. **J Virol,** 79**,** 1084-98.

Su, F. & Schneider, R.J. (1997) Hepatitis B virus HBx protein sensitizes cells to apoptotic killing by tumor necrosis factor alpha. **Proc Natl Acad Sci U S A,** 94**,** 8744-9.

Su, F., Theodosis, C.N. & Schneider, R.J. (2001) Role of NF-kappaB and myc proteins in apoptosis induced by hepatitis B virus HBx protein. **J Virol,** 75**,** 215-25.

Su, L. & David, M. (1999) Inhibition of B cell receptor-mediated apoptosis by IFN. **J Immunol,** 162**,** 6317-21.

Su, Q., Schroder, C.H., Hofmann, W.J., Otto, G., Pichlmayr, R. & Bannasch, P. (1998) Expression of hepatitis B virus X protein in HBV-infected human livers and hepatocellular carcinomas. **Hepatology,** 27**,** 1109-20.

Summers, J. & Mason, W.S. (1982) Replication of the genome of a hepatitis B--like virus by reverse transcription of an RNA intermediate. **Cell,** 29**,** 403-15.

Summers, J., Smolec, J.M. & Snyder, R. (1978) A virus similar to human hepatitis B virus associated with hepatitis and hepatoma in woodchucks. **Proc Natl Acad Sci U S A,** 75**,** 4533-7.

Sundararajan, R., Cuconati, A., Nelson, D. & White, E. (2001) Tumor necrosis factor-alpha induces Bax-Bak interaction and apoptosis, which is inhibited by adenovirus E1B 19K. **J Biol Chem,** 276**,** 45120-7.

Sureau, C., Romet-Lemonne, J.L., Mullins, J.I. & Essex, M. (1986) Production of hepatitis B virus by a differentiated human hepatoma cell line after transfection with cloned circular HBV DNA. **Cell,** 47**,** 37-47.

Tagashira, M., Yamamoto, K., Fujio, K., Nagano, T., Okamoto, R., Ibuki, N., Yabushita, K., Matsumura, S., Okano, N. & Tsuji, T. (2000) Expression of perforin and Fas ligand mRNA in the liver of viral hepatitis. **J Clin Immunol,** 20**,** 347-53.

Takahashi, K., Imai, M., Tsuda, F., Takahashi, T. & Miyakawa, Y. (1976) Association of dane particles with e antigen in the serum of asymptomatic carriers of hepatitis B surface antigen. **J Immunol,** 117**,** 102-5.

Tang, H., Oishi, N., Kaneko, S. & Murakami, S. (2006) Molecular functions and biological roles of hepatitis B virus x protein. **Cancer Sci,** 97**,** 977-83.

Tang, T.J., Kwekkeboom, J., Laman, J.D., Niesters, H.G., Zondervan, P.E., de Man, R.A., Schalm, S.W. & Janssen, H.L. (2003) The role of intrahepatic immune effector cells in inflammatory liver injury and viral control during chronic hepatitis B infection. **J Viral Hepat,** 10**,** 159-67.

Taylor, R.C., Cullen, S.P. & Martin, S.J. (2008) Apoptosis: controlled demolition at the cellular level. **Nat Rev Mol Cell Biol,** 9**,** 231-41.

Terradillos, O., de La Coste, A., Pollicino, T., Neuveut, C., Sitterlin, D., Lecoeur, H., Gougeon, M.L., Kahn, A. & Buendia, M.A. (2002) The hepatitis B virus X protein abrogates Bcl-2-mediated protection against Fas apoptosis in the liver. **Oncogene,** 21**,** 377-86.

Terradillos, O., Pollicino, T., Lecoeur, H., Tripodi, M., Gougeon, M.L., Tiollais, P. & Buendia, M.A. (1998) p53-independent apoptotic effects of the hepatitis B virus HBx protein in vivo and in vitro. **Oncogene,** 17**,** 2115-23.

Thimme, R., Wieland, S., Steiger, C., Ghrayeb, J., Reimann, K.A., Purcell, R.H. & Chisari, F.V. (2003) CD8(+) T cells mediate viral clearance and disease pathogenesis during acute hepatitis B virus infection. **J Virol,** 77**,** 68-76.

Thornberry, N.A. (1998) Caspases: key mediators of apoptosis. **Chem Biol,** 5**,** R97-103.

Tobian, A.A., Harding, C.V. & Canaday, D.H. (2005) Mycobacterium tuberculosis heat shock fusion protein enhances class I MHC cross-processing and -presentation by B lymphocytes. **J Immunol,** 174**,** 5209-14.

Trobonjaca, Z., Leithauser, F., Moller, P., Schirmbeck, R. & Reimann, J. (2001) Activating immunity in the liver. I. Liver dendritic cells (but not hepatocytes) are potent activators of IFN-gamma release by liver NKT cells. **J Immunol,** 167**,** 1413-22.

Tuttleman, J.S., Pugh, J.C. & Summers, J.W. (1986) In vitro experimental infection of primary duck hepatocyte cultures with duck hepatitis B virus. **J Virol,** 58**,** 17-25.

Varfolomeev, E., Blankenship, J.W., Wayson, S.M., Fedorova, A.V., Kayagaki, N., Garg, P., Zobel, K., Dynek, J.N., Elliott, L.O., Wallweber, H.J., Flygare, J.A., Fairbrother, W.J., Deshayes, K., Dixit, V.M. & Vucic, D. (2007) IAP antagonists induce autoubiquitination of c-IAPs, NF-kappaB activation, and TNFalpha-dependent apoptosis. **Cell,** 131**,** 669-81.

Vilarinho, S., Ogasawara, K., Nishimura, S., Lanier, L.L. & Baron, J.L. (2007) Blockade of NKG2D on NKT cells prevents hepatitis and the acute immune response to hepatitis B virus. **Proc Natl Acad Sci U S A,** 104**,** 18187-92.

Voll, R.E., Herrmann, M., Roth, E.A., Stach, C., Kalden, J.R. & Girkontaite, I. (1997) Immunosuppressive effects of apoptotic cells. **Nature,** 390**,** 350-1.

Wang, G.H. & Seeger, C. (1993) Novel mechanism for reverse transcription in hepatitis B viruses. **J Virol,** 67**,** 6507-12.

Wang, W.H., Hullinger, R.L. & Andrisani, O.M. (2008) Hepatitis B virus X protein via the p38MAPK pathway induces E2F1 release and ATR kinase activation mediating p53 apoptosis. **J Biol Chem,** 283**,** 25455-67.

Wang, X.W., Gibson, M.K., Vermeulen, W., Yeh, H., Forrester, K., Sturzbecher, H.W., Hoeijmakers, J.H. & Harris, C.C. (1995) Abrogation of p53-induced apoptosis by the hepatitis B virus X gene. **Cancer Res,** 55**,** 6012-6.

Watanabe, T., Sorensen, E.M., Naito, A., Schott, M., Kim, S. & Ahlquist, P. (2007) Involvement of host cellular multivesicular body functions in hepatitis B virus budding. **Proc Natl Acad Sci U S A,** 104**,** 10205-10.

Webster, G.J., Reignat, S., Brown, D., Ogg, G.S., Jones, L., Seneviratne, S.L., Williams, R., Dusheiko, G. & Bertoletti, A. (2004) Longitudinal analysis of CD8+ T cells specific for structural and nonstructural hepatitis B virus proteins in patients with chronic hepatitis B: implications for immunotherapy. **J Virol,** 78**,** 5707-19.

Webster, G.J., Reignat, S., Maini, M.K., Whalley, S.A., Ogg, G.S., King, A., Brown, D., Amlot, P.L., Williams, R., Vergani, D., Dusheiko, G.M. & Bertoletti, A. (2000) Incubation phase of acute hepatitis B in man: dynamic of cellular immune mechanisms. **Hepatology,** 32**,** 1117-24.

Westendorp, M.O., Shatrov, V.A., Schulze-Osthoff, K., Frank, R., Kraft, M., Los, M., Krammer, P.H., Droge, W. & Lehmann, V. (1995) HIV-1 Tat potentiates TNF-induced NF-kappa B activation and cytotoxicity by altering the cellular redox state. **EMBO J,** 14**,** 546-54.

Wieland, S., Thimme, R., Purcell, R.H. & Chisari, F.V. (2004) Genomic analysis of the host response to hepatitis B virus infection. **Proc Natl Acad Sci U S A,** 101**,** 6669-74.

Will, H., Reiser, W., Weimer, T., Pfaff, E., Buscher, M., Sprengel, R., Cattaneo, R. & Schaller, H. (1987) Replication strategy of human hepatitis B virus. **J Virol,** 61**,** 904-11.

Winau, F., Hegasy, G., Weiskirchen, R., Weber, S., Cassan, C., Sieling, P.A., Modlin, R.L., Liblau, R.S., Gressner, A.M. & Kaufmann, S.H. (2007) Ito cells are liver-resident antigen-presenting cells for activating T cell responses. **Immunity,** 26**,** 117-29.

Wisher, M.H. & Evans, W.H. (1975) Functional polarity of the rat hepatocyte surface membrane. Isolation and characterization of plasma-membrane subfractions from the blood-sinusoidal, bile-Canalicular and contiguous surfaces of the hepatocyte. **Biochem J,** 146**,** 375-88.

Wu, J., Meng, Z., Jiang, M., Pei, R., Trippler, M., Broering, R., Bucchi, A., Sowa, J.P., Dittmer, U., Yang, D., Roggendorf, M., Gerken, G., Lu, M. & Schlaak, J.F. (2009) Hepatitis B virus suppresses toll-like receptor-mediated innate immune responses in murine parenchymal and nonparenchymal liver cells. **Hepatology,** 49**,** 1132-40.

Xu, N., Yao, H.P., Sun, Z. & Chen, Z. (2008) Toll-like receptor 7 and 9 expression in peripheral blood mononuclear cells from patients with chronic hepatitis B and related hepatocellular carcinoma. **Acta Pharmacol Sin,** 29**,** 239-44.

Yamada, T., Yamaoka, S., Goto, T., Nakai, M., Tsujimoto, Y. & Hatanaka, M. (1994) The human T-cell leukemia virus type I Tax protein induces apoptosis which is blocked by the Bcl-2 protein. **J Virol,** 68**,** 3374-9.

Yang, P.L., Althage, A., Chung, J. & Chisari, F.V. (2002) Hydrodynamic injection of viral DNA: a mouse model of acute hepatitis B virus infection. **Proc Natl Acad Sci U S A,** 99**,** 13825-30.

Yang, X., Stennicke, H.R., Wang, B., Green, D.R., Janicke, R.U., Srinivasan, A., Seth, P., Salvesen, G.S. & Froelich, C.J. (1998) Granzyme B mimics apical caspases. Description of a unified pathway for trans-activation of executioner caspase-3 and -7. **J Biol Chem,** 273**,** 34278-83.

Yang, Y., Ertl, H.C. & Wilson, J.M. (1994) MHC class I-restricted cytotoxic T lymphocytes to viral antigens destroy hepatocytes in mice infected with E1-deleted recombinant adenoviruses. **Immunity,** 1**,** 433-42.

Yee, J.K. (1989) A liver-specific enhancer in the core promoter region of human hepatitis B virus. **Science,** 246**,** 658-61.

Yuh, C.H. & Ting, L.P. (1993) Differentiated liver cell specificity of the second enhancer of hepatitis B virus. **J Virol,** 67**,** 142-9.

Zou, H., Henzel, W.J., Liu, X., Lutschg, A. & Wang, X. (1997) Apaf-1, a human protein homologous to C. elegans CED-4, participates in cytochrome c-dependent activation of caspase-3. **Cell,** 90**,** 405-13.

.

6 Appendix

6.1. Sequencing Data of HBx ORF

The translation of the HBx has been blocked by a premature stop codon at the 5´ end of the HBx ORF (TGC **C**AA C was mutated to TGC **T**AA C). To confirm the point mutation, cccDNA from was isolated from generated stable ΔxHBV-producing hepatoma cell lines (HepG2-H1.3x-) and amplified by specific primers (92-, 2251+); subsequently, purified PCR products were sequenced (sequencing primer 2459+).

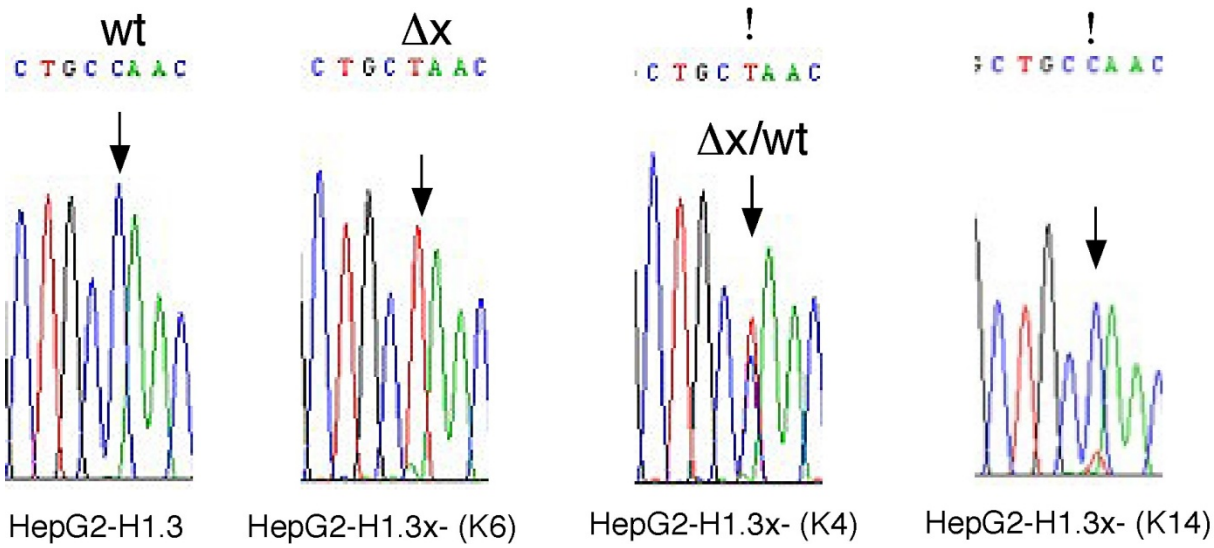

Results: Only the cell clone HepG2-H1.3x- (K6) carries the specific point mutation in the ORF of HBx on cccDNA level; all other HepG2-H1.3x- cell clones being selected re-mutated back to wild type for still undefined reasons.

6.2. Liver Histology of AdHBV-infected Mice

Detailed record of stained liver sections of AdHBV infected mice (concerning second experimental part). Detailed description see page 96 -99.

Legend: first row shows H&E stain, second and third row show HBcAg immunohistochemical stain. (**d**x) = days post infection; **M**x = male animal + specific number; **F**x = female animal+ specific number; **K**x = control animal + specific number **P** = portal tract; **CV** = central vein; arrow／ marks infiltrating lymphocytes;

gld (d0)

a) K2

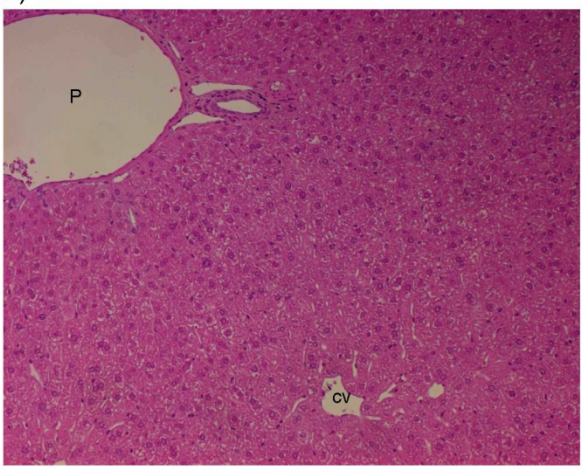

gld (d3)

c) M4

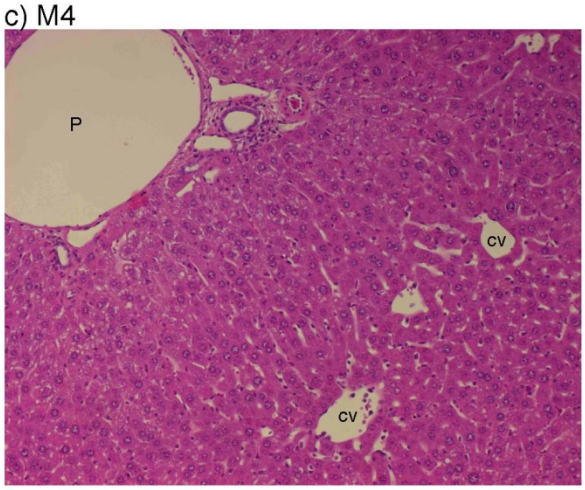

b) K2

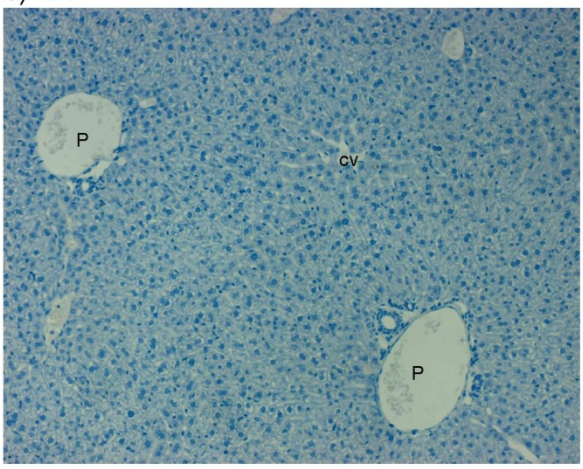

d) M4

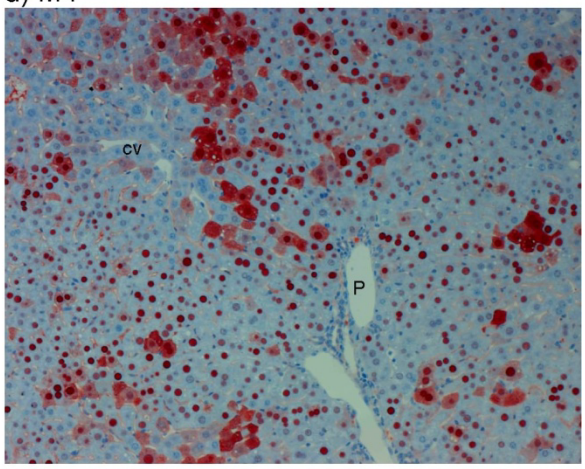

gld (d7)

a) M3

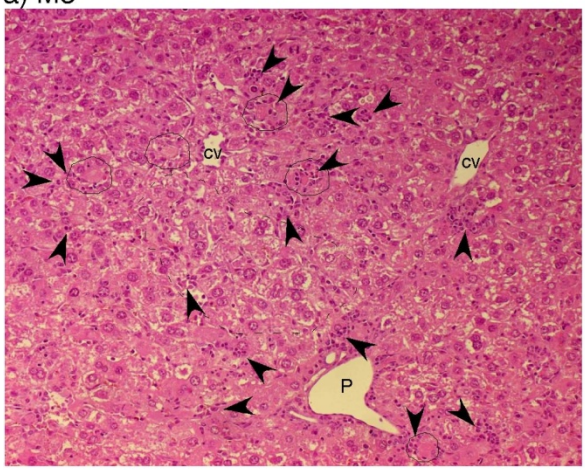

b) M4

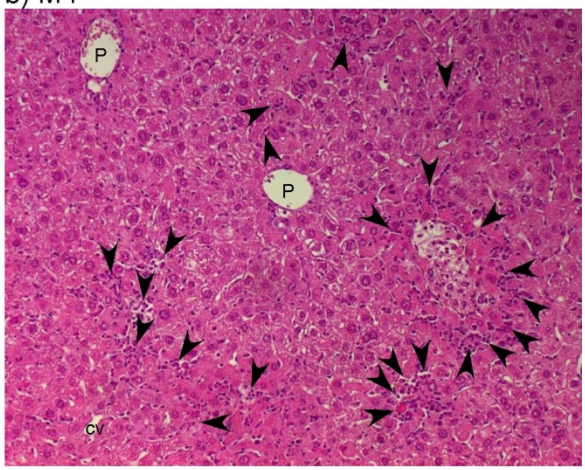

c) M3

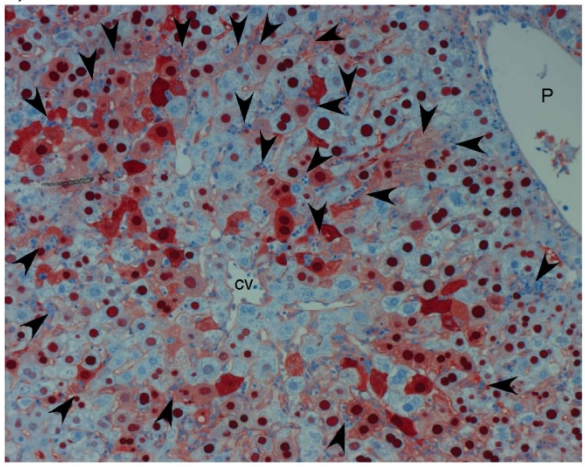

d) M4

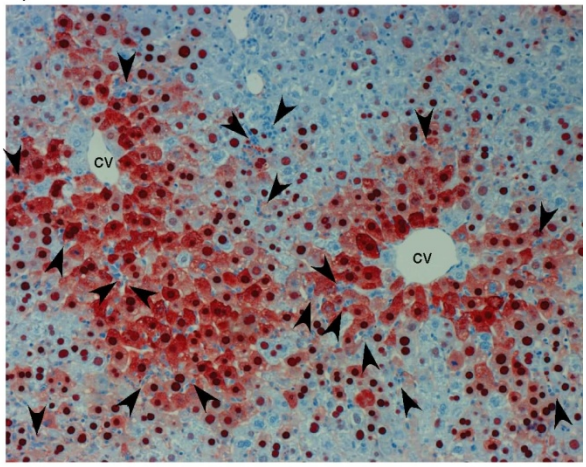

e) M3

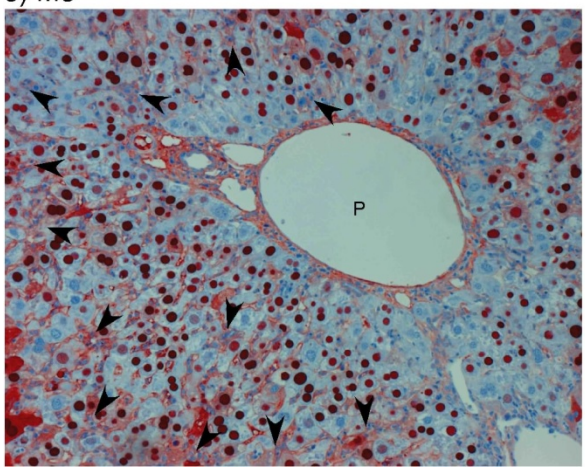

f) M4

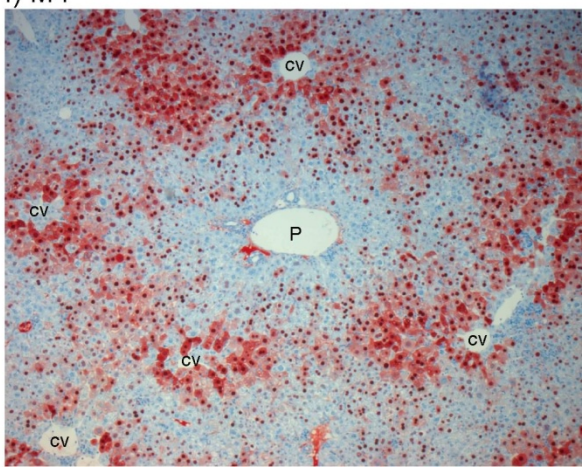

gld (d14)

a) M3

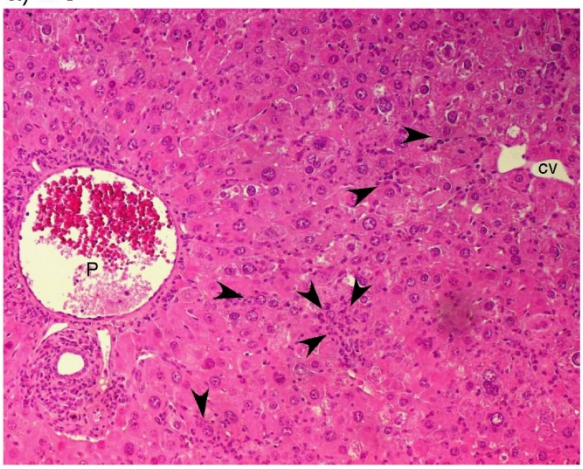

b) M3

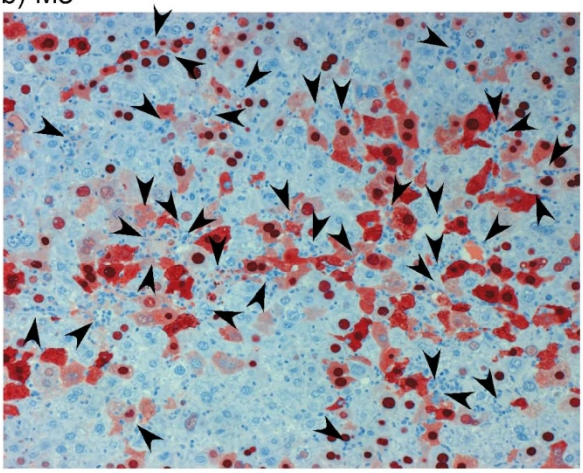

c) M3

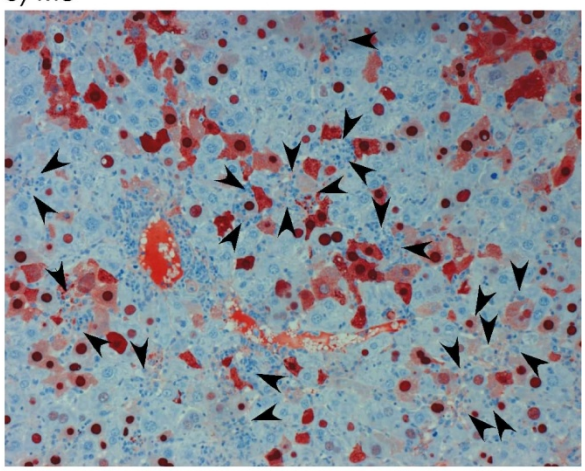

d) M3

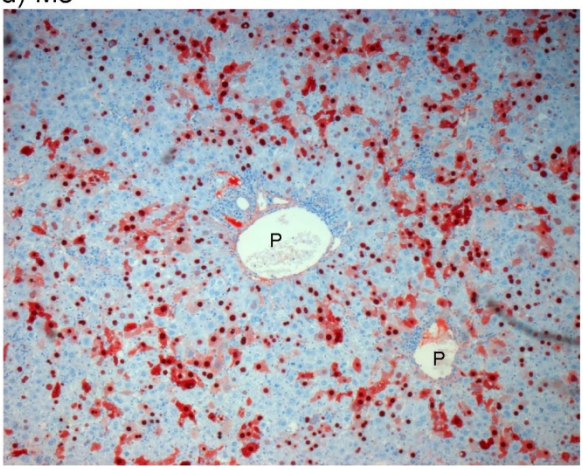

gld (d21)

a) F2

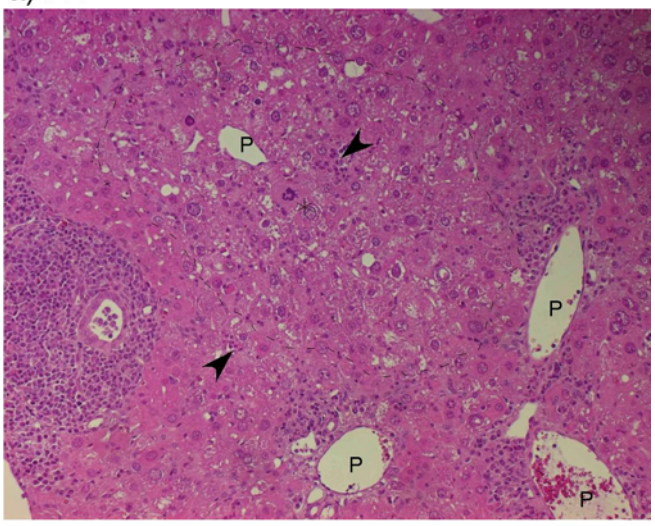

b) F2

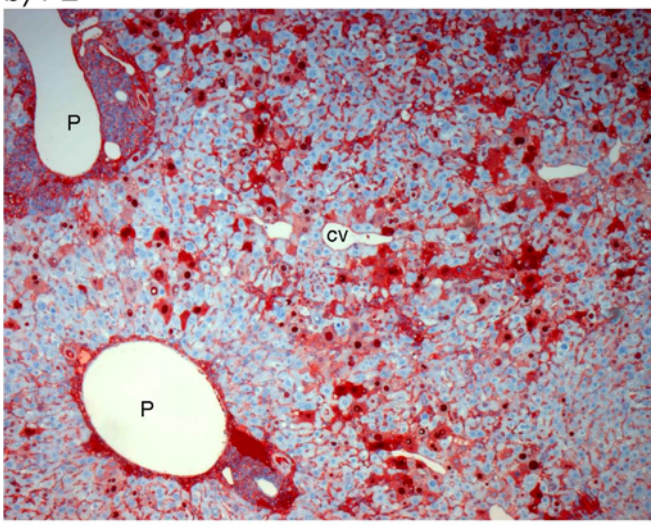

c) F2

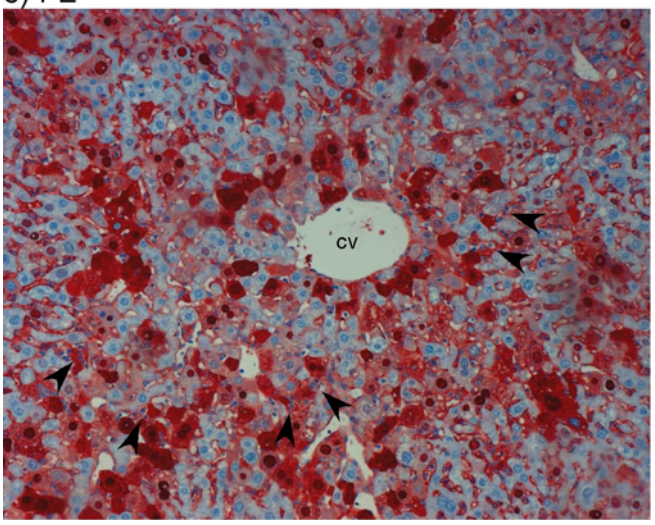

gld (d28)

a) M4

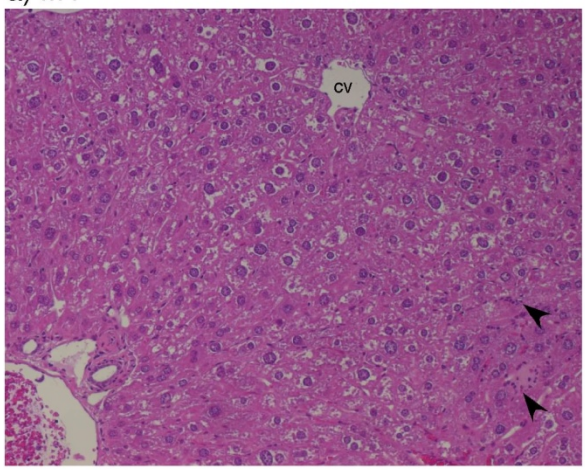

b) F1

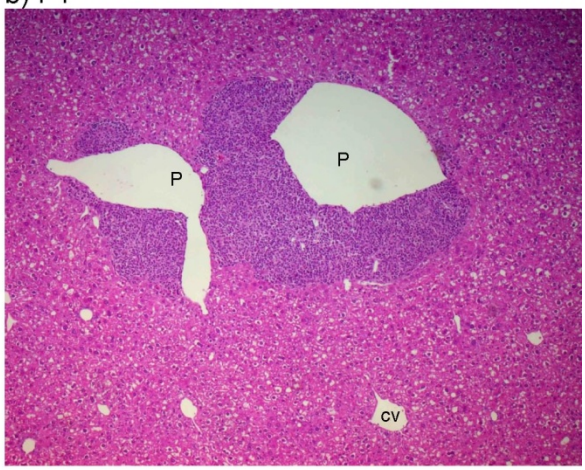

c) M4

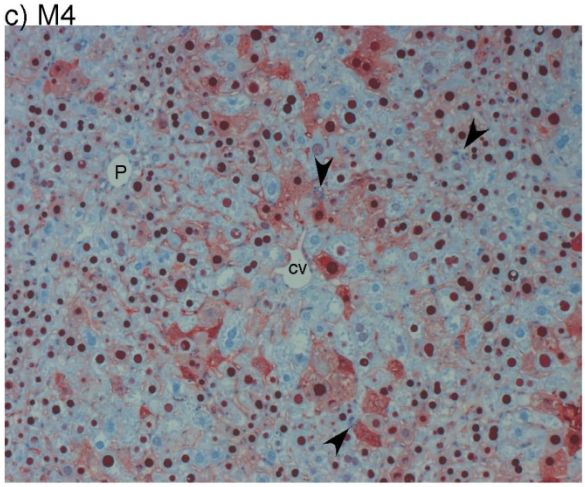

d) F1

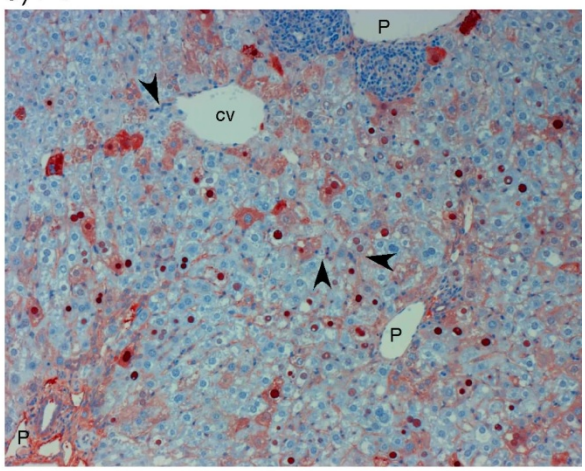

d) M4

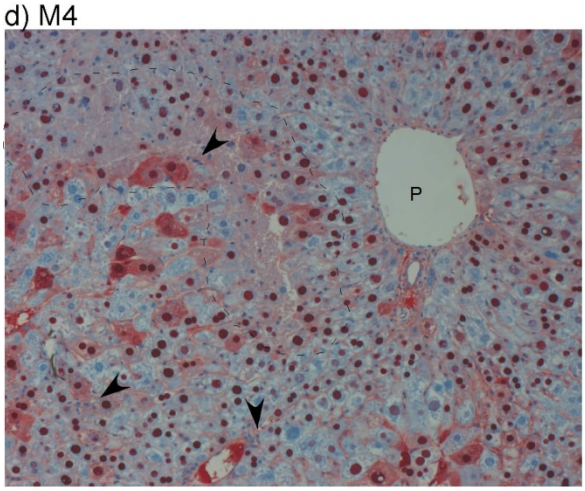

gld (d56)

a) F2

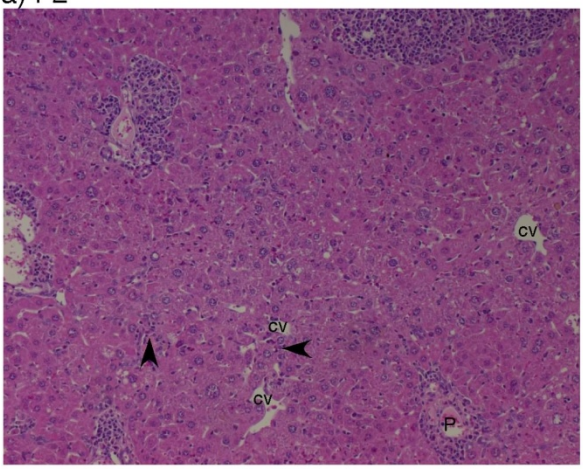

b) F2

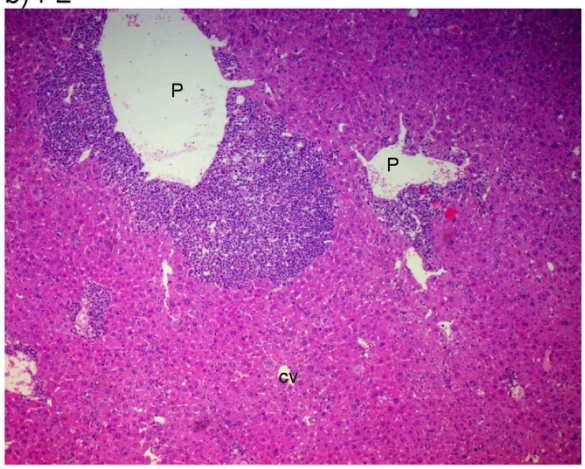

c) M4

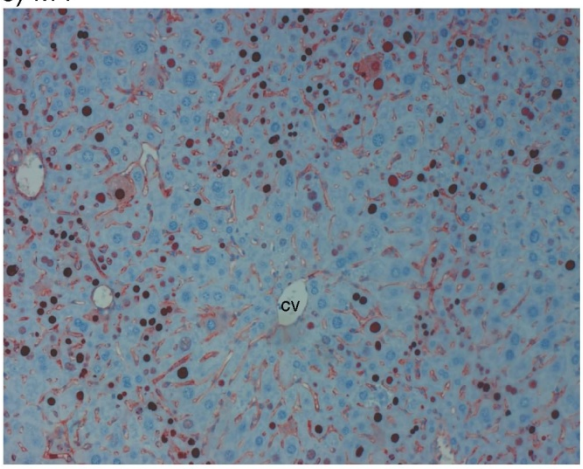

d) M4

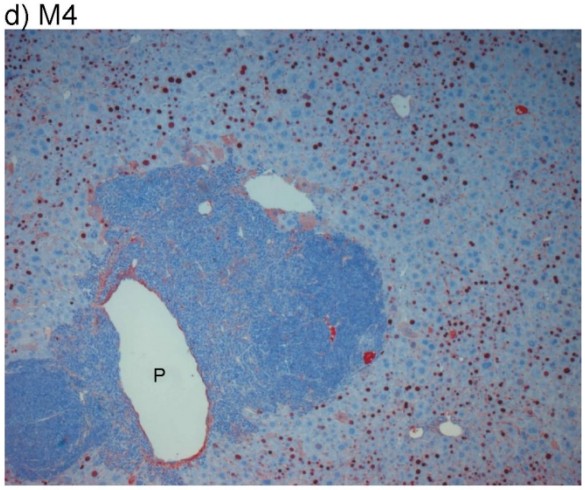

e) F2

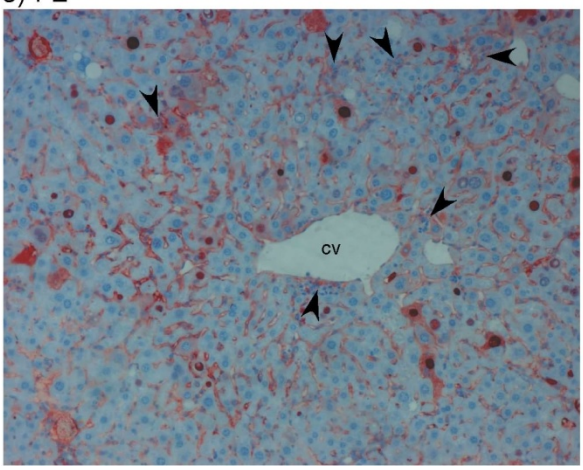

f) M3

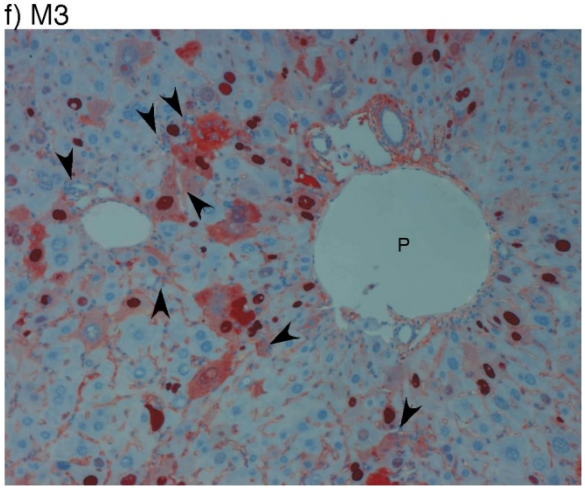

gld (d84)

a) F2

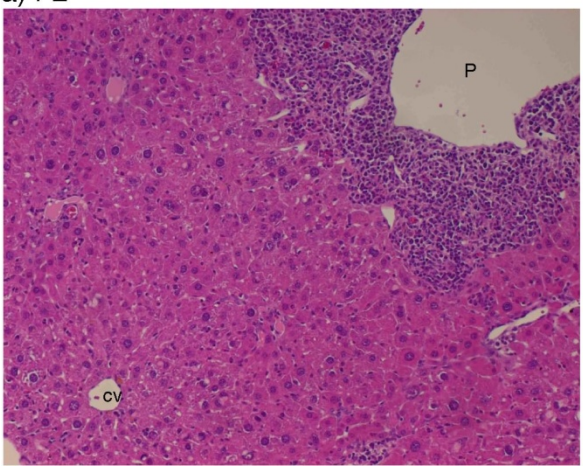

b) M2

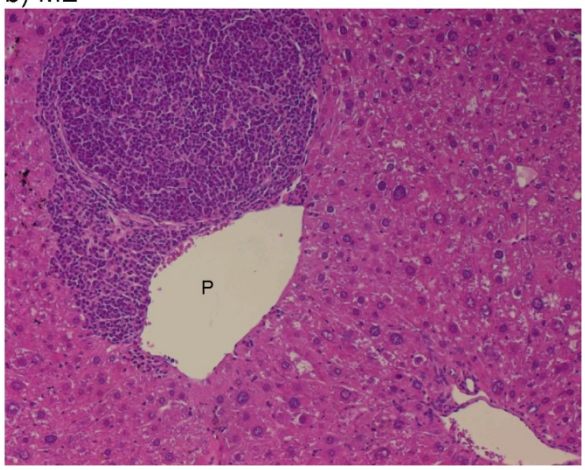

C57BL/6

a) K **(d0)**

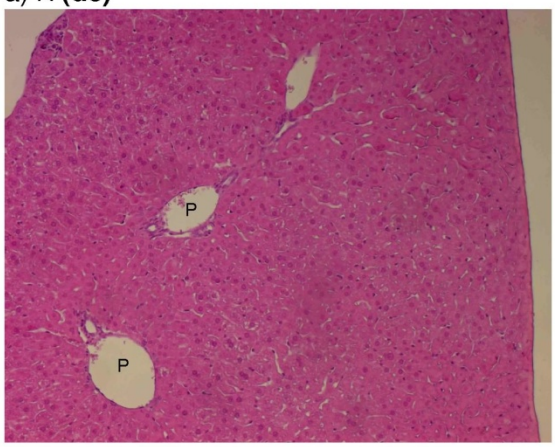

b) M2 **(d3)**

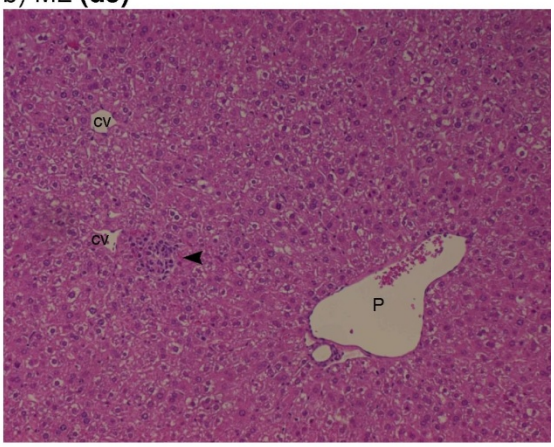

c) M4 **(d7)**

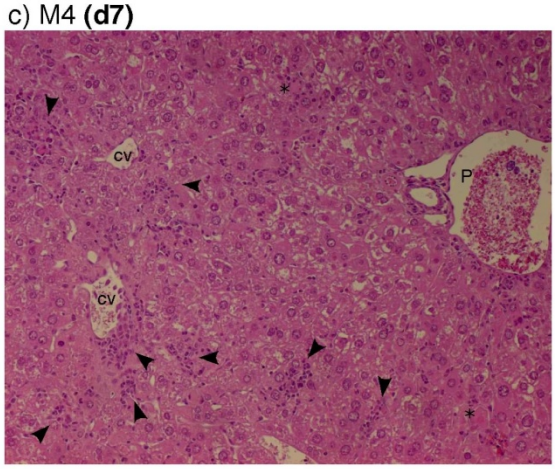

d) M3 **(d14)**

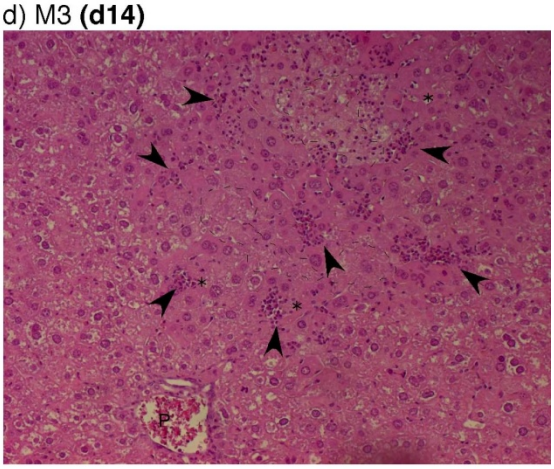

e) M2 **(d21)**

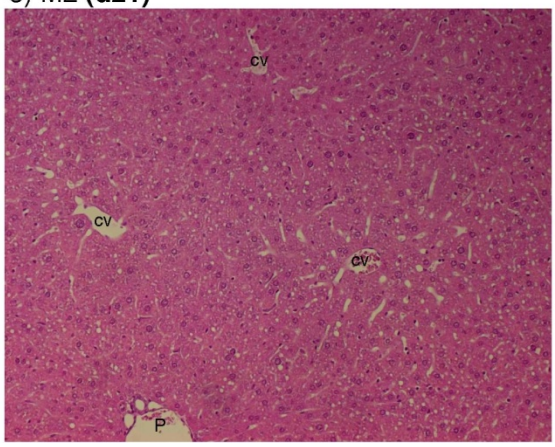

f) M4 **(d28)**

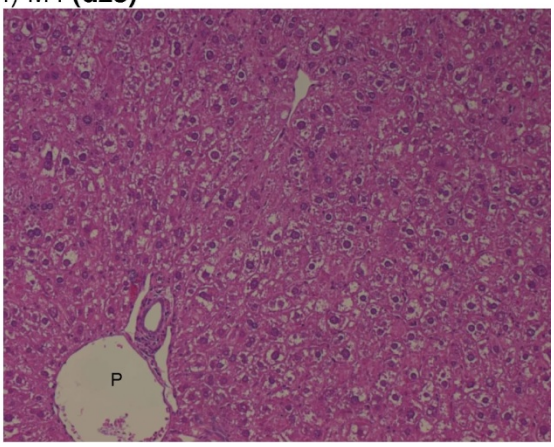

C57BL/6

a) M3 **(d56)**

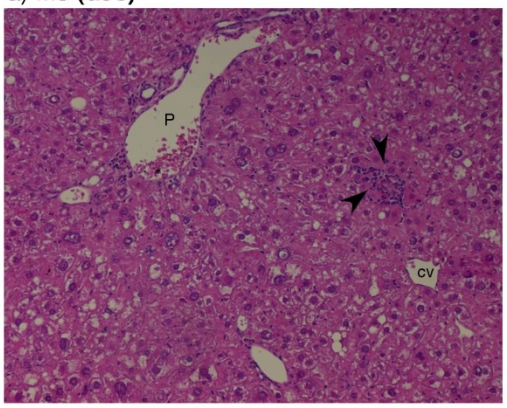

b) M3 **(84)**

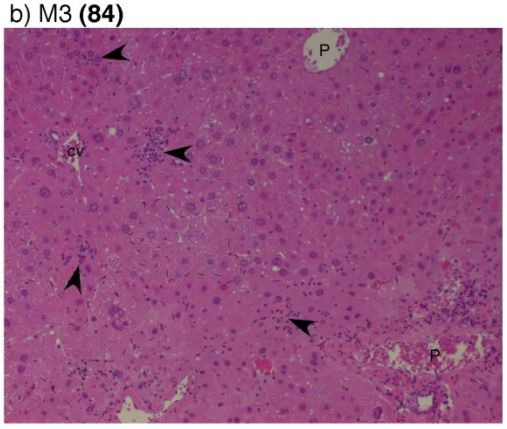

c) F1 **(d84)**

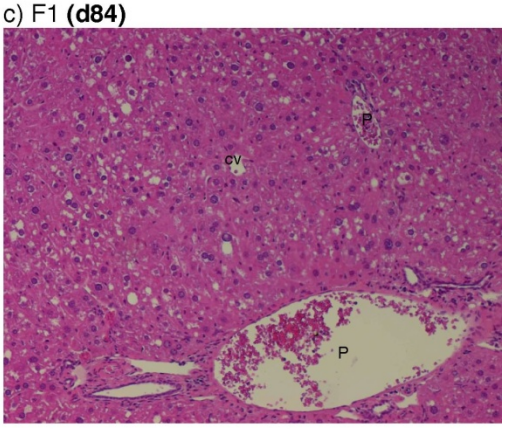

d) F1 **(d112)**

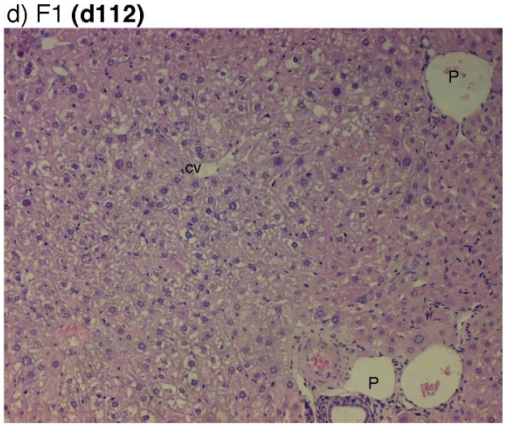

FADD/cre neg. **[FADD+] (d3)**

a) M1

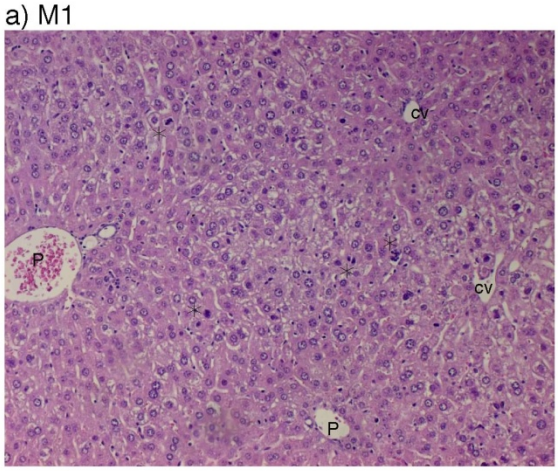

b) M4

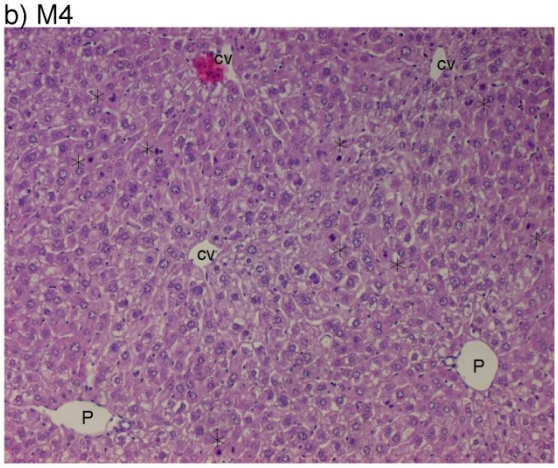

c) M1

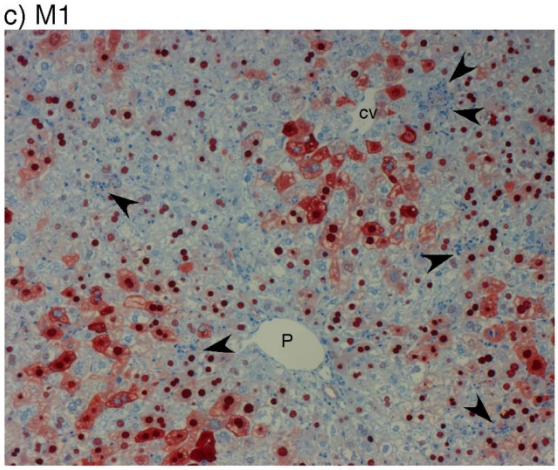

d) M4

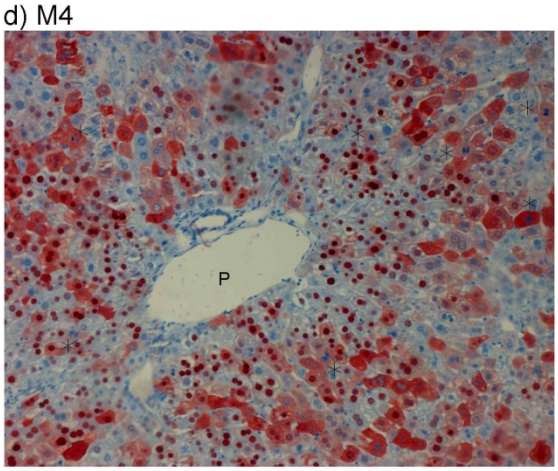

e) M4

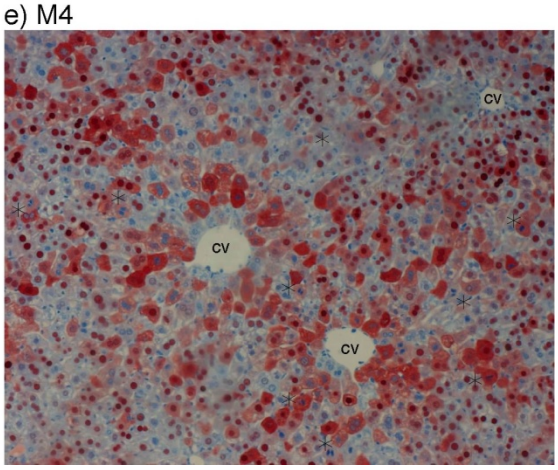

FADD/cre neg. **[FADD+] (d7)**

a) F1

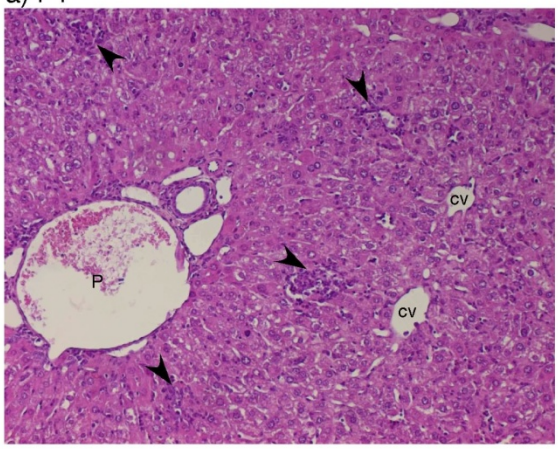

b) M4

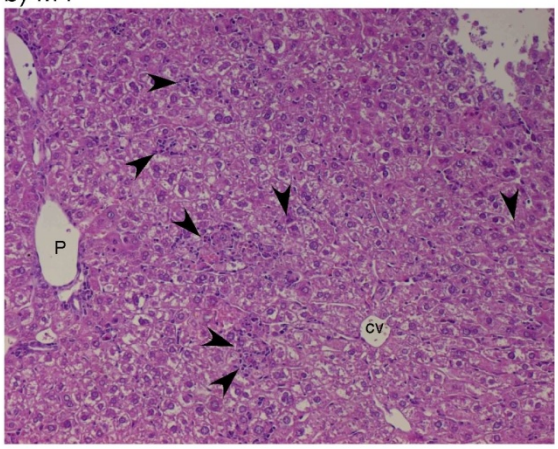

c) F1

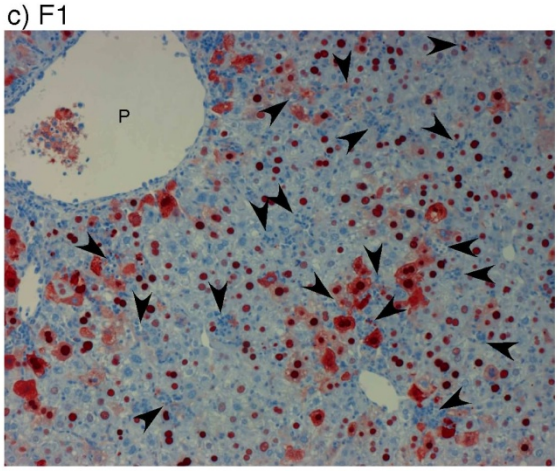

d) M4

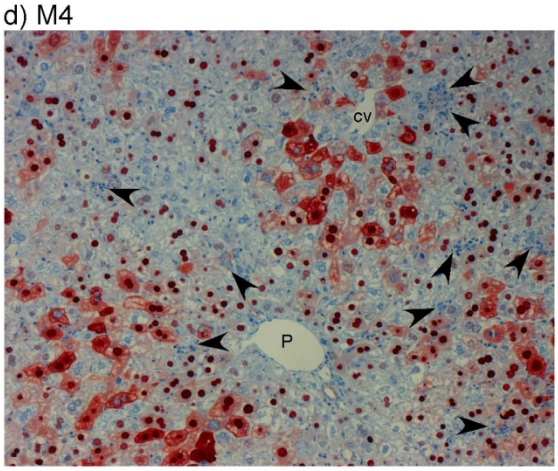

e) M4

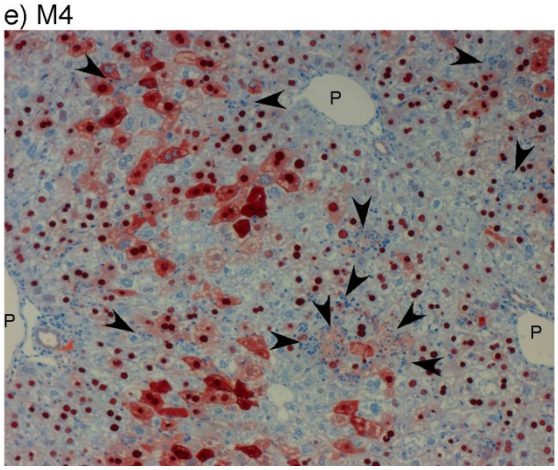

FADD/cre neg. **[FADD+] (d14)**

a) M4

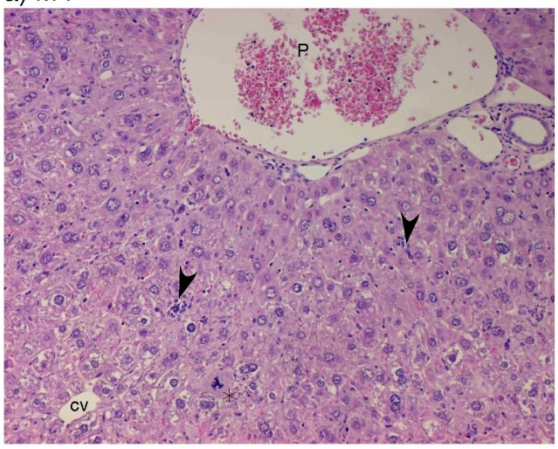

b) F1

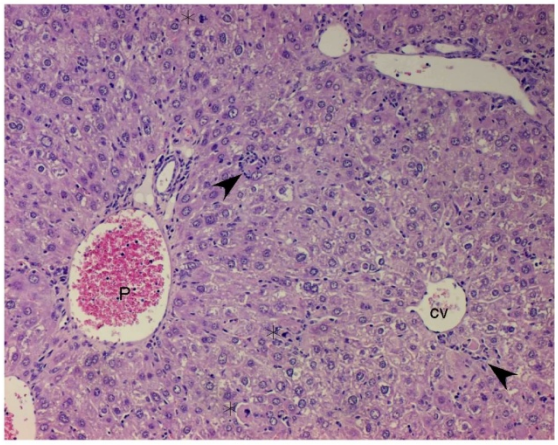

c) M4

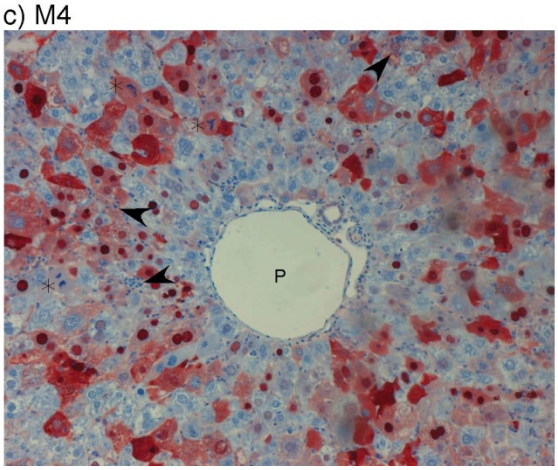

d) F1

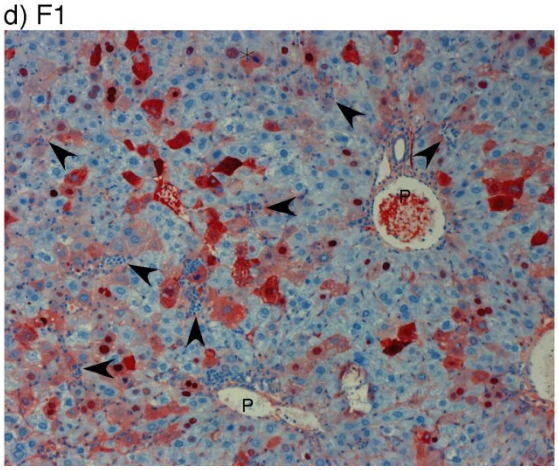

FADD/cre neg. **[FADD+] (d21)**

a) F2

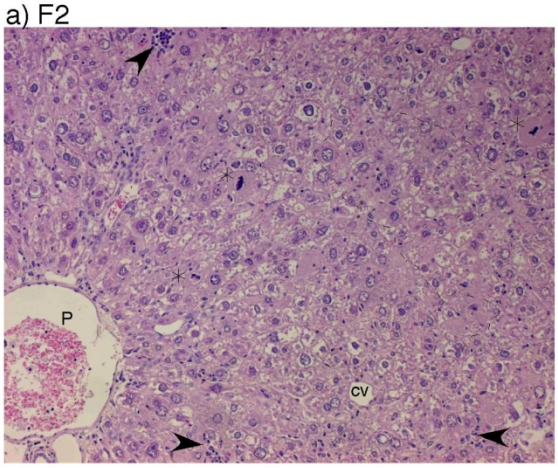

b) M3

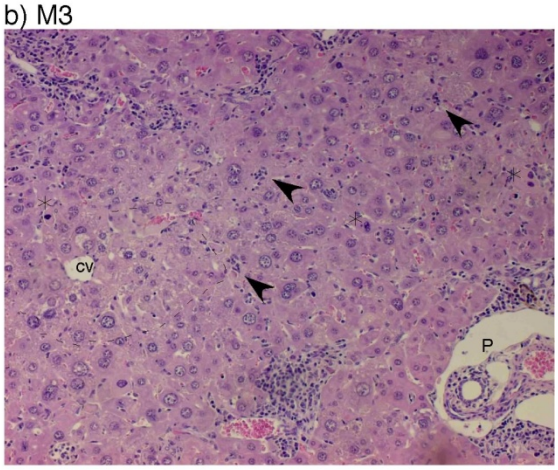

c) F2

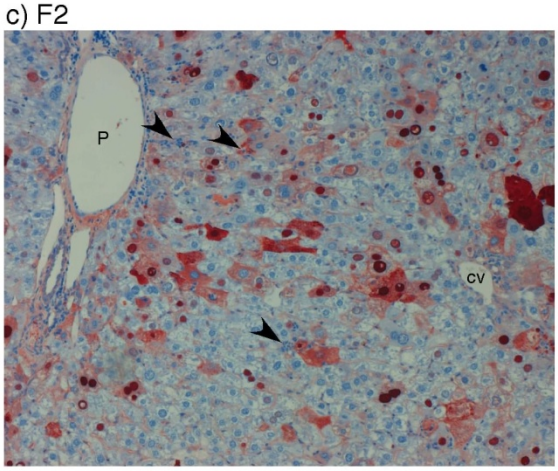

d) M3

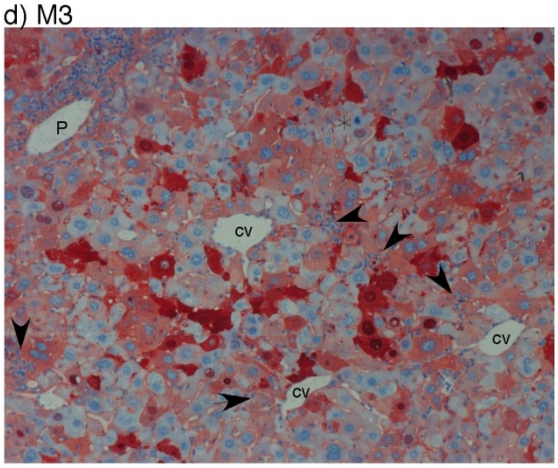

e) M3

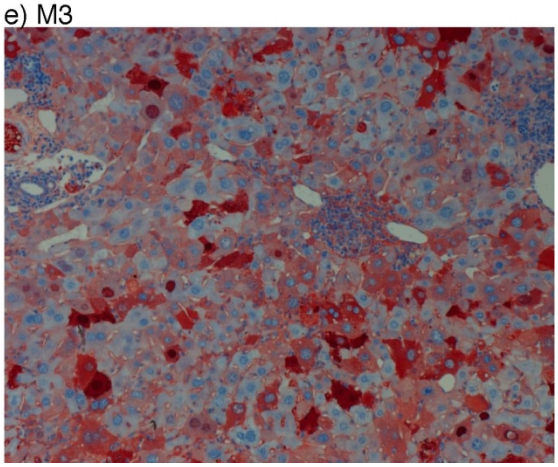

FADD/cre neg. **[FADD+] (d28)**

a) F2

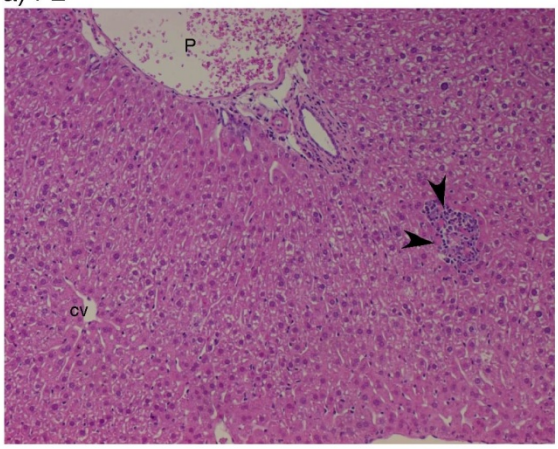

b) M3

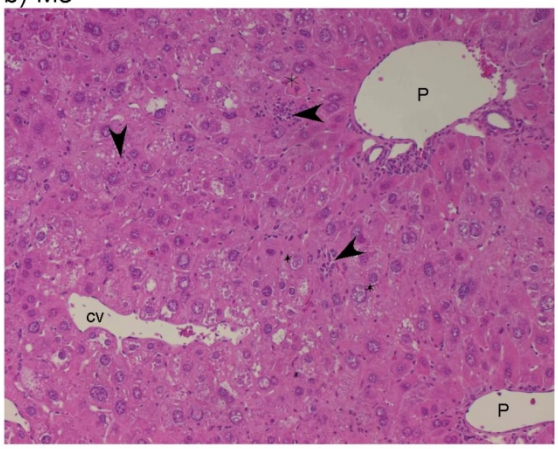

c) F2

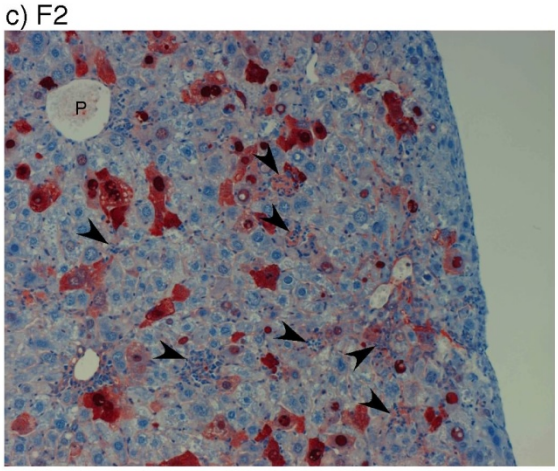

d) M3

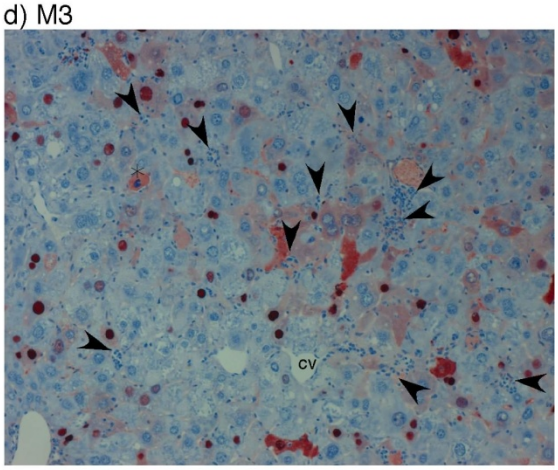

e) M3

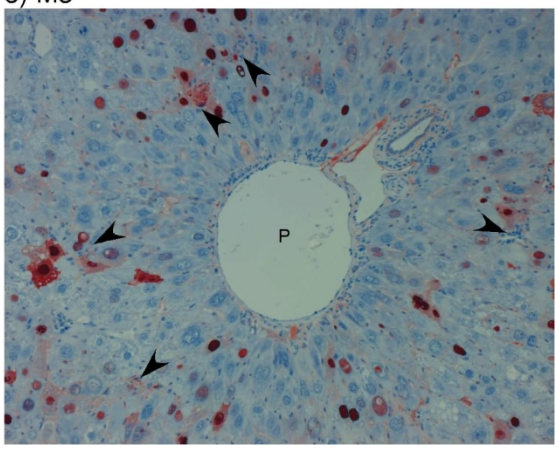

FADD/cre neg. **[FADD+] (d56)**

a) F1

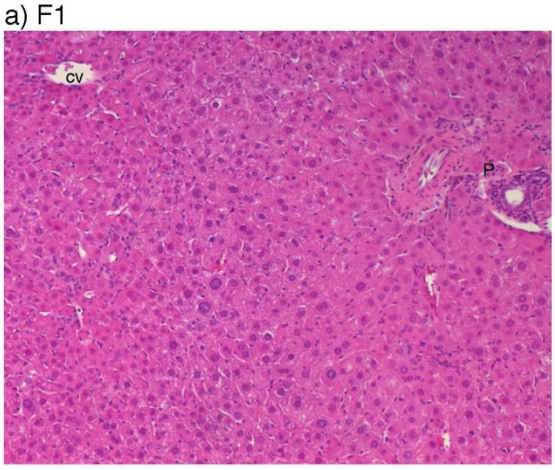

b) M4

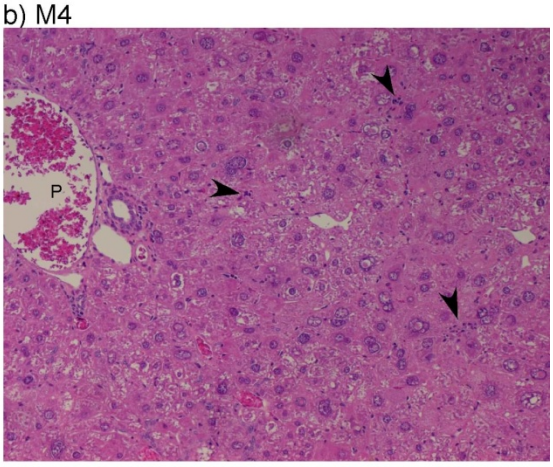

c) F1

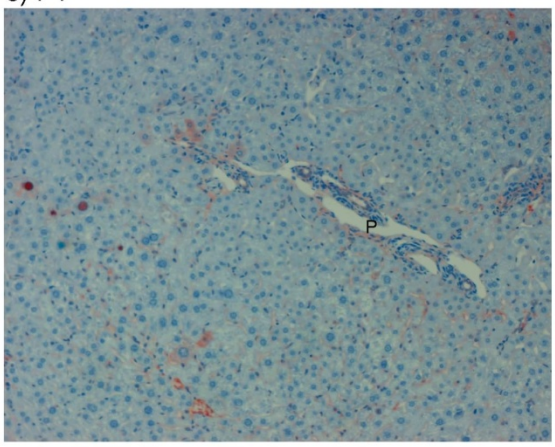

d) M4

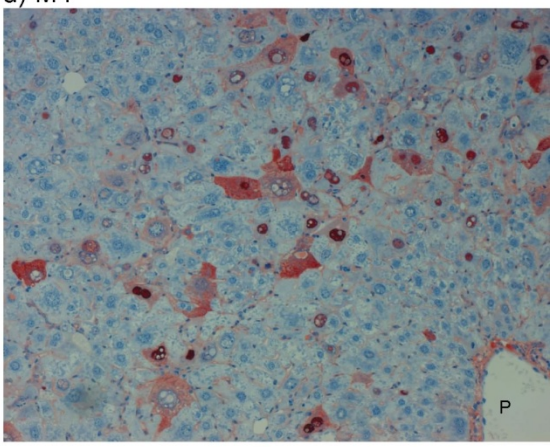

e) M4

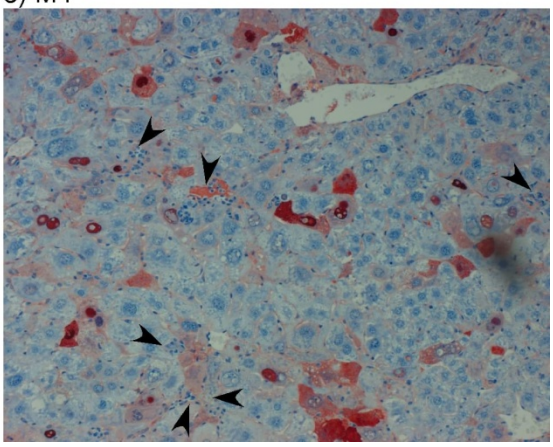

FADD/cre neg. **[FADD+] (d84)**

M3

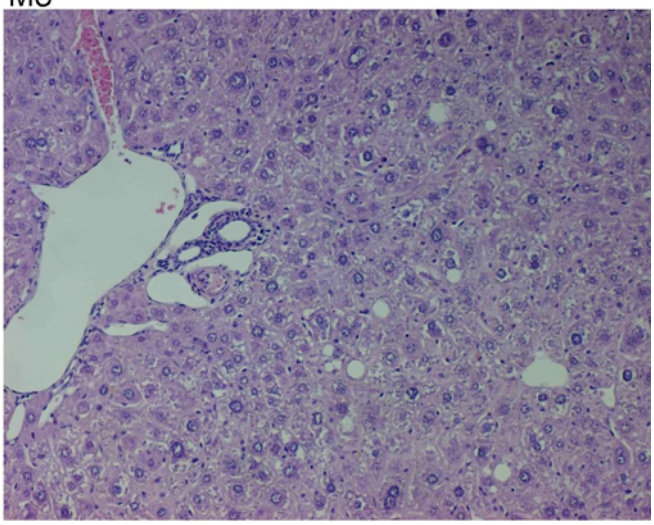

FADD/cre neg. **[FADD+] (d0)**

F2

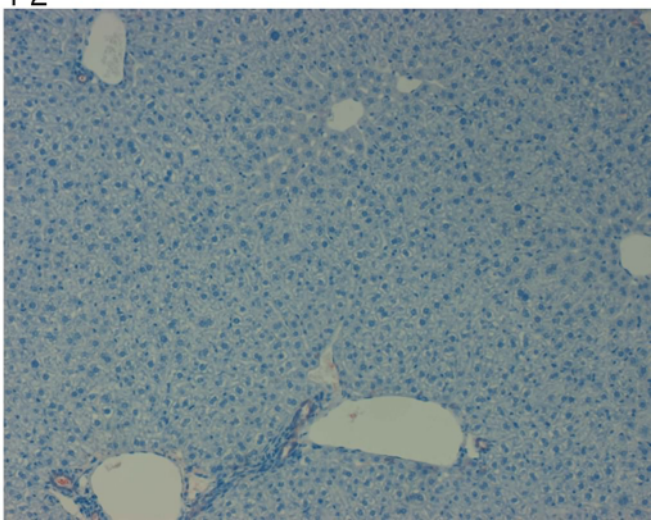

FADD/cre pos. **[FADD-]**

a) K **(d0)**

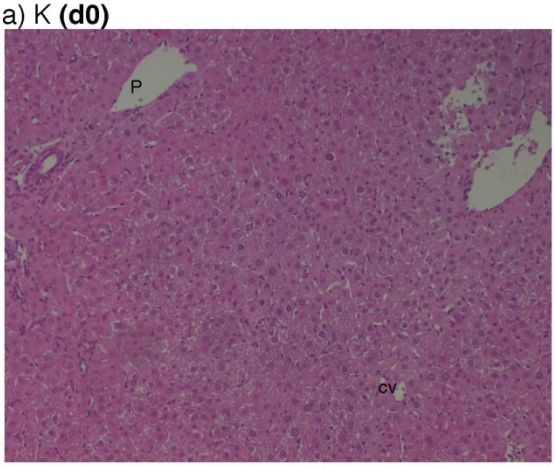

b) F1 **(d3)**

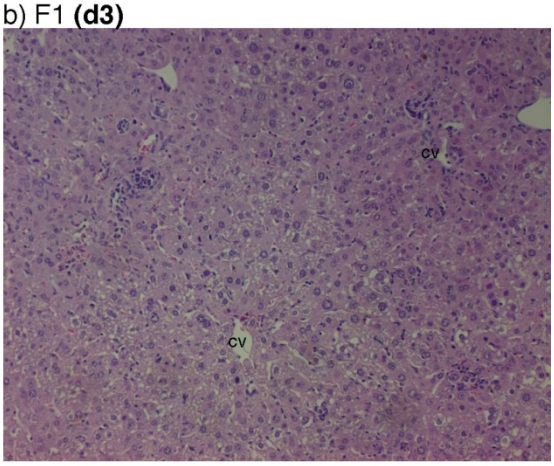

c) M4 **(d7)**

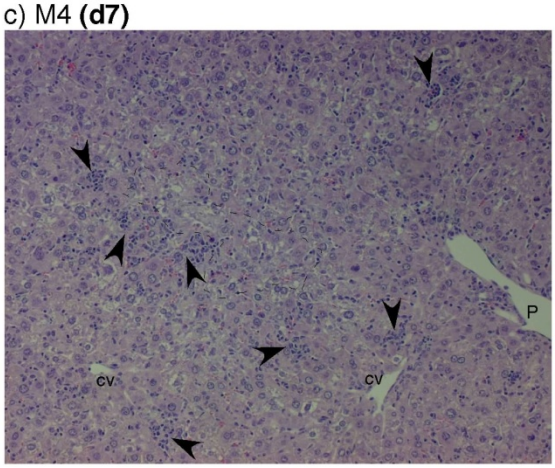

d) M4 **(d14)**

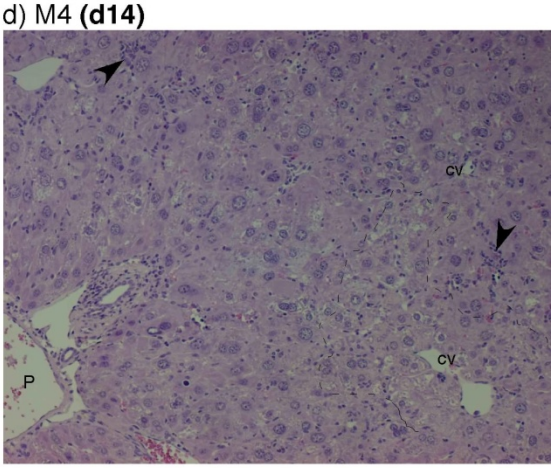

e) F1 **(d21)**

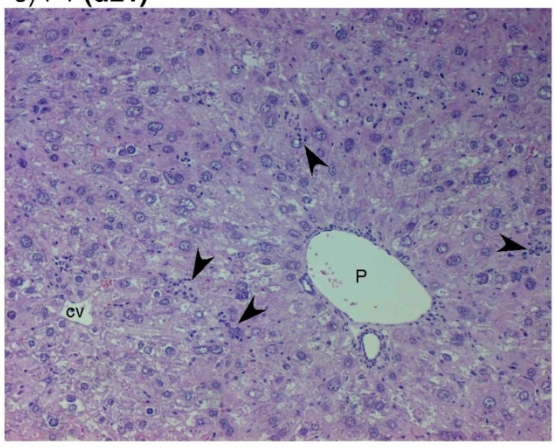

f) M3 **(d28)**

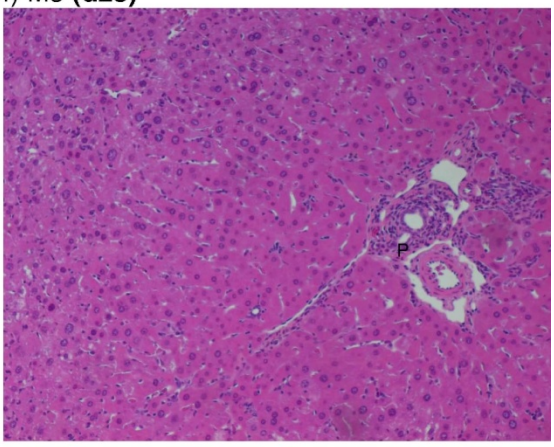

FADD/cre pos **[FADD-]**

a) F1 **(d56)**

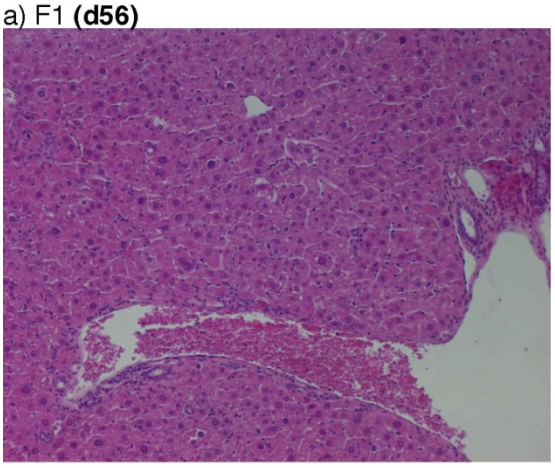

b) M4 **(d84)**

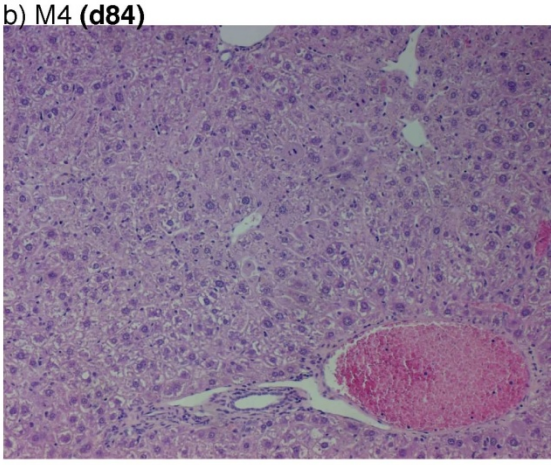

Danksagung

Mein ganz besonderer Dank gebührt *Frau Prof. Dr. Ulrike Protzer*, für die Überlassung interessanter Themen, vieler anregender und kritischer Diskussionen sowohl über meine Arbeit aber natürlich auch über das gesamte Gebiet HBV. Darüber hinaus möchte ich mich bei ihr für die optimalen experimentellen Arbeitsbedingungen, die regelmäßige Teilnahme an internationalen Kongressen, die Unterstützung beim wissenschaftlichen Schreiben sowie für die Wohnungssuche in München ganz herzlich bedanken.

Bei Herrn *Prof. Hrabé de Angelis* bedanke ich mich für die offizielle Begutachtung meiner Arbeit. Herrn *Prof. Dr. Volker Bruss* danke ich ganz herzlich für das kritische Lektorat des Apoptose-Papers, für manche anregende Diskussion im Seminar und für die Begutachtung meiner Arbeit. Herrn *Prof. Dr. Küster* danke ich für seine Bereitschaft den Vorsitz meines gesamten Dissertationsverfahrens zu übernehmen.

Ein ganz großes Dankeschön geht an alle *meine Arbeitskollegen* und Freunde der Arbeitsgruppe von Frau Prof. Dr. Ulrike Protzer (Ehemalige natürlich mit eingeschlossen) für die unglaublich gute und kollegiale Atmosphäre.

Ganz besonders hervorheben möchte ich *Dr. Marianna Hösel* für ihre Freundschaft, ihre Fröhlichkeit, die vielen intensiven wissenschaftlichen und privaten Gespräche, ihre aufbauenden Worte und natürlich für das sehr kritische Lektorat meiner Arbeit aus weiter Ferne (das z.T. nur durch die Ballettstunden ihrer Tochter Lisa erst möglich wurde ;-)). Ein ebenso dickes Dankeschön gebührt *Dr. Uta Zedler*, die auch bei eigenen turbulenten Zeiten in weiter Ferne immer konstant zu mir gestanden hat und mit sehr viel konstruktiver Kritik und aufmunternden Worten das Schreiben meiner Arbeit begleitet und bereichert hat. Ganz herzlich bedanken möchte ich mich auch bei *Karin Krebs* für ihre Freundschaft, ihre moralische Unterstützung (insbesonders im Kampf des Laboralltags in München) und für ihre konstruktive Kritik weiter Teile meiner Arbeit.

Für die absolut zuverlässige technische Unterstützung meiner Mausexperimente möchte ich mich bei *Raindy Tedjokusumo* und *Katrin Tinnefeld* bedanken, insbesondere für das Messen sämtlicher serologischer Proben auf dem Axym System sowie für ihre Hilfe in der Aufbereitung von DNA und RNA aus Gewebe. Hervorheben möchte ich auch *Joana Fischer,* die mir bei so mancher

Mauspräparation in Köln tatkräftig zur Seite stand. *Leonhard Stross* danke ich für die technische Planung der FACS Analyse und seine Bereitschaft dafür extra einige Tage mit nach Köln zu kommen. *Knud Esser* danke ich für sehr konstruktive und unterhaltsame Diskussionen. *Dr. Miriam John von Freyend* danke ich für so manche lustige Stunde im Laboralltag. Ganz besonders hervorheben möchte ich ihre Zuverlässigkeit bei der Bereitstellung des Kölner Tierstallschlüssels und wichtiger Utensilien für die Mausexperimente, was bei meiner Anreise aus München eine große Erleichterung für mich darstellte. *Theresa Asen* danke ich für ihre Mithilfe in der Isotypenbestimmung der HB Antikörper. *Dr. Julie Lucifora* danke ich herzlich für das kritisches Lektorat des ersten Ergebnisteiles meiner Arbeit aber auch für ihr Engagement sich in die HBx-Thematik einzuarbeiten. Durch ihre Mithilfe wurde maßgeblich ein publizierbares Ergebnis außerhalb dieser Arbeit erreicht.

Herzlich Bedanken möchte ich mich bei allen ehemaligen *Arbeitskollegen aus der Medizinischen Mikrobiologie in Köln*. Hervorheben möchte ich *Katja Wiegman-Krönke* die mich bei meinem ständigen Pendeln immer richtig freundlich Empfangen und unterstützt hat. Danken möchte ich auch *Prof. Dr. Martin Krönke*, ohne sein Einverständnis wäre das bestehende Mausprojekt in Köln sicherlich nicht so einfach möglich gewesen. *Dr. Hamid Kaschka*r danke ich für sehr fruchtbare Diskussionen rund um das Thema Apoptose. Danken möchte ich auch *Diana Wagner-Stippich*, die mehrfach für mich eingesprungen ist, um Mäuse zu bluten. Gudrun Suckau und Gisela Holz danke ich für das zuverlässige Bereitstellen von Trockeneis, ohne ihre Hilfe wäre so mancher Probentransport nach München ein Desaster gewesen.

Dr. Jens Seeger, *Christian Bach* und *Ke Zhang* danke ich ganz herzlich für das zügige Lösen der Microsoft eigenen EDV Probleme.

Unserem Kooperationspartner *Prof. Dr. Peter Schirmacher* danke ich für die histologische Begutachtung sämtlicher Mäuselebern, aber natürlich auch für die grundsätzliche Ermöglichung der histologischen Analysen. *Sahra Meißnard* danke ich für die technische Durchführung der histologischen Schnitte und Färbungen. *Prof. Dr. Manolis Pasparakis* danke ich für das Bereitstellen der FADD Mäuse. Des weiteren möchte ich mich bei *Dr. Svenja Debey-Pascher* bedanken für die Durchführung der Microarray Analyse und für die telefonische Unterstützung bei Fragen rund um den Microarray. *Prof. Dr. Percy Knolle* danke ich für seine sehr konstruktiven Anregungen zum Apoptose Paper.

Ein großer Dank gilt *Dale Richardson* für das sprachliche Korrekturlesen dieser Arbeit.

Ganz besonders bedanken möchte ich mich bei meiner *Familie und Freuden* außerhalb des Laboralltags für Ihr Interesse und die Unterstützung in allen Lebenslagen. Besonders hervorheben möchte ich meinen Lebensgefährten *Ralph Zumkier,* der geduldig alle Höhen und Tiefen der letzten Jahre mit durchlitten hat, mich auf unglaubliche Weise unterstützte und mir jederzeit mit Rat und Tat zur Seite stand. Danke!